Exploring Stereochemical Constraints and Chemical Reactivity of Vinylogous Amino acids in the Design of Foldamers

A thesis
Submitted in partial fulfillment of the requirements
Of the degree of
Doctor of Philosophy

By

Mothukuri Ganesh Kumar

ID: 20103065

Indian Institute of Science Education and Research, Pune

Dedicated to My family and Teachers……

CERTIFICATE

This is to certify that the work incorporated in the thesis entitled "**Exploring Stereochemical Constraints and Chemical Reactivity of Vinylogous Amino acids in the Foldamers Design and Molecular Rearrangements**" submitted by **Mothukuri Ganesh Kumar** carried out by the candidate at the Indian Institute of Science Education and Research (IISER), Pune, under my supervision. The work presented here or any part of it has not been included in any other thesis submitted previously for the award of any degree or diploma from any other University or Institution.

Date:

Dr. Hosahudya N. Gopi
(Research Supervisor)
Associate Professor, IISER-Pune
Pune-411008, India

Declaration

I hereby declare that the thesis entitled "**Exploring Stereochemical Constraints and Chemical Reactivity of Vinylogous Amino acids in the Foldamers Design and Molecular Rearrangements**" submitted for the degree of Doctor of Philosophy in Chemistry at Indian Institute of Science Education and Research (IISER), Pune has not been submitted by me to any other University or Institution. This work was carried out at Indian Institute of Science Education and Research (IISER), Pune, India under the supervision of Dr. Hosahudya N. Gopi.

Date:

Mothukuri Ganesh Kumar

ID: 20103065

Senior Research Fellow

Dept. of Chemistry, IISER-Pune

Pune-411008

Acknowledgement

First I would like to thank my supervisor Dr. Hosahudya N. Gopi for his unconditional support throughout five years to conduct my research. He is prolific and brilliant chemist. He is by far the hardest working person I know. His commitment at work, punctuality, motivating students and constant support at their difficult times and many more qualities I always admire at. I am fortunate to work with him.

My sincere thanks to our Director Prof. K. N. Ganesh for providing excellent facilities and financial support during my research here at Indian Institute of Science Education and Research (IISER)-Pune. I am also thankful to the CSIR-India for my five years research fellowship. Special thanks to Dr. C. V. Ramana and Dr. Aloke Das for being my RAC committee members. Their valuable suggestions and critics always encouraged me to pursue in the right direction. I would like to acknowledge Dr. K. M. P. Raja from Madurai Kamaraj University, Tamil Nadu for building the NMR structure models, Dr. T. S. Mahesh for helping me to setup 2D-NMR and other special experiments and I am very much thankful to all chemistry faculties, technicians (Pooja, Swathi, Archana, Nayana, Chinmay, Nitin, Deepali) and admin staff of IISER-Pune for their numerous support.

I am lucky to have wonderful labmates. I would extend my sincere thanks to all of them. Dr. Anupam Bandyopadhyay, Dr. Sandip V. Jadhav and Dr. Schitanand M. Mali were seniors to me when I have joined in the group. They are very helpful from the beginning of my Ph.D and I am lucky to have such colleagues. Shiva Shankar (Shiva) and Sushil N. Benke (Suhil) are one of my best buddies to whom I always share my thoughts and they are highly motivated, hardworking, and cheerful persons I have to mention especially about Rajkumar Misra (Razz). He played best part in learning Hindi language and he is higly motivated and joyful person. Anindita Adak, Veeresh (Raina), Rupal (Rinku), Rahi Masoom Reja (Rahi) and Sachin Nalawade (Master Blaster) are really good and supportive in maintaining lab facilities and ambience of the lab. They are cheerful and full of energy. Rupal is very cool, calm and good singer also. Among them I got opportunities to work with Veeresh and Sachin Nalawade. I was highly impressed with their motivation and interest in science. We have got highly motivated undergraduate and project students Neha, Sumeet (Babu), Ankita, Rohini, Varsha, Mona, Anur, Swathi, Rinku, Abhijit and Sereena to work in our lab as part of their summer internship or fifth year project, they keep joyful atmosphere in lab. Our advisor is fortunate enough to have such enthusiastic and motivated students. Because of all these people all my five years in IISER passed just like few days.

From last five years, I am fortunate to have many good friends from IISER apart from my labmates. I thank my roommates Dharma, Gopal, Sathish, Kiran and Rajesh. We have great time in two years stay at Someshwar Wadi. I got to learn so many things from them. Dharma is like my brother, who always motivates and encourages doing things what I like. We together have great time in Cooking, playing Cricket, watching movies, scientific discussions etc. Gopal, Kiran, Rajesh, Sathish and Bapu had been with me from last 5 years. They were very good with me and helped in numerous ways. Madhan Gopal had been with me from last three years. We used to discuss about various topics science, politics, philosophy and movies etc. He is cool, quiet, critical thinker and good human being. I am sure will continue their friendship for lifetime. I would extend my thanks to Krishna, Venki, Ravi Kiran, Kishore, Subbu, Palvai, Gurivi, Rajkumar, Ashok, Koti, Hari, Narasimha, Rajendra, Rangu, Jagadheesh, Siva and Sarath for keeping playful atmosphere in IISER hostels and had a great time with them in many "Ugadi (telugu new year)" functions. Further I would thank all chemistry department friends of IISER-Pune and NCL-Pune for their support and help.

I would also like to express my deepest gratitude to my family. My family has been encouraging, supportive and shown belief in me and my work. Without them I wouldn't have chance to be at IISER-Pune. My father Mothukuri Satyanarayana is my role model in life. My mother Bhadravathi and father made lot of sacrifices to raise me and my sister. My sister (Rohini Laxmi) and my brother-in-Law (Suresh) are the one who stood like a backbone to me. I never forget their support in my life time. I extend my thanks to my friends Guptha, Ramakrishna, BSR garu, Suresh (NCL-Pune), Dr. Gopikrishna (IITH), Nag, Muvva, Suresh, Rajesh, Bapuji, Rama krishna, Balakrishna, Chaitanya who encouraged me throughout my carrier.

Finally I thank almighty God for giving me strength and courage to pursue what I would like to do in my life.

Mothukuri Ganesh Kumar

Contents

Abbreviations……vi

Abstract……..……ix

Publications……x

Chapter 1: Engineering Polypeptide Folding through *trans* Double Bonds

1.1 Introduction……2

1.1.1 Protein Secondary structures…….3

1.1.2 Protein Super secondary structures…….…..5

1.1.3 Mimicking protein structures ……..…....7

1.1.3.1 β-Peptide foldamers……..……..…..8

1.1.3.2 γ-Peptide foldamers ……..…11

1.2 (*E*)-Vinylogous γ-amino acids in the design of foldamers……..13

1.2.1 Natural occurrence and Biological importance of (*E*)-vinylogous γ-amino acids…….…..13

1.2.2 Previous work ……..…15

1.3 Aim and rationale of the present work……16

1.4 Results and discussion……..…...17

1.4.1 Design and synthesis of Hexapeptides P1 and P2……17

1.4.2 Crystal structure analysis of P1……...….….18

1.4.3 NMR structure analysis of P1 and P2…….…..21

1.4.4 Functional transformation of α, α, dγXaa -hybrid peptides into α,α,γ^4-hybrid peptides……..31

1.4.5 Structural analysis of P3 and P4…….……..31

1.4.6 Analogy with 3_{10}- helix and β-peptide 12-helix……...…35

1.5 Design and synthesis of heptapeptide P5 (Ac-Aib-γPhe-Ala-dγVal-Aib-γPhe-Aib-$CONH_2$)…….36

1.6 Conclusions…….39

1.7 Experimental section……40

1.8 References…….…...51

1.9 Appendix I: Characterization data of synthesized compounds …….…….58

Chapter 2: Exploring Reactivity of (*E*)-Vinylogous γ-Amino Acids and their Utility in the Design of Peptide Foldamers

2.1 Introduction…….....67

SECTION 2A: Design, synthesis and functionalization of multifaceted β-nitromethyl γ-amino acids and peptides

2A.1 Introduction…..…..……...68

2A.2 Aim and Rationale of the Present Work.……..…69

2A.3 Results and Discussion ….……....69

2A.3.1 High Diastereoselective Synthesis of β-Nitromethyl γ-Amino Acids from Naturally Occurring α, β-Unsaturated γ-Amino Acids…….…….....69

2A.3.2 Synthesis of Nitro-Peptides……75

2A.3.3 Synthesis and Conformational Analysis of $\gamma^{3,4}$-Homooligomers……..76

2A.3.4 Synthesis and Conformational Analysis of α, $\gamma^{3,4}$-Hybrid peptides……...85

2A.4 Chemistry on Nitro Peptides…..…….....90

2A.5 $\beta^{2,3}$-Amino Acids and Peptides……....91

SECTION 2B: Synthesis and Stereochemical Analysis of thiostatines (β-sulfhydryl γ-amino acids)

2B.1 Introduction……...……....94

2B.2 Results and Discussion……..94

2B.2.1 Synthesis of β-Sulfhydryl γ-Amino Acids…….....94

2B.2.2 Synthesis and Conformational Analysis of β-Sulfhydryl γ-Amino Acid in Hybrid Helix……...95

2.2 Conclusions…….....98

2.3 Experimental Section…….....99

2.3.1 General Experimental details……99

2.3.2 Synthesis procedure and characterization of compounds in Section 2A……99

2.3.3 Synthesis procedure and characterization of compounds in Section 2B……119

2.4 References……..123

2.5 Appendix: Characterization of synthesized compounds……127

Chapter 3: Peptide Foldamers with Heterogeneous Backbone: Utilization of *Z*-Vinylogous Amino Acids in the Design of α, γ-Hybrid Helices

3.1 Introduction……....137

3.2 Aim and Rationale of the Present Work……139

3.3 Results and Discussion……..139

3.3.1 Synthesis of (Z)-α, β-Unsaturated γ-Amino acids……..139

3.3.2 Incorporation of (Z)-α, β-Unsaturated γ-Amino acids in Known α, γ-Hybrid Helix: Synthesis and Conformational Analysis of Peptide P1 …….….141

3.3.3 Design, Synthesis and Conformational Analysis of Peptides P2-P5…….143

3.4 Comparison of α,γ-Hybrid Helices containing (*E*)-α, β-Unsaturated γ-Amino acids and (*Z*)-α, β-Unsaturated γ-Amino acids……..155

3.5 Conclusions…….……..157

3.6 Experimental Section…….……....157

3.7 References…….……167

3.8 Appendix I: Characterization of synthesized Compounds and Peptides……...170

Chapter 4: Unprecedented Rearrangement in (*E*)-Vinylogous Amides through α, β→β, γ Double Bond Migration

4.1 Introduction …….180

4.2 Aim and Rationale of the Present Work……..……..180

4.3 Results and Discussion……...……...180

4.3.1 Synthesis of Boc-Pro-dγPhe-Pro-dγPhe-Pro-dγPhe-OEt Hexapeptide……..……180

4.3.2 Unusual α, β → β, γ Double Bond Migration in Hybrid Peptide……182

4.4 Unprecedented Rearrangement in α, β-Unsaturated γ-Amino Amides……186

4.5 Future Perspective …….....191

4.6 Conclusions…….....191

4.7 Experimental Section ……192

4.8 References …….208

4.9 Appendix I: Characterization Data of Synthesized Compounds and Peptides……..210

Abbreviations

Ac_2O = Acetic anhydride

ACN = Acetonitrile

AcOH = Acetic acid

Aib = α-Amino isobutyric acid

aq. = Aqueous

Bn = Benzyl

Boc = tert-Butoxycarbonyl

$(Boc)_2O$ = Boc anhydride

^tBu = tertiary Butyl

Calcd. = Calculated

Cbz = Bezyloxycarbonyl

Cbz-Cl = Benzyl chloroformate

CCDC no. = Cambridge Crystallographic Data Centre number

CD = Circular Dichroism

COSY = **CO**rrelation **S**pectroscop**Y**

CIF = Crystallographic Information File

dγ = dehydro gamma

dr = Diastereomeric ratio

DBU = 1,8-Diazabicyclo[5.4.0]undec-7-ene

DCC = N, N' –Dicyclohexylcarbodiimide

DCM = Dichloromethane

DiPEA = Diisopropylethyl Amine

DMAP = 4-Dimethylaminopyridine

DMF = Dimethylformamide

DMSO = Dimethylsulfoxide

EtOH = Ethanol

Et = Ethyl

EtOAc = Ethyl acetate

Fmoc = 9-Fluorenylmethoxycarbonyl

Fmoc-OSu = N-(9-Fluorenylmethoxycarbonyloxy) succinimide

g = gram

h = hours

HBTU = 2-(1H-benzotriazol-1-yl)-1, 1, 3, 3-tetramethyluronium hexafluorophosphate

H-bond = Hydrogen bond

HOBt = Hydroxybenzotriazole

HCl = Hydrochloric acid

IR = Infrared spectroscopy

IBX = 2-Idoxybenzoic acid

LAH = Lithium Aluminium Hydride

M = Molar

MALDI-TOF/TOF = Matrix-Assisted Laser Desorption/Ionization-Time of Flight

MBHA = Methyl bezydrylamine

Me = Methyl

MeOH = Methanol

mg = Milligram

min = Minutes

µL = Micro liter

mL = Milliliter

mM = Millimolar

mmol = millimoles

m.p = Melting Point

MS = Mass Spectroscopy

N = Normal

NHS = N-hydroxy succinimide

NMP = N-methyl pyrrolidone

NMR = Nuclear Magnetic Resonance

NOE = Nuclear Overhauser Effect

ORTEP = Oak Ridge Thermal-Ellipsoid Plot Program

PG = Protecting Group

ppm = Parts per million

Py = Pyridine

R_f = Retention factor

R_t = Retention time

ROESY = **R**otating-frame nuclear **O**verhauser **E**ffect correlation **S**pectroscop**Y**

RP- HPLC = Reversed Phase-High Performance Liquid Chromatography

RT = Room Temperature

TFA = Trifluoroacetic acid

THF = Tetrahydrofuran

UV = Ultraviolet–Visible Spectroscopy

TOCSY = **TO**tal **C**orrelation **S**pectroscop**Y**

*Z*dγ = Z-dehydro gamma

Abstract

The relationship between a well-defined structure and function of proteins inspire the creation of foldamers from non-natural building blocks. Among them, the most widely studied foldamers are constructed from β- and γ-amino acid subunits. The remarkable protein secondary structure mimetics displayed by these β- and γ-peptide oligomers have been exploited in designing inhibitors for various protein-protein interactions, antimicrobials and biomaterials. Previously, we have showed the utilization of naturally occurring *E*-vinylogous amino acids in the design of β-hairpins and β-sheet mimetics. In the present study, we investigated the utility of these conformationally constrained yet highly reactive α, β-unsaturated γ-amino acids to engineer the folding in polypeptides and as Michael acceptors to derive a variety of 3,4-disubstituted γ-amino acids. We showed that by selective insertion of *E*-vinylogous amino acids in the α-peptide sequence, it is possible to design novel miniature β-meander as well as helix-turn-helix type of motifs even in small peptide sequences. Further, utilizing *E*-vinylogous residues as Michael acceptors, we derived highly functionalizable β-nitromethyl γ-amino acids as well as thiostatines (β-sulfhydryl γ-amino acids). Besides their utility as templates in the design of 14- and 12-helical foldamers, we showed the multifaceted nature of alkyl nitro group on peptides by transforming it into various functional groups including amines, carboxylic acids, oximes, and 1, 3-dipolar addition products. Further, as *E*-vinylogous amino acids preferred to adopt extended β-sheets type structures, we investigated whether *Z*-vinylogous amino acids can be used to design helical peptide foldamers with conjugated double bond in the helix backbone. Finally, in the course of our investigation on structural and chemical characterization of unsaturated γ-amino acids and peptides, we encountered a base mediated novel rearrangement transforming the vinylogous amides into γ-lactams through double bond migration. Overall, these basic results on vinylogous amino acids open wide opportunities to further explore them as building blocks for the foldamers design as well as templates to perform various organic reactions.

Publications

1. γ- and β-Peptide Foldamers from Common Multifaceted Building Blocks: Synthesis and Structural Characterization. **Ganesh Kumar, M.;** Gopi, H. N., *Org. Lett*., **2015,** *17*, 4738.

2. Design of Stable β-Hairpin Mimetics through Backbone Disulfide Bonds. **Ganesh Kumar, M.;** Mali, S. M.; Raja, K. M. P.; Gopi, H. N. *Org. Lett*., **2015**, *17*, 230.

3. Engineering Polypeptide Folding through *trans* Double Bonds: Transformation of Miniature β-meanders to Hybrid Helices. **Ganesh Kumar, M.;** Benke, S. N.; Raja, K. M. P.; Gopi, H. N. *Chem. Comm*., **2015**, *51*, 13397.

4. Synthesis of Tetrasubstituted Symmetrical Pyrazines from β-Keto γ-Amino Esters: A Mild Strategy for Self-Dimerization of Peptides. **Ganesh Kumar, M.;** Thombare, V. J.; Bhaisare, R. D.; Adak, A.; Gopi, H. N. *Eur. J. Org. Chem.*, **2015**, 135.

5. HBTU Mediated 1-Hydroxybenzotriazole (HOBt) Conjugate Addition: Synthesis and Stereochemical Analysis of β-Benzotriazole N-Oxide Substituted γ-Amino Acids and Hybrid Peptides. Mali, S. M.; **Ganesh Kumar, M.;** Katariya, M. M.; Gopi, H. N. *Org. Biomol. Chem.*, **2014**, *12*, 8462.

6. Exploring β-Hydroxy γ-Amino Acids (Statines) in the Design of Hybrid Peptide Foldamers. Bandyopadhyay, A.; Malik, A.; **Ganesh Kumar, M.;** Gopi, H. N. *Org. Lett*., **2014**, *16*, 294-297.

7. Synthesis and Stereochemical Analysis of β-Nitromethane Substituted γ-Amino Acids and Peptides. **Ganesh Kumar, M.;** Mali, S. M.; Gopi, H. N. *Org. Biomol. Chem.*, **2013**, *11*, 803.

8. Synthesis of α, β-unsaturated γ-Amino Esters with Unprecedented High (*E*)-Stereo selectivity and their Conformational Analysis in Peptides. Mali, S. M.; Bandyopadhyay, A.; Jadhav**,** S. V.; **Ganesh Kumar, M.;** Gopi, H. N. *Org. Biomol. Chem.*, **2011**, *9*, 6566.

Chapter 1

Engineering Polypeptide Folding Through *trans* Double Bonds

1.1 Introduction

Proteins play a crucial role in all biological events of life. Three dimensional structures of proteins are very important for their functions. Inspection of protein three dimensional structures suggests their complex tertiary folds and quaternary associations. The disintegration of protein tertiary structure, hypothetically, leads to a limited number of secondary structural elements such as β-sheets, helices, and turns, which are assembled using loosely structured loops (Figure 1.1).[1] These protein secondary structures are locally defined, meaning that there can be many different secondary motifs present in one single protein molecule. These protein secondary structures are further connected by loosely structured loops leads to the supersecondary structures such as β-hairpins (β-β motifs), helix-turn-helix, coiled-coils, β-meanders, β-α-β motifs, Greek key motifs etc. Understanding the folding processes of proteins is of paramount importance in the *de novo* design of protein structures.

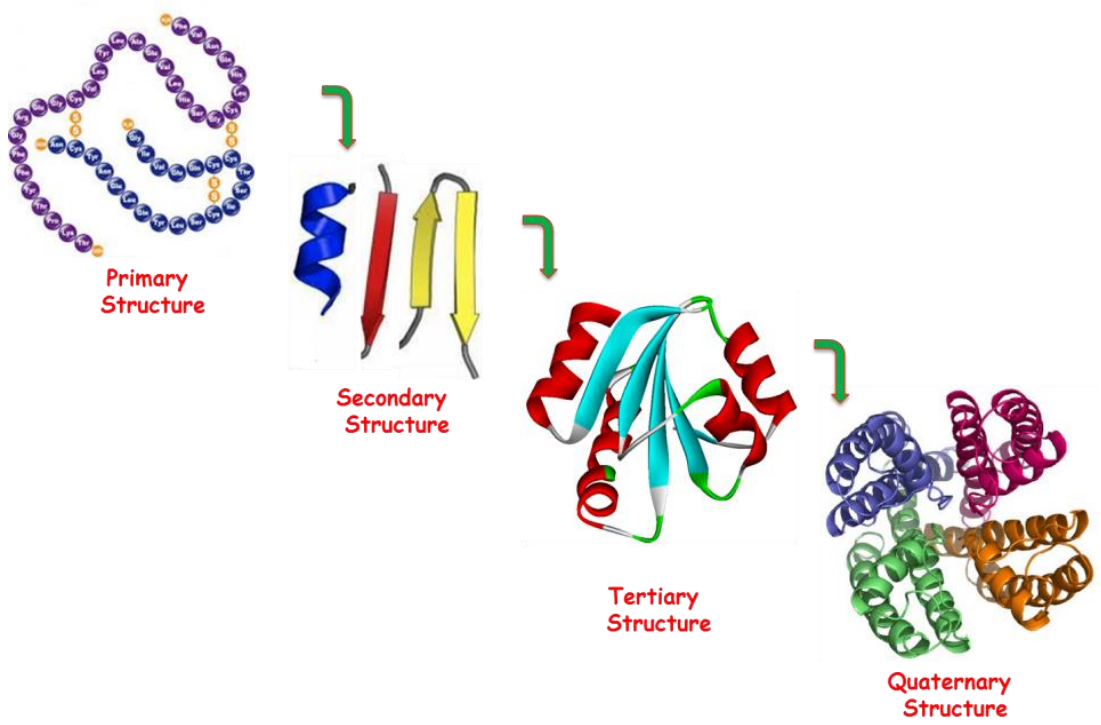

Fig 1.1: Structural description of proteins (PDB codes: 1AIU and 1BL8).

Protein structures are mainly described at four levels as shown in Fig. 1.1., where primary structure of protein represents the number and sequence of amino acids arranged in a poly

peptide chain. Secondary structure describes the local organization of peptide backbone in a specific three dimensional conformation. Tertiary structure explains the overall structure of single polypeptide chain resulting from interactions of amino acid side chains and secondary structural elements. Whereas quaternary structure defines the spatial arrangement of two or more polypeptide chains in a specific oligomer complex which is accompanied by a variety of non-covalent interactions and disulfide cross linkages.

1.1.1 Protein Secondary Structures

Protein secondary structures are classified mainly into helices, β-sheets and reverse turns. In their seminal work, Linus Pauling and colleagues first described the α-helix and β-sheet structures. These secondary structures are characterized by the definite pattern of hydrogen bonding between the main chain NH and CO groups. Protein structures are built up by the combination of secondary structures which are connected by loops of various lengths. The loop regions which connects two adjacent anti-parallel β-strands are called reverse turns. In their pioneering work, G. N. Ramachandran and colleagues[2] delineated the stereochemically allowed conformations of polypeptide secondary structures using two degrees of torsional freedom ϕ and ψ (Figure 1.2C). Brief descriptions regarding secondary structures are given below.

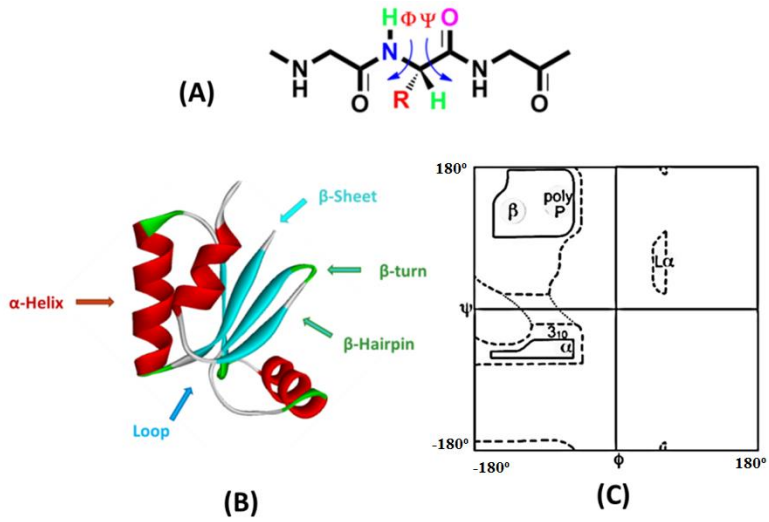

Fig 1.2: (A) Depiction of torsional angles ϕ and ψ on peptide backbone, (B) Secondary structural elements shown in a protein ribbon model (PDB code: 1H75) and (C) Ramachandran plot depicting the torsional angles of different secondary structures.

Helices: Based on the H-bonding pattern and number of residues per turn, helices are classified into 2.2_7 (γ-helix), 3_{10}, 3.6_{13}(α-helix) and 4.4_{16} (π)-helices. α-Helix is the most abundant secondary structure present in proteins and predominant motif over the other types of helices. The structure of α-helix was proposed in 1951 by Linus Pauling.[3] α- Helix is right-handed screw (Right-handedness and Left-handedness are represented by P and M, respectively) like structure which constitutes 3.6 residues per turn and 13-atoms in the H-bond pseudo cycle. General nomenclature of the α-helix is represented by 3.6_{13}-P-helix with average ϕ and ψ values -60° and -45°, respectively. Unlike α-helix, 3_{10}-helix is rarely present in proteins. The average ϕ and ψ values of 3_{10}-P-helix is -49° and -26°, respectively. The nomenclature 3_{10}-helix describes the three residues per turn and 10-atoms in H-bond pseudo cycle. Similarly, π-helix is denoted by 4.4_{16}-P-helix (ϕ = -55°, ψ = -70°) and γ-helix as 2.2_7 helix (ϕ = -70°, ψ = 70°).

β-Sheets: β-Pleated sheets are the second major structural elements found in proteins. β-Sheets are usually 5 to 10 residues long with extended conformation. The ϕ and ψ values are found to be within the broad structurally allowed region in the upper left quadrant of Ramachandran Map. In 1930, William Astbury proposed the first β-sheet structure. However, the refined version of β-sheet structure was proposed by Linus Pauling and Robert Corey in 1951.[4] Based on the directionality of β-strands arranged in β-pleated sheets, they are classified into (i) parallel β-sheets, in which the chains are aligned in parallel manner and (ii) anti-parallel β-sheets, in which the chains are connected by H-bonds in anti-parallel manner (Fig 1.3). β-sheets usually exhibit a right-handed twist (ϕ = -135°, ψ = 135°) rather than a perfect extended character (ϕ = -180°, ψ = 180°), which is favored by intrastrand non-bonded interactions and interstrand geometric

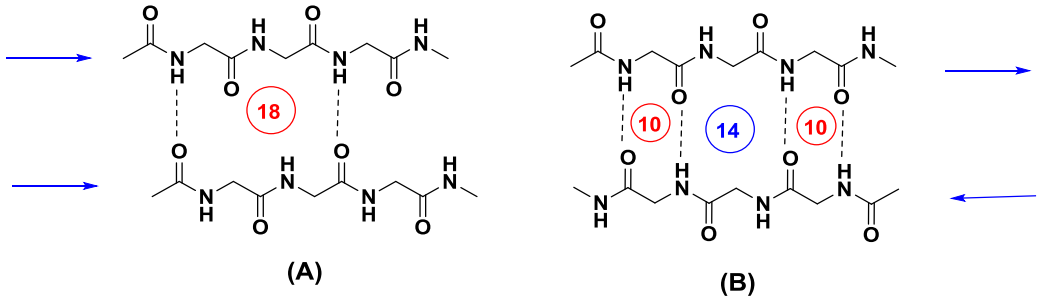

Fig 1.3: Hydrogen bonding and directionality of β-sheets shown in parallel β-sheets **(A)** and anti-parallel β-sheets **(B)**.

constraints. At the tertiary structure level, layers of β-sheets are generally oriented to each other at a small angle (-30°) in aligned β-sheet packing or close to 90° in orthogonal β-sheet packing.

Reverse Turns: Reverse turns are also considered as secondary structures of proteins. Reverse turns are classified based on the number of residues involved in inducing the reverse directionality of the polypeptide chain. They are classified as δ-turn (2 amino acids), γ-turn (3 amino acids), β-turn (4 amino acids), α-turn (5 amino acids) and π-turn (6 amino acids). Based on the dihedral angles ϕ and ψ of *i+1* and *i+2* residues, the predominantly occurring β-turns are further classified into type I, II and III as well as their mirror images type I', II' and III' turns respectively.[5]

1.1.2 Protein Supersecondary Structures

Supersecondary structural motifs have been found frequently in many protein structures. Supersecondary structures are nothing but the combination of few secondary structures with a specific geometrical arrangement. These motifs have been associated with the many functions of proteins such as DNA binding, receptor recognition etc. The supersecondary structures are classified based on the involvement of secondary structures such as ββ (β-hairpin), helix-turn-helix, coiled-coils, sheet-helix-sheet (β-α-β), β-meander, helix-loop-helix, Greek Key motif etc. (Fig 1.4). A brief description of these supersecondary structures is given below.

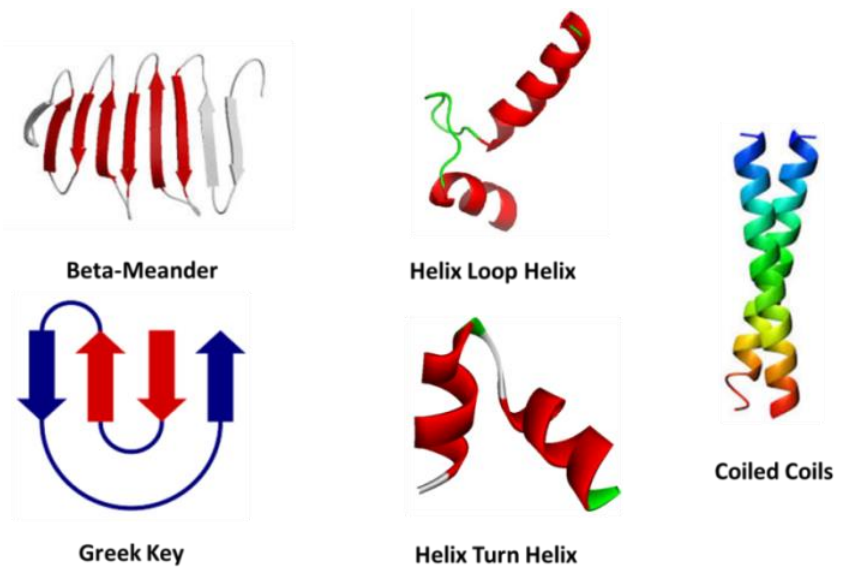

Fig 1.4: Model diagrams of diverse supersecondary structures of proteins.

β-Hairpins (ββ): β-Hairpins are the simplest protein supersecondary structures. The β-hairpin motif consists of two anti-parallel β-strands and a reverse turn. The β-hairpin structure is generally stabilized by intramolecular H-bonds existed between the two antiparallel β-strands and van der Waals interactions between the side chains. Based on the number of residues involved in the reverse turn, β-hairpins are classified as one residue β-hairpin to four residue β-hairpin.

β-Meander: The β-meander is a common protein supersecondary structural motif consists of two or more anti-parallel *β*-strands and each adjacent strands are connected by *β*-hairpin loops.[7] The β-meander structural motif is frequently observed in many proteins including proteases and enzymes.[8] In addition, β-barrel and β-propeller structural motifs are also constituted from β-meander topology.[9]

Greek key (β_4): Greek key motif is formed by four adjacent β-sheets connected by loops. In details, first three strands are connected by hairpin loops and fourth strand connected to first strand with longer loop (Fig 1.4).

Helix-turn-helix motif: This motif can also be represented as *αα* motif. In this type of motifs, two helices are joined by a loop. These helix-turn-helix architectures are found frequently in DNA binding as well as in calcium binding proteins (EF motifs) (Fig 1.4).

Sheet-helix-sheet motif: This is represented by β-α-β as it is comprised of β-strand, α-helix and β-strand connected by two loops. Two parallel β-sheets are connected via α-helix and form a common hydrophobic core. These motifs are frequently found in many proteins mostly in ion channels.

Coiled coil motif: Coiled coil motifs are widely present in protein structures.[10] In this motif, two alpha helices are wound with each other either in parallel or in anti-parallel way to form coiled coil super helix. The conformations of coiled-coils are prescribed primarily by a seven-residue ('heptad') sequence repeat, denoted as *a-b-c-d-e-f-g*. Positions *a* and *d* are predominantly occupied by the hydrophobic residues.[11] In addition to the hydrophobic interactions between '*a*' and '*d*', coiled coils are also stabilised by the polar/ionic interactions between side-chains of amino acids at '*e*' and '*g*' positions. Coiled coil α-helices occur in many fibrous proteins like α-keratin, tropomyosin etc.[12] Left handed coiled coils are predominant in nature.

1.1.3 Mimicking protein structures

Our understanding of protein structure and function has advanced rapidly in recent years, providing a mechanistic insight into a wide variety of biological processes. *De novo* design of existing or novel protein folds demands a thorough understanding of the rules that underlie protein structure and stability. Considerable attention has been paid over the past several decades on polypeptides composed of α-amino acids, the use of stereochemically constrained amino acids and templates in the design of folded polypeptides.[13] The *de novo* design of protein secondary structural elements is not only useful in our understanding of structure, function and folding of proteins, but also provides widespread opportunity in structure based drug design.

Polymers that show both secondary and tertiary structures are not limited to natural proteins. RNA also adopts characteristic secondary and tertiary structures. In RNA, as in proteins, specific folding underlies diverse informational and catalytic functions, even though proteins and RNA have very different backbones. Thus, it underlines that it should be possible for the chemist to design functional polymers with biological, catalytic, and organizational properties that are not precedent in nature.

In this context, a variety of unnatural amino acids and organic templates have been explored as building blocks in the design of protein secondary structures. Among the various unnatural amino acids and organic templates, the most widely studied foldamers are constructed from β- and γ-amino acid subunits.

1.1.3.1 β-peptide Foldamers

The β-amino acids are homologated species of α-amino acids. Depending on the position of the side chain, they are classified as β^3- and β^2-amino acids (Figure 1.5). Double homologation of α-amino acids leads to γ^2-, γ^3-, and γ^4-amino acids. In contrast to α-peptides, *β*-peptides and higher homologue oligomers have proved to be proteolytically and metabolically stable .[14] These properties make *β*-peptides and higher homologue oligomers very attractive from a biomedical perspective. In the past two decades, β-peptides composed of β-amino acids emerged as very promising tools in the construction of protein secondary structures. In their pioneering work, Gellman and Seebach introduced cyclic β-amino acids and chiral acyclic β-

amino acids, respectively and investigated the conformational properties of polypeptides generated from these amino acids.[15] In addition, Sharma and colleagues extensively investigated β-peptide oligomers generated from carbo-β-amino acids.[16] Reiser et al. showed the utilization of the cyclic β-amino acids in the design of β-peptides.[17] Further, Aitken and colleagues[18] and Fulop *et al*.[19] showed the utilization of various cyclic β-amino acids in the design of β-peptide foldamers. Different types of acyclic and cyclic β-amino acids utilized in the protein structure mimetics are shown in the Fig 1.5. The structures adopted by peptides assembled from β-amino acid units are again classified as helices, sheets and turns. β-Peptide and higher homologue peptides produced a variety of helical secondary structures which are not seen in the alpha-peptides. The helices produced by the β-peptides are recognized as C_{14}-, C_{12}-, C_{10}- and C_8-helices.[20-22] The helices from β-peptides have different polarities with respect to their C and N-termini. The C_8- and C_{12}-helices have a hydrogen bond direction (C ←N), which is the same as that observed in α-peptides, whereas in the C_{10}- and C_{14}- structures the hydrogen bond directions (N ←C) are reversed. The structural diversity of the helices increases upon progressing from α- to β- to γ-peptides. The structural diversity of γ-amino acids and γ-peptides, however, has not been elucidated nearly as well as that of β-peptides.

In their initial attempt, Balaram and colleagues demonstrated the hybrid peptide structures composed of β-amino acids and higher homologous amino acids into host α-peptide helices and β-hairpin structures.[23a,b] The concept of hybrid peptides was further explored by Gellman and others.[23c-f] The hybrid peptides with heterogeneous backbone (peptides with α and other β- and γ-amino acids) displayed a variety of hydrogen bonded helical structures compared to that of homooligomers of β- and γ-amino acids. The advantage of hybrid helices is that it is possible to design a variety of helices by simply varying the amino acid sequence patterns.

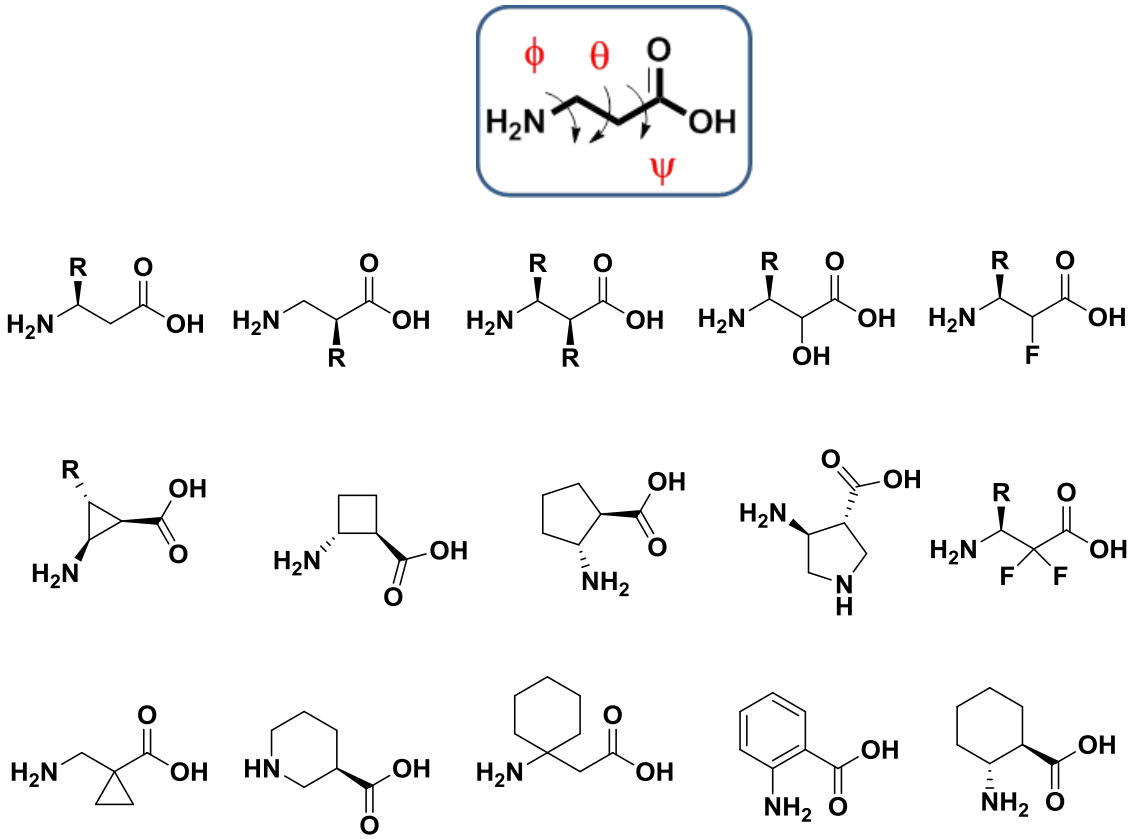

Fig 1.5: The list of β-amino acids used in the design of foldamers. The torsional variables for β-amino acid were depicted.

Gellman and colleagues showed that short α, β-hybrid peptides contained backbone constrained *trans*-ACPC amino acids (*trans*-2-aminocyclopentane carboxylic acid and its derivatives) are able to adopt both C_{11}-helix and$C_{14/15}$-helix.[24a, 24b] Recently, Amblard *et al*. showed the conformational conversion between $C_{9/11}$-helix and $C_{18/16}$-helix using tri-substituted β-amino acid [(S)-ABOC] in α, β-hybrids.[24c] Further, Gellman *et al*. demonstrated $C_{11/11/12}$-helix and $C_{10/11/11}$-helix formation in 1:2 and 2:1 α, β-hybrids.[24d] Fulop and colleagues evaluated the stereochemical patterns in the folding of α, β-hybrid peptides.[24e] Similar results are also observed from Sharma and colleagues.[24f-24i] Moreover, Gellman and colleagues reported spectacular helix bundle quaternary structures in oligomers composed of α-β_2-α-β_2 and α_3-β-α_2-β sequence patterns.[24j,24k]

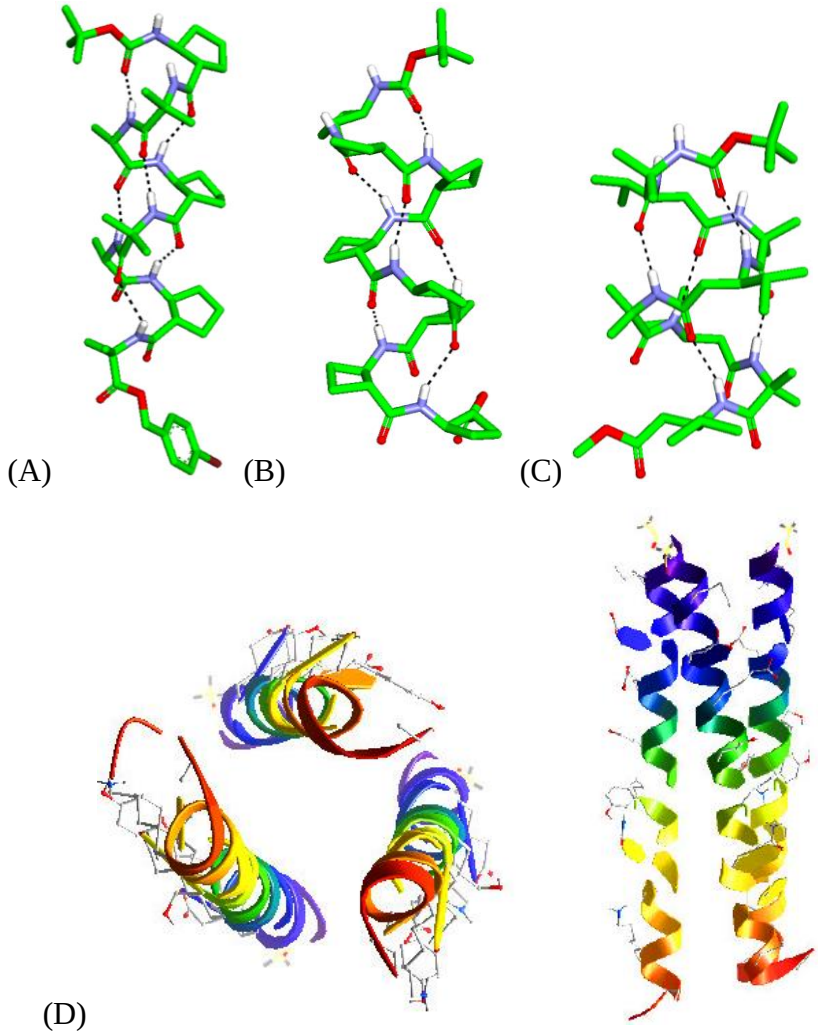

Fig 1.6: (A) *trans*-ACPC α, β-hybrid C_{11}-helix, (B) *trans*-ACPC C_{12}-helix, (C) C_{14}-helix of α,β^3-hybrid peptide. (D) Three helix bundle from the crystal structure of α/β-hybrid peptide (PDB-2OXJ). Crystallographic information is taken from *ref*. 22 and *ref*. 24.

Biologically active β- and hybrid β-peptides:

In addition to the design and understanding the conformations of homo and hetero oligomers of β- and γ- amino acids, the structural properties of these foldamers have also been exploited in the design of antimicrobials,[25] antiproliferative agents,[26] somatostatin analogues,[27] p53-hDM2 inhibitors,[28] HIV inhibitors,[29] Human cytomegalovirus entry inhibitors[30] etc. Nylon-3 polymers made up of β-amino acids showed potent activity and selectivity against planktonic forms of multiple fungal species.[31a] In addition, these peptides also have showed good inhibitory profiles against biofilm formation of drug-resistant *candida albicans*.[31b]

Ordered supramolecular assemblies of β-peptide helices:

Extensive investigations from the Fulop and colleagues[32] and others[33,34] showed the ordered supramolecular assemblies from the β-peptide helices. The β-peptide helices displayed a well-defined 3D molecular architectures such as nanostructured fibrils,[32a] vesicles,[32b] hexagons, molar tooth shape[33] and rod-shaped assemblies.[35] In addition, the cyclic α, β-hybrid peptides self-assembled into excellent nanotubes and these nanotubes have been utilized in many biomedical applications.[36]

1.1.3.2 γ-peptide Foldamers

γ-Amino acids are double homologated α-amino acids having two $–CH_2$- groups between C^{α} carbon and C=O carbon. These two methylene groups introduced two additional torsional variables θ_1 and θ_2 along with regular ϕ and ψ. Unlike β-amino acids, γ-amino acids have not been much explored probably due to the difficulties in the synthesis and isolation of stereo-chemically pure γ-amino acids. However, in their preliminary investigations Seebach and colleagues[37] and Hanessian *et al*.[38] recognized the 14-helical conformations of the oligomers of γ^4-amino acids as well as 2, 3, 4 substituted γ-amino acids. In addition, Hofmann and colleagues predicted a wide range of helical organizations from the oligomers of unsubstituted γ-amino acids and hybrid peptides composed of 1:1 alternating α- and γ- amino acids using *ab initio* theoretical calculations.[39] In their pioneering work, Balaram and colleagues reported a variety of helical conformations from the homo and heterooligomers of gabapentin (3, 3-dialkyl-γ-amino acid) as well as γ^4-amino acids. In contrast to the γ-peptides with backbone homologated γ-amino acids,[40] the homooligomers of gabapentin displayed C_9 and C_7 helical conformations. Further, the α,γ-hybrid peptides composed of gabapentin displayed C_{12} and combinations of C_{12} and C_{10} H-bonding patterns.[41] In continuation, Sharma and colleagues reported the left-handed helical conformations of γ-peptides composed of carbo-γ-amino acids (γ-Caas) along with γ-aminobutyric acid (GABA), helix-turn-helix motifs etc., in solution .[42] Recently, Gellman and colleagues reported a verity of helical conformations from both single crystals and in solution.[43] Further, Smith and colleagues showed extended sheet structures with bifurcated H-bonds from the $\gamma^{2,3}$-cyclopropane amino acids.[44] In addition to the cyclic and acyclic γ-amino acids, many different types of γ-amino acids containing backbone heteroatoms such as O (Oxygen) and N

(Nitrogen) have also been reported. Yang and colleagues demonstrated the conformational properties of oligomers constructed from both α-aminoxy peptides and β-aminoxy peptides.[45] They observed C_8 helical conformations in α-aminoxy peptides and C_9 helices and turns in the case of β-aminoxy peptides. Further, Le Grel *et al*. showed the synthesis and conformational properties of γ-peptides composed of aza-amino acids.[46] Similar to that of aminoxy peptides, the structures of azapeptides are also stabilized by short range turn like H-bonds. Further, Guichard and colleagues derived new γ-amino acids, where the α-carbon has been replaced with NH group and constructed a variety of urea-oligomer peptidomimetics.[47] The structural investigation of the urea peptides revealed that they adopted 14-helical conformations. In addition, conformational properties of γ-amino acids with thiazole backbone has also been reported.[48] The structures of γ-amino acids utilized in the design of foldamers are shown in Figure 1.5. The helical structures obtained from various γ-amino acids are shown in Figure 1.10.

In contrast to various unnatural γ-amino acids described above, a variety of non-ribosomal γ-amino acids such as α, β-unsaturated γ-amino acids, β-hydroxy γ-amino acids, β-keto-γ-amino acids have been found in many biologically active peptide natural products. However, little is known regarding the conformational properties of these amino acids. In this chapter, we explored the geometrically constrained *trans* α, β unsaturated γ-amino acids in the design of novel peptide foldamers.

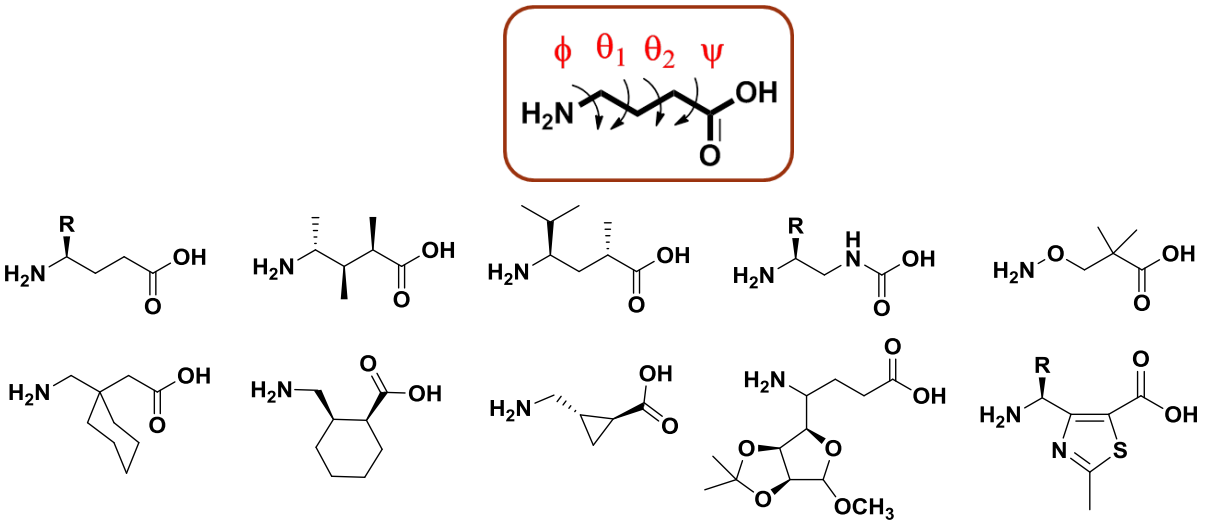

Fig 1.7: The list of γ-amino acids used in the design of foldamers. The torsional variables for γ-amino acid were depicted.

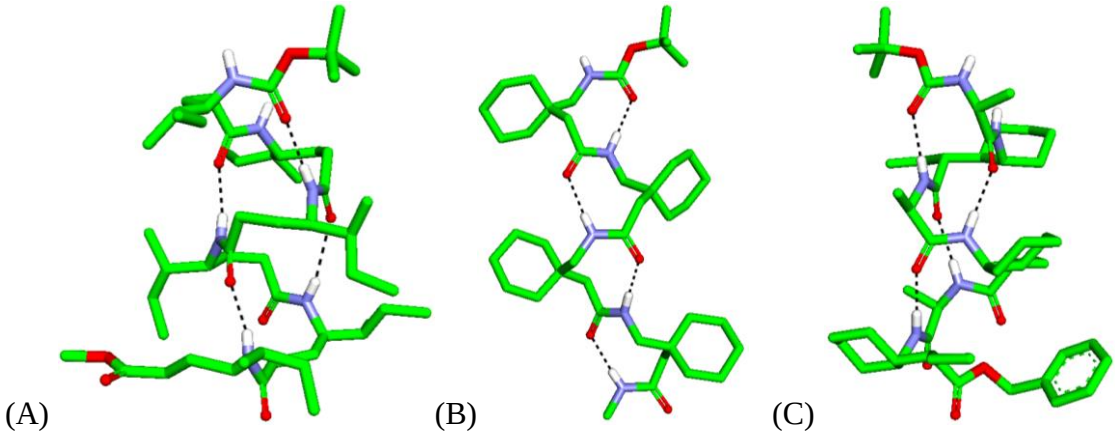

Fig 1.8: (A) C_{14}-helix of γ^4 –peptide, (B) C_9-helix of gabapentin oligomer and (C) C_{14}-helix of $\gamma^{2,3,4}$ -oligomer peptide. Crystallographic information is taken from *ref*. 40 and 43.

1.2 (*E*)-vinylogous γ-amino acids in the design of foldamers

1.2.1 Natural occurrence and Biological importance of vinylogous amino acids

(*E*)-α, β-unsaturated γ-amino acids (*E*-vinylogous amino acids) are non-ribosomal amino acids often found in many natural products like Cyclotheonamide (A, B, C, D, E), Gallinamide A, Miraziridine A and Luminmycin (A, B, C) (Fig 1.9**)**. Further, Schreiber and colleagues reported the detailed mechanistic study of Cyclotheonamides binding to serine protease and bovine β-trypsin and act as strong inhibitors.[49] Gallinamide A also shown a potent anti-malarial activity.[50] Miraziridine A is a natural cyclic peptide that inhibits variety of proteases like trypsine-like protease, papain-like cysteine protease and pepsin-like aspartyl protease.[51] These excellent biological activity and natural occurrence of vinylogous amino acid residues motivated many synthetic chemists to design peptide inhibitors against serine and cysteine proteases (Fig 1.10).[52]

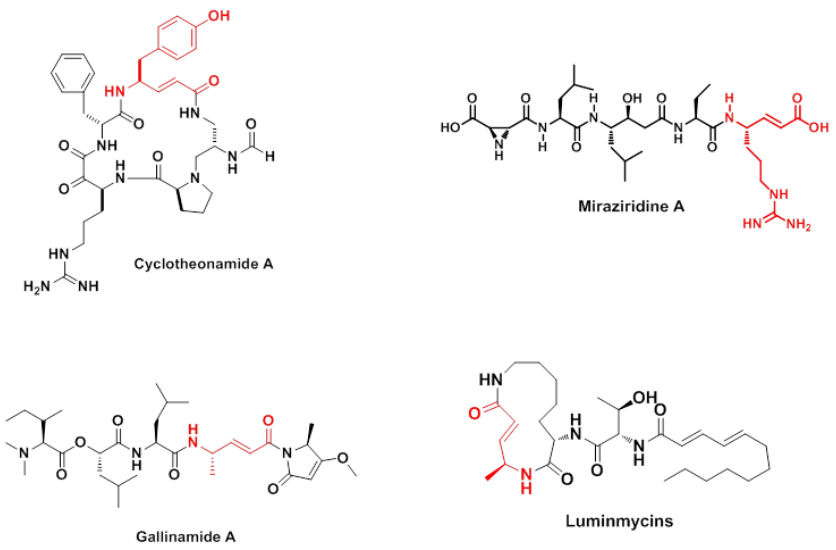

Fig 1.9: Chemical structures of naturally occurring α, β-unsaturated γ-amino acid contained cyclic and linear peptides.

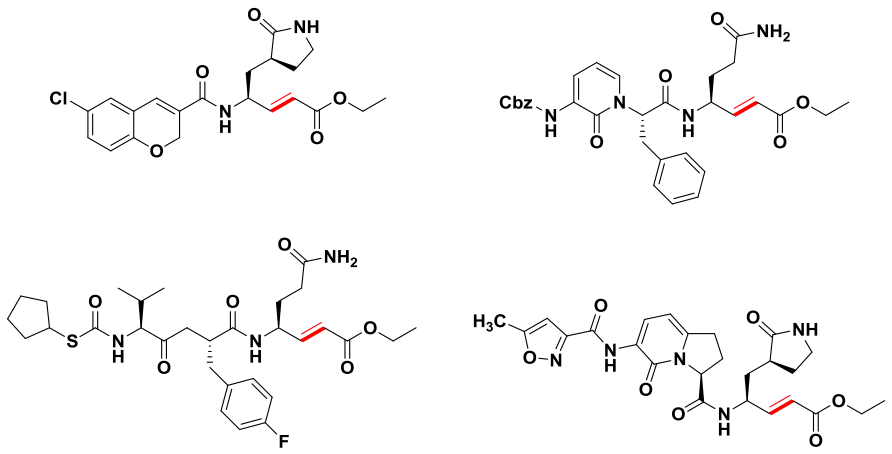

Fig 1.10: Synthetic peptides contained α, β-unsaturated γ-amino acids used for various protease inhibitors.[52]

1.2.2 Previous Work

Besides their potential protease inhibition property, *E*-vinylogous amino acids have also served as starting material for many organic reactions like Diels-Alder reaction, epoxidation and Michael addition reactions to generate a variety of γ-amino acids. These biological and chemical properties of (*E*)-vinylogous residues motivated many chemists to study their conformational behavior in monomers as well as peptides. In their preliminary investigation, Schreiber and

colleagues showed the β-sheet formation of dipeptide and unusual helical structure from the hybrid tetrapeptide.[53] Chakraborty *et. al.* showed the utilization of *E*- vinylogous amino acids to induce reverse turn in β-hairpins.[54] In continuation, Hoffmann and colleagues[55] reported a variety of helical organizations with larger H-bond pseudo cycles from the homooligomers of (*E)*-and (*Z*)-vinylogous amino acids through **s**ystematic theoretical calculations using *ab initio* MO theory (Figure 1.11A). It is also been proposed that it is possible to construct single walled nanotubes from the *E*-vinylogous amino acid homooligomers.[56] Recently, our group studied the single crystal conformations of stable β-hairpin by incorporating (*E*)-vinylogous amino acids at the facing positions of the anti-parallel β-strands. In continuation, our group also studied the unusual planar structures in 1:1 α,dγX-hybrid peptides(Fig 1.11)[57] and the direct transformation of this unusual planar structure into α,γ-hybrid peptide 12-helix through single step catalytic hydrogenation.

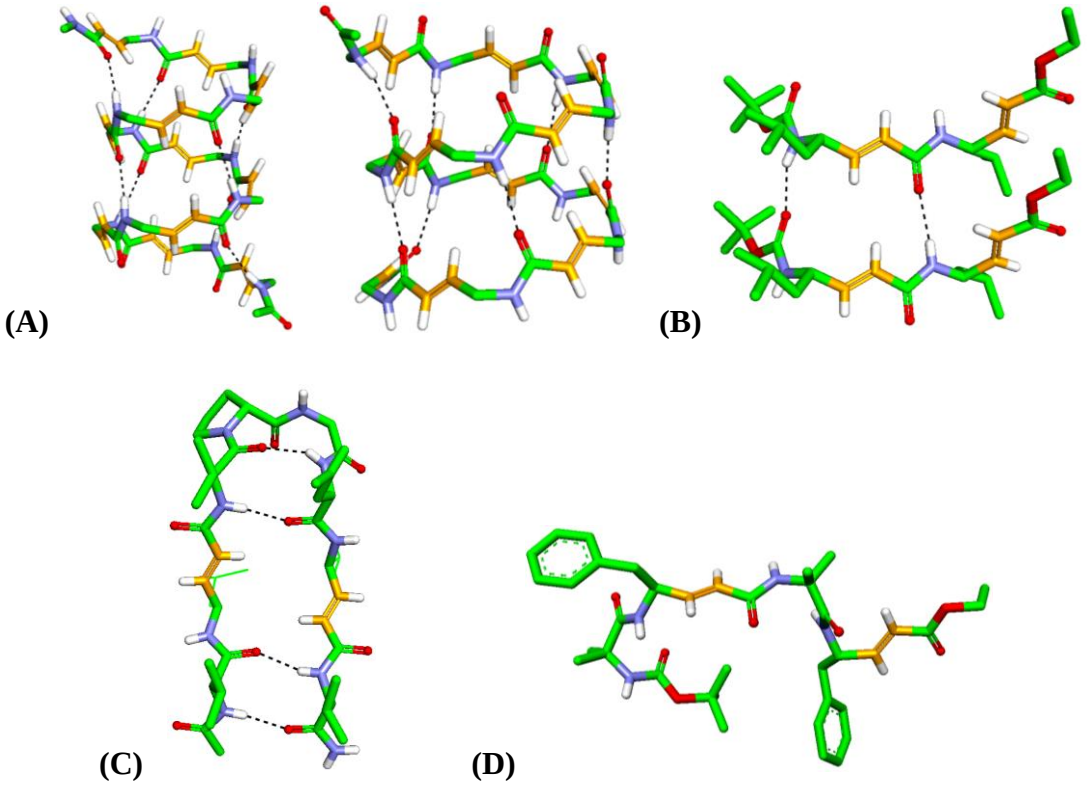

Fig 1.11: Structure of Foldamers contained (*E*)-α, β-unsaturated γ-amino acids. (**A**) Theoretical models of C_{22}- and C_{27}-helical structures (Data is taken from *ref.* 54), Crystal structures: Boc-dγLeu-dγVal-OEt (**B**), Ac-Val-dγLeu-Val-^{D}Pro-Gly-Leu-dγVal-Val-NH_2 (**C**) and Boc-Aib-dγPhe-Aib-dγPhe-OEt (D). Crystallographic data is taken from *ref.* 56 and *ref.* 57.

1.3 Aim and rationale of the present work

(*E*)-α, β-unsaturated γ-amino acids have been utilized in the design of β-sheets, β-hairpins and turns. In addition, 1:1 alternating α-and *E*-vinylogous amino acids showed the unusual planar conformation. We anticipated that the exceptional conformational properties of (*E*)-vinylogous amino acids can be exploited to design highly organized protein supersecondary structural mimetics (β-meander, Greek key and helix-turn-helix etc.) beyond the conventional secondary structures (helix, β-sheets and turns). Based on the previous results described above, we hypothesized that β-sheet promoting and turn inducing properties of (*E*)-vinylogous amino acids can be readily exploited in the design of miniature β-meander and miniature Helix-Turn-Helix mimetics (for protein structures see section 1.1.2).

We envisaged that in contrast to 1:1 alternating α, and *E*-vinylogus sequences, by using 2:1 α- and *E*-vinylogous sequences it may be possible to achieve cross β-sheet structures. In addition to this, we also sought to investigate whether *E*-vinylogous amino acids can be accommodated into the hybrid peptide helix. Herein, we are reporting the design of novel miniature β-meanders from αα*E*-vinylogous hybrid hexapeptides, single step transformation of miniature β-meanders into 10/12 ααγ-hybrid helices using catalytic hydrogenation, the design of novel miniature helix-turn-helix motif, and their solution and single crystal conformations.

1.4 Results and Discussion

1.4.1 Design and Synthesis of Hexapeptides P1 and P2

Required (*E*)-α, β-unsaturated γ-amino esters were synthesized through Wittig reaction starting from α-amino aldehydes as reported earlier.[56] The schematic representation of the synthesis of *E*-vinylogous amino esters is shown in Scheme 1.

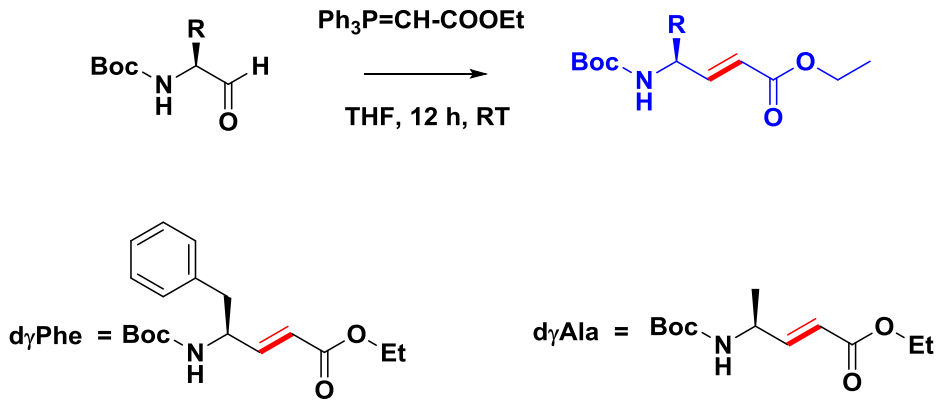

Scheme 1: Synthesis of (*E*)-α, β-unsaturated γ-amino esters using Wittig reaction.

To understand the conformational behavior of hybrid peptides composed of both α- and α,β-unsaturated γ-amino acids, we designed two hexapeptides **P1** and **P2** consists of repeated αα*E*-vinylogous amino acid repeats. The sequences of **P1** and **P2** are shown in Scheme 2. Peptides **P1** and **P2** consist of α, β-unsaturated γ-phenylalanine and α, β-unsaturated γ-alanine, respectively. Peptides were synthesized using Boc-chemistry by a solution phase using DCC/HOBt coupling conditions. Details of the peptide synthesis are given in the experimental section. Crude peptides were purified by reverse phase HPLC using MeOH/H_2O in gradient method. Pure peptides were subjected to conformational analysis in solution as well as to grow single crystals in various solvent combinations.

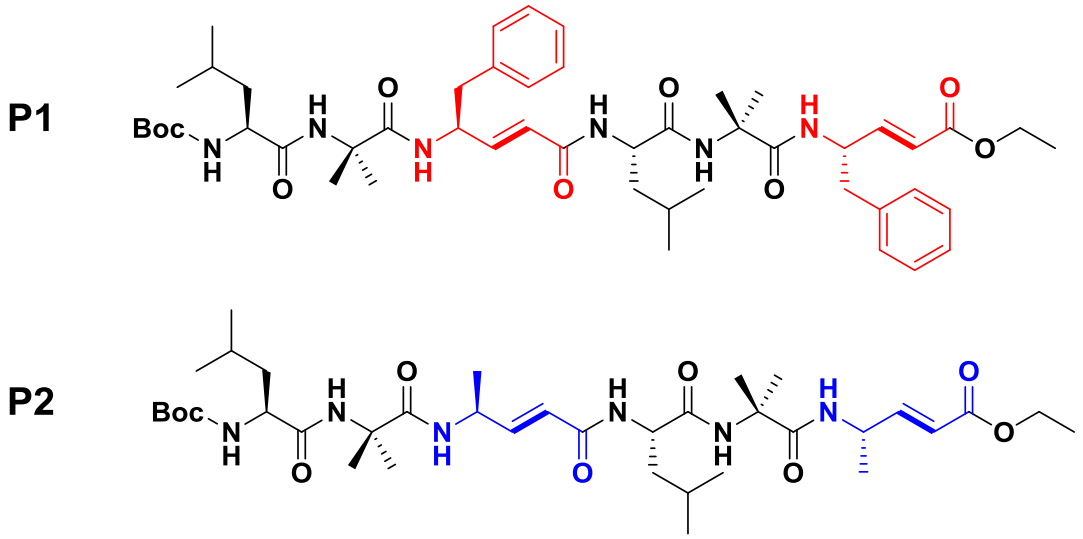

Scheme 2: Sequences of two hexapeptides **P1** and **P2** composed of *E*-vinylogous amino acids.

1.4.2. Crystal Structure analysis of P1

Single crystals of **P1** obtained from the slow evaporation of a methanol/toluene solution yielded the single crystals suitable for X-ray diffraction. The crystal structure is shown in Fig 1.12. Peptide **P2** did not give X-ray diffraction quality single crystals. Instructively, **P1** adopted a novel miniature β-meander type of structural motif with two reverse-turns. The analysis of the crystal structure of **P1** reveals that two C=O----NH intramolecular hydrogen bonds between the urethane carbonyl and the NH of Leu4 (1 ←4) and between the carbonyl of dγPhe3 and NH of dγPhe6 (1 ← 4) stabilize the overall folding of the molecule.

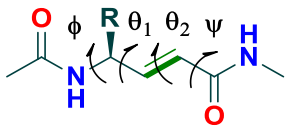

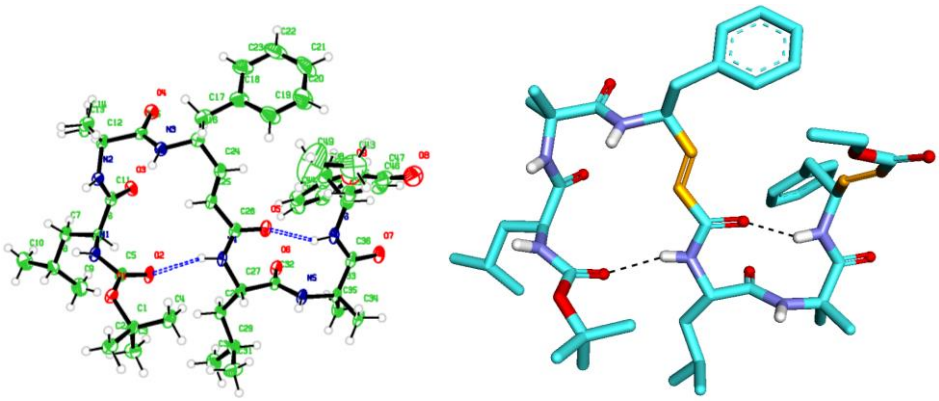

(A) **(B)**

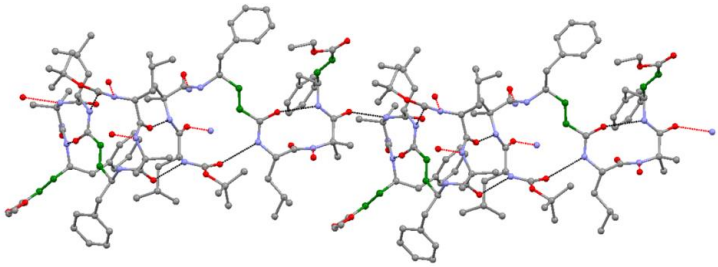

(C)

Fig 1.12: (A) ORTEP diagram of hybrid peptide Boc-(Leu-Aib-dγPhe)$_2$-OEt (**P1**) where ellipsoids are drawn to 40% probability. Hydrogen bonds are represented in dotted lines (CCDC number 1063358). (B) 15-membered and 10-membered H-bond pseudocycles depicted in crystal structure of **P1** and (C) View of crystal packing for **P1** along b-axis.

The torsional angles of α,β-unsaturated γ-amino acids were measured by introducing two new additional variables θ_1 and θ_2 along with ϕ and ψ (Fig 1.12). The torsional angles and H-bond parameters of **P1** are tabulated in Table 1 and 2, respectively. Inspection of the crystal structure reveals that Aib2 and dγPhe3 adopted a reverse turn type of conformation stabilized by a 15-membered H-bond. Furthermore, analysis of the central segment, Leu4-Aib5, reveals that it adopted a type II β-turn conformation by displaying torsional values ϕ4 = -48° , ψ4 = 128°, ϕ5 = 68° and ψ5 = 11° [for a typical type II β-turn ϕ(i) = -60°, ψ(i) = 120°, ϕ(i + 1) = 80° and ψ(i + 1) = 0°]. The type II β-turn is stabilized by the 1 ← 4 hydrogen bond between the carbonyl of dγPhe 3 and NH of dγPhe 6.

Table 1: Torsional variables (in deg) of Boc-Leu-Aib-dγPhe-Leu-Aib-dγPhe-OEt(**P1**)

Peptide	**Residue**	**ϕ**	**θ_1**	**θ_2**	**ψ**	**ω**
P1	Leu1	-95	-	-	-46	-163
	Aib2	-60	-	-	-45	-174
	dγPhe3	-129	18	-178	178	-178
	Leu4	-48	-	-	128	177
	Aib5	68	-	-	11	173
	dγPhe6	-122	118	-178	-10	-

Table 2: Hydrogen bond parameters of Boc-Leu-Aib-dγPhe-Leu-Aib-dγPhe-OEt (**P1**)

i) Intramolecular Hydrogen bond parameters

Donor (D)	**Acceptor (A)**	**D….A (Å)**	**DH….A (Å)**	**∠NH….O (deg)**
N4	O2	2.944	2.235	139.70
N6	O5	2.853	2.055	153.98

ii) Intermolecular Hydrogen bond parameters

Donor (D)	Acceptor (A)	D….A (Å)	DH….A (Å)	∠NH….O (deg)
N1	O4[§]	2.931	2.160	148.05
N2	O3[§]	3.063	2.238	160.90
N5	O7[†]	2.934	2.075	176.72
O3	N2[‡]	3.063	2.238	160.90
O4	N1[‡]	2.931	2.160	148.05
O7	N5[*]	2.934	2.075	176.72

Symmetry transformations used to generate equivalent atoms: **§** 1.5-x, 1/2+y, 2-z; **†** 1.5-x, 1/2+y, 1-z; **‡** 1.5-x, 1/2+y, 2-z; ***** 1.5-x, 1/2+y, 1-z.

1.4.3 NMR structure analysis of P1 and P2

In order to understand the conformations of **P1** and **P2** in solutions, we recorded 2D NMR (TOCSY, ROESY and COSY) in $CDCl_3$. The ^{1}H NMR reveals that all amide NHs are in the range of δ 6.5–7.3 ppm. The amino acid residues and their positions in the peptide sequences were identified using TOCSY and ROESY spectra, respectively. The strong sequential NH↔NH connectivity between Aib2↔dγPhe 3 and Aib5↔dγPhe 6 residues observed in **P1** suggests the reverse turn conformations of dipeptide segments in the hexapeptide. In addition, a strong NOE between the dγPhe3 C_αH and Leu4 NH indicates the extended conformation of the conjugated amide. The solution conformation analysis of **P2** also reveals a similar type of NOE pattern. Adding to the characteristic sequential NH↔NH NOEs between Leu1↔Aib2, Aib2↔dγAla 3 and Aib5↔ dγAla6, the peptide also showed the NOEs between Aib2 side chains with both Leu1 NH as well as NH of dγAla3. The long range strong NOE is observed between dγAla3 βH and the dγAla6 side-chain which further supports a well folded conformation of **P2** in solution. The intramolecular H-bonds are further examined using temperature-dependent ^{1}HNMR. It has been established that if the values of temperature coefficient are less negative than −4.5 ppb K^{-1}, such amide NHs are considered to be less solvent exposed and are involved in the intramolecular H-bonds. The residues which are exposed to the solvent exhibited a dδ/dt value above −5.9 ppb

K−1. The unexpected -2.8 and -3.7 ppb K−1 observed for Aib3 and Aib5 indicates their probable involvement in the strong intermolecular H-bond with other β-meanders or solvent molecules.The unexpected value observed for Leu4 may be due to solvent invasion at the N-terminal H-bond of the peptide. The peptide **P2** also displayed a similar trend revealed from the dδ/dt values of backbone amide protons. The chemical shifts and temperature coefficients of both the peptides are tabulated in Tables 3 and 4. Using unambiguous NOEs and variable temperature data, solution structure models of **P1** and **P2** are generated and shown in Fig 1.15. Instructively, both peptides adopt distinctively different and a spectacular 3-dimensional folded miniature β-meander type of structures in solution as compared to the 2-dimensional flat crystal structure. We understand that the crystal packing forces possibly directed the 3-dimentional architecture of **P1** in single crystals. Overall, the crystal structure and the NMR models suggested that both **P1** and **P2** adopted novel and distinct miniature β-meander type of structures.

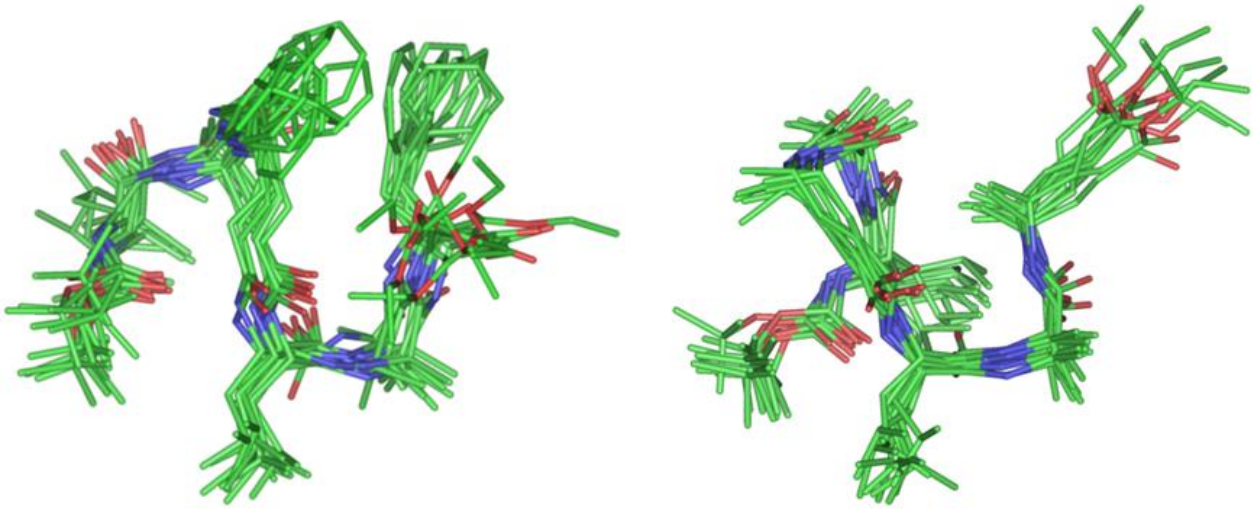

(A) (B)

Fig 1.13: The solution structures of peptide **P1** (A) and **P2** (B) in chloroform. The ensembles of ten low energy structures are calculated based on observed NOEs. H-atoms are omitted for clarity.

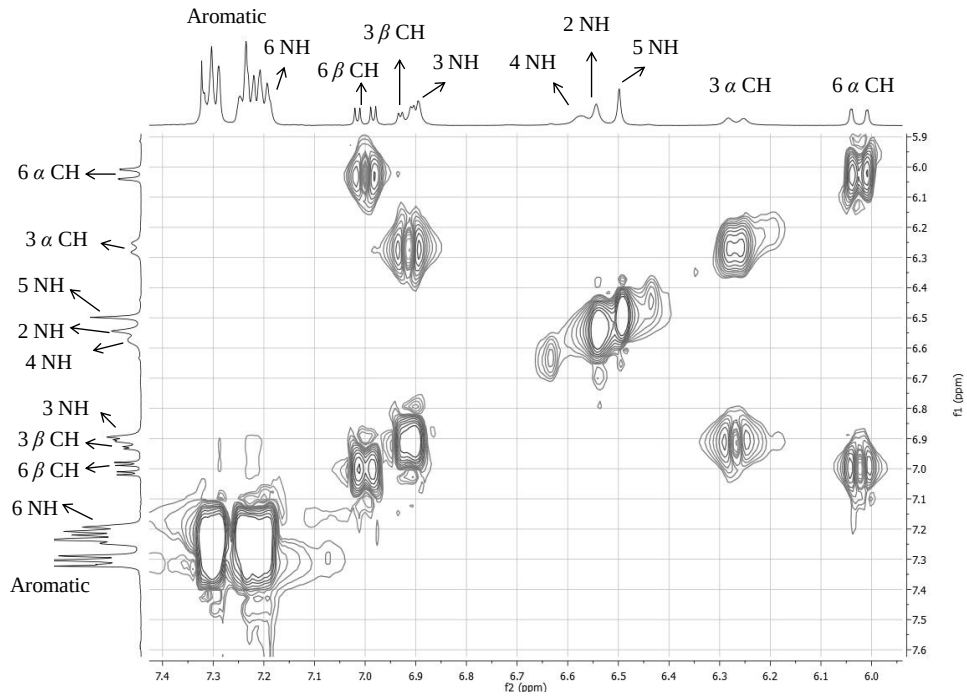
Aromatic
6 NH
3 β CH
6 β CH
3 NH
4 NH
2 NH
5 NH
3 α CH
6 α CH
f2 (ppm)
f1 (ppm)

(A)

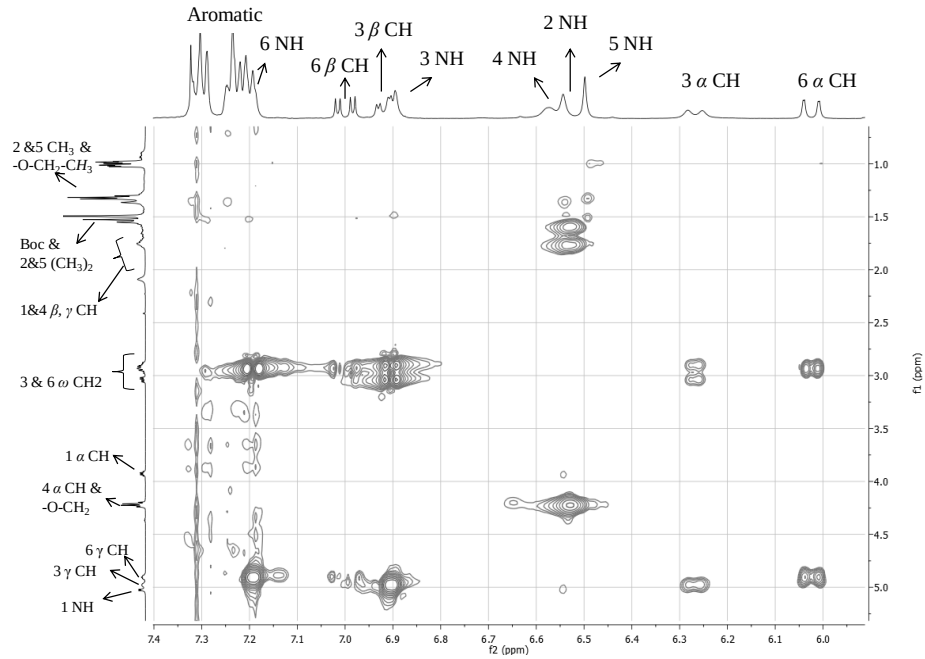
Aromatic
6 NH
3 β CH
6 β CH
3 NH
4 NH
2 NH
5 NH
3 α CH
6 α CH
2 &5 CH3 &
-O-CH2-CH3
Boc &
2&5 (CH3)2
1&4 β, γ CH
3 & 6 ω CH2
1 α CH
4 α CH &
-O-CH2
6 γ CH
3 γ CH
1 NH
f2 (ppm)
f1 (ppm)

(B)

Fig 1.14: Partial TOCSY spectra of peptide **P1** in $CDCl_3$ shown in (A) and (B). The sequential assignments of amino acids were performed using ROESY.

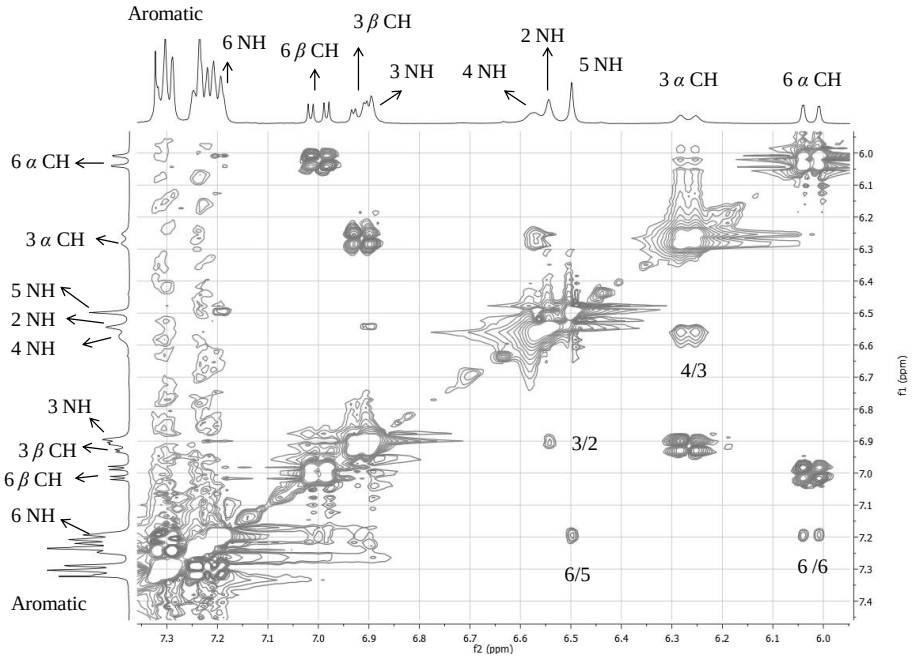

(A)

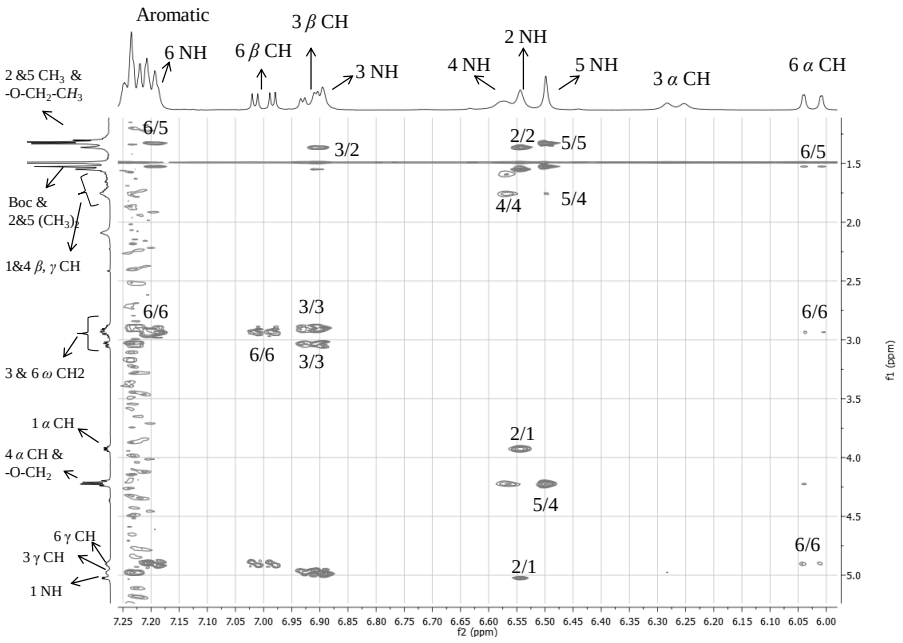

(B)

Fig 1.15: Partial ROESY spectrum of **P1** showing sequential NOEs of (A) NH↔NH and NH↔C_{α}H and (B) NH↔C_{α}H, NH↔C_{γ}H, NH↔side-chain, C_{α}H ↔ sidechain.

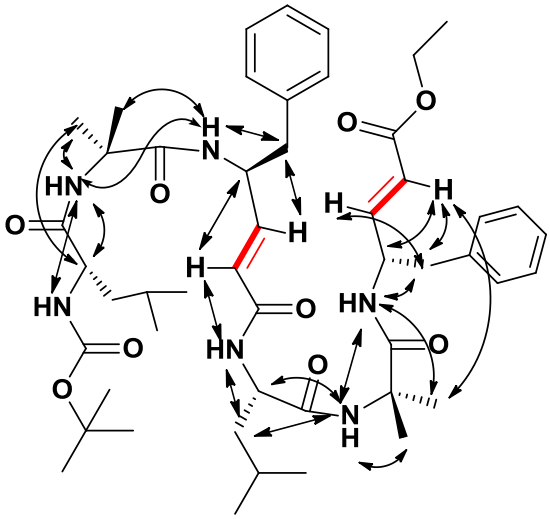

Fig 1.16: Observed NOEs of **P1** from ROESY spectrum are schematically represented by double headed arrows.

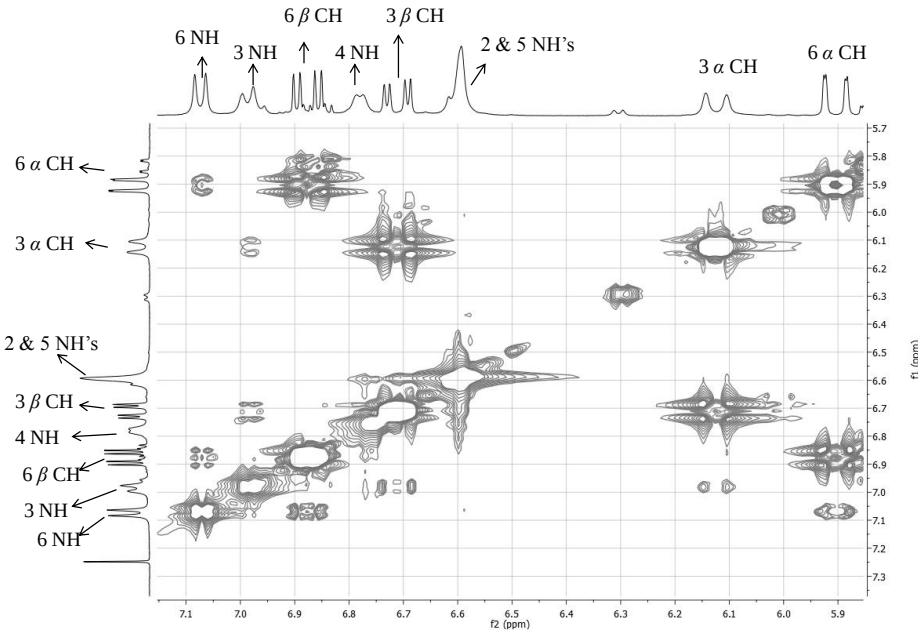

(A)

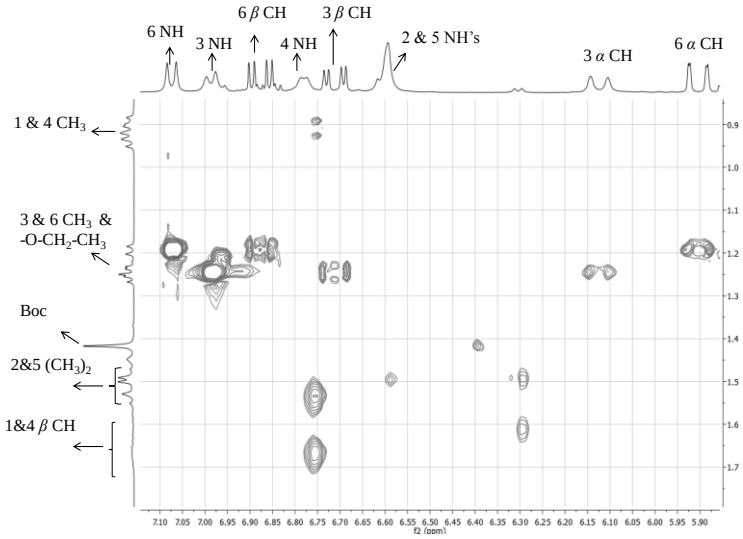

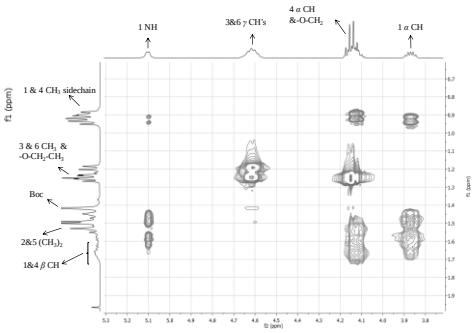

(B) **(C)**

Fig 1.17: Partial TOCSY spectra of peptide **P2** in $CDCl_3$ shown in (A), (B) and (C). The sequential assignments of amino acids were performed using ROESY.

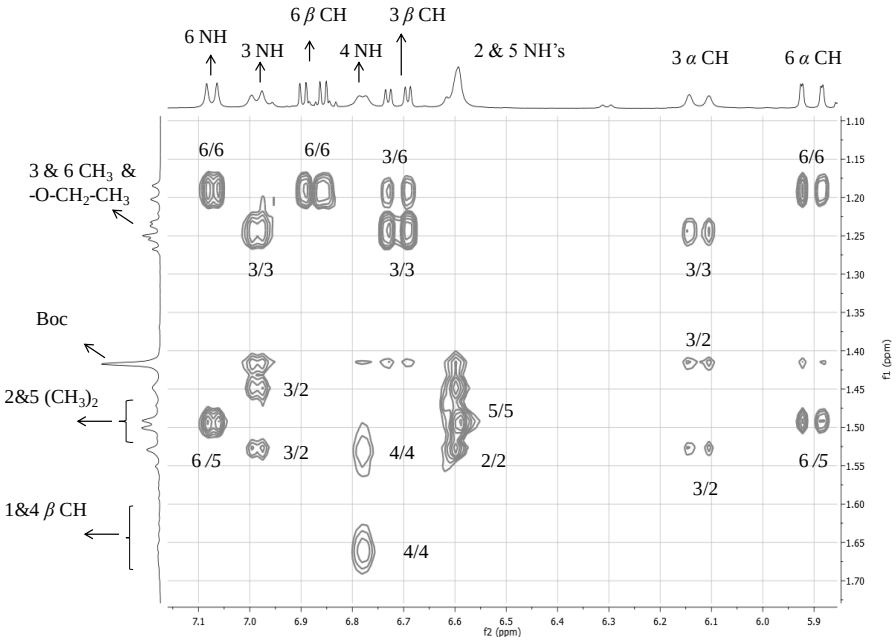

(a)

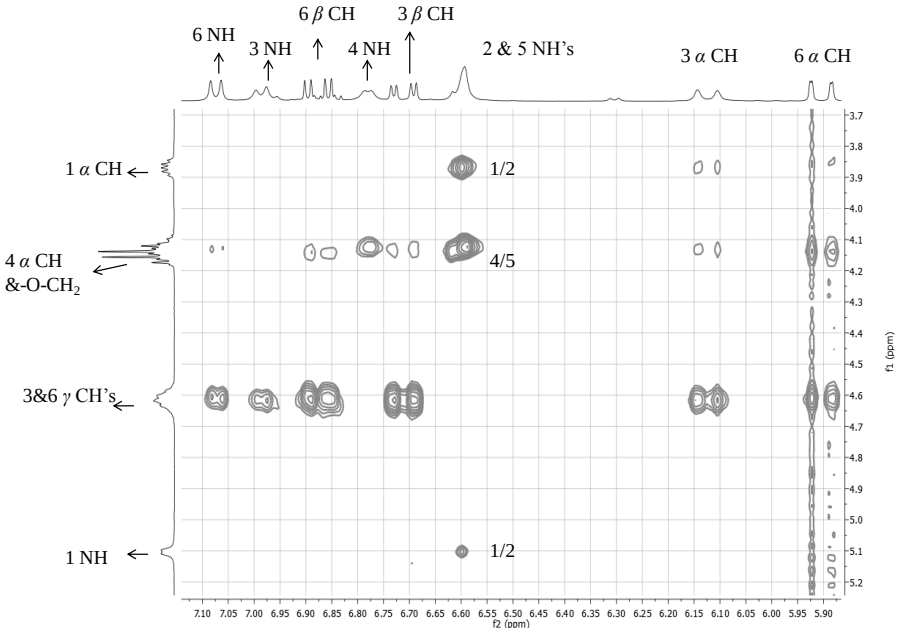

(b)

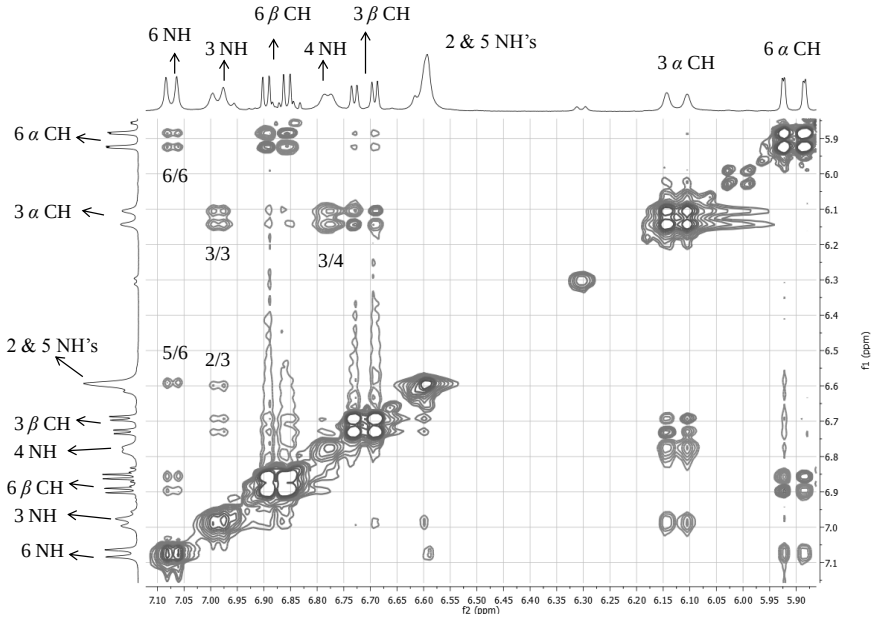

(c)

Fig 1.18: Partial ROESY spectrum of **P2** showing sequential NOEs of (a) NH↔side-chain, $C_{\alpha}H$ ↔ sidechain, (b) NH↔$C_{\alpha}H$, NH↔$C_{\gamma}H$ and (c) NH↔NH and NH↔$C_{\alpha}H$.

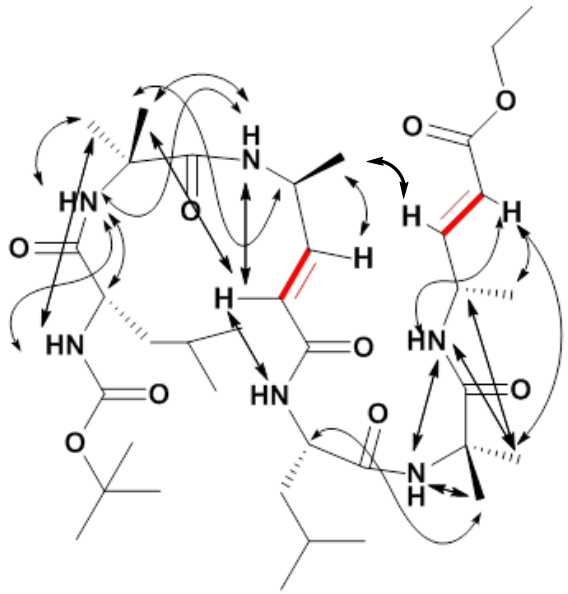

Fig 1.19: Observed NOEs of the peptide **P2** in the ROESY spectrum are schematically represented by double headed arrows.

Variable Temperature Study of Beta-meanders P1 and P2:

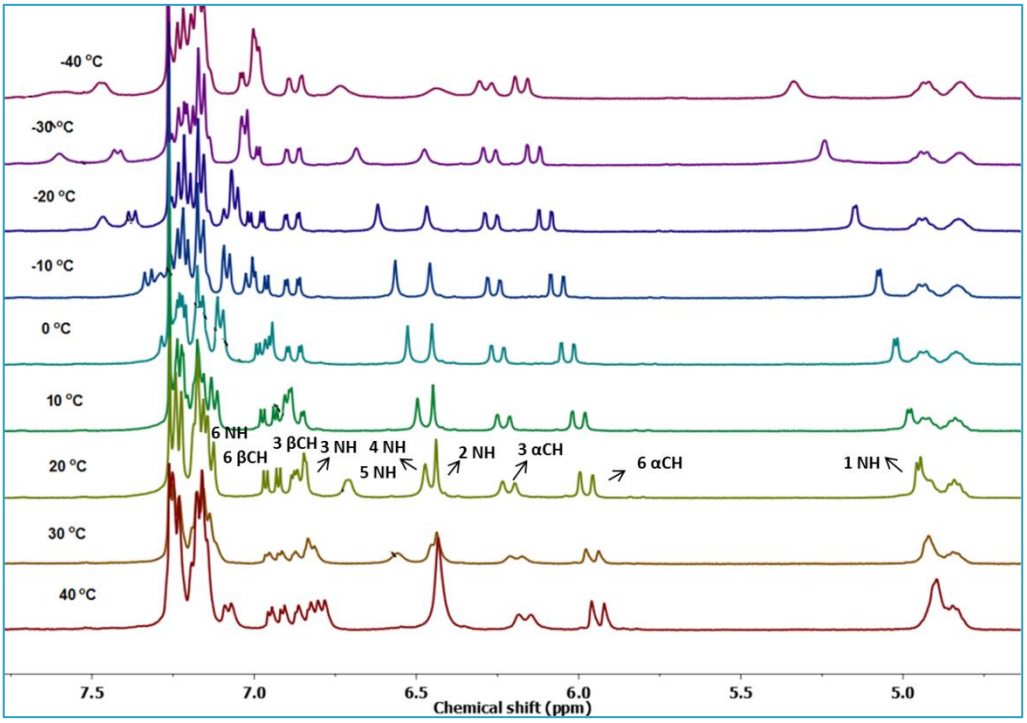

Fig 1.20: Temperature dependent ^{1}H NMR spectra of amide NH region of **P1**.

Table 3: Chemical shifts (in ppm) of amide NHs of peptide **P1**

Temp. (°C)	Leu1	Aib2	dγPhe3	Leu4	Aib5	dγPhe6
-40	5.34	6.73	6.99	7.59	6.44	7.47
-30	5.24	6.69	7.03	7.60	6.48	7.42
-20	5.15	6.62	7.06	7.47	6.47	7.38
-10	5.08	6.57	7.02	7.29	6.46	7.33
0	5.03	6.53	6.95	n.d	6.45	n.d
10	4.98	6.50	6.90	n.d	6.45	n.d
20	4.96	6.47	6.85	6.71	6.44	n.d
30	4.93	6.46	6.82	6.56	6.44	n.d
40	4.89	6.43	6.78	6.43	6.43	7.08
dδ/dT (ppb K^{-1})	**-5.4 (± 0.49)**	**-3.8 (± 0.29)**	**-3.4 (± 0.56)**	**-16.0 (± 0.99)**	**-0.4 (± 0.17)**	**-4.9 (± 0.75)**

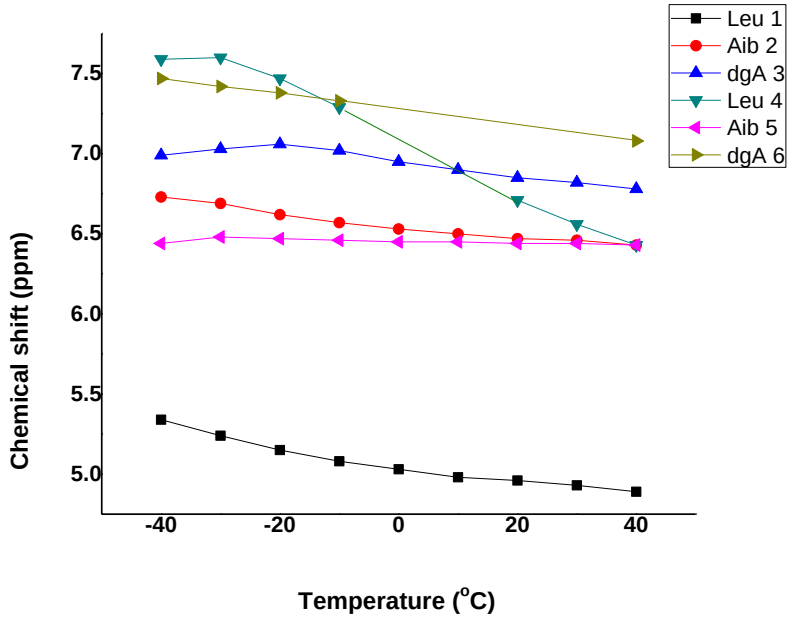

Fig 1.21: Plot of amides chemical shift and the temperature for peptide **P1**. The slope dδ/dt for all NH's is given in the Table 3.

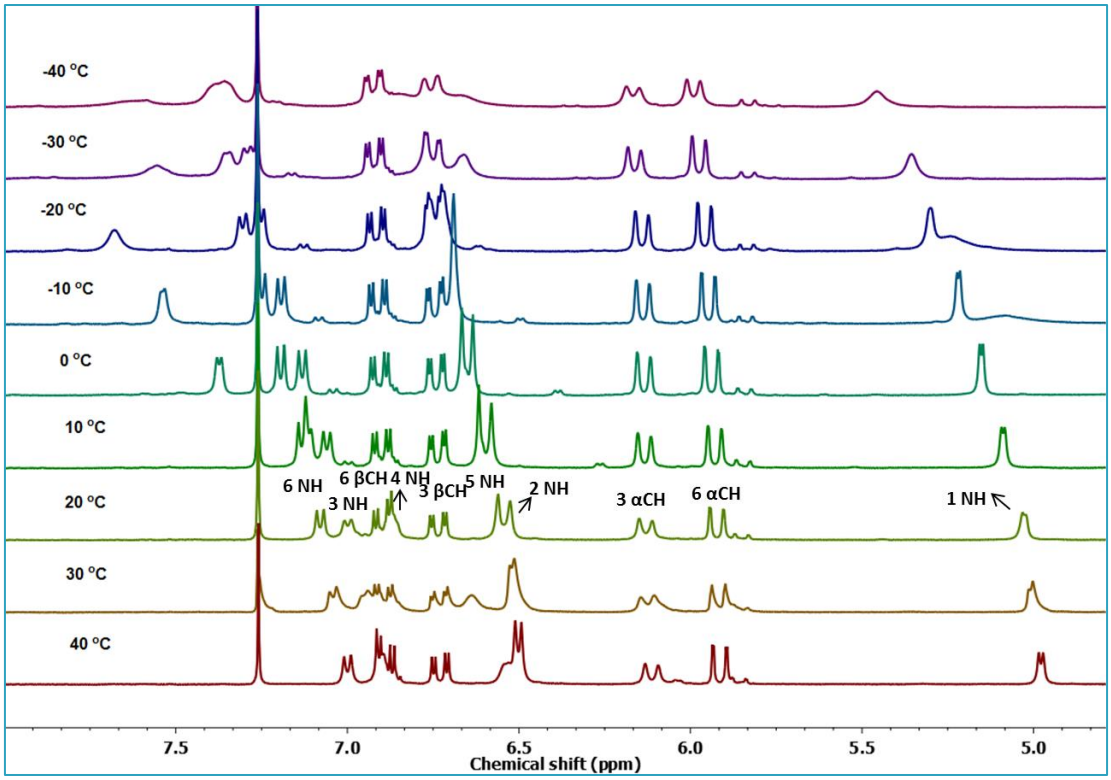

Fig 1.22: Temperature dependent ^{1}H NMR spectra of amide NH region of **P2**

Table 4: Chemical shifts (in ppm) of amide NH's of peptide **P2**

Temp. (°C)	**Leu1**	**Aib2**	**dγAla3**	**Leu4**	**Aib5**	**dγAla6**
-40	5.46	6.68	7.36	7.58	6.84	7.36
-30	5.36	6.66	7.29	7.55	6.67	7.35
-20	5.31	6.71	7.25	7.68	6.75	7.30
-10	5.22	6.69	7.19	7.54	6.69	7.25
0	5.15	6.63	7.13	7.38	6.67	7.19
10	5.09	6.58	7.06	7.11	6.62	7.13
20	5.02	6.53	7.00	6.86	6.56	7.08
30	5.00	6.51	6.95	6.64	6.53	7.04
40	4.98	6.49	6.89	6.54	6.51	7.00
dδ/dT (ppb K^{-1})	**-6.2 (±0.4)**	**-2.8 (±0.46)**	**-5.9 (±0.09)**	**-14.9 (±2.0)**	**-3.7 (±0.5)**	**-4.9 (±0.18)**

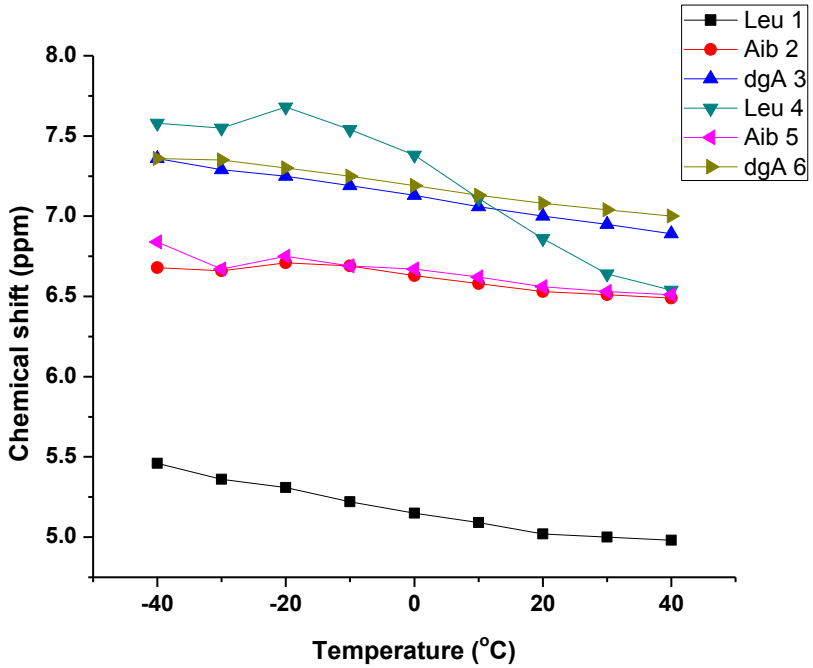

Fig 1.23: Plot of amides chemical shift and the temperature for peptide **P2**. The slope dδ/dt for all NHs is given in the Table 4.

1.4.4 Functional transformation of α,α,dγXaa-hybrid peptides into α,α,γ^4-hybrid peptides

To test whether **P1** and **P2** will adopt the same miniature β-meander structures upon reduction of double bonds or not, we subjected the two peptides to catalytic hydrogenation using 20% Pd/C in ethanol. The complete conversion of unsaturated hybrid peptides **P1** and **P2** into their saturated analogues **P3** [Boc-Leu-Aib-γ^4Phe-Leu-Aib-γ^4Phe-OEt] and **P4** [Boc-Leu-Aib-γ^4Ala-Leu-Aib-γ^4Ala-OEt], respectively, was achieved within six hours and isolated with 92–95% yield (Scheme 3). This transformation also provides an alternative opportunity to synthesize hybrid γ-peptides without starting from saturated γ-amino acids. To understand their conformations, both peptides were subjected to crystallization in various solvent combinations. Both **P3** and **P4** gave X-ray quality single crystals in an aqueous methanol solution and their X-ray structures are shown in Fig 1.24 and Fig 1.25.

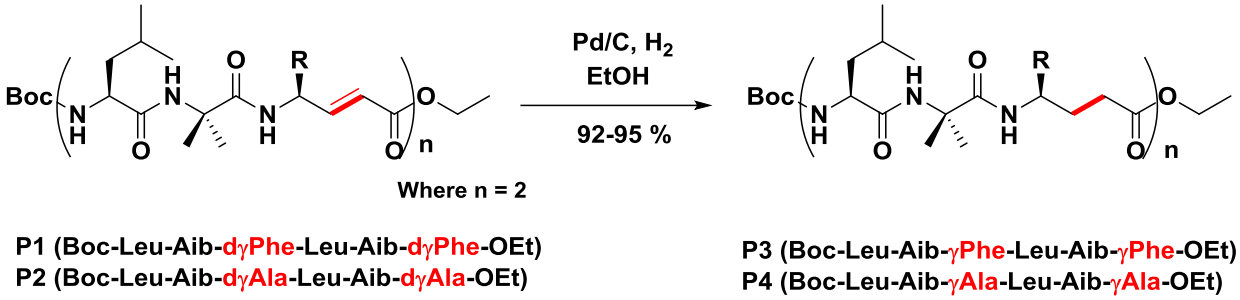

Scheme 3: Direct transformation of αα*E*-vinylogous hybrid peptides (**P1** and **P2**) into ααγ^4-hybrid peptides (**P3** and **P4**).

1.4.5 Structural analysis of P3 and P4

Both peptides adopted helical conformations in single crystals. The release of the geometrical constraints of vinylogous double bonds in the miniature β-meanders leads to the formation of hybrid helices. Analysis of the crystal structure of **P3** reveals that the helical structure is stabilized by four intramolecular H-bonds between i and i + 3 residues similar to the 3_{10}-helix[58] and the β-peptide 12-helix,[59] however, with 10- and 12-membered H-bonds. The 10-membered H-bonds were observed at both N- and C-termini of the helix, while two consecutive

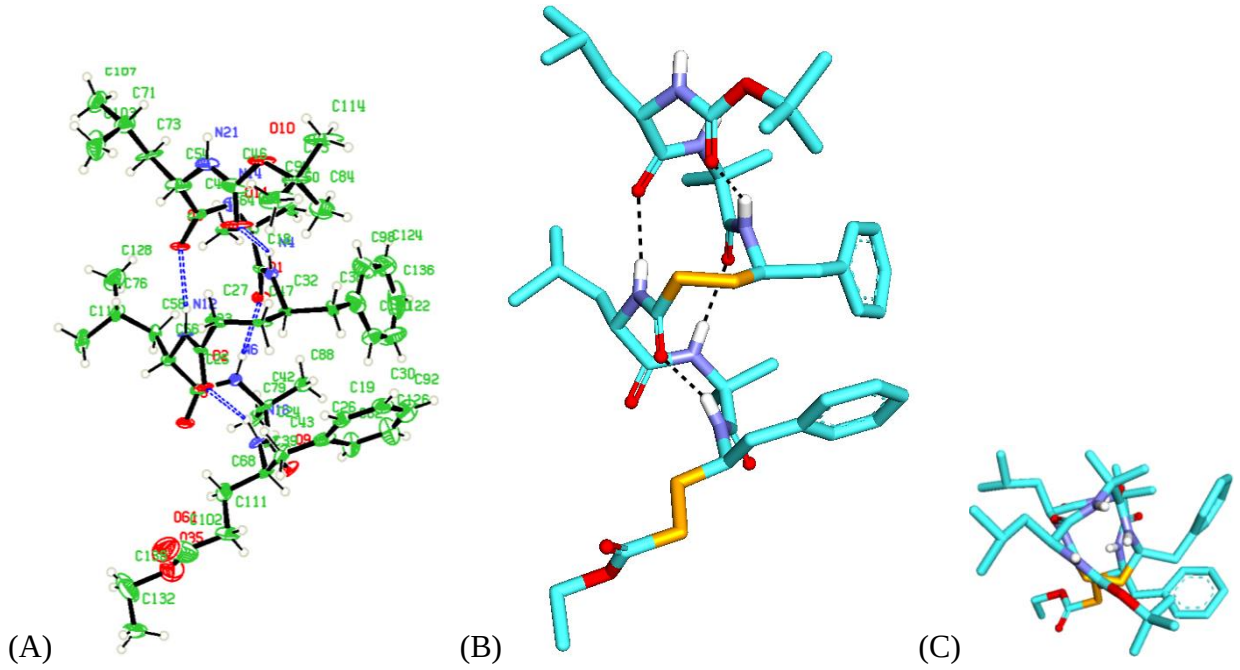

Fig 1.24: (A) ORTEP diagram of peptide **P3** and thermal ellipsoids are drawn at 50% probability, side view and top view of peptide **P3** are shown in (B) and (C), respectively.

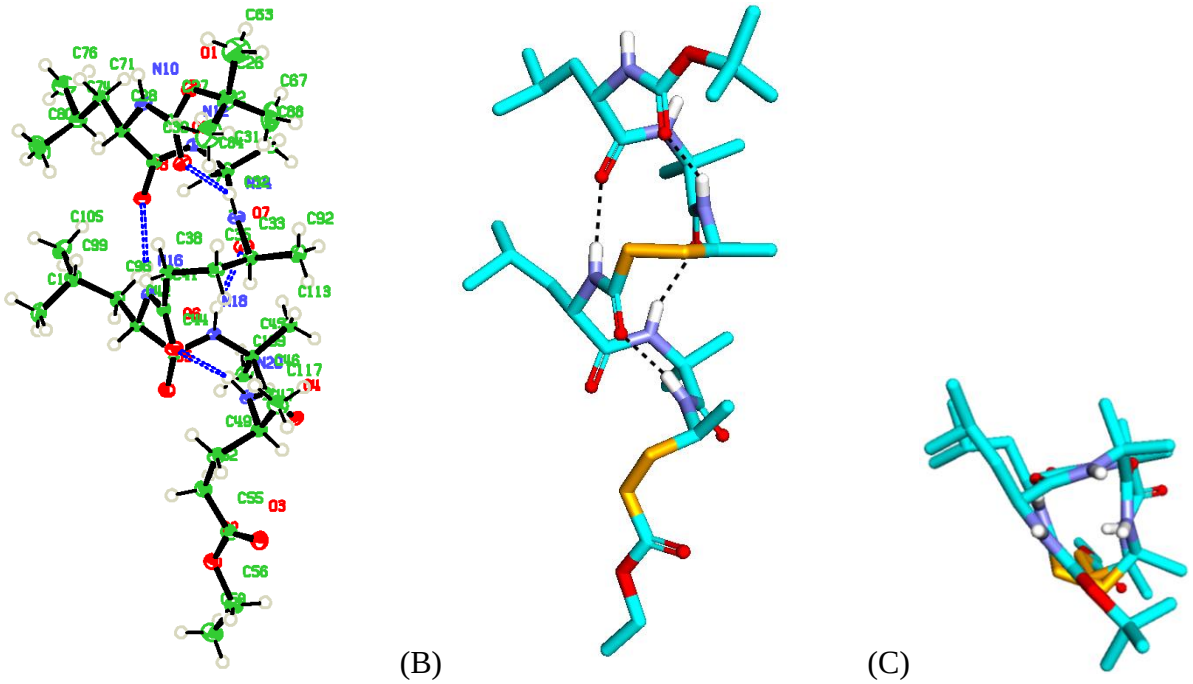

Fig 1.25: (A) ORTEP diagram of peptide **P4** and thermal ellipsoids are drawn at 50% probability, side view and top view of peptide **P4** are shown in (B) and (C), respectively.

12-membered H-bonds were observed at the centre of the helix. Similar to **P3**, **P4** also adopted a 10/12 helical structure. These helical structures of ααγ-hybrid peptides are consistent with the hybrid helices of $-(\alpha\gamma\alpha)_n-$ sequences reported by Balaram and colleagues.[60] The stereochemical analysis of γ^4-residues in both **P3** and **P4** adopted *gauche*$^+$, *gauche*$^+$ (g^+, g^+, $\theta_1 \approx \theta_2 \approx 60°$) conformation about the C_β–$C_\gamma$and C_α–C_β bonds, while the C-terminal γ-residues displayed *gauche*$^+$ (C_β–C_γ), *anti* (C_α–C_β) conformation due to the lack of a terminal H-bond donor (NH) to participate in the helix. Similar to the *E*-vinylogous amino acids, the torsional angles of γ-amino acids were measured by introducing additional torsional variables θ_1 and θ_2 along with ϕ and ψ. The torsional angels and H-bond parameters of γ-residues are tabulated in the Table 5-7.

Table 5: Torsional angles (in deg) of peptides **P3** and **P4**.

Peptide	Residue	ϕ	θ_1	θ_2	ψ	ω
P3	Leu1	-53	-	-	-40±2	-175±2
	Aib2	-57	-	-	-34	-174
	γPhe3	-127±1	52	61	-114	-175±1
	Leu4	-55±2	-	-	-39	178
	Aib5	-59	-	-	-25	-173±1
	γPhe6	-104	172±4	176/-161	98±15	-
P4	Leu1	-46	-	-	-41	-177
	Aib2	-54	-	-	-37	-173
	γAla3	-132	55	59	-122	-169
	Leu4	-62	-	-	-37	-178
	Aib5	-67	-	-	-12	-177
	γAla6	-121	74	82	172	-

Table 6: Peptide **P3** (Boc-Leu-Aib-γPhe-Leu-Aib-γPhe-OEt)

i) Intramolecular Hydrogen bond parameters for two molecules A and B in the asymmetric unit

Acceptor (A)	Donor (D)	D….A (Å)	DH….A (Å)	∠NH….O (deg)
O2 (A)	N19 (A)	3.08	2.35	142.8
O3 (A)	N16 (A)	2.95	2.12	163.5
O4 (A)	N18 (A)	2.99	2.14	169.5
O5 (A)	N17 (A)	2.84	2.04	153
O11 (B)	N26 (B)	2.99	2.25	143.9
O12 (B)	N23 (B)	2.92	2.07	164.8
O13 (B)	N24(B)	3.04	2.20	165
O14 (B)	N25 (B)	2.84	2.03	157.4

ii) Intermolecular Hydrogen bond parameters for two molecules A and B in the asymmetric unit

Donor (D)	Acceptor (A)	D….A (Å)	DH….A (Å)	∠NH….O (deg)
Molecule A				
N14	O16 *	2.90	2.153	161
N15	O19 *	3.00	2.068	169
O00B	O21 #	2.70	-	-
O8 †	O21#	2.97	-	-
O7	O20	2.84	-	-
O7	N20 (B)	2.87	2.04	161
Molecule B				
N20	O7 (A)	2.87	2.04	161
N21	O20	2.99	2.14	167
O16	O19	2.84	-	-
N14 (A) ‡	O16	2.90	2.07	161

Symmetry transformations used to generate equivalent atoms:

*x, y, -1+z; # -1+x, y, z; † 1+x, y, z; ‡ x, y, 1+z

Table 7: Peptide **P4** (Boc-Leu-Aib-γAla-Leu-Aib-γAla-OEt)

i) Intramolecular Hydrogen bond parameters

Acceptor (A)	Donor (D)	D….A (Å)	DH….A (Å)	∠NH….O (deg)
O9	N3	2.92	2.162	146.95
O8	N4	2.94	2.0841	171.6
O7	N5	2.93	2.102	160.68
O6	N6	3.00	2.209	153.93

ii) Intermolecular Hydrogen bond parameters

Acceptor (A)	Donor (D)	D….A (Å)	DH….A (Å)	∠NH….O (deg)
N1	O4 *	2.80	1.95	168
O4	N1 †	2.80	1.95	168
O4 ‡	O10 #	2.88	2.14	165

Symmetry transformations used to generate equivalent atoms:

* 1+x, 1+y, 1+z; † -1+x, -1+y, -1+z; # x, -1+y, z; ‡ x, 1+y, z

1.4.6 Analogy with 3_{10}- helix and β-peptide 12-helix

Interestingly, the top view of the helical peptides in ααγ-hybrid peptides showed the projection of side-chains at three faces of the helical cylinder similar to the β-peptide 12-helices and 3_{10}-helix.[58, 59] In contrast, αγ-hybrid peptide 12-helices showed the projection of the side-chains at four corners of the helical cylinder.[61] The side-chain correlation of 10/12 hybrid helices with 3_{10}-helix and β-peptide 12-helix is shown in Fig 1.26. Analysis suggests that the ααγ-hybrid peptides can mimic β-peptide 12-helices as well as 3_{10}-helices.

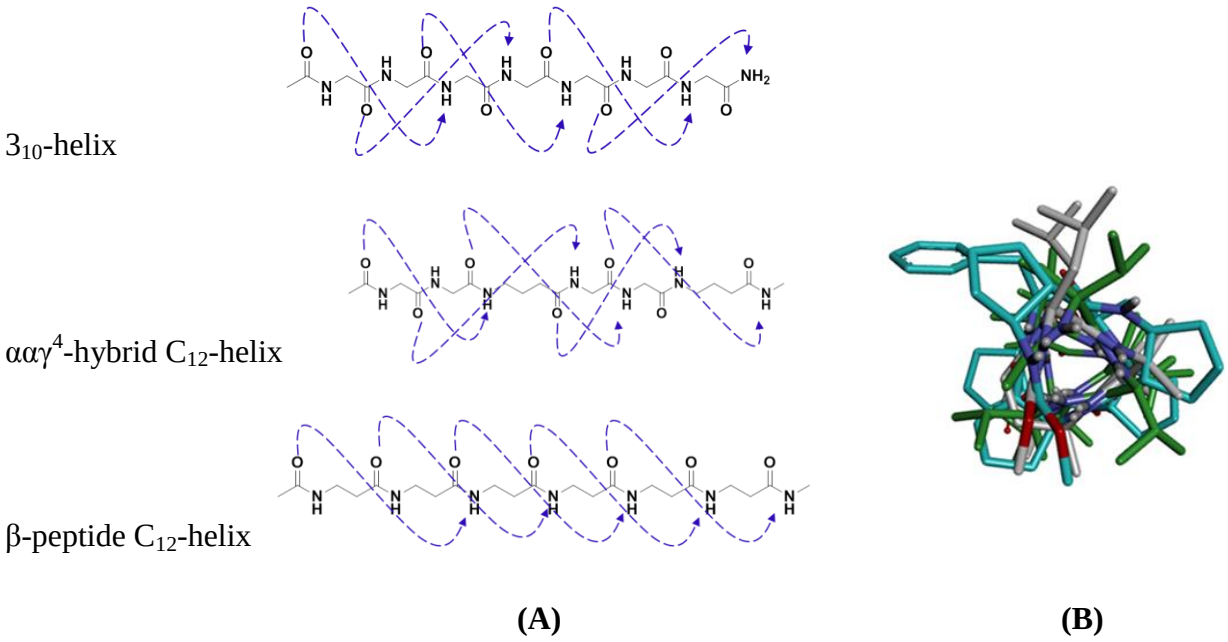

Fig 1.26: (A) Backbone H-bond directionality shown for 3_{10}-, ααγ^4- and β-peptide helices and (B) Side-chain correlation of 3_{10}-(green), ααγ^4-(grey) and β-peptide (cyan) helices (top view).

1.5 Design and synthesis of heptapeptide P5 (Ac-Aib-γPhe-Ala-dγVal-Aib-γPhe-Aib-$CONH_2$)

Earlier studies by Schreiber *et al.*[56] and recent advancements from our group[57] clearly showed that (*E*) α, β-unsaturated γ-amino acids are prone to adopt an extended conformation in homo- and hybrid oligomers irrespective of their sequence. In the above section, we studied the miniature β-meander type conformation in the short ααdγX-hexapeptide sequences. In the present section we sought to exploit these *E*-vinylogous amino acids in the design of another interesting supersecondary structure, helix-turn-helix (HTH).

We reasoned that selective incorporation of (*E*) α, β-unsaturated γ-amino acid in αγ-hybrid C_{12}-helix sequence can potentially lead to the construction of miniature helix-turn-helix (HTH) motifs. To test our hypothesis, we have taken known sequence of αγ-hybrid C_{12}-helix heptapeptide (Ac-Aib-γPhe-Aib-γPhe-Aib-γPhe-Aib-$CONH_2$) (Fig 1.27) as a model.[61c] We have designed the peptide **P5** (Ac-Aib-γPhe-Ala-dγVal-Aib-γPhe-Aib-$CONH_2$) by selective replacement of the third and fourth residues of model peptide with Ala (Alanine) and dγVal (α, β-unsaturated γ-Valine) residues respectively.

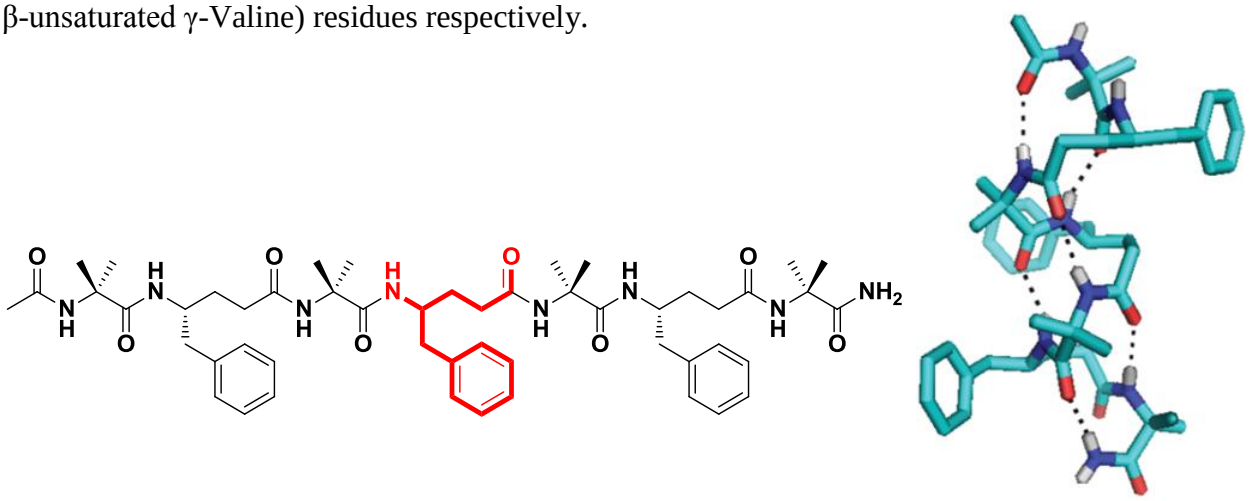

(A) **(B)**

Fig 1.27: (A) Model peptide (Ac-Aib-γPhe-Aib-γPhe-Aib-γPhe-Aib-$CONH_2$) and (B) crystallographic data is taken from *ref*. 61c.

Peptide P5: Ac-Aib-γPhe-Ala-dγVal-Aib-γPhe-Aib-$CONH_2$

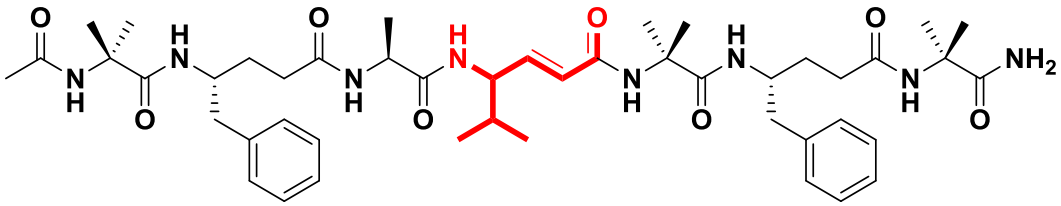

We have synthesized the peptide **P5** using standard solid-phase Fmoc-chemistry on Rink-amide resin at 0.2 mmol scale. After synthesis, the peptide was cleaved from the resin using TFA/H_2O/Phenol/TIPS (88:5:5:2) cocktail. The crude peptide was subjected to reverse phase-HPLC purification on C_{18}-column with methanol/water as a gradient at a flow rate of 3 mL/min. We attempted to crystallize the pure peptide **P5** in various solvent combinations to understand its unambiguous structure in single crystals. After repeated attempts we were fortunate enough to get single crystals of the peptide from the slow evaporation of aqueous methanol solution. The X-ray structure of **P5** is shown in Fig 1.28.

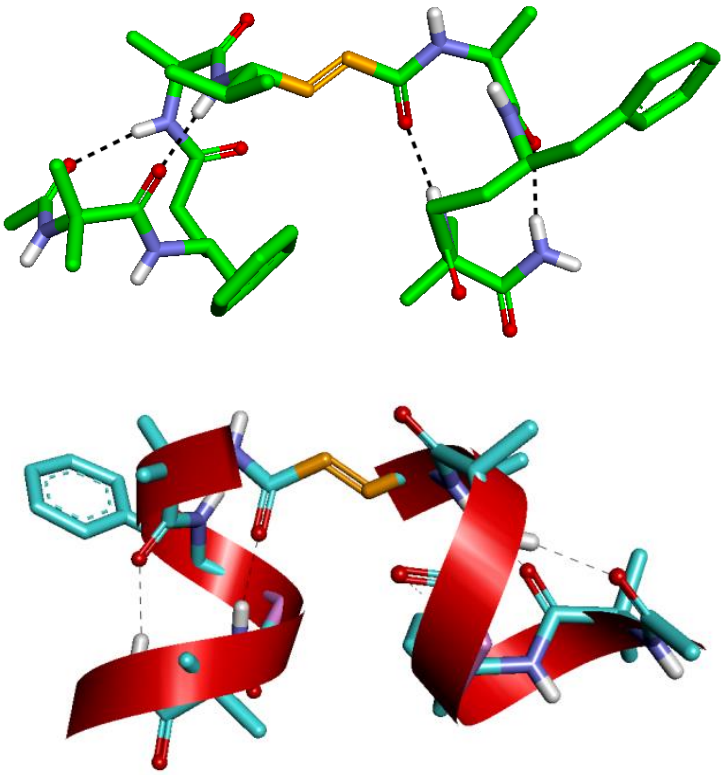

Fig 1.28: X-ray structure of peptide **P5** and its ribbon diagram depicting helix-turn-helix supersecondary structure motif of protein.

The engineered αγ-hybrid heptapeptide **P5** (Ac-Aib-γPhe-Ala-dγVal-Aib-γPhe-Aib-$CONH_2$) was crystallized in triclinic space group P_1, with two independent peptide molecules and seven water molecules in the crystallographic asymmetric unit. The backbone conformations of two peptide molecules showed that the peptide folds into a bended C_{12}-helix stabilized with 4 → 1 intramolecular H-bonds. The conformation was found to be very similar to protein supersecondary structure "helix-turn-helix" motif (Fig 1.28**)**. Careful observation of crystal structure revealed that all γ-residues have adopted g^+, g^+ conformations except fourth residue (α, β-unsaturated γ-Valine) due to the presence of constrained *trans* double bond (Table 8). This remarkable character of vinylogous amino acid induces the continuous C_{12}-helix to fold into a miniature "HTH" motif (a bend like structure). In summary, these results suggested that α, β-unsaturated γ-amino acids can be readily utilized to design different types of protein supersecondary structures using short hybrid peptide sequences.

Table 8: Torsional variables (in deg) for peptide **P5**

Peptide	ϕ	θ_1	θ_2	ψ	ω
Aib 1	-54	-	-	-55	-180
γPhe 2	-118	58	63	-129	-172
Ala 3	-71	-	-	-32	-175
dγVal 4	-80	121	-177	-169	-177
Aib 5	-52	-	-	-52	-177
γPhe 6	-122	54	67	-114	-179
Aib 7	-54	-	-	-43	-

1.6 Conclusions

In conclusion, we presented the utilization of geometrically constrained *trans* double bonds to engineer folding in peptides. The solution and crystal conformations suggested that the designed unsaturated hybrid peptides **P1** and **P2** adopted a novel miniature "β-meander" type of structure. Furthermore, these peptides also provide a prospect to transform them into 10/12-hybrid helices through simple catalytic hydrogenation. The structural analogy of ααγ-hybrid 10/12 helices suggests that they can be used to mimic surface topology of β-peptide 12-helices as well as 3_{10} helices. Additionally, we have shown that selective incorporation of α, β-unsaturated γ-amino acids into αγ-hybrid 12 helices leads to a novel miniature "helix-turn-helix" type of motif. The miniature β-meander and helix-turn-helix type structures from the short peptide sequences offers a glimpse of the potential to generate higher order structures using the combinations of α- and α,β-unsaturated γ-amino acids. As peptide foldamers have been emerging as promising candidates in medicinal chemistry and chemical biology, the novel miniature β-meanders, novel miniature helix-turn-helix and ααγ-hybrid peptide helices reported here can be further explored to design functional hybrid peptide foldamers.

1.7 Experimental Section

General experimental details

All amino acids, triphenylphosphine, TFA, Ethyl bromoacetate, DCC, HOBt and LAH were commercially available. DCM, DMF, ethyl acetate and pet-ether (60-80 ^{o}C) have used after distillation. THF was dried over sodium and distilled immediately prior to use. Column chromatography was performed on silica gel (120-200 mesh). Final peptides were purified on reverse phase HPLC (C18 column, MeOH/H_2O 60:40-95:5 as gradient with flow rate 1.00 mL/min). ^{1}H spectra were recorded on 500 MHz (or ^{13}C on 125 MHz) and 400 MHz (or ^{13}C on 100 MHz) using residual solvents as internal standards ($CDCl_3$ δ_H 7.26 ppm, δ_C77.3 ppm). Chemical shifts (δ) reported in *ppm* and coupling constants (J) reported in Hz.

NMR spectroscopy: All NMR studies were carried out by using a Bruker AVANCE^{III}-500 MHz spectrometer. Resonance assignments were obtained by TOCSY and ROESY analysis. All two-dimensional data were collected in phase-sensitive mode, by using the time-proportional phase

incrementation (TPPI) method. Sets of 1024 and 512 data points were used in the t_2 and t_1 dimensions, respectively. For TOCSY and ROESY analysis, 32 and 72 transients were collected, respectively. A spectral width of 6007 Hz was used in both dimensions. A spin-lock time of 256 ms was used to obtain ROESY spectra. Zero-filling was carried out to finally yield a data set of 2 K × 1 K. A shifted square-sine-bell window was used before processing.

Molecular Dynamics (MD): Model building and molecular dynamics simulation of P2 was carried out using Insight II (97.0) / Discover program on a Silicon Graphics Octane workstation. The cvff force field with default parameters was used throughout the simulations. Minimization's were done first with steepest decent, followed by conjugate gradient methods for a maximum of 1000 iterations each or RMS deviation of 0.001 kcal/mol, whichever was earlier. The energy-minimized structures were then subjected to MD simulations. A number of inter atomic distance constraints obtained from NMR data were used as restraints in the minimization as well as MD runs. For MD runs, a temperature of 300 K was used. The molecules were initially equilibrated for 50 ps and subsequently subjected to a 1 ns dynamics with a step size of 1 fs, sampling the trajectory at equal intervals of 10 ps. In trajectory 50 samples were generated and the best structures were again energy minimized with above protocol and superimposed these structures.

Table 9: List of NOEs used for MD calculation for peptide **P1**.

Residue	H-atom	Residue	H-atom	NOE observed
Leu (1)	α CH	Aib (2)	NH	Strong
Leu (1)	NH	Aib (2)	NH	Strong
Leu (1)	NH	Leu (1)	αCH	Medium
Leu (1)	NH	Leu (1)	β CH	Strong
Leu (1)	NH	Leu (1)	γ CH	Strong
Leu (1)	NH	Leu (1)	δ CH	Strong
Leu (1)	α CH	Aib (2)	$(CH_3)_2$	Strong
Aib (2)	NH	dγPhe (3)	NH	Strong
Aib (2)	NH	Aib (2)	$(CH_3)_2$	Strong
dγPhe (3)	NH	Aib (2)	$(CH_3)_2$	Medium
dγPhe (3)	αCH	Leu (4)	NH	Strong
dγPhe (3)	NH	dγPhe (3)	ω CH_2	Strong
dγPhe (3)	β CH	dγPhe (3)	ω CH_2	Strong
dγPhe (3)	γ CH	dγPhe (3)	Aromatic	Strong
dγPhe (3)	αCH	dγPhe (3)	γ CH	Weak
Leu (4)	NH	Leu (4)	β CH	Medium
Leu (4)	NH	Leu (4)	γ CH	Weak
Aib (5)	NH	Leu (4)	β CH	Weak
Aib (5)	NH	Leu (4)	αCH	Strong
Aib (5)	NH	dγPhe (6)	NH	Strong
Aib (5)	NH	Aib (5)	$(CH_3)_2$	Strong
dγPhe (6)	NH	Aib (5)	$(CH_3)_2$	Medium
dγPhe (6)	NH	dγPhe (6)	ω CH_2	Strong
dγPhe (6)	NH	dγPhe (6)	αCH	Strong
dγPhe (6)	αCH	dγPhe (6)	ω CH_2	Weak
dγPhe (6)	αCH	dγPhe (6)	γCH	Weak
dγPhe (6)	αCH	Aib (5)	$(CH_3)_2$	Weak
dγPhe (6)	β CH	dγPhe (6)	ω CH_2	Strong

Table 10: List of NOEs used for MD calculation for peptide **P2**.

Residue	H-atom	Residue	H-atom	NOE observed
Leu (1)	NH	Aib (2)	NH	Strong
Leu (1)	α CH	Aib (2)	NH	Strong
Leu (1)	NH	Aib (2)	$(CH_3)_2$	Medium
Leu (1)	NH	Leu (1)	β CH	Strong
Leu (1)	NH	Leu (1)	γ CH	Weak
Aib(2)	NH	dγAla (3)	NH	Weak
Aib(2)	NH	Aib (2)	$(CH_3)_2$	Strong
Aib(2)	$(CH_3)_2$	dγAla (3)	NH	Strong
Aib(2)	$(CH_3)_2$	dγAla (3)	α CH	Weak
Aib(2)	$(CH_3)_2$	dγAla (3)	γ CH	Weak
dγAla (3)	NH	dγAla (3)	CH_3	Strong
dγAla (3)	β CH	dγAla (3)	CH_3	Strong
dγAla (3)	β CH	dγAla (6)	CH_3	Strong
dγAla (3)	α CH	Leu (4)	NH	Strong
dγAla (3)	α CH	dγAla (3)	NH	Strong
dγAla (3)	α CH	dγAla (3)	CH_3	Medium
Leu (4)	NH	Leu (4)	β CH	Medium
Leu (4)	NH	Leu (4)	γ CH	Medium
Leu (4)	α CH	Aib (5)	NH	Strong
Leu (4)	α CH	Leu (4)	δ CH	Strong
Aib (5)	NH	dγAla (6)	NH	Medium
Aib (5)	NH	Aib (5)	$(CH_3)_2$	Strong
Aib (5)	$(CH_3)_2$	dγAla (6)	NH	Strong
Aib (5)	$(CH_3)_2$	dγAla (6)	α CH	Weak
Aib (5)	$(CH_3)_2$	dγAla (6)	γ CH	Strong
dγAla (6)	α CH	dγAla (6)	NH	Medium
dγAla (6)	α CH	dγAla (6)	CH_3	Weak
dγAla (6)	NH	dγAla (6)	CH_3	Strong
dγAla (6)	β CH	dγAla (6)	CH_3	Strong

Crystallographic Information

Crystal structure analysis of Boc-Leu-Aib-dγPhe-Leu-Aib-dγPhe-OEt (P1): Crystals of peptide were grown by slow evaporation from a solution of methanol/toluene (1:1). A single crystal (0.21 × 0.08 × 0.1 mm) was mounted on loop with a small amount of the paraffin oil. The X-ray data were collected at 100K temperature on a Bruker APEX(II) DUO CCD diffractometer using Mo K_α radiation (λ = 0.71073 Å), ω-scans (2θ = 52.52), for a total of 14074 independent reflections. Space group C2, a = 35.352(11), b = 10.430(3), c = 17.876(5), β = 107.549(5), V = 6285 (3) $Å^3$, Monoclinic C, Z = 4 for chemical formula $C_{49}H_{72}N_6O_9$ (C_7H_8), with one molecule in asymmetric unit; ρcalcd = 1.037 gcm^{-3}, μ = 0.070 mm^{-1}, F(000) = 2120, R_{int}= 0.0506. The structure was obtained by direct methods using SHELXS-97.[62] The final R value was 0.0542 (wR2 = 0.1280) 14074 observed reflections ($F_0 \geq 4\sigma$($|F_0|$)) and 589 variables, S = 0.832. The largest difference peak and hole were 0.228 and -0.256 $eÅ^3$, respectively.

There is some partially occupied solvent molecule also present in the asymmetric unit. A significant amount of time was invested in identifying and refining the disordered molecule. Option SQUEEZE of program PLATON[63] was used to correct the diffraction data for diffuse scattering effects and to identify the solvent molecule. PLATON calculated the upper limit of volume that can be occupied by the solvent to be 1740 $Å^3$, or 27.7% of the unit cell volume. The program calculated 118 electrons in the unit cell for the diffuse species. No data are given for the diffusely scattering species. Outputs of SQUEEZE report are appended in cif file **P1**.

Crystal structure analysis of Boc-Leu-Aib-γPhe-Leu-Aib-γPhe-OEt (P3): Crystals of peptide were grown by slow evaporation from a solution of methanol. A single crystal (0.12 × 0.09 × 0.1 mm) was mounted on loop with a small amount of the paraffin oil. The X-ray data were collected at 100K temperature on a Bruker APEX(II) DUO CCD diffractometer using Mo K_α radiation (λ = 0.71073 Å), ω-scans (2θ = 56.7), for a total of 90866 independent reflections. Space group P 21, a = 9.286 (3), b = 20.892 (7), c = 27.661 (9), β = 98.639 (6), V = 5305 (3) $Å^3$, Monoclinic C, Z = 2 for chemical formula C_{49} H_{76} N_6 O_9 (C H_4 O, 3 O), with two molecule in asymmetric unit; ρcalcd = 1.168 gcm^{-3}, μ = 0.082 mm^{-1}, F (000) = 1936, R_{int}= 0.1470. The structure was obtained by direct methods using SHELXS-97.[62] The final R value was 0.1509 (wR2 = 0.3727) 26002 observed reflections ($F_0 \geq 4\sigma$ ($|F_0|$)) and 1224 variables, S = 1.642.

There are partially occupied solvent molecules along with peptide molecules. Option SQUEEZE of program PLATON[63] was used to correct the diffraction data for diffuse scattering effects and to identify the solvent molecule. PLATON calculated the upper limit of volume that can be occupied by the solvent to be 470 Å ^{3}, or 8.8% of the unit cell volume. Outputs of SQUEEZE report are appended in CIF file **P4**. This structure contains ethyl ester groups. Even though this structure was collected at 100K the thermal parameters for one of the ethyl ester group was very high. This was attempted to be modeled as disorder but this was not successful. The conclusion is that this group is not well defined and thus was refined isotropically.

Crystal structure analysis of Boc-Leu-Aib-γAla-Leu-Aib-γAla-OEt (P4): Crystals of peptide were grown by slow evaporation from a solution of methanol. A single crystal (0.15 × 0.04 × 0.07 mm) was mounted on loop with a small amount of the paraffin oil. The X-ray data were collected at 100K temperature on a Bruker APEX(II) DUO CCD diffractometer using Mo K_α radiation (λ = 0.71073 Å), ω-scans (2θ = 56.9), for a total of 7174 independent reflections. Space group P1, a = 9.7972 (4), b = 10.4809 (5), c = 12.3285 (6), β = 102.4740 (10), V = 1132 (9) Å^3, Triclinic, Z = 1 for chemical formula C_{37} H_{68} N_6 O_9 (C_2 H_6 O), with one molecule in asymmetric unit; ρcalcd = 1.129 gcm^{-3}, μ = 0.081 mm^{-1}, F (000) = 419, R_{int}= 0.0401. The structure was obtained by direct methods using SHELXS-97.[52]The final R value was 0.035 (wR2 = 0.1052) 7363 observed reflections ($F_0 \geq 4\sigma$ ($|F_0|$)) and 514 variables, S = 0.908.

Crystal structure analysis of Ac-Aib-γPhe-Ala-dγVal-Aib-γPhe-Aib-CONH (P5): Crystals of peptide were grown by slow evaporation from aqueous solution of methanol. A single crystal (0.13 × 0.05 × 0.08 mm) was mounted on loop with a small amount of the paraffin oil. The X-ray data were collected at 100K temperature on a Bruker APEX(II) DUO CCD diffractometer using Mo K_α radiation (λ = 0.71073 Å), ω-scans (2θ = 59.9), for a total of 7174 independent reflections. Space group P1, a = 10.154(13), b = 16.17(2), c = 17.35(2), β = 107.002(15), V = 2522(6) Å^3, Triclinic, Z = 1 for chemical formula 2($C_{46}H_{68}N_8O_8$), 7(O) with two molecules in asymmetric unit; ρcalcd = 1.208 gcm^{-3}, μ = 0.087 mm^{-1}, F (000) = 985, R_{int}= 0.0415. The structure was obtained by direct methods using SHELXS-97.[62] The final R value was 0.115 (wR2 = 0.328) 14027 observed reflections ($F_0 \geq 4\sigma$ ($|F_0|$)) and 1201 variables, S = 0.962.

General procedure for the Synthesis of Boc-N- α, β-unsaturated γ-amino esters:

Boc-α,β-unsaturated γ-amino esters: *N*-Boc-Amino aldehyde (10 mmol) was dissolved in 30 mL of dry THF followed by Wittig ylide (11 mmol) was added at RT. Reaction mixture was stirred for about 5 h at RT. Completion of the reaction was monitored by TLC. After completion, solvent was evaporated and the crude product was purified by column chromatography using EtOAc/pet ether to get (88%) of pure product.

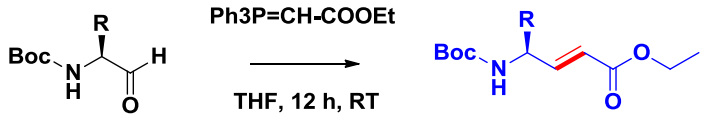

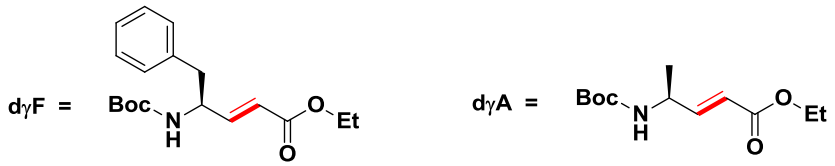

(*S*, *E*)-ethyl 4-((tert-butoxycarbonyl)amino)-5-phenylpent-2-enoate (1): White powder solid; Yield 88%; ^{1}H NMR (400 MHz, $CDCl_3$) δ 7.30-7.14 (m, 5H), 6.89 (dd, J = 16 Hz, J = 4 Hz, 1H), 5.84 (dd, J = 16 Hz, J = 2 Hz, 1H), 4.59 (b, 1H), 4.16 (q, J = 7 Hz, 2H), 2.88 (m, 2H), 1.37 (s, 9H), 1.25 (t, J = 7.1 Hz, 3H); ^{13}C NMR (100 MHz, $CDCl_3$) δ 166.3, 155.2, 147.6, 136.4, 129.4, 128.6, 126.9, 121.1, 79.9, 60.5, 52.3, 40.9, 28.3, 14.2; MALDI TOF/TOF *m/z* calculated value for $C_{18}H_{25}NO_4$ [M+Na$^+$] 342.1676 and observed 342.1657.

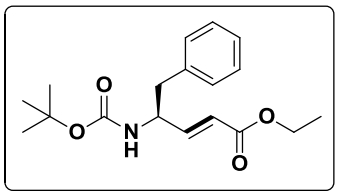

(*S*, *E*)-ethyl 4-((tert-butoxycarbonyl)amino)pent-2-enoate (2): Colourless Oil; Yield 93%; ^{1}H NMR(400 MHz, CDCl3) δ 6.87-6.82 (dd, J = 16 Hz, J = 4 Hz, 1H), 5.89-5.85 (d, J = 16 Hz, 1H), 4.5 (br, 1H), 4.38 (br, 1H), 4.19-4.14 (q, J = 8 Hz, 2H), 1.43 (s, 9H), 1.26-1.24 (m, 6H); ^{13}C NMR(100 MHz, CDCl3) 166.4, 154.9, 120.2, 79.8, 60.5, 47.0, 28.4, 20.4, 14.3; MALDI.TOF/TOF*m/z* Calculated value for $C_{12}H_{21}NO_4$ [M+Na]$^+$ 266.1368 and Observed 266.1365.

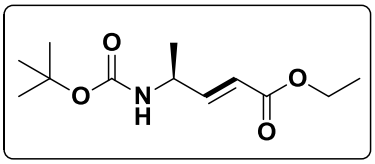

General procedure for the Synthesis of Peptide P1 and P2:

Boc-Leu-Aib-dγX-Leu-Aib-dγX-OEt: Tripeptide and hexapeptide were prepared by conventional solution-phase fragment condensation strategy. Deprotections were performed with trifloroacetic acid and saponification for *N*- and *C*-termini respectively. Couplings were carried out using N, N'-dicyclohexylcarbodiimide (DCC) and 1-hydroxybenzotriazole (HOBt). Tripeptide was synthesized using 1+2 condensation strategy involving Boc-Leu-OH and NH_2-Aib-dγX-OEt. Hexapeptide was synthesized by 3+3 condensation strategy involving Boc-Leu-Aib-dγX-COOH and NH_2-Leu-Aib-dγX-OEt. All peptides were purified by RP-HPLC using MeOH/H_2O system.

Boc-Leu-Aib-dγPhe-OEt (T1): White solid; yield 88%; ^{1}H NMR (400 MHz, $CDCl_3$) δ 7.30 (bs, 1H), 7.29-7.17 (m, 5H), 7.06 (d, J = 7.8 Hz, 1H), 6.92 (dd, J = 15.8 Hz, J = 4.8 Hz, 1H), 6.47 (bs, 1H) 5.90 (d, J = 15.57 Hz, 1H), 4.90 (m, 2H), 4.16 (q, 2H, J = 8 Hz), 2.91 (m, 2H) , 1.65 (m, 2H), 1.50-1.40 (m, 16H), 1.26 (t, J = 7.1, 3H), 0.94 (m, 6H); ^{13}C NMR (100 MHz, $CDCl_3$) δ 173.53, 172.38, 147.05, 136.92, 129.35, 128.56, 126.83, 121.21, 80.82, 60.44, 57.54, 54.05, 53.53, 51.26, 40.62, 40.17, 34.03, 28.35, 25.61, 25.46, 25.03, 24.86, 23.03, 21.92, 14.33; HR-MS *m/z* calculated for $C_{28}H_{43}N_3O_6$ $[M+Na]^+$ 540.3050, observed 540.3057.

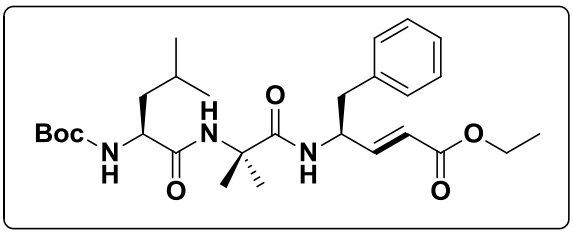

Boc-Leu-Aib-dγAla-OEt (T2):^{1}H NMR (400 MHz, $CDCl_3$) δ 7.08 (d, J = 8 Hz, 1H), 6.88 (dd, J = 16 Hz, J = 4 Hz, 1H), 6.48 (s, 1H), 5.92 (d, J = 16 Hz, 1H), 4.99 (bs, 1H), 4.65 (m, 1H), 4.16 (q, J = 8 Hz, 2H), 3.90 (m, 1H), 1.65 (m, 2H), 1.52 (s, 3H), 1.51 (s, 3H), 1.42 (s, 9H), 1.26 (m, 6H), 0.93 (m, 6H); ^{13}C NMR (100 MHz, $CDCl_3$) δ 173.5, 172.2, 166.7, 156.3, 149.1, 120.4, 80.8,

60.5, 57.5, 54.4, 46.1, 40.3, 28.4, 25.8, 24.9, 23.0, 22.0, 20.0, 14.4; HR-MS *m/z* value calculated for $C_{22}H_{39}N_3O_6$ [M+Na$^+$] 464.2736, observed 464.2740.

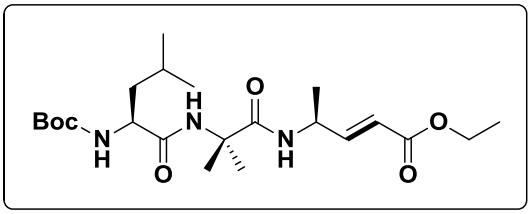

Boc-Leu-Aib-dγPhe-Leu-Aib-dγPhe-OEt (P1): White color solid; Yield 50%; ^{1}H NMR (500 MHz, $CDCl_3$) δ 7.12-7.02 (m, 11H), 6.66 (dd, J = 15.6 Hz, J = 5 Hz, 1H), 6.77 (m, 2H), 6.43 (b, 1H), 6.40 (s, 1H), 6.35 (s, 1H), 6.13 (d, J = 15 Hz, 1H), 5.88 (dd, J = 16 Hz, J = 1 Hz, 1H), 4.88 (d, J = 5 Hz, 1H), 4.83 (m, 1H), 4.76 (m, 1H), 4.07 (m, 2H), 3.78 (m, 1H), 2.91-2.73 (m, 4H), 1.66-1.42 (m, 6H), 1.40-1.16 (m, 25H), 0.86 (m, 12H); HR-MS *m/z* calculated value for $C_{49}H_{72}N_6O_9$ [M+Na$^+$] 911.5253, observed 911.5266.

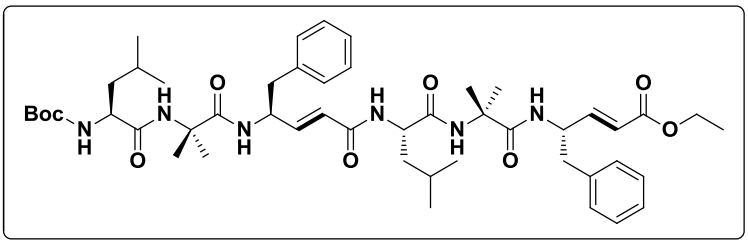

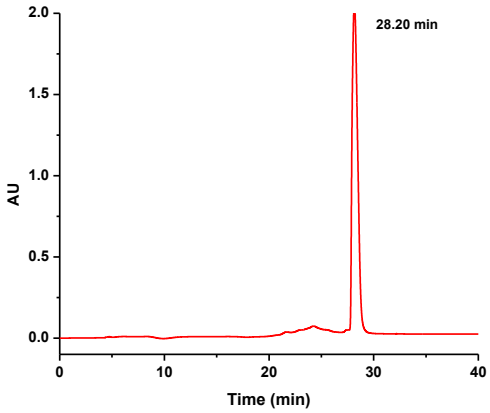

Fig 1.29: Reverse phase HPLC profile of peptide **P1**(λ = 220 nm). MeOH/H_2O was used as solvent system at a flow rate of 1.00 mL/min.

Boc-Leu-Aib-dγAla-Leu-Aib-dγAla-OEt (P2): White color solid; Yield 72%; ^{1}H NMR (400 MHz, $CDCl_3$) δ 7.09 (d, *J* = 8 Hz, 1H), 7.01 (d, *J* = 8 Hz, 1H), 6.93 (d, *J* = 4 Hz, 1H), 6.89 (d, *J* = 4 Hz, 1H), 6.80 (d, *J* = 4 Hz, 1H), 6.76 (d, *J* = 4 Hz, 1H), 6.72 (d, *J* = 8 Hz, 1H), 6.58 (s, 1H), 6.57 (s, 1H), 6.14 (d, *J* = 16 Hz, 1H), 5.93 (d, *J* = 16 Hz, 1H), 5.08 (d, *J* = 4 Hz, 1H), 4.70-4.60 (m, 2H), 4.20-4.12 (m, 4H), 3.92-3.87 (m, 1H), 1.74-1.47 (m, 22H), 1.44 (s, 9H), 1.29-1.21 (m, 11H), 0.98-0.91 (m, 15H); HR-MS *m/z* calculated value for $C_{37}H_{64}N_6O_9$ [M+Na$^+$] 759.4632, observed 759.4623.

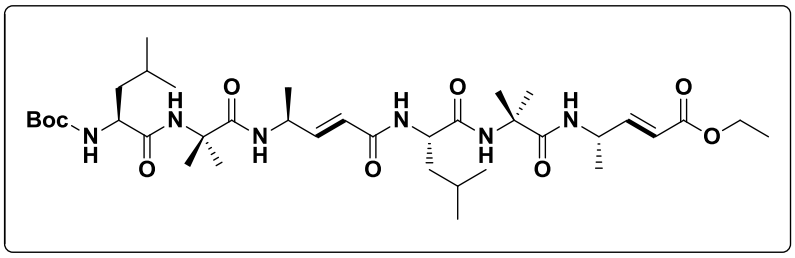

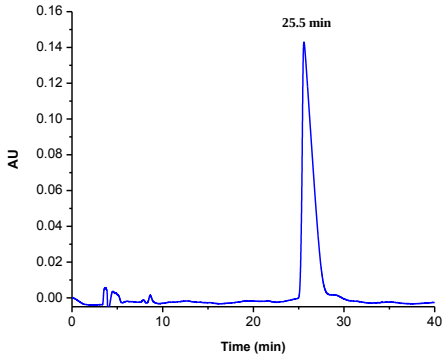

Fig 1.30: Reverse phase HPLC profile of peptide **P2** (λ = 220 nm). MeOH/H_2O was used as solvent system at a flow rate of 1.00 mL/min.

Transformation of β-miniature peptides into their saturated analogs of 10/12-helices through catalytic hydrogenation: Boc-Leu-Aib-dγX-Leu-Aib-dγX-OEt (0.10 mmol, 100 mg) was dissolved in EtOH (4 mL), and was treated with 20 mg of 20% Pd/C. The hydrogen gas was supplied through balloon. The reaction mixture was stirred under hydrogen atmosphere for about 5 h. The completion of the reaction was monitored by MALDI-TOF/TOF and RP-HPLC. After the completion of reaction, the reaction mixture was diluted with EtOH (10 mL) and it was filtered through sintered funnel using celite bed and celite bed was washed with

EtOH (3 × 15 mL). The filtrate was evaporated under *vacuum* to get white crystalline pure product.

Boc-Leu-Aib-γPhe-Leu-Aib-γPhe-OEt (P3): White color solid; Yield 90%; ^{1}H NMR (500 MHz, $CDCl_3$) δ 7.92 (bs, 1H), 7.62 (bs, 1H), 7.40 (d, *J* = 15 Hz), 7.29-7.10 (m, 11H), 6.92-6.90 (m, 2H), 6.74-6.63 (m, 2H), 5.53 (bs, 1H), 4.36-4.27 (m, 1H), 4.12-4.04 (m, 3H), 3.89-3.80 (m, 2H), 2.96-2.64 (m, 4H), 2.53-2.35 (m, 5H), 2.23-2.17 (m, 3H), 1.94-1.85 (m, 3H), 1.72-1.67 (m, 2H), 1.57 (s, 3H), 1.49 (s, 9H), 1.42 (s, 3H), 1.30 (s, 3H), 1.22 (t, *J* = 5 Hz, 3H), 1.02 (s, 3H), 0.98-0.88 (m, 12H); HR-MS *m/z* calculated value for $C_{49}H_{76}N_6O_9$ [M+Na$^+$] 915.5571, observed 915.5574.

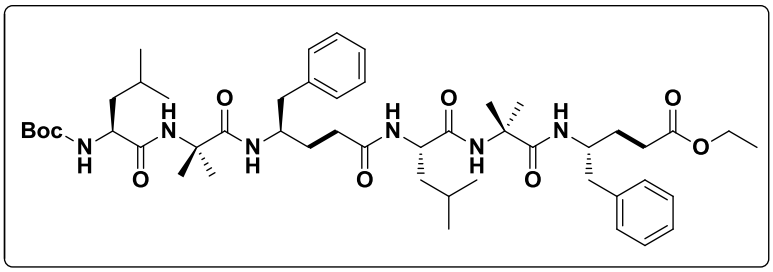

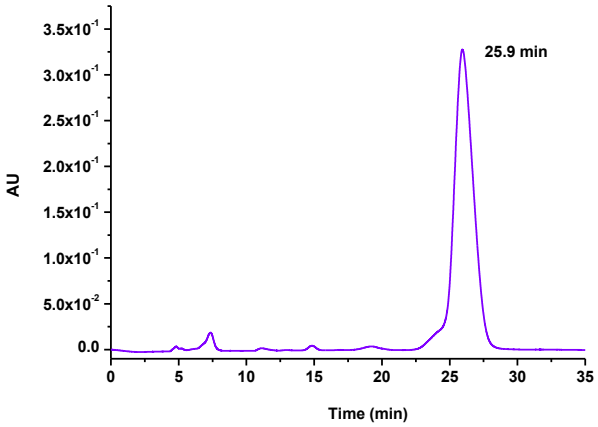

Fig 1.31: Reverse phase HPLC profile of peptide **P3**. MeOH/H_2O was used as solvent system at a flow rate of 1.00 mL/min.

Boc-Leu-Aib-γAla-Leu-Aib-γAla-OEt (P4): White color solid; Yield 95%; ^{1}H NMR (400 MHz, $CDCl_3$) δ 8.03 (s, 1H), 7.15 (s, 1H), 7.08 (s, 1H), 6.83 (d, *J* = 10 Hz, 1H), 6.63 (s, 1H), 5.10 (d, *J* = 5 Hz, 1H), 4.13-4.06 (m, 2H), 4.03-3.86 (m, 5H), 2.55-2.34 (m, 4H), 2.16-2.13 (m, 1H), 2.03-1.97 (m, 1H), 1.86-1.73 (m, 10H), 1.60 (s, 3H), 1.53 (s, 3H), 1.48 (s, 9H), 1.44 (s, 3H), 1.37 (s,

3H), 1.23 (t, J = 5 Hz), 1.14 (d, J = 5 Hz, 3H), 1.04 (d, J = 5 Hz, 3H), 1.00-0.90 (m, 14H); HR-MS *m/z* calculated value for $C_{37}H_{68}N_6O_9$ [M+Na$^+$] 763.4945, observed 763.4940.

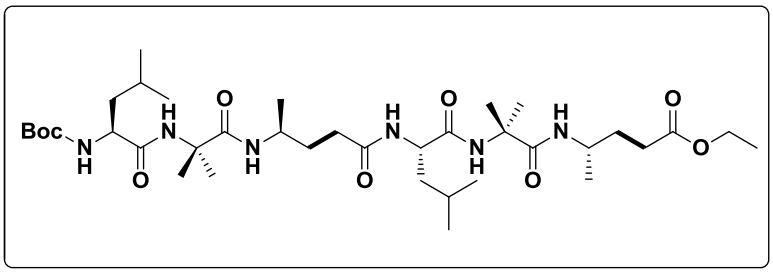

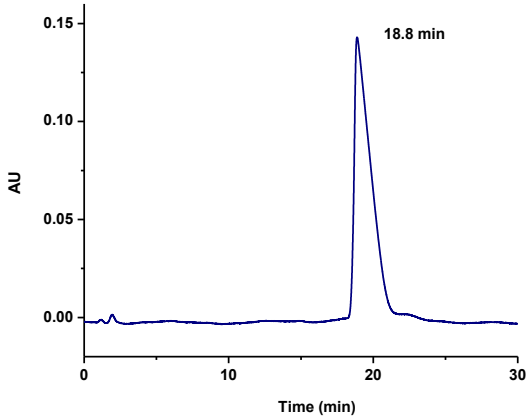

Fig 1.32: Reverse phase HPLC profile of peptide **P4**. MeOH/H_2O was used as solvent system at a flow rate of 1.00 mL/min.

Ac-Aib-γPhe-Ala-dγVal-Aib-γPhe-Aib-CONH$_2$ (P5) : ^{1}H NMR (400 MHz, DMSO-d_6) δ 8.19 (s, 1H), 8.00 (d, J = 12Hz, 1H), 7.95 (s, 1H), 7.82 (d, J = 16 Hz, 1H), 7.77 (d, J = 8Hz, 1H), 7.60 (s, 1H), 7.52 (d, J = 12Hz, 1H), 7.40 (d, J = 12Hz, 1H), 7.22-7.11 (m, 10H), 6.72 (s, 1H), 6.60 (dd, J = 8 Hz, J =8 Hz, 1H), 6.04 (d, J = 16 Hz, 1H), 4.36-4.10 (m, 2H), 3.91 (m, 1H), 2.65 (m, 2H), 2.20-1.99 (m, 4H), 1.87-1.47 (m, 8H), 1.29-1.15 (m, 22H), 0.80 (m, 8H); HRMS *m/z* calculated value for $C_{46}H_{68}N_8O_8$ [M+Na$^+$] is 883.5052 and observed 883.5010.

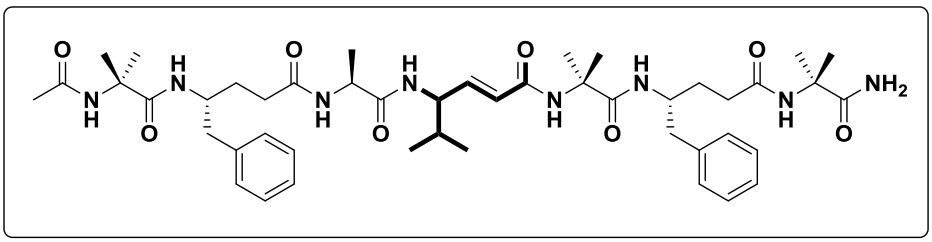

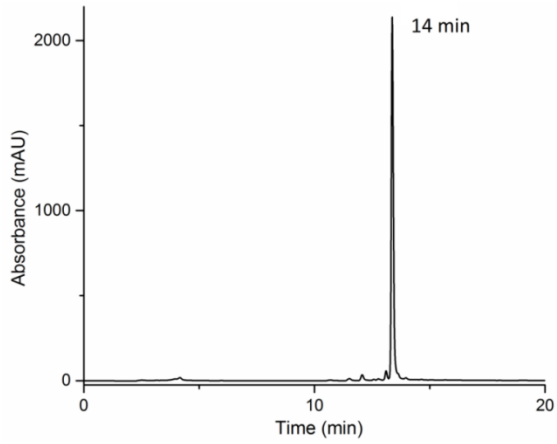

Fig 1.33: Reverse phase HPLC profile of peptide **P5**. MeOH/H_2O was used as solvent system at a flow rate of 1.00 mL/min.

1.8 References

1. Linderstrom-Lang, K. U.; Schellman, J. A. (**1959**), *The Enzymes*, (P. D. Boyer, Ed.), *Vol. 1*, 2nd ed., pp. 443-510. Academic Press, New York.
2. Ramachandran, G. N.; Sasisekaran, V. *Advan. Protein Chem*. **1968**, *23*, 283-437.
3. Pauling, L.; Corey, R. B.; Branson, R. *Proc. Nat. Acad. Sci. USA*, **1951**, *37*, 205.
4. Pauling, L.; Corey, R. B. *Proc. Nat. Acad. Sci. USA* **1951**, *37*, 729.
5. Venkatachalam, C. M. *Biopolymers* **1968**, *6*, 1425.
6. (a) Sibanda, B. L.; Blundell, T. L.; Thorton, J. M. *Nature(London)***1985**, *316*, 170. (b) Milner-White, J.; Poet, R. *Biochemical Journal* **1986**, *240*, 289.
7. T. E. Creighton, *Proteins: structure and molecular properties* 2nd Ed., W. H. Freeman and Co., New York, **1993**, p. 227.
8. (a) Shotton, D. M.; Watson, H. C. *Nature* **1970**, *225*, 811. (b) Matthews, B. W.; Remington, S. J. *Proc. Nat. Acad. Sci. USA*, **1974**, *71*, 4178. (c) Rossmann, M. G.; Adams, M. J.; Buehner, M.; Ford, G. C.; Hackert, M. L.; Lentz, Jr. P. J.; McPherson, Jr. A, Schevitz, R. W.; Smiley, I. E. *Cold SpringHarbor Symp. Quant. Biol*. **1971**, *36*, 179. (d) Woolfson, D. N.; Bartlett, G. J.; Burton, A. J.; Heal, J. W.; Niitsu, A.; Thomson, A. R.; Wood, C. W. *Curr. Opin. Struct. Biol*. **2015**, *33*, 16.
9. (a) Balaji, S. *Curr. Opin. Struct. Biol*. **2015**, *32*, 156. (b) Wimley, W. C. *Curr. Opin. Struct. Biol.* **2003**, *13*, 404. (c) Schulz, G. E. *Curr. Opin. Struct. Biol*. **2000**, *10*, 443. (d) Zhang, C.;

Kim, S.-H. *J. Mol. Biol*. **2000**, *299*, 1075. (e) Murzin, A. G. *Proteins* **1992**, *14*, 191. (f) Murzin, A.; Lesk, A.; Chothia, C. *J. Mol. Biol*. **1994**, *236*, 1369.

10. (a) Lupas, A. N.; Gruber, M. *Adv. Protein. Chem.* **2005**, *70*, 37. (b) Woolfson, D. N. *Adv. Protein. Chem*. **2005**, *70*, 79; (c) Scholtz, J. M.; Baldwin, R. L. *Annu. Rev*. *Biophys. Biomol. Struct*. **1992**, *21*, 95. (d) Rackham, O. J. L.; Madera, M.; Armstrong, C. T.; Vincent, T. L.; Woolfson, D. N.; Gough, J. *J. Mol. Biol*. **2010**, *403*, 480.
11. Crick, F. H. C. *Acta Crystallogr*. **1953**, *6*, 689.
12. (a) Fraser, R. D. B.; MacRae, T. P. *Nature* **1971**, *233*, 138. (b) Parry, D. A. D.; Crewther, W. G.; Fraser, R. D. B.; MacRae, T. P. *J. Mol. Biol*. **1977**, *113*, 449. (c) Caspar, D. L. D.; Cohen, C.; Longley, W. *J. Mol. Biol*. **1969**, *41*, 87.
13. (a) Ramachandran, G. N.; Chandrasekaran, R. *Progress in Peptide Research*. Lande, S., Ed.; Gordon & Breach: New York, 1972; Vol. II (Proceedings of the Second American Peptide Symposium, Cleveland, 1970), p 195. (b) Marshall, G. R.; Bosshard, H. E. *Circ. Res*. **1972**, *31*, 143. (c) Toniolo, C.; Benedetti, E. *ISI Atlas Sci. Biochem*. **1988**, *1*, 225. (d) Bosch, R.; Schmitt, H.; Jung, G.; Winter, W. *Biopolymers* **1985**, *24*, 961. (e) Karle, I. L.; Balaram, P. *Biochemistry* **1990**, *29*, 6747. (f) Marshall, G. R.; Hodgkin, E. E.; Langs, D. A.; Smith, G. D.; Zabrocki, J.; Leplawy, M. T. *Proc. Natl. Acad. Sci. U.S.A.* **1990**, *87*, 487. (g) Toniolo, C.; Benedetti, E. *Trends Biochem. Sci*. **1991**, *16*, 350. (h) Karle, I. L. *Acc. Chem. Res*. **1999**, *32*, 693. (i) Kaul, R.; Balaram, P. *Bioorg. Med. Chem*. **1999**, *7*, 105. (j) Balaram, P. *J. Pept. Res*. **1999**, *54*, 195. (k) Venkatraman, J.; Shankaramma, S. C.; Balaram, P. *Chem. Rev*. **2001**, *101*, 3131.
14. (a) Frackenpohl , J.; Arvidsson , P. I.; Schreiber , J. V.; Seebach , D. *ChemBioChem* **2001** , *2* , 445. (b) Goodman, C. M.; Choi, S.; Shandler, S.; DeGrado, W.F. *Nat. Chem. Biol*. **2007**, *3*, 252.
15. (a) Arvidsson, P. I.; Rueping, M.; Seebach, D. *Chem. Commun*. **2001**, 649. (b) Appella, D. H.; Christianson, L. A.; Klein, D. A.; Powell, D. R.; Huang, X. L.; Barchi J. J.; Gellman, S. H. *Nature* **1997**, *387*, 381.
16. (a) Sharma, G. V. M.; Reddy, V. G.; Chander, A. S.; Reddy, K. R. *Tetrahedron: Asymmetry* **2002**, *13*, 21. (b) Sharma, G. V. M.; Reddy, K. R.; Krishna, P. R.; Sankar, A. R.; Narsimulu, K.; Kumar, S. K.; Jayaprakash, P.; Jagannadh, B.; Kunwar, A. C. *J. Am. Chem. Soc*. **2003**,

125, 13670; (c) Sharma, G. V. M.; Reddy, K. R.; Krishna, P. R.; Sankar, A. R.; Jayaprakash, P.; Jagannadh, B.; Kunwar, A. C. *Angew. Chem., Int. Ed*. **2004**, *43*, 3961.

17. (a) Pilsl, L. K. A.; Reiser, O. *Amino Acids* **2011**, *41*, 709. (b) De Pol, S.; Zorn, C; Klein, C. D.; Zerbe, O.; Reiser, O. *Angew. Chem., Int. Ed*. **2004**, *43*, 511.
18. Fernandes, C.; Faure, S.; Pereira, E.; Thery, V.; Declerck, V.; Guillot, R.; Aitken, D. J. *Org. Lett*. **2010**, *12*, 3606.
19. (a) Hetenyi, A.; Mandity, I. M.; Martinek, T. A.; Toth, G. K.; Fulop, F. *J. Am. Chem. Soc*. **2005**, *127*, 547. (b) Mandity, I. M.; Weber, E.; Martinek, T. A.; Olajos, G.; Toth, G. K.; Vass E.; Fulop, F. *Angew. Chem., Int. Ed*. **2009**, *48*, 2171. (c) Martinek, T. A.; Toth, G. K.; Vass, E.; Hollosi, M.; Fulop, F. *Angew. Chem., Int. Ed*. **2002**, *41*, 1718. (d) Martinek, T. A.; Mandity, I. M.; Fulop, L.; Toth, G. K.; Vass, E.; Hollosi, M.; Forro, E.; Fulop, F. *J. Am. Chem. Soc*. **2006**, *128*, 13539.
20. (a) Gellman, S. H. *Acc. Chem. Res.* **1998**, *31*, 173. (b) Hill, D. J.; Mio, M. J.; Prince, R. B.; Hughes, T. S.; Moore, J. S. *Chem. Rev*. **2001**, *101*, 3893. (c) Cheng, R. P.; Gellman, S. H.; DeGrado, W. F. *Chem. Rev*. **2001**, *101*, 3219. (d) Venkatraman, J.; Shankaramma, S. C.; Balaram, P. *Chem. Rev*. **2001**, *101*, 3131. (e) Seebach, D.; Beck, A. K.; Bierbaum, D. J. *Chem. Biodiversity* **2004**, *1*, 1111. (f) Hecht, S.; Huc, I. *Foldamers: Structure, Properties and Applications*; Wiley-VCH: Weinheim, **2007**. (g) Seebach, D.; Gardiner, J. *Acc. Chem. Res.* **2008**, *41*, 1366. (h) Cummings, C. G.; Hamilton, A. D. *Curr. Opin. Chem. Biol*. **2010**, *14*, 341.
21. (a) Petersson, E. J.; Schepartz, A. *J. Am. Chem. Soc*. **2008**, *130*, 821. (b) Price, J. L.; Horne, W. S.; Gellman, S. H. *J. Am. Chem. Soc*. **2010**, *132*, 12378.
22. (a) Arvidsson, P. I.; Rueping, M.; Seebach, D. *Chem. Commun*. **2001**, 649. (b) Appella, D. H.; Christianson, L. A.; Klein, D. A.; Powell, D. R.; Huang, X. L.; Barchi J. J.; Gellman, S. H. *Nature* **1997**, *387*, 381. (c) Seebach, D.; Schreiber, V. J.; Abele, S.; Daura, X.; Gunsteren, F. W. *Helv. Chim. Acta* **2000**, *83*, 34. (d) Daura, X.; Bakowies, D.; Seebach, D.; Fleischhauer, J.; van Gunsteren, W. F.; Kruger, P. *Eur. Biophys. J*. **2003**, *32*, 661. (e) Hetenyi, A.; Mandity, I. M.; Martinek, T. A.; Toth, G. K.; Fulop, F. *J. Am. Chem. Soc*. **2005**, *127*, 547. (f) Threlfall, R. ; Davies, A. ; Howarth, N.M. ; Fisher, J. ; Cosstick, R. *Chem. Commun*. **2008**, 585. (g) Rua, F.; Boussert, S.; Parella, T.; Diez-Perez, I.; Branchadell, V.; Giralt, E.; Ortuno, R. M. *Org. Lett*. **2007**, *9*, 3643. (h) Arvidsson, P. I.;

Ryder, N. S.; Weiss, H. M.; Gross, G.; Kretz, O.; Woessner, R.; Seebach, D. *ChemBioChem* **2003**, *4*, 1345. (i) Mandity, I. M.; Weber, E.; Martinek, T. A.; Olajos, G.; Toth, G. K.; Vass E.; Fulop, F. *Angew. Chem., Int. Ed*. **2009**, *48*, 2171. (j) Seebach, D.; Abele, S.; Gademann, K.; Jaun, B. *Angew. Chem., Int. Ed*. **1999**, *38*, 1595. (k) Martinek, T. A.; Toth, G. K.; Vass, E.; Hollosi, M.; Fulop, F. *Angew. Chem., Int. Ed*. **2002**, *41*, 1718. (l) Martinek, T. A.; Mandity, I. M.; Fulop, L.; Toth, G. K.; Vass, E.; Hollosi, M.; Forro, E.; Fulop, F. *J. Am. Chem. Soc*. **2006**, *128*, 13539.

23. (a) Roy, R. S.; Karle, I. L.; Raghothama, S.; Balaram, P. *Proc. Natl. Acad. Sci. USA* **2004**, *101*, 16478. (b) Karle, I. L.; Pramanik, A.; Banerjee, A.; Bhattacharjya, S.; Balaram, P. *J. Am. Chem. Soc.* **1997**, *119*, 9087. (c) De Pol, S.; Zorn, C.; Klein, C. D.; Zerbe, O.; Reiser, O. *Angew. Chem., Int. Ed.* **2004**, *43*, 511–514. (d) Hayen, A.; Schmitt, M. A.; Ngassa, F. N.; Thomasson, K. A.; Gellman, S. H. *Angew. Chem., Int. Ed.* **2004**, *43*, 505–510. (e) Schmitt, M. A.; Choi, S. H.; Guzei, I. A.; Gellman, S. H. *J. Am. Chem. Soc.* **2005**, *127*, 13130-13131. (f) Schmitt, M. A.; Choi, S. H.; Guzei, I. A.; Gellman, S. H. *J. Am. Chem. Soc.* **2006**, *128*, 4538-4539.

24. (a) Hayen, A.; Schmitt, M. A.; Ngassa, F. N.; Thomasson, K. A.; Gellman, S. H. *Angew. Chem., Int. Ed*. **2004**, *43*, 505. (b) Choi, S. H.; Guzei, I. A.; Spencer, L. C.; Gellman, S. H. *J. Am. Chem. Soc*. **2008**, *130*, 6544. (c) Legrand, B.; Andre, C.; Moulat, L.; Wenger, E.; Didierjean, C.; Aubert, E.; Averlant-Petit, M. C.; Martinez, J.; Calmes, M.; Amblard, M. *Angew. Chem., Int. Ed*. **2014**, *53*, 13131. (d) Schmitt, M. A.; Choi, S. H.; Guzei, I. A.; Gellman, S. H. *J. Am. Chem. Soc*. **2006**, *128*, 4538. (e) Mándity, I. M.; Weber, E.; Martinek, T. A.; Olajos, G.; Tóth, G. K.; Vass, E.; Fülöp, F. *Angew. Chem., Int. Ed*. **2009**, *48*, 2171. (f) Sharma, G. V. M.; Reddy, K. R.; Krishna, P.R.; Sankar, A. R.; Narasimulu, K.; Kumar, S. K.; Jayaprakash, P.; Jagannadh, B.; Kunwar, A. C. *J. Amer. Chem. Soc*. **2003**, *125*, 13670. (g) Sharma, G. V. M.; Reddy, K. R.; Krishna, P. R.; Sankar, A. R.; Jayaprakash, P.; Jagannadh, B.; Kunwar, A. C. *Angew. Chem., Int. Ed. Engl*. **2004**, *43*, 3961. (h) Sharma, G. V. M.; Nagendar, P.; Krishna, P. R.; Ramakrishna K. V. S.; Jayaprakash, P.; Kunwar, A. C. *Angew. Chem., Int. Ed. Engl*. **2005**, *44*, 5878. (i) Sharma, G. V. M.; Subash, V.; Narasimulu, K.; Sankar, A. R.; Kunwar, A. C. *Angew. Chem. Int. Ed. Engl*. **2006**, *45*, 8207. (j)Horne, W. S.; Price, J. L.; Keck, J. L.; Gellman, S. H. *J. Am. Chem. Soc*. **2007**, *129*, 4178. (k) Giuliano, M. W.; Horne, W. S.; Gellman, S. H. *J. Am. Chem. Soc*. **2009**, *131*, 9860.

25. (a) Hamuro, Y.; Schneider, J. P.; DeGrado, W. F. *J. Am. Chem. Soc*. **1999**, *121*, 12200. (b) Karlsson, A. J.; Pomerantz, W. C.; Weisblum, B.; Gellman, S. H.; Palecek, S. P. *J. Am. Chem. Soc*. **2006**, *128*, 12630.
26. Gademann, K.; Seebach, D. *Helv. Chim. Acta* **2001**, *84*, 2924.
27. (a) Gademann, K.; Ernst, M.; Hoyer, D.; Seebach, D. *Angew. Chem. Int. Ed*. **1999**, *38*, 1223. (b) Gademann, K.; Ernst, M.; Seebach, D.; Hoyer, D. *Helv. Chim. Acta* **2000**, *83*, 16. (c) Gademann, K.; Kimmerlin, T.; Hoyer, D.; Seebach, D. *J. Med. Chem*. **2001**, *44*, 2460.
28. Kritzer, J. A.; Lear, J. D.; Hodsdon, M. E.; Schepartz, A. *J. Am. Chem. Soc*. **2004**, *126*, 9468.
29. Stephens, O. M.; Kim, S.; Welch, B. D.; Hodsdon, M. E.; Kay, M. S.; Schepartz, A. *J. Am. Chem. Soc.* **2005**, *127*, 13126.
30. English, E. P.; Chumanov, R. S.; Gellman, S. H.; Compton, T. *J. Biol. Chem.* **2006**, *281*, 2661.
31. (a) Liu, R.; Chen, X.; Falk, S. P.; Mowery, B. P.; Karlsson, A. J.; Weisblum, B.; Palecek, S. P.; Masters, K. S.; Gellman, S. H. *J. Am. Chem. Soc*. **2014**, *136*, 4333. (b) Liu, R.; Chen, X.; Falk, S. P.; Masters, K. S.; Weisblum, B.; Gellman, S. H. *J. Am. Chem. Soc*. **2015**, *137*, 2183.
32. (a) Martinek, T. A.; Hetenyi, A.; Fulop, L.; Mandity, I. M.; Toth, G. K.; Dekany, I.; Fulop, F. *Angew.Chem., Int. Ed*. **2006**, *45*, 2396. (b) Mándity, I. M.; Fülöp, L.; Vass, E.; Tóth, G. K.; Martinek, T. A.; Fulop, F. *Org. Lett*. **2010**, *12*, 5584.
33. Kwon, S.; Shin, H. S.; Gong, J.; Eom, J-. H.; Jeon, A.; Yoo, S. H.; Chung, I. S.; Cho, S. J.; Lee, H-. S. *J. Am. Chem. Soc*. **2011**, *133*, 17618.
34. Rua, F.; Boussert, S.; Parella, T.; Diez-Perez, I.; Branchadell, V.; Giralt, E.; Ortuno, R. M. *Org. Lett*. **2007**, *9*, 3643.
35. (a) Balamurugan, D.; Muraleedharan, K. M. *Soft Matter*. **2012**, *8*, 11857. (b) Balamurugan, D.; Muraleedharan, K. M. *Chem. Eur. J*., **2012**, *18*, 9516.
36. (a) Montenegro, J.; Ghadiri, M. R.; Granja, J. R. *Acc. Chem. Res*. **2013**, *46*, 2955. (b) Bonetti, A.; Pellegrino, S.; Das, P.; Yuran, S.; Bucci, R.; Ferri, N.; Meneghetti, F.; Castellano, C.; Reches, M.; Gelmi, M. L. *Org. Lett*. **2015**, *17*, 4468.
37. Hintermann, T.; Gademann, K.; Jaun, Seebach, D. *Helv. Chim. Acta.* **1998**, *81*, 893.
38. Hanessian, S.; Luo, X.; Schaum, R.; Michnick, S. *J. Am. Chem. Soc.* **1998**, *120*, 8569.

39. (a) Baldauf, C.; Gunther, R.; Hofmann, H. J. *Helv. Chim. Acta*. **2003**, *86*, 2573. (b) Baldauf, C.; Gunther, R.; Hofmann, H. -J. *J. Org. Chem.* **2006**, *71*, 1200.
40. Basuroy, K.; Dinesh, B.; Reddy, M. B. M.; Chandrappa, S.; Raghothama, S.; Shamala, N.; Balaram, P. *Org. Lett*. **2013**, *15*, 4866.
41. Vasudev, P. G.; Shamala, N.; Ananda, K.; Balaram, P. *Angew. Chem., Int. Ed*. **2005**, *44*, 4972.
42. (a) Sharma, G. V. M.; Jayaprakash, P.; Narsimulu, K.; Sankar, A. R.; Reddy, K. R.; Kunwar, A. C. *Angew. Chem. Int. Ed.* **2006**, *45*, 2944. (b) Sharma, G. V. M.; Reddy, K. R.; Krishna, P.R.; Sankar, A. R.; Narasimulu, K.; Kumar, S. K.; Jayaprakash, P.; Jagannadh, B.; Kunwar, A. C. *J. Amer. Chem. Soc*. **2003**, *125*, 13670. (c) Sharma, G. V. M.; Subash, V.; Narasimulu, K.; Sankar, A. R.; Kunwar, A. C. *Angew. Chem. Int. Ed. Engl*. **2006**, *45*, 8207. (d) G. V. M. Sharma.; Thodupunuri, P.; Sirisha, K.; Basha, S. J.; Reddy, P. G.; Sarma, A. V. S. *J. Org. Chem.* **2014**, *79*, 8614.
43. (a) Giuliano, M. W.; Maynard, S. J.; Almeida, A. M.; Guo, L.; Guzei, L. A.; Spencer, L. C.; Gellman, S. H. *J. Am. Chem. Soc*. **2014**, *136*, 15046. (b) Fisher, B. F.; Guo, L.; Dolinar, B. S.; Guzei, L. A.; Gellman, S. H. *J. Am. Chem. Soc*. **2015**, *137*, 6484.
44. Khurram, M.; Qureshi, N.; Smith, M. D. *Chem. Commun*. **2006**, 5006.
45. (a) Lee, X.; Yang, D. *Chem. Commun*. **2006**, 3367. (b) Chen, F.; Zhu, N.-Y.; Yang, D. *J. Am. Chem. Soc.* **2004**, *126*, 15980.
46. Cheguillaume, A.; Salaun, A.; Sinbandhit, S.; Potel, M.; Gall, P.; Baudy-Floch, M.; Le Grel, P. *J. Org. Chem.* **2001**, *66*, 4923.
47. (a) Pendem, N.; Nelli, Y. R.; Douat, C.; Fischer, L.; Laguerre, M.; Ennifar, E.; Kauffman, B.; Guichard, G. *Angew. Chem. Int. Ed*. **2013**, *52*, 4147. (b) Collie, G. W.; Pulka-Ziach, K.; Lombardo, C. M.; Fremaux, J.; Rosu, F.; Decossas, M.; Mauran, L.; Lambert,O.; Gabelica, V.; Mackereth, C. D.; Guichard, G. *Nature Chemistry* **2015**, *7*, 871.
48. Mathieu, L.; Legrand, B.; Deng, C.; Vezenkov, L.; Wenger, E.; Didierjean, C.; Amblard, M.; Averlant-Petit, M. C.; Masurier, N.; Lisowski, V.; Martinez, J.; Maillard, L. T. *Angew. Chem. Int. Ed*. **2013**, *52*, 6006.
49. Hagihara, M.; Schreiber, S. L. *J. Am. Chem. Soc*. **1992**, *114*, 6570.
50. Linington, R. G.; Clark, B. R.; Trimble, E. E.; Almanza, A.; Uren, L.-D.; Kyle, D. E.; Gerwick, W. H. *J. Nat. Prod*. **2009**, *72*, 14.

51. Nakao, Y.; Fujita, M.; Warabi, K.; Matsunaga, S.; Fusetani, N. *J. Am. Chem. Soc*. **2000**, *122*, 10462.
52. (a) Hanzlik, R. P.; Thompson, S. A. *J. Med. Chem*. **1984**, *27*, 711. (b) Bastiaans, H. M. M.; Van der Baan, J. L.; Ottenheijm, H. C. J. *J. Org. Chem*. **1997**, *62*, 3880. (c) Liu, S.; Hanzlik, R. P. *J. Med. Chem*. **1992**, *35*, 1067. (d) Kong, J-S.; Venkatraman, S.; Furness, K.; Nimkar, S.; Shepherd, T. A.; Wang, Q. M.; Aube, J.; Hanzlik, R. P. *J. Med. Chem*. **1998**, *41*, 2579. (e) Schaschke, N.; Sommerhoff, C. P. *ChemMedChem* **2010**, *5*, 367.
53. Hagihara, M.; Anthony, N. J.; Stout, T. J.; Clardy, J.; Schreiber, S. L. *J. Am. Chem. Soc*. **1992**, *114*, 6568.
54. Chakraborty, T. K.; Ghosh, A.; Kumar, S. K.; Kunwar, A. C. *J. Org. Chem*. **2003**, *68*, 6459.
55. Baldauf, C.; Gunther, R.; Hofmann, H.-J. *J. Org. Chem*. **2005**, *70*, 5351.
56. (a) Bandyopadhyay, A.; Mali, S. M.; Lunawat, P.; Raja, K. M. P.; Gopi, H. N. *Org. Lett*. **2011**, *13*, 4482. (b) Bandyopadhyay, A.; Gopi, H. N. *Org. Lett*. **2012**, *14*, 2770.
57. Mali, S. M.; Bandyopadhyay, A.; Jadhav, S. V.; Ganesh Kumar, M.; Gopi, H. N. *Org. Biomol. Chem*. **2011**, *9*, 6566.
58. (a) Karle, I. L.; Balaram, P. *Biochemistry* **1990**, *29*, 6747; (b) Toniolo, C.; Crisma, M.; Formaggio, F.; Peggion, C. *Biopolymers* **2001**, *60*, 396.
59. (a) Chatterjee, S.; Vasudev, P. G.; Raghothama, S.; Ramakrishnan, C.; Shamala, N.; Balaram, P. *J. Am. Chem. Soc*. **2009**, *131*, 5956. (b) Guo, L.; Chi, Y.; Almeida, A. M.; Guzei, I. A.; Parker, B. K.; Gellman, S. H. *J. Am. Chem. Soc*. **2009**, *131*, 16018. (c) Bandyopadhyay, A.; Jadhav, S. V.; Gopi, H. N. *Chem. Commun*. **2012**, *48*, 7170.
60. Basuroy, K.; Dinesh, B.; Shamala, N.; Balaram, P. *Angew. Chem., Int. Ed*. **2013**, *52*, 3136.
61. (a) Bandyopadhyay, A.; Gopi, H. N. *Org. Lett*. **2012**, *14*, 2770. (b) Bandyopadhyay, A.; Jadhav, S. V.; Gopi, H. N. *Chem. Commun*. **2012**, *48*, 7170. (c) Jadhav, S. V.; Bandyopadhyay, A.; Gopi, H. N. *Org. Biomol. Chem*. **2013**, *11*, 509.
62. (a) SHELXS-97: G. M. Sheldrick, *Acta Crystallogr. Sect A*, **1990**, *46*, 467. (b) M.Sheldrick, G. SHELXL-97, UniversitätGöttingen (Germany) 1997.
63. Spek, A. L. *ActaCryst*. **1990,** A46, C34.

1.9 Appendix I: Characterization Data of Synthesized Compounds

Designation	Description	Page
Boc-dγPhe-OEt (**1**)	^{1}H & ^{13}C NMR	59
Boc-dγAla-OEt (**2**)	^{1}H & ^{13}C NMR	60
Boc-Leu-Aib-dγPhe-OEt (**T1**)	^{1}H & ^{13}C NMR	61
Boc-Leu-Aib-dγAla-OEt (**T2**)	^{1}H & ^{13}C NMR	62
Boc-Leu-Aib-dγPhe-Leu-Aib-dγPhe-OEt (**P1**)	^{1}H NMR	63
Boc-Leu-Aib-dγAla-Leu-Aib-dγAla-OEt (**P2**)	^{1}H NMR	63
Boc-Leu-Aib-γPhe-Leu-Aib-γPhe-OEt (**P3**)	^{1}H NMR	64
Boc-Leu-Aib-γAla-Leu-Aib-γAla-OEt (**P4**)	^{1}H NMR	64
Ac-Aib-γPhe-Ala-dγVal-Aib-γPhe-Aib-CONH2 (**P5**)	^{1}H NMR	65
	& MALDI-TOF/TOF spectrum	65

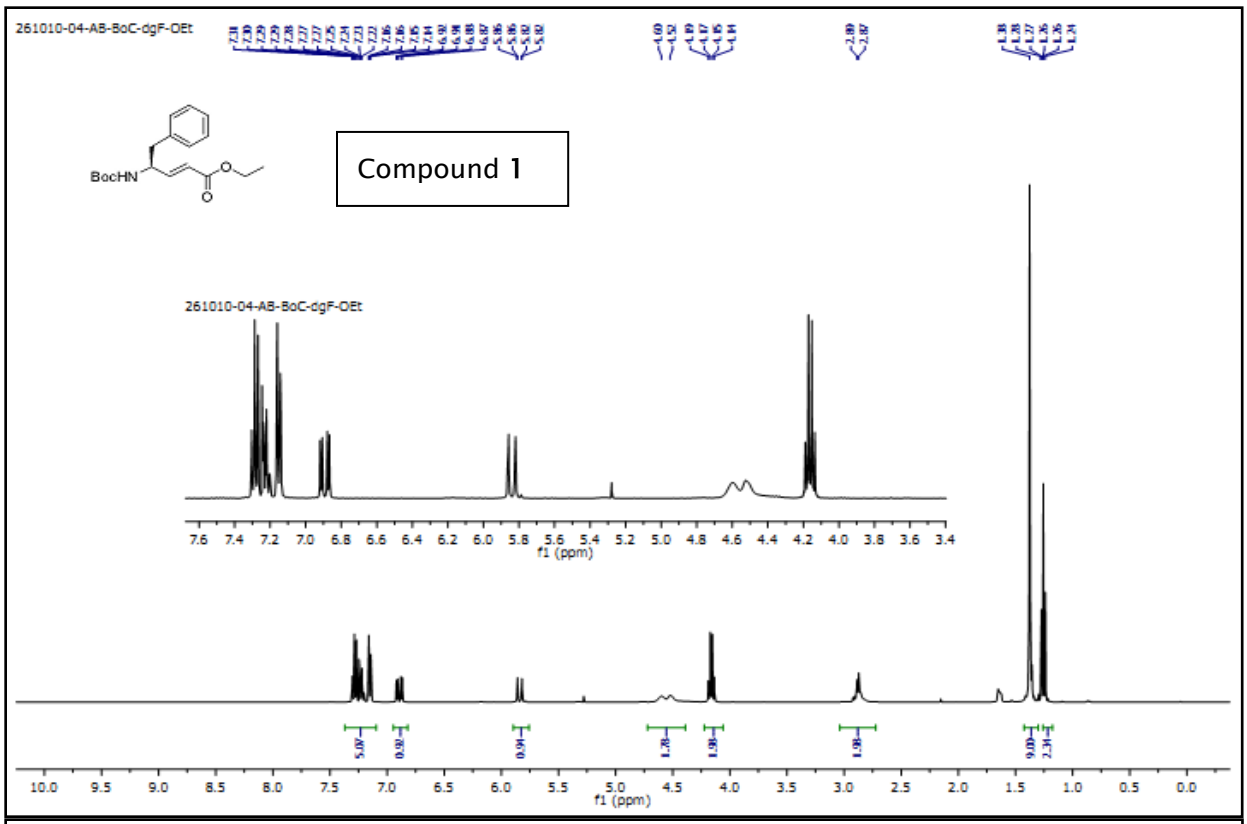
261010-04-AB-BoC-dgF-OEt
BocHN
Compound 1
261010-04-AB-BoC-dgF-OEt
f1 (ppm)
f1 (ppm)

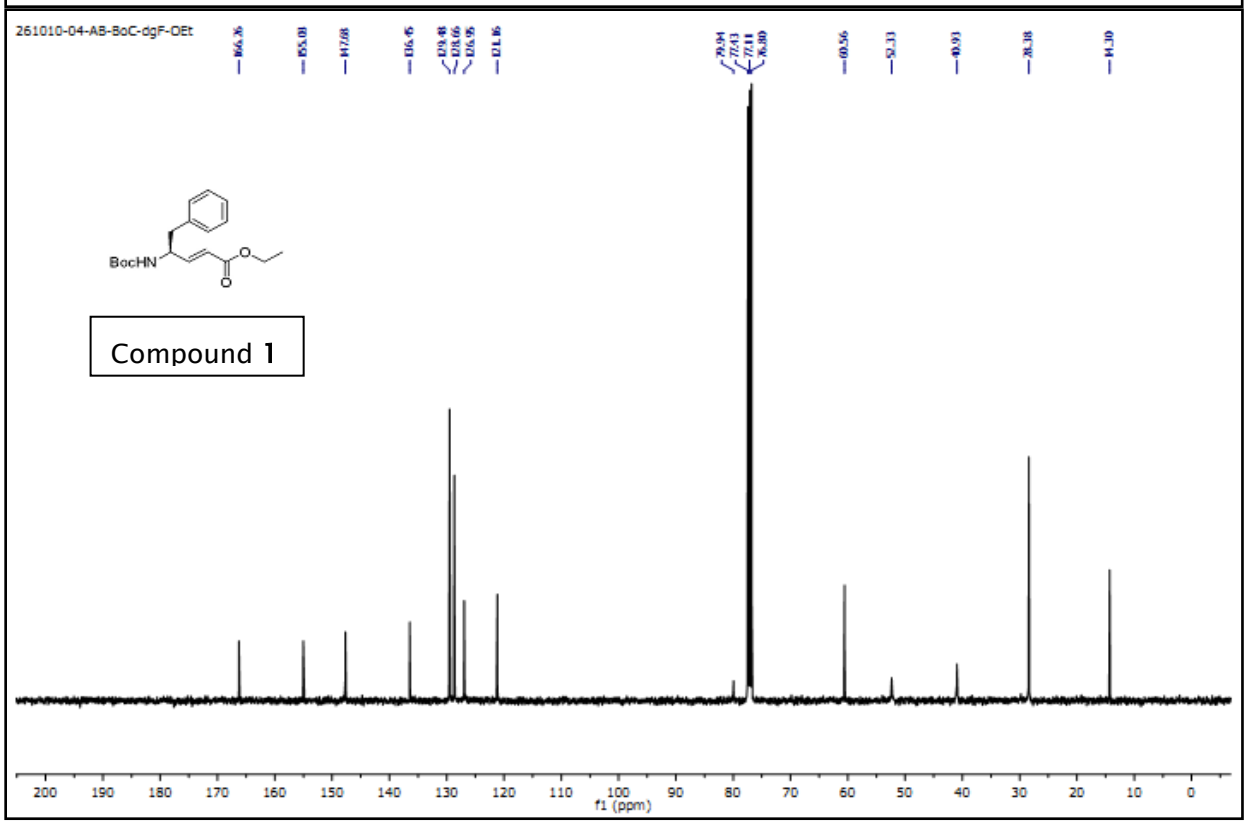
261010-04-AB-BoC-dgF-OEt
BocHN
Compound 1
f1 (ppm)

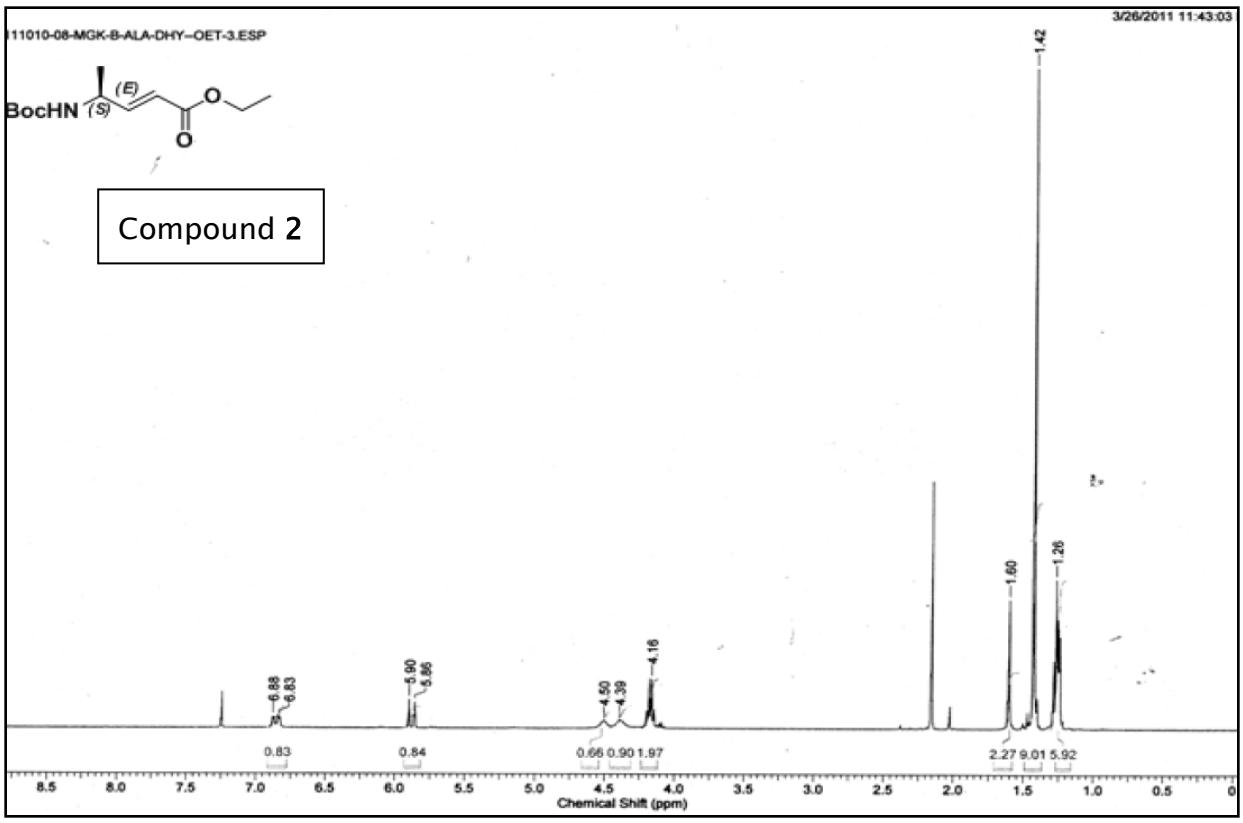
111010-08-MGK-B-ALA-DHY--OET-3.ESP
3/26/2011 11:43:03
BocHN
(E)
(S)
O
O
Compound 2
1.42
1.60
1.26
6.88
6.83
5.90
5.86
4.50
4.39
4.16
0.83
0.84
0.66 0.90 1.97
2.27 9.01 5.92
Chemical Shift (ppm)

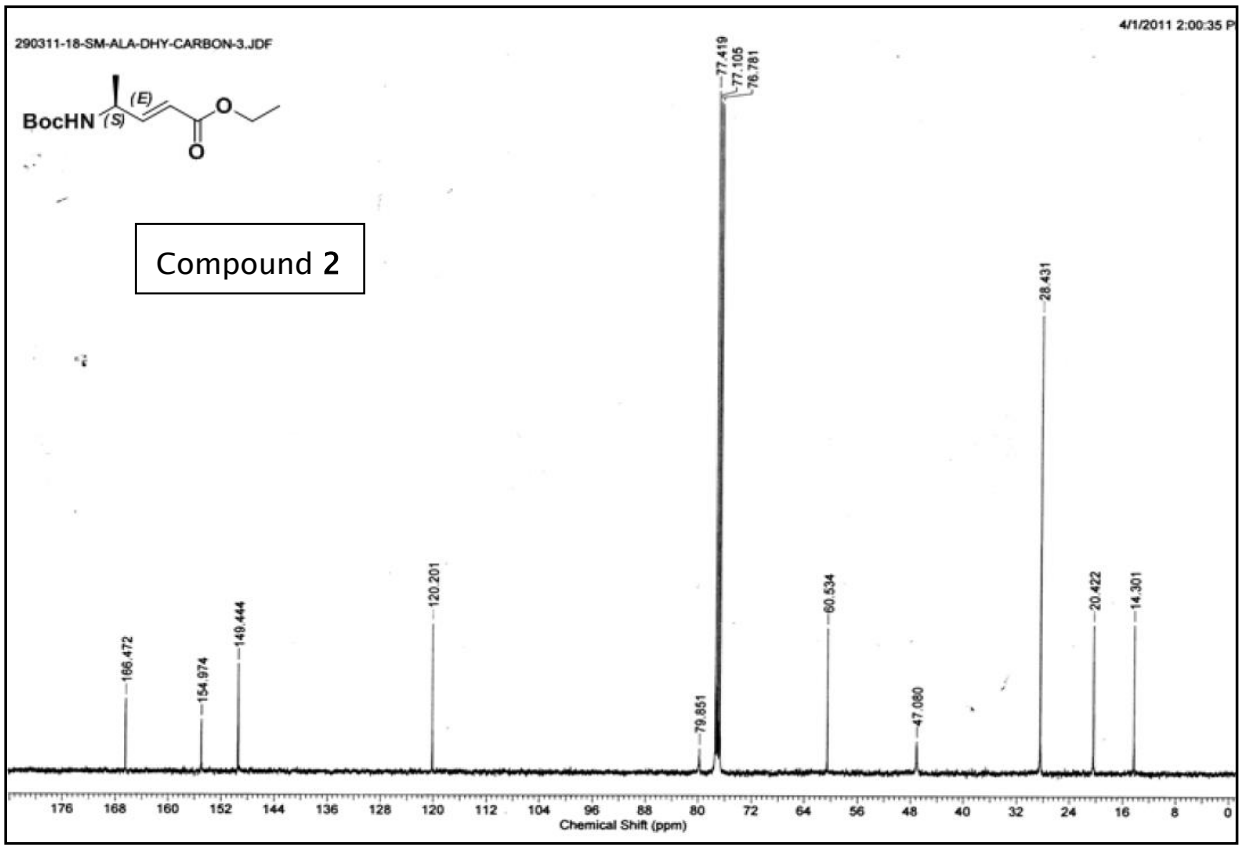
290311-18-SM-ALA-DHY-CARBON-3.JDF
4/1/2011 2:00:35 P
BocHN
(E)
(S)
O
O
Compound 2
77.419
77.105
76.781
28.431
120.201
60.534
20.422
14.301
166.472
154.974
149.444
79.851
47.080
Chemical Shift (ppm)

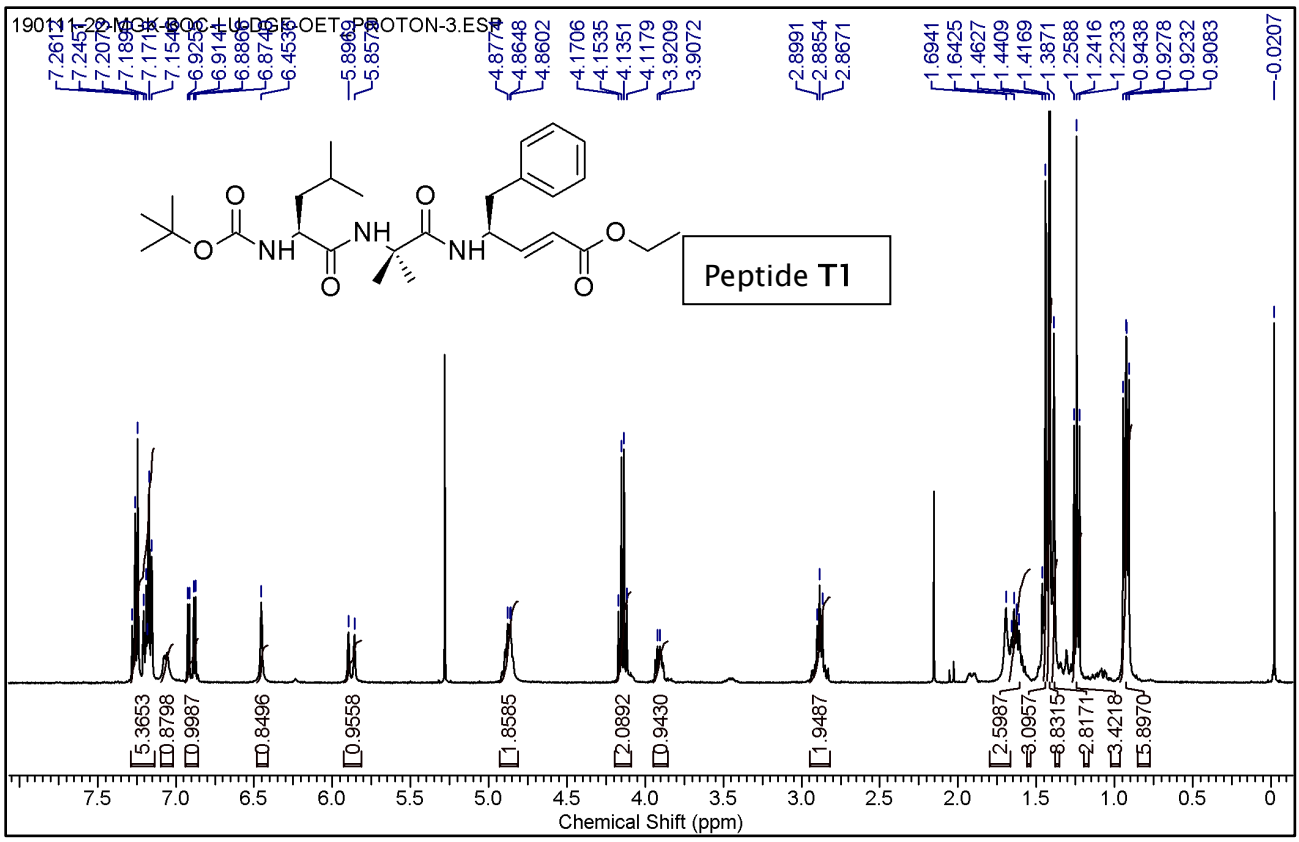
190111-22-MGK-BOC-LUDCF-OETo-PROTON-3.ESP
Peptide T1
Chemical Shift (ppm)

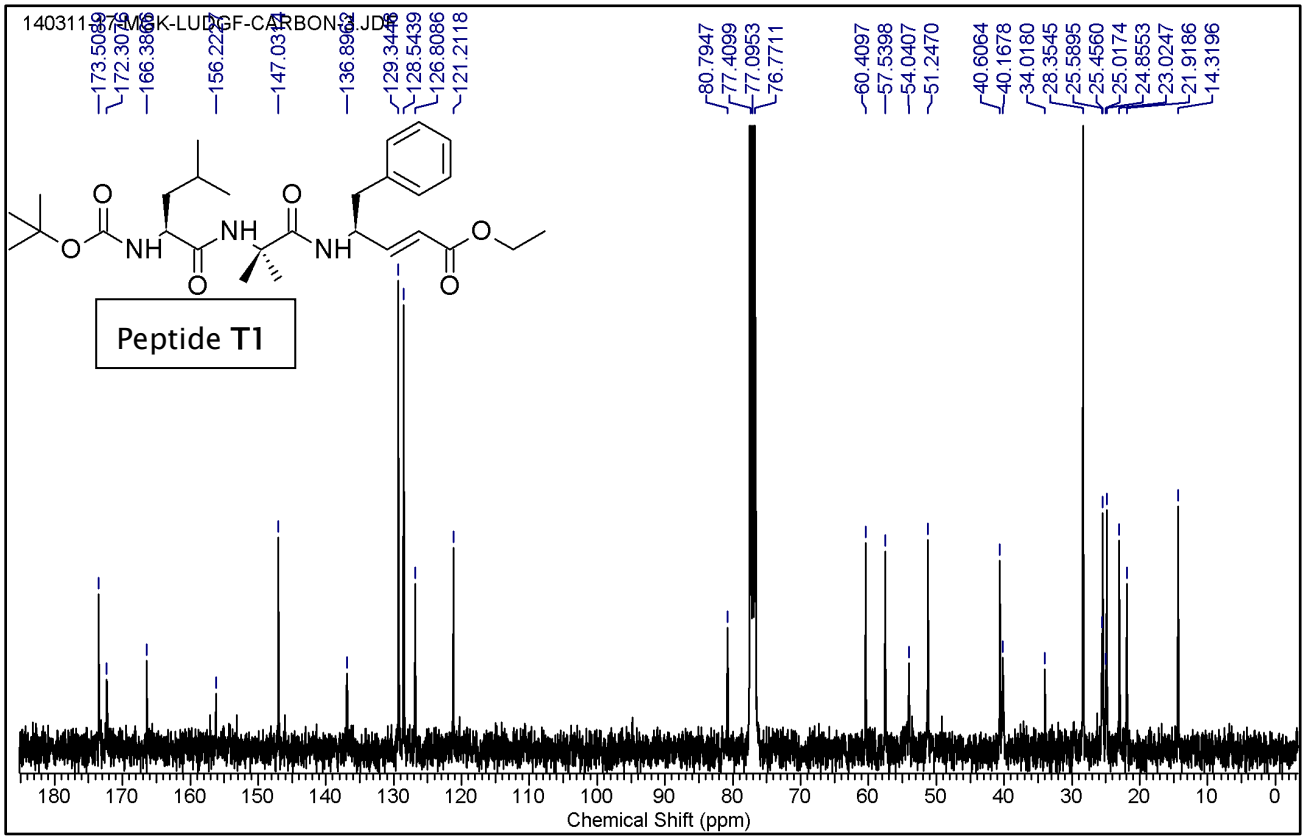
140311-37-MGK-LUDCF-CARBON-2.JDF
Peptide T1
Chemical Shift (ppm)

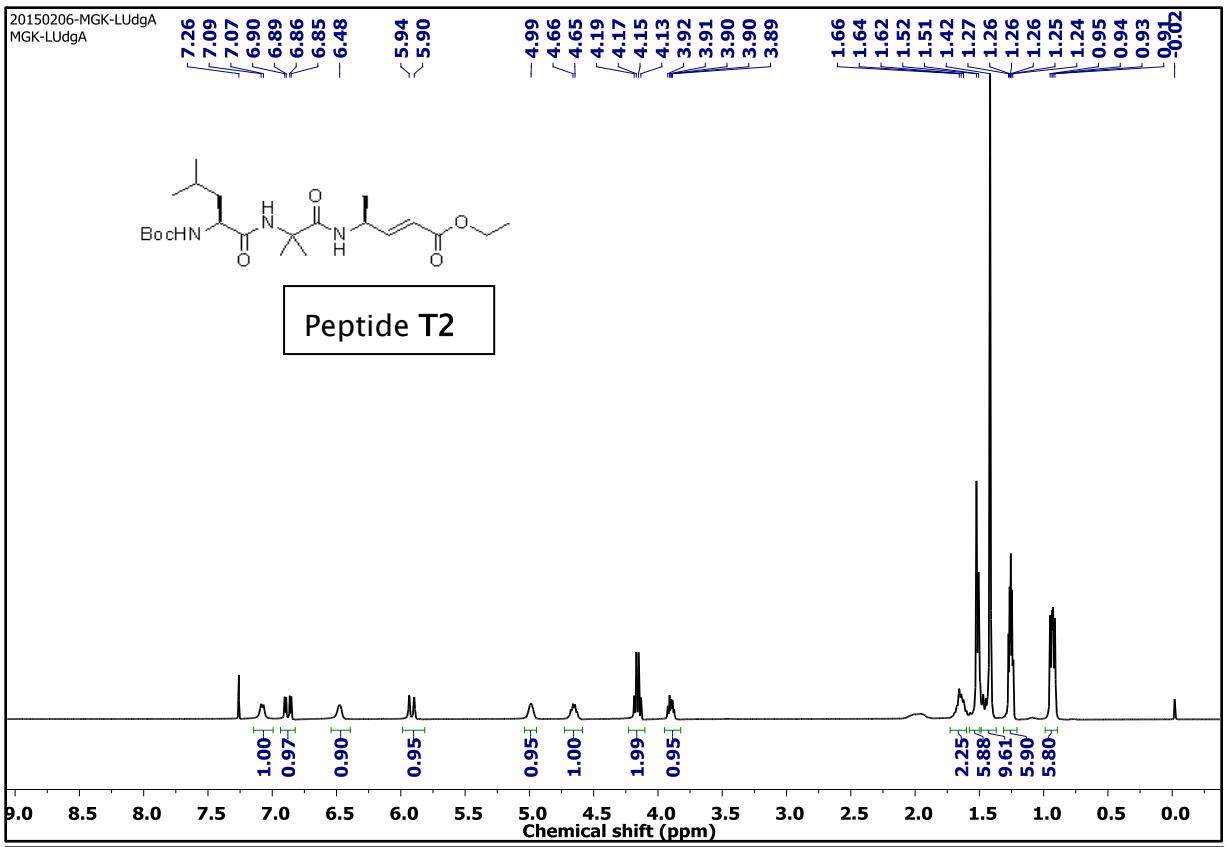
20150206-MGK-LUdgA
MGK-LUdgA
7.26 7.09 7.07 6.90 6.89 6.86 6.85 6.48 5.94 5.90 4.99 4.66 4.65 4.19 4.17 4.15 4.13 3.92 3.91 3.90 3.90 3.89 1.66 1.64 1.62 1.52 1.51 1.42 1.27 1.26 1.26 1.26 1.25 1.24 0.95 0.94 0.93 0.91 0.02
BocHN
Peptide T2
1.00 0.97 0.90 0.95 0.95 1.00 1.99 0.95 2.25 5.88 9.61 5.90 5.80
9.0 8.5 8.0 7.5 7.0 6.5 6.0 5.5 5.0 4.5 4.0 3.5 3.0 2.5 2.0 1.5 1.0 0.5 0.0
Chemical shift (ppm)

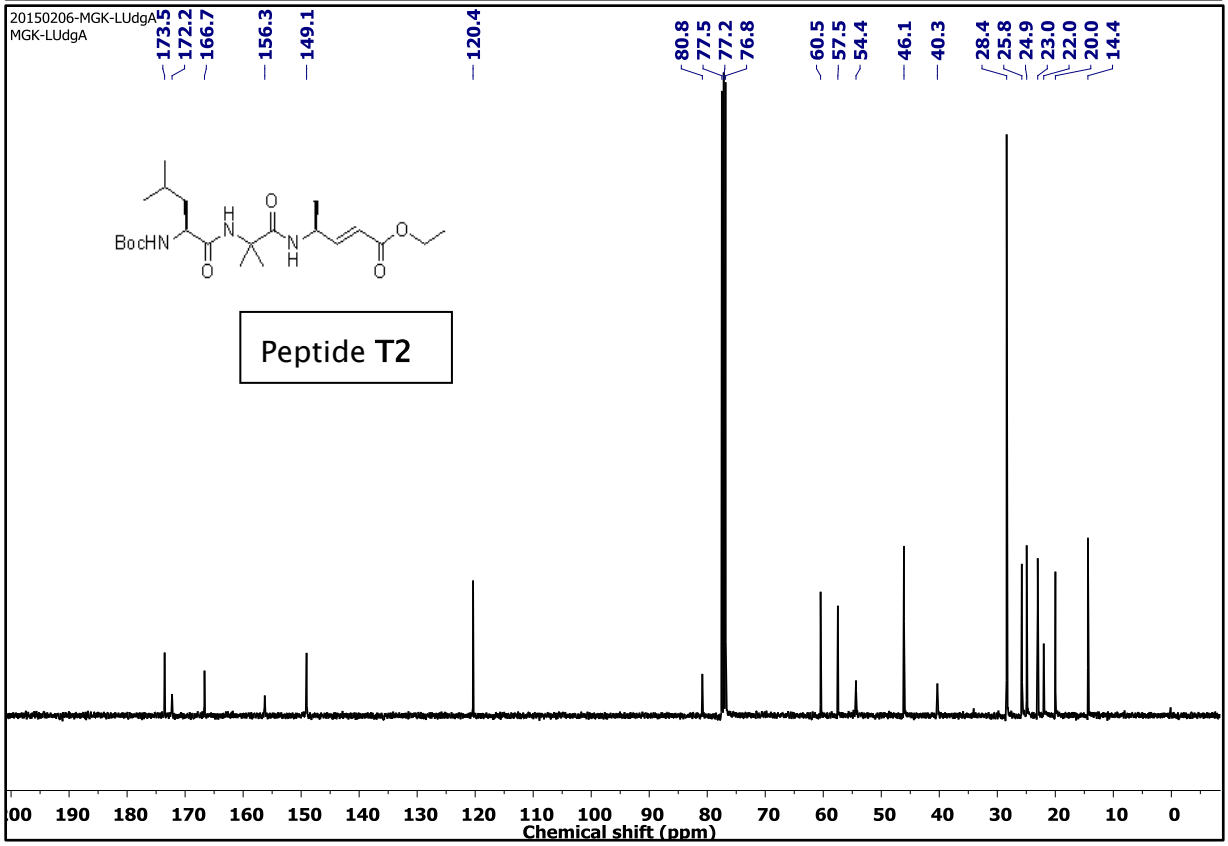
20150206-MGK-LUdgA
MGK-LUdgA
173.5 172.2 166.7 156.3 149.1 120.4 80.8 77.5 77.2 76.8 60.5 57.5 54.4 46.1 40.3 28.4 25.8 24.9 23.0 22.0 20.0 14.4
BocHN
Peptide T2
00 190 180 170 160 150 140 130 120 110 100 90 80 70 60 50 40 30 20 10 0
Chemical shift (ppm)

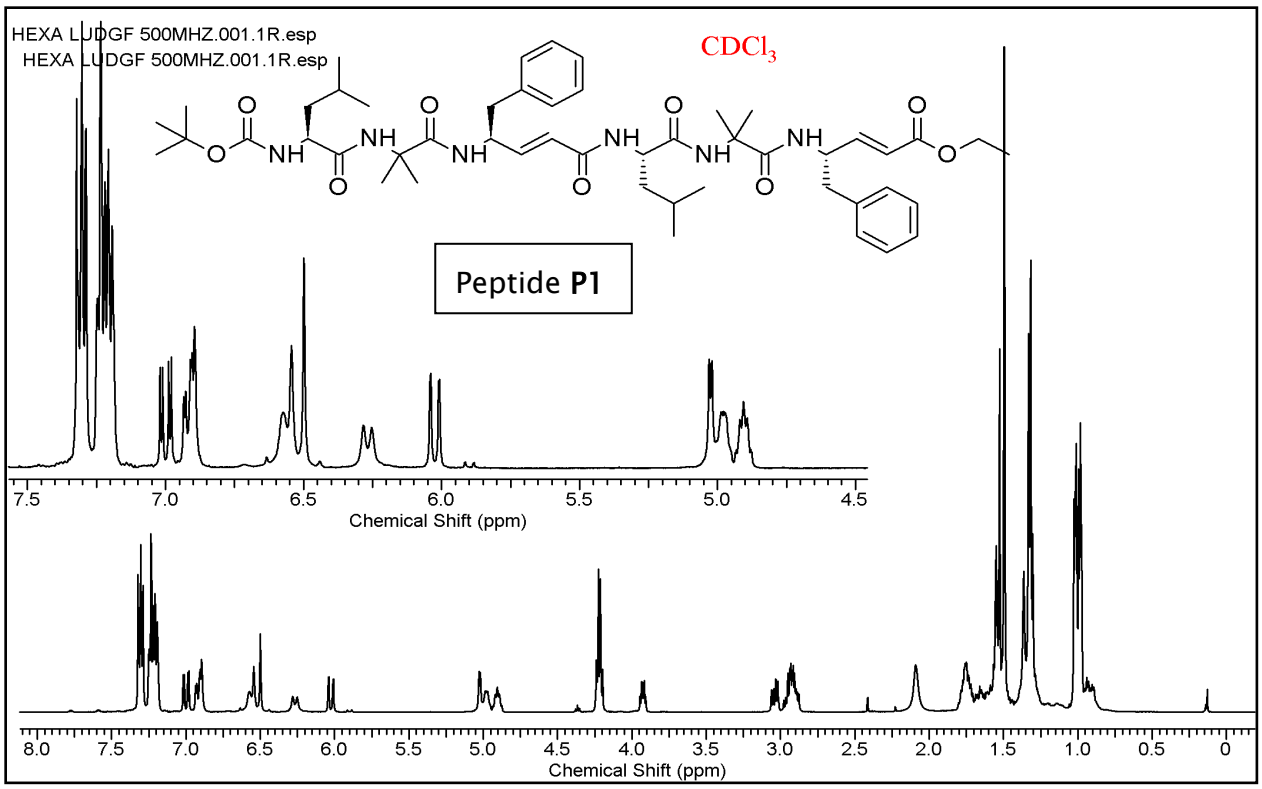
HEXA LUDGF 500MHZ.001.1R.esp
HEXA LUDGF 500MHZ.001.1R.esp
CDCl3
Peptide P1
Chemical Shift (ppm)
Chemical Shift (ppm)

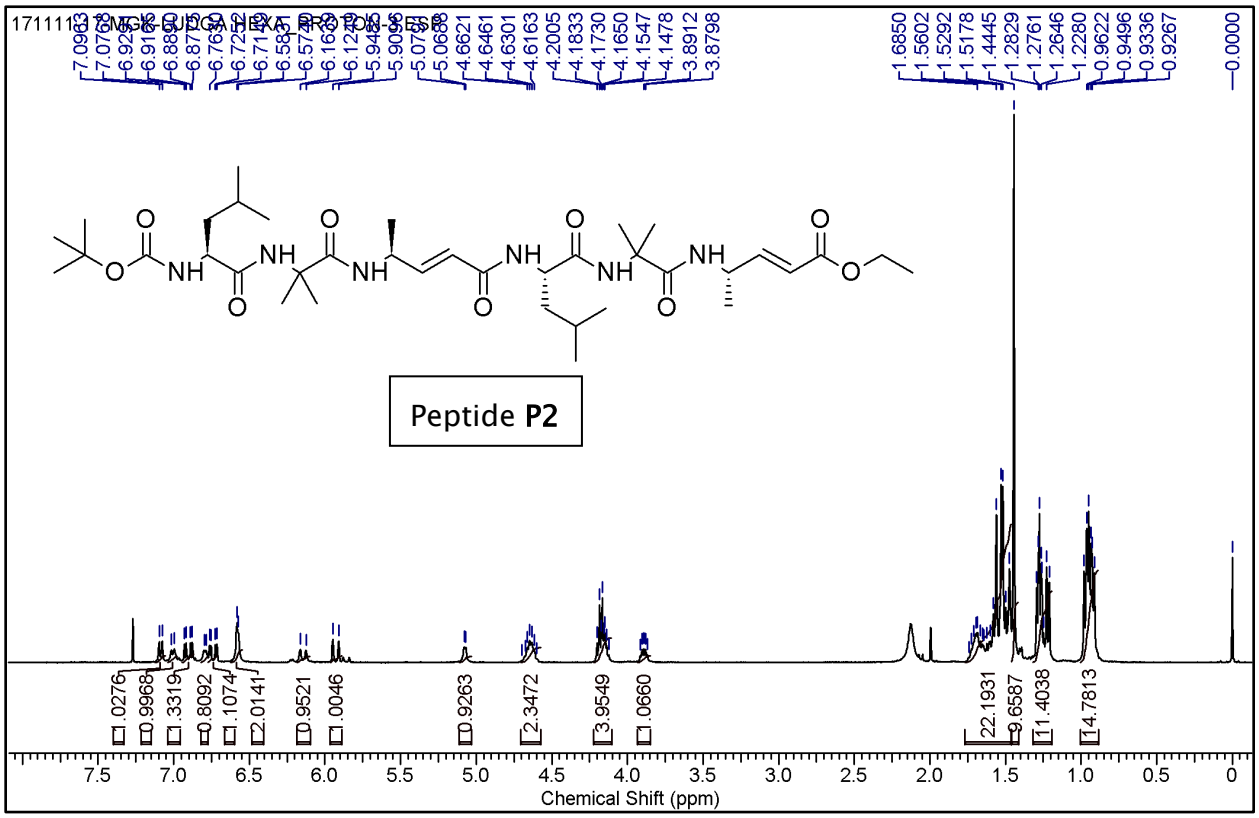
Peptide P2
Chemical Shift (ppm)

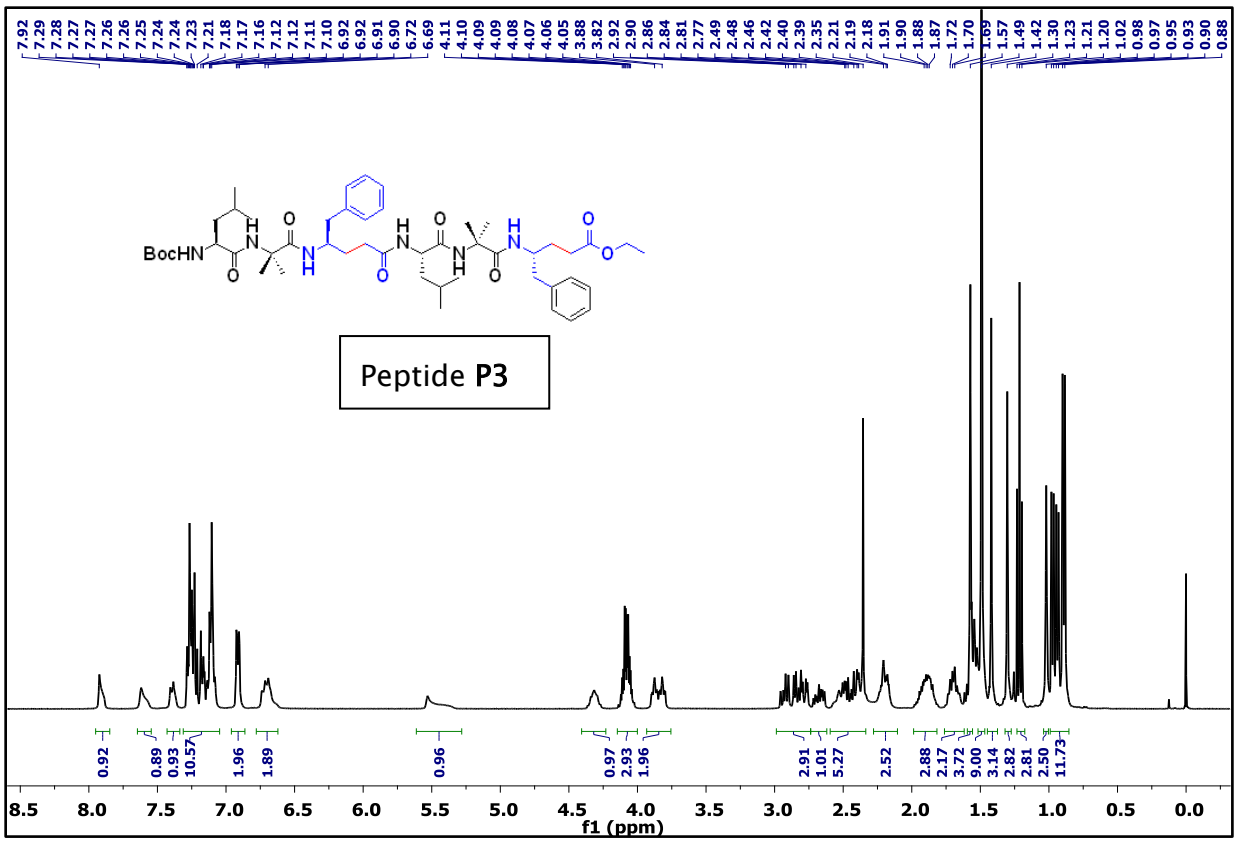
Peptide P3
BocHN
f1 (ppm)

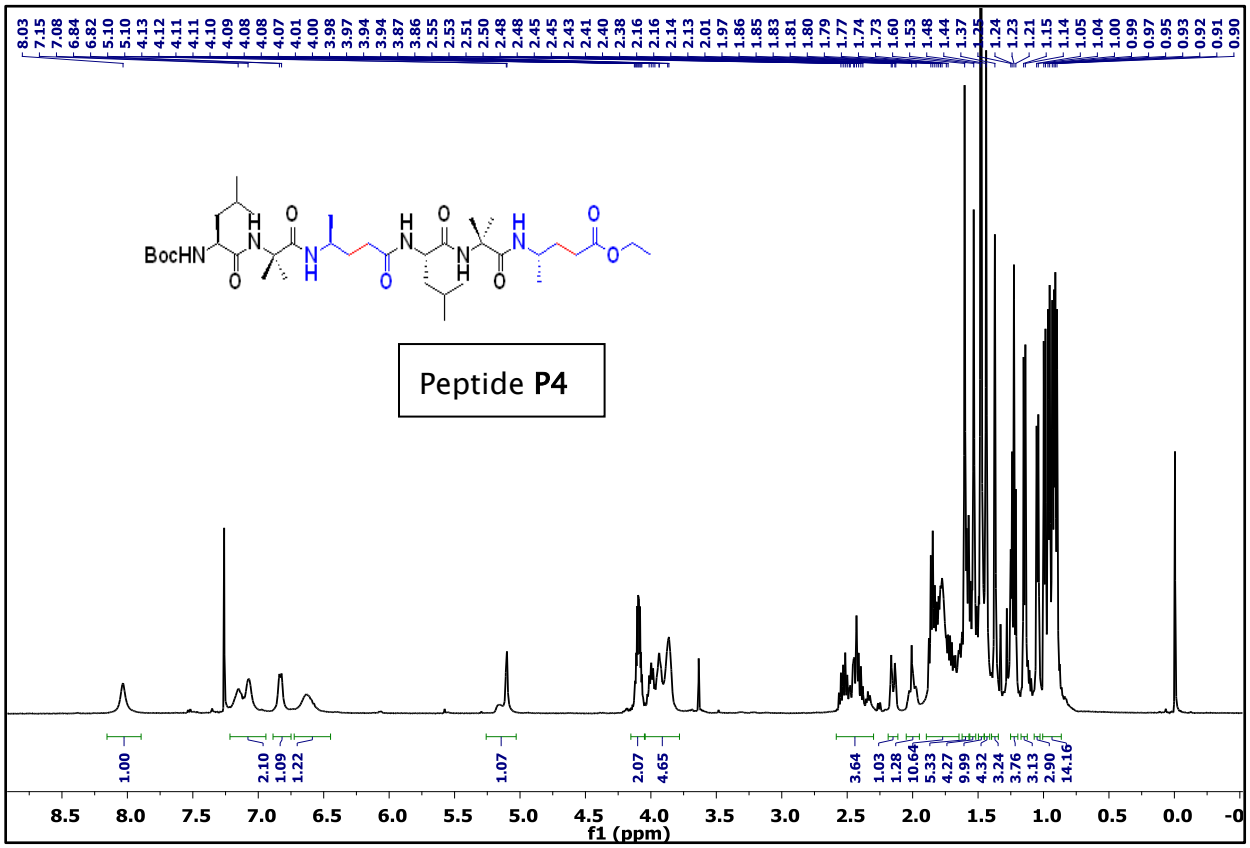
Peptide P4
BocHN
f1 (ppm)

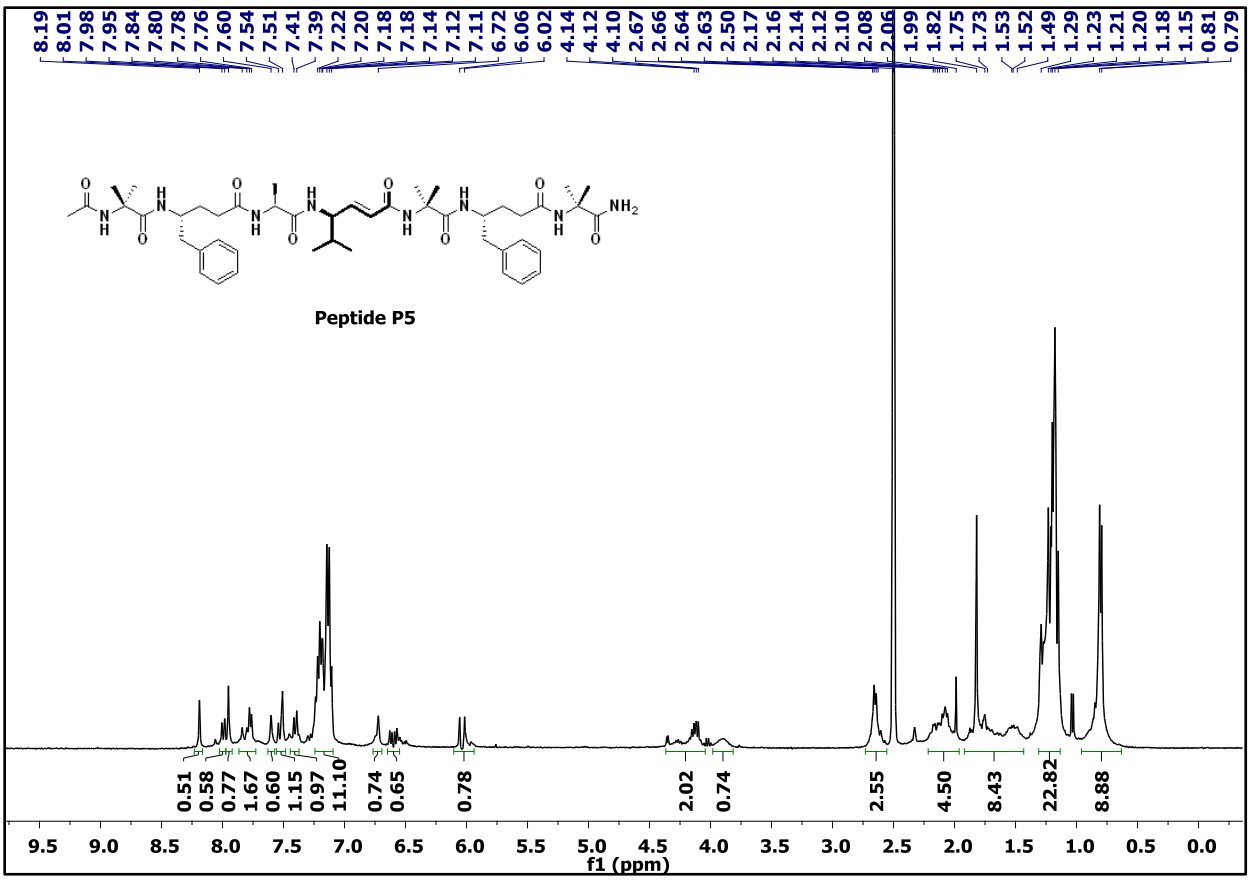
Peptide P5
f1 (ppm)

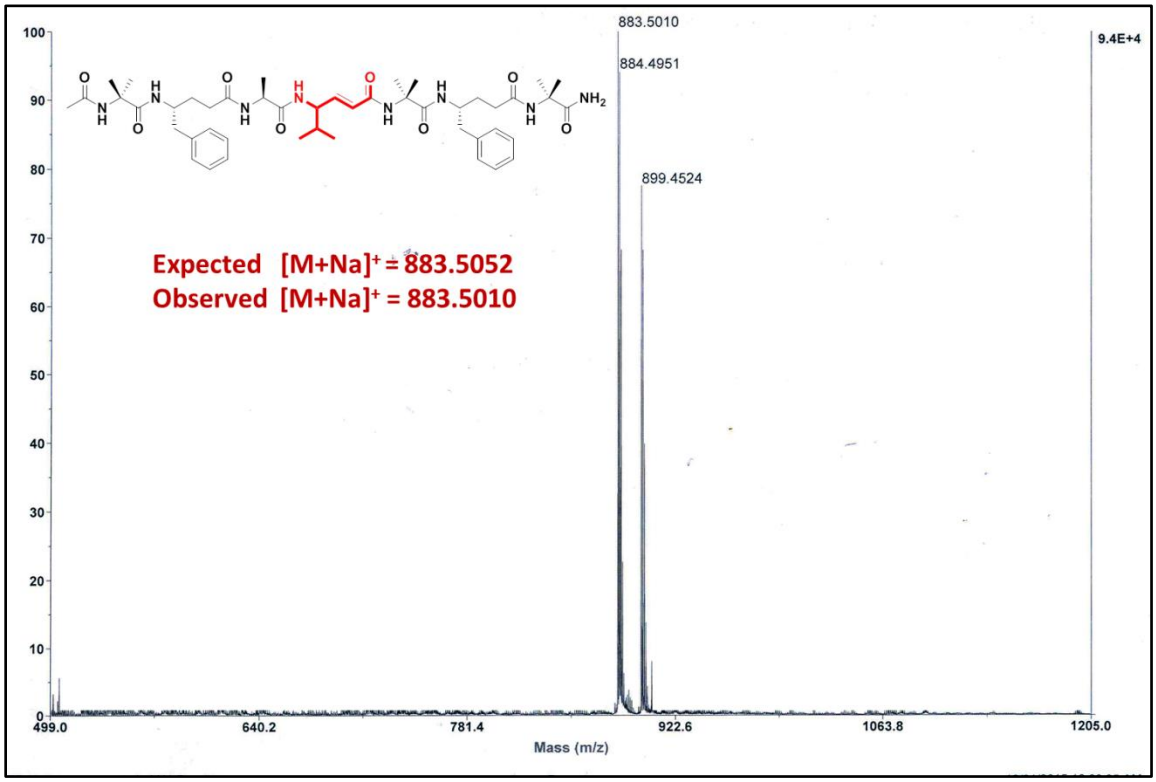
Expected [M+Na]+ = 883.5052
Observed [M+Na]+ = 883.5010
883.5010
884.4951
899.4524
9.4E+4
Mass (m/z)

Chapter 2

Exploring Reactivity of (*E*)-Vinylogous Amino Acids and their Utility in the Design of Peptide Foldamers

2.1 Introduction

Due to their structural diversity and functional versatility, backbone homologated α-amino acids and their oligomers, such as β-and γ-peptides, emerged as a very important class of molecules in medicinal chemistry.[1] As described in the previous Chapter 1, the β- and γ-peptides have been shown to adopt stable secondary structures, such as helices, β-sheets and reverse turns, similar to the natural protein secondary structures.[2] In addition, simple unprotected β-alkyl or dialkyl substituted γ-amino acids (pregabalin and gabapentin) have also been marketed as anticonvulsant drugs for the neuropathic pain as well as for the treatment of epilepsy.[3] In comparison with α- and β-peptides, the structural diversity of γ- and hybrid γ-peptide foldamers is expected to be richer due to the presence of additional backbone C-C bonds.[4] The structural characterization of homooligomers of γ^4, $\gamma^{2,4}$ and $\gamma^{2,3,4}$ substituted γ-peptides[5] and peptides from cyclic γ-amino acids[6] reveal that they adopt the C_{14}-helical conformations. In a sharp contrast to these helical γ-peptide foldamers, the 4, 4-dimethyl substituted γ-amino acid oligomers exhibit extended structures.[7] The growing body of literature infers that γ-amino acids and peptides have a huge potential in the design of peptidomimetics and biomaterials. In the previous chapter, we explored the *E*-vinylogous γ- amino acids in the design of protein supersecondary structure mimetics such as miniature β-meanders as well as helix-loop-helix structures through selective incorporation. [8] We anticipate that these β-sheet promoting *E*-α, β-unsaturated γ-amino acids may serve as excellent starting materials to introduce functional diversity into the γ-peptides through simple Michael addition of nitromethane, thiols as well as other nucleophiles.[9] In addtion, $\gamma^{3,4}$ substiuted amino acids have not been explored in the design of foldamers and the Michael addtion products of nitromethane and other nucleophiles may also provide new building blocks to construct peptide foldamers. In this context, we sought to explore the chemical reactivity of unsatured γ-amino esters. Chapter 2 is divided into Section 2A and Section 2B. The first part, section 2A deals with the synthesis and isolation of diastereomerically pure β-nitromethyl substituted γ-amino acids through the Michael addition of nitromethane, utility of these multifaceted nitromethyl substituted γ-amino acids in the design of foldamers and the transformation of nitro functional group into a variety of other functional groups. The second part, section 2B deals with the Michael addition of thiols to *E*-vinylogous amino esters to derive thiostatines (β-sulfhydryl γ-amino acids) and the stereochemistry of thiol conjugate addition products.

<u>SECTION 2A:</u> Design, synthesis and functionalization of multifaceted β-nitromethyl γ-amino acids and peptides

2A.1 Introduction

This section deals with Michael addition reaction of nitromethane to *E*-vinylogous amino esters to derive disubstituted γ-amino acids and their utility in the design of peptide foldamers. The reason to introduce nitromethyl group is that nitroalkanes are unique with respect to the diverse functional group transformations. Nitroalkanes have been used as effective precursors for the synthesis of amines, carboxylic acids, aldehydes, ketones, substituted alkanes, alkenes, complex heterocyclic structures and more (Figure 1).[10] With these multifaceted functional group transformations of nitroalkanes, we asked the question whether these functional properties of nitroalkanes can be transformed to the γ-amino acids and to the peptides, since they are very attractive entities from the perspective of medicinal chemistry.

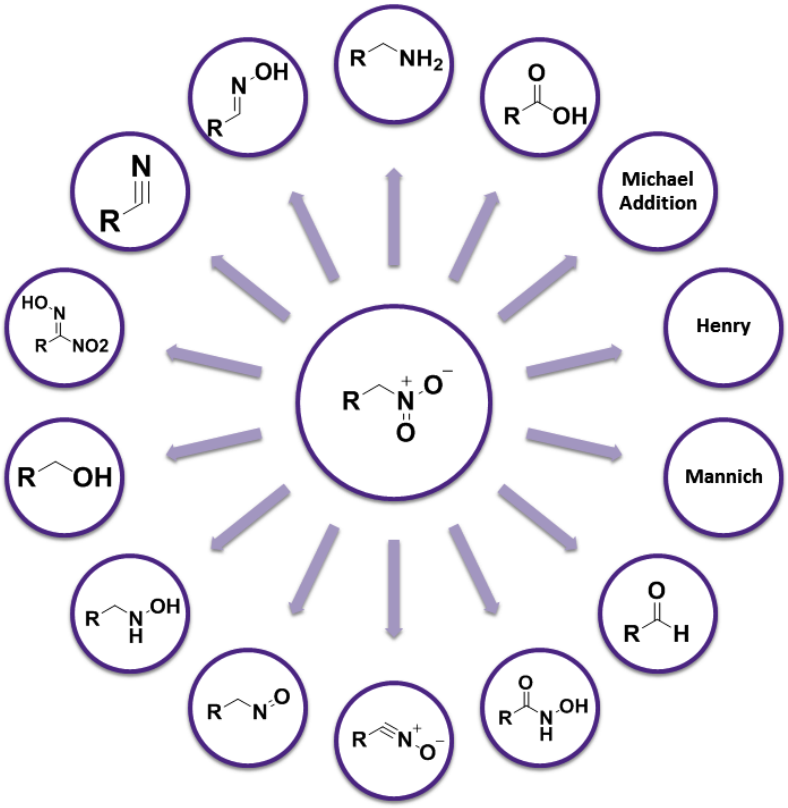

Fig 1: Diverse functional group transformations of nitroalkanes.

2A.2 Aim and Rationale of the Present Work

We anticipate that α, β-unsaturated γ-amino esters may serve as ideal precursors for the synthesis of β-nitromethane functionalized γ-amino acids using Michael addition. A variety of nucleophiles and catalysts have been demonstrated for the C–C and C–X (X = N, S, O, etc.) bond formation using the Michael addition reaction.[11] In addition, nitromethane Michael addition to the *N*-carbamate protected vinylogous amino esters has also been reported, however, these reports have offered no insight into the diastereoselectivity and the mechanism of the conjugate addition.[12] We sought to utilize these amino acids as substrates in the Michael addition reaction with nitromethane to understand the diastereoselectivity as well as to obtain stereochemically pure β-nitromethane substituted γ-amino acids to synthesize hybrid peptide foldamers. Herein, we are reporting the highly diastereoselective Michael addition of nitromethane to various N-Boc-(*S*, *E*)-α,β-unsaturated γ-amino esters, single crystal conformations of β-nitromethane substituted γ-amino acids as well as various β-nitromethyl γ-amino acid homooligomers and hybrid peptides. In addition to that we are also reporting the functional transformation of nitro group into various other functional groups on both monomers as well as on hybrid peptides.

2A.3 Results and Discussion

2A.3.1 Highly Diastereoselective Synthesis of β-Nitromethyl γ-Amino Acids from Naturally Occurring α, β-Unsaturated γ-Amino Acids

Synthesis of (E)-vinylogous amino esters from α-amino acids

The N-protected (*S*, *E*)-vinylogous amino esters (**1**) were synthesized starting from the N-protected amino aldehydes using the Wittig reaction[13] as shown in Scheme 1. The N-Boc amino aldehydes were synthesized from the oxidation of corresponding amino alcohols.[14] A variety of *E*-vinylogous amino esters were synthesized using this protocol (Scheme 1, **1a–l**). Instructively, many of these N-protected *E*-vinylogous amino esters were prone to crystallize immediately after the column purification. The crystal conformations of the compounds **1b** and **1c** are shown in Fig 2.

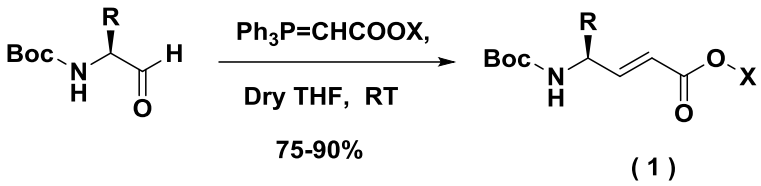

1a: R = $-CH(CH_3)_2$, X = $-CH_2-CH_3$; 1b: R = $-CH(CH_3)-CH_2-CH_3$, X = $-CH_2-CH_3$;
1c: R = $-CH_2-CH(CH_3)_2$, X = $-CH_2-CH_3$; 1d: R = $-CH_2-NHBoc$, X = $-CH_2-CH_3$;
1e: R = $-CH_2-C_6H_5$, X = $-CH_2-CH_3$; 1f: R = $-CH_2-O^tBu$, X = $-CH_2-CH_3$;
1g: R = $-CH_2-COO^tBu$, X = $-CH_2-CH_3$; 1h: R = $-CH_3$, X = $-CH_2-CH_3$;
1i: R = -Proline, X = $-CH_2-CH_3$; 1j: R = $-CH(CH_3)_2$, X = $-CH_2-C_6H_5$;
1k: R = $-CH_2-CH(CH_3)_2$, X =$-CH_2-C_6H_5$; 1l: R = $-CH_2-C_6H_5$, X = $-CH_2-C_6H_5$;

1i =

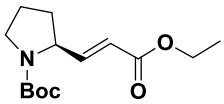

Scheme 1*:* Synthesis of *α*, *β*-unsaturated *γ*-amino esters using Wittig reaction.

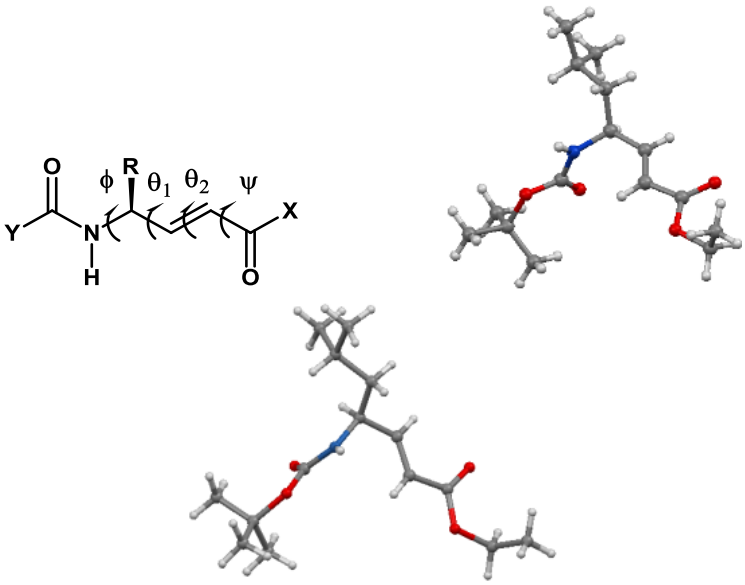

1b **1c**

(A) **(B)**

Fig 2: (A) The local torsional variables of vinylogous residues and **(B)** X-ray structures of *N*-Boc-(*S*, *E*)-vinylogous amino esters **1b** and **1c** showing the N-C^{γ}-C^{β}=C^{α} eclipsed conformations.

Conjugate addition of nitromethane to (*E*)-vinylogous amino esters

We anticipate that Michael addition of nitromethane to all *E*-vinylogous esters (**1a-l**) can be performed in the presence of a base. The schematic representation of the conjugate addition in

the presence of a base is shown in Scheme 2. Conditions for the Michael addition were optimized using the base DBU.[12a] To begin with, ethyl ester of N-Boc-(*S*, *E*)-α, β-unsaturated γ-valine (Boc-(*S*, *E*)-dγVal-OEt, **1a**) was subjected to the Michael addition reaction using nitromethane in the presence of DBU.

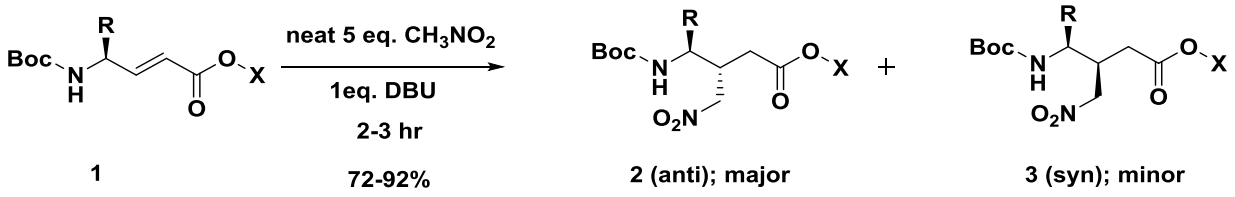

Scheme 2: Synthesis of *β*-nitromethane substituted *γ*-amino esters.

Table 1: List of *β*-nitromethane substituted *γ*-amino acids and their diastereomeric ratios.

Entry	**R**	**X**	**product** *(% yield)*	***dr*** (*anti:syn*)
1			**2+3**	**2 : 3**
a	$-CH(CH_3)_2$	$-C_2H_5$	90	89:11†*
b	$-CH(CH_3)-CH_2-CH_3$	$-C_2H_5$	89	83:17†*
c	$-CH_2-CH(CH_3)_2$	$-C_2H_5$	86	82:18†
d	$-CH_2-NHBoc$	$-C_2H_5$	87	90:10*
e	$-CH_2-C_6H_5$	$-C_2H_5$	88	80:20†
f	$-CH_2-O^tBu$	$-C_2H_5$	84	100:0†*
g	$-CH_2-COO^tBu$	$-C_2H_5$	82	81:19*
h	$-CH_3$	$-C_2H_5$	92	80:20‡
i	Proline side chain	$-C_2H_5$	91	61:39*
j	$-CH(CH_3)_2$	$-CH_2C_6H_5$	80	86:14*
k	$-CH_2-CH(CH_3)_2$	$-CH_2C_6H_5$	79	81:19‡
l	$-CH_2-C_6H_5$	$-CH_2C_6H_5$	72	89:11*

Note: †Determined by isolated products; *Determined by reverse phase HPLC; ‡Determined by NMR analysis.

The Michael addition product was isolated with 90% yield in 2.5 h at room temperature. Interestingly, the HPLC analysis of the crude product reveals the 89.5:10.5 diastereomeric ratio of *anti* (**2a**): *syn* (**3a**) products, respectively. Both major (**2a**) and minor (**3a**) products were separated using column chromatography and analyzed. Encouraged by the high

diastereoselectivity, we further subjected other vinylogous amino acids (**1b-l**) to the Michael addition reaction and the diastereomeric products were isolated in moderate to good yields (72-92%). The analyses of all nitromethane conjugate addition products reveal that *anti* (**2b-l**) is a major product in all the cases. The diastereomeric major (**2a, 2b, 2c** and **2e**) and minor (**3a, 3b, 3c** and **3e**) products of **1a**, **1b**, **1c** and **1e** were separated using column chromatography and the diastereomeric ratio was measured using the isolated yields. Surprisingly, compound **1f** gave a

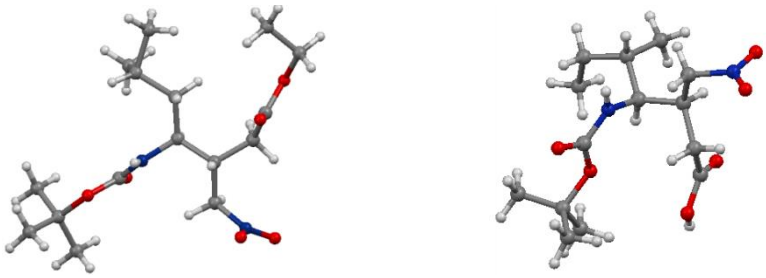

2c **2b acid**

Fig 3: X-ray crystal structures of Boc-NH-γLeu(β-CH_2NO_2)-COOEt (**2c**) and Boc-γleu(β-CH_2NO_2)-COOH (**2b acid**).

single *anti* isomer **2f**. As the reactions were performed in small scale, only major *anti* Michael addition products of **2g**, **2j**, **2k** and **2l** were isolated using column chromatography for the compounds **1g**, **1j**, **1k** and **1l,** respectively. In addition, we found difficult to separate the diastereomers for the compounds **1d**, **1h** and **1i** from the column chromatography. However, the diastereomeric ratio (**2**: **3**) was measured for all the crude products either using RP-HPLC or by the ^{1}H NMR (Table 1). Instructively, high diastereoselectivity was observed for all *E*-vinylogous esters except the proline side-chain containing compound **1i**. In addition, both benzyl and ethyl esters gave similar yields and diastereoselectivity of the nitromethane Michael addition. Out of all Michael addition products (**2a-l** and **3a-l**) in the Table 1, we were able to obtain the single crystals for **2c** and its X-ray structure is shown in Figure 3.

In contrast to the nucleophilic addition at the carbonyl compounds containing α-chiral center, the stereochemical outcome of 1, 4 nucleophilic addition to α, β-unsaturated esters containing γ-stereogenic center is sometimes bewildering to rationalize. However, the intriguing results of conjugate addition of nitromethane to *N*-Boc-protected vinylogous amino esters **1a-e**, **1h** and **1j-k**, single *anti* isomer of **1f** and the almost equal diastereomeric ratio from **1i**, enable us to rationalize plausible mechanism of the Michael addition starting from the crystal structures of

E-vinylogous amino esters. The local conformations of vinylogous residues were determined by introducing additional torsional variables θ_1 (N-C$^{\gamma}$-C$^{\beta}$=C$^{\alpha}$) and θ_2 (C$^{\gamma}$- C$^{\beta}$=C$^{\alpha}$-C') along with the ϕ and ψ as shown in Figure 1. The crystal conformations of vinylogous amino esters from the literature[8, 10] and from the present work, suggest that they mainly adopt either N-C$^{\gamma}$-C$^{\beta}$=C$^{\alpha}$ (θ_1=~0°) or H-C$^{\gamma}$-C$^{\beta}$=C$^{\alpha}$ (θ_1=~120°) eclipsed conformations (Figure 1). This is not surprising because in their seminal work Houk and colleagues[15] and Wiberg *et al.*[16] proposed that the eclipsed conformations of olefins and the carbonyls are stabilized by σ→π* donations. As C-C bond is a better σ donor than the C-N bond, from the analysis of twenty one units of vinylogous resides in both monomers as well as in peptide crystals,[8] we observed that the amino acid side-chains are always perpendicular to the double bonds. In addition, the analysis also reveals the preference of N-C$^{\gamma}$-C$^{\beta}$=C$^{\alpha}$ eclipsed conformation in monomer esters and H-C$^{\gamma}$-C$^{\beta}$=C$^{\alpha}$eclipsed conformation in amides/peptides. Based on these analyses, we speculate that both eclipsed conformers **A** and **B** are in equilibrium in solution (Scheme 3).

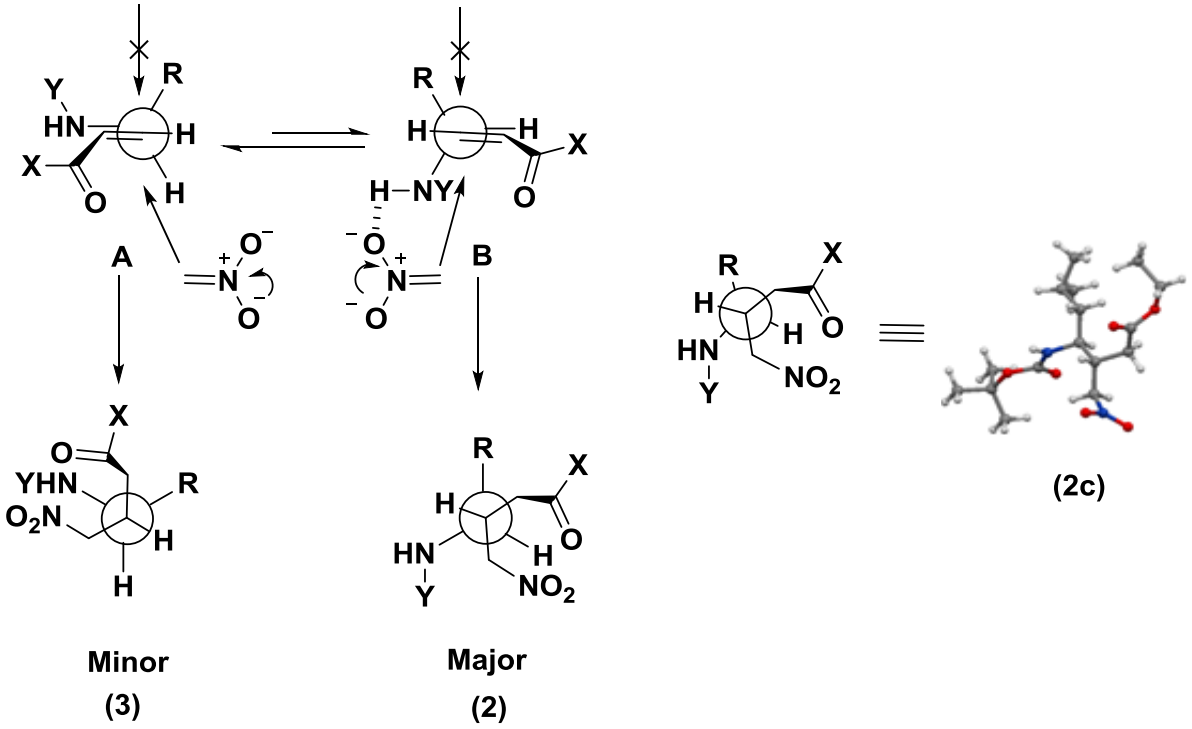

Scheme 3: Schematic representation of the highly diastereoselective Michael addition of nitromethane to the *E*-vinylogous amino esters. The crystal structure of **2c** representing the stereochemical outcome from the conformer **B**.

The preference for **A** over **B** is may be due to the reduced $A^{1,3}$ strain. In the conformer **B**, both C^{γ}-H and C^{α}-H are in the same plane separated by a distance of 2.3 Å, where as in the conformer **A**, N-H is twisted upwards in all N-C^{γ}-C^{β}=C^{α} eclipsed conformations (in single crystals) probably to reduce the steric strain (N-**H**---**H**-C^{α} distance 2.75 Å and **N**-**H**---**H**-C^{α} angle 67°) with C^{α}-H. The crystal structure analysis also suggests that the approach of the nucleophile from top is restricted due to the steric clash with R group (Scheme 3) as the R-group projected perpendicular to the double bonds. Based on these analyses, we propose that nucleophile must approach the conjugated ester from the opposite face of the R group to avoid the steric clash. In addition, the excellent diastereoselcetivity observed in all *E*-vinylogous amino esters containing amide NH except proline (**1i**), suggesting the significant role of the carbamate NH's in dictating the high diastereoselectivity. In order to understand the role of NH in the conjugate addition, we performed the conjugate addition reaction on ethyl ester of *N, N*-di-Boc-protected (*S, E*)-α, β-unsaturated γ-phenylalanine (**4**, Scheme 4). Instructively, the conjugate addition of nitromethane yield the diastereomeric ratio (**5**+**6**) 52:48 similar to the compound **1i** suggesting the crucial role of amide NH. We speculate that carbamate NH may be involving in the H-bond formation with the incoming nucleophile and stabilizing the nucleophilic approach. Based on these results, we

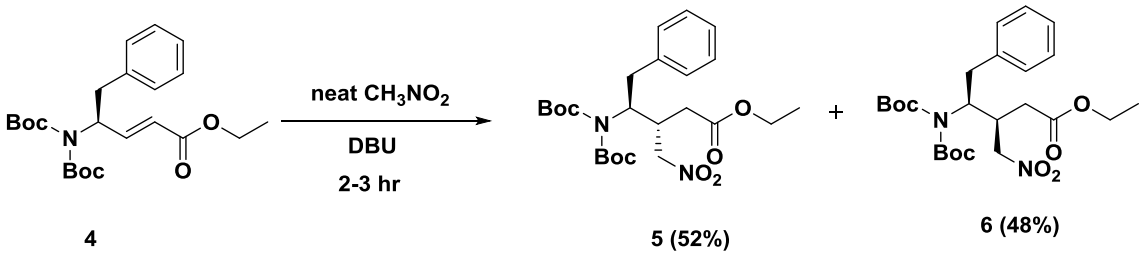

Scheme 4: Conjugate addition of nitromethane to *N,N*-di-Boc-protected *E*-vinylogous amino ester.

propose the possible reaction mechanism for the conjugate addition of the nitromethane as shown in Scheme 3. The conformer **B** leads to the major (*anti*) product due to the H-bond mediated stabilization of the nucleophile in the conjugate addition, whereas in the conformer **A** disfavored the formation of major (*syn*) as there is no favorable H-bond stabilization for the nucleophilic approach. Further, the analysis of the crystal structure **2c** reveal that it adopted the similar structure as anticipated from the conformer **B**.

2A.3.2 Synthesis of Nitro-Peptides

To understand the conformations of β-nitromethane substituted γ-amino acids in peptides, we synthesized various homo and heterooligomers. In order to synthesize β-nitromethane substituted γ-peptides, we subjected ethyl esters of *N*-protected nitroamino acids for the saponification and *N*-Boc deprotection using 1N NaOH and 50% TFA in DCM, respectively.

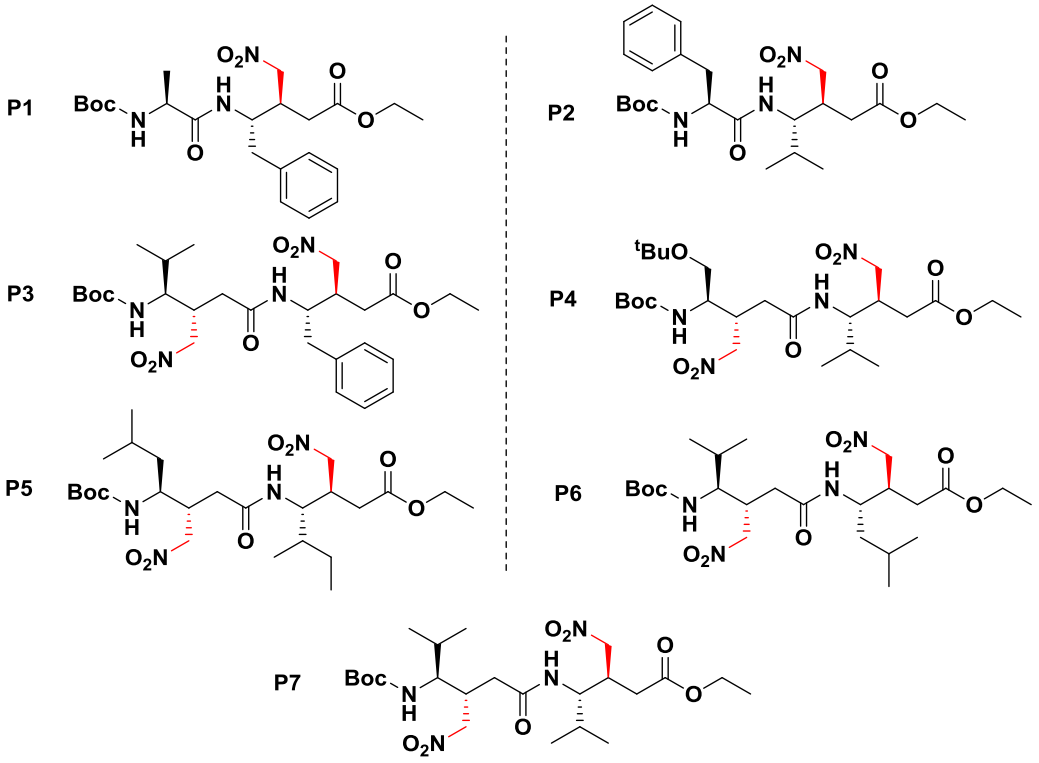

Scheme 5: Sequences of peptides **P1-P7** containing β-nitromethane substituted γ-amino acids.

The free amines and carboxylic acids were directly used for the peptide synthesis without further characterization. However, we were able to obtain the single crystals for the **2b** after the ester hydrolysis and its structure is shown in Figure 3. The peptide couplings were carried out using standard DCC/HOBt coupling conditions. The list of β-nitromethane substituted γ- dipeptides (**P1-P7)** were synthesized using this procedure is shown in Scheme 5. All peptides were isolated in moderate to good yields (55-78%) after column chromatography. Out of all the peptides in Scheme 5, **P6** and **P7** gave single crystals after the slow evaporation from the solution of EtOAc and their X-ray structures are shown in Figure 4. Similar to the vinylogous amino acids (Figure

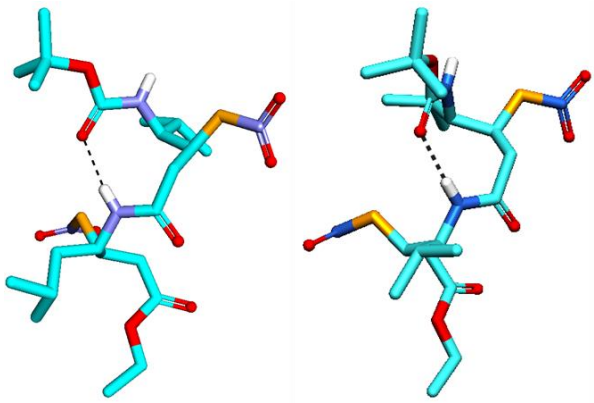

P6 **P7**

Fig 4: X-ray structures of **P6** and **P7**.

1), the backbone torsional angles of β-nitromethane substituted γ-amino acids were also analyzed by introducing additional torsional variables θ_1 and θ_2.[13] The torsional variables of β-nitromethane substituted γ-amino residues are tabulated in Table 2. Inspection of the crystal structures of P6 and P7 reveal that the independent amino acids in the dipeptides adopted g^+, g^+ backbone conformations similar to the amino acid crystal structure **2b**. In contrast to the *anti*-conformation of **2c** (along C3-C4 bond), the amino acid **2b** and amino acid residues in the

Table 2: Torsional values of Nitro amino acids and nitropeptides

Compound	residue	ϕ	θ_1	θ_2	ψ	Back bone Conformation
2c	γLeu(β-CH_2NO_2)	-110	-179	89	-146	t, g^+
2 b acid	γIleu(β-CH_2NO_2)	-110	67	72	-145/36	g^+, g^+
P6	γVal(β-CH_2NO_2)-1	-100	68	72	-87	g^+, g^+
	γLeu(β-CH_2NO_2)-2	-99	69	66	36	g^+, g^+
P7	γVal(β-CH_2NO_2)-1	-100	65	76	-88	g^+, g^+
	γVal(β-CH_2NO_2)-2	-98	66	71	27	g^+, g^+

dipeptides **P6** and **P7** follow the general trend of tetra alkyl substituted ethane by adopting the *gauche* conformations.[17] Instructively, the analysis of the crystal structures of **P6** and **P7** reveal that they adopt C_9-helical type of structure in single crystals.[18] The helial structures are stabilized by single nine membered intramolecular H-bond [average C=**O**---**H**-N distance 1.99 Å, **O**---**N** dist. 2.85 Å and **O**---**H**-**N** bond angle 173] existed between Boc-amide CO and the NH of C-terminal residue (i→i+2). These structures are resembling the γ-turn in α-peptides.[19] Similar type of 9-helices have also been observed in the homooligomers of gabapentin, however, with mirror image torsional values.[20]

2A.3.3 Synthesis and Conformational Analysis of $\gamma^{3,4}$-Homooligomers

In order to understand the conformations of β-nitromethyl γ-amino acids in higher homooligomers, we synthesized peptides **P8** and **P9** in solution phase using standard DCC/HOBt coupling conditions. The sequences of the peptides **P8** and **P9** are shown in Scheme 6. The deprotection of *N*-Boc and ethyl esters was carried out using TFA and NaOH, respectively. We adopted stepwise couplings from C- to N- terminus to avoid unexpected impurities during the hydrolysis of peptide esters. Both peptides were subjected to grow the X-ray quality crystals in various solvent combinations to understand their unambiguous conformations. In contrast to the γ^4-, $\gamma^{2,4}$-, $\gamma^{3,3}$, $\gamma^{4,4}$- and $\gamma^{2,3,4}$-peptides,[21] the conformations of $\gamma^{3,4}$-peptides have not been systematically investigated. We speculated greater helical propensity from $\gamma^{3,4}$-peptides due to the favorable gauche interactions of side-chains similar to the tetra substituted ethanes.[17]

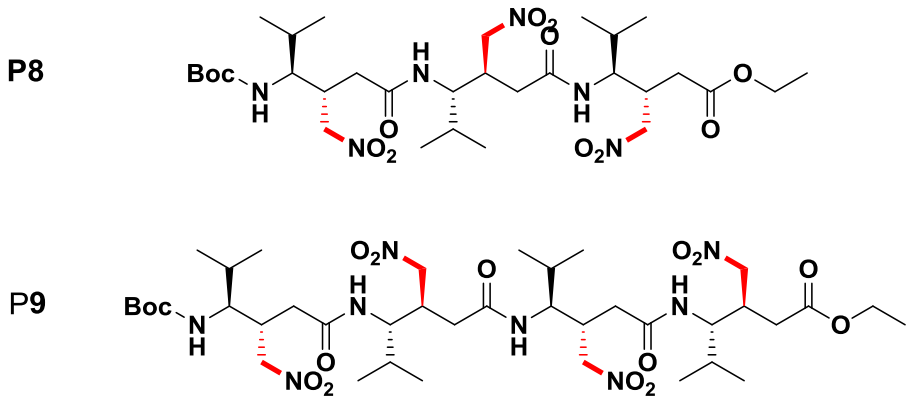

Scheme 6. Sequences of $\gamma^{3,4}$-peptides derived from the major *anti*-isomers.

Single crystal structures of **P8** and **P9** are shown in Figure 5. Intriguingly, the extension of dipeptide (**P7**) to tri (**P8**) and tetrapeptide (**P9**) leads to (P)-14-helical conformations similar to the γ^4-peptides.[22] The helical conformation in **P8** and **P9** is stabilized by one and two intramolecular H-bonds between the *i* and *i+3* residues, respectively. The torsional values and H-bond parameters are tabulated in the Table 5-9. The helical structure in **P8** is stabilized by the 14-membered H-bond between the Boc amide CO (*i*) and the NH of the C-terminal γ-residue (*i+3*), while **P9** structure is stabilized by two intramolecular 14-membered H-bonds between Boc amide CO (*i*) and NH of $\gamma^{3,4}$ Val3 (*i+3*) and between the Val1 CO (*i*) and $\gamma^{3,4}$ Val4 NH (*i+3*). Though there is a possibility to attain C_9-helices similar to the **P7**, both **P8** and **P9** attained the C_{14}-helical conformation.

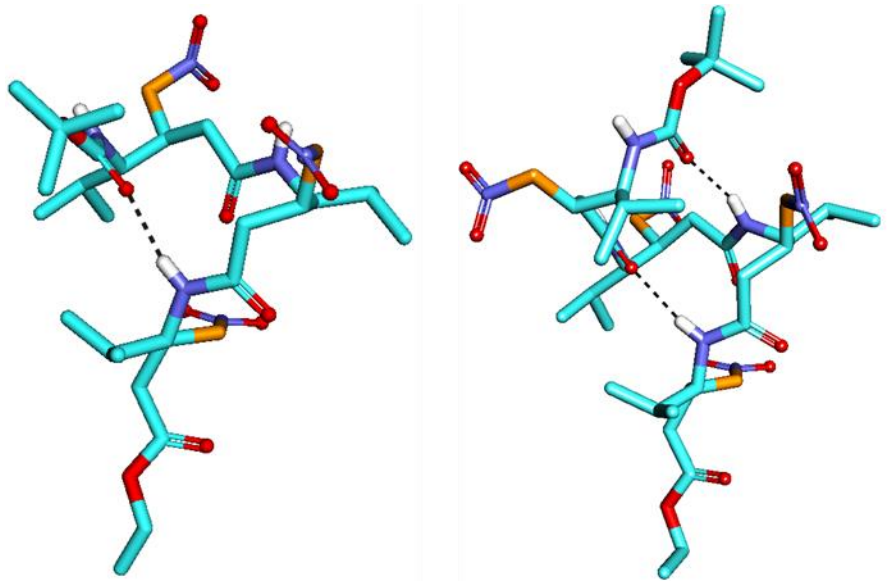

P8 **P9**

Fig 5: Single crystal structures of peptides **P8** and **P9**.

Crystal structure analysis of **P8** and **P9** reveal that except the C-terminal $\gamma^{3,4}$-residue, the other $\gamma^{3,4}$-residues adopted *g+*, *g+* conformations. The directionality and the pattern of H-bonding (*i→i+3*) observed in the $\gamma^{3,4}$- tri and tetrapeptides resemble the 3_{10}-helix in α-peptides as well as 14-helix of γ^4-peptides.[23, 22] The torsional angles of **P8** and **P9** are given in Table 3-6. Careful analysis of the intramolecular H-bonds in **P7**-**P9** revealed that the H-bond distance is

relatively lager in 14-helix compared to the 9-helix. Overall, these novel $\gamma^{3,4}$-disubstituted amino acids favor the helical conformations even in simple dipeptides.

In addition, single crystals of **P9** were simultaneously grown in methanol and ethanol solutions along with EtOAc and their X-ray structures, **P3(m)** and **P3(e)** are shown in Figure 6. Instructively, the structural analysis reveals that **P9** adopted different type of helical conformation. The solvent molecules MeOH and EtOH were invaded the intramolecular 14-membered H-bond which existed between the Boc urethane CO and NH of $\gamma^{3,4}$ Val(3) and bridges the Boc CO (i) and NH of $\gamma^{3,4}$ Val (i+3) through two strong H-bonds. With this solvent invasion, a new nine membered intramolecular H-bond is observed between the residues $\gamma^{3,4}$ Val2 (CO) and $\gamma^{3,4}$ Val4 (NH) instead of the regular 14-membered H-bond observed between the residues $\gamma^{3,4}$ Val1 (CO) and $\gamma^{3,4}$ Val4 (NH). All independent $\gamma^{3,4}$ Val residues adopted *g*+, *g*+ conformations without much deviation in their original torsional values observed in the C_{14}-helix. These results demonstrated that solvent dependent helical switch between 14-to distorted C9 helix. In addition, these studies also provide the realistic information regarding the conformational transition of solvent dependent helical types.

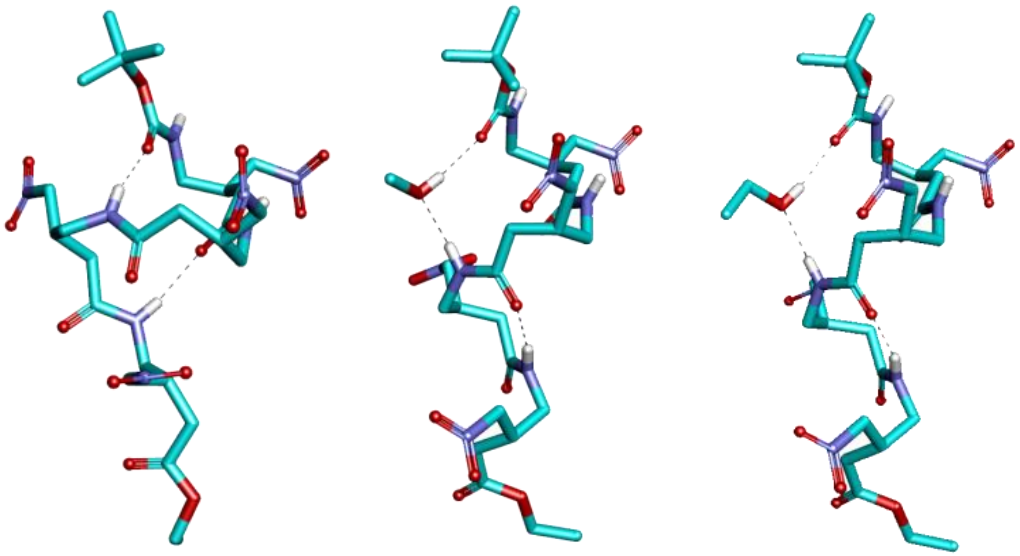

P9 **P9(m)** **P9(e)**

Fig 6: Solvent dependent reversible C_{14}- and C_9-helical types in single crystals of **P9** (m = methanol and e = ethanol). Amino acid side-chains are removed for clarity.

Table 3: Back bone torsional variables of peptide **P8**.

Compound	Residue	ϕ	θ_1	θ_2	ψ	ω	Back bone conformation
P8 Molecule A	γVal(β-CH_2NO_2)-1	-110	58	72	175	175	g^+, g^+
	γVal(β-CH_2NO_2)-2	-108	62	66	-148	-173	g^+, g^+
	γVal(β-CH_2NO_2)-3	-106	-171	-60	156	-	t, g^+
P8 Molecule B	γVal(β-CH_2NO_2)-1	-114	59	68	175	172	g^+, g^+
	γVal(β-CH_2NO_2)-2	-115	67	68	-135	-177	g^+, g^+
	γVal(β-CH_2NO_2)-3	-99	65	111	-7	-	g^+, t
P8 Molecule C	γVal(β-CH_2NO_2)-1	-109	69	68	176	173	g^+, g^+
	γVal(β-CH_2NO_2)-2	-119	61	72	-140	174	g^+, g^+
	γVal(β-CH_2NO_2)-3	-120	177	-69	-121	-	t, g^+

Mean torsional values of three peptides tabulated with e.s.d. value					
Residue	ϕ	θ_1	θ_2	ψ	ω
γVal(β-CH_2NO_2)-1	-111 (2)	62 (6)	69 (2)	176 (1)	173 (2)
γVal(β-CH_2NO_2)-2	-114 (6)	63 (3)	69 (3)	141 (6)	-
γVal(β-CH_2NO_2)-3	-108	-	-	-	-

Table 4: Intra and Intermolecular H-bond parameters of **P8A - P8C**.

P8 Molecule A	**Donor (D)**	**Acceptor (A)**	**D….A (Å)**	**DH….A (Å)**	**NH….O (deg)**	**N….O=C (deg)**
Intermolecular	N5	O2	2.938	2.091	167.78	164.97
Intramolecular H-bond	N1	O38 (**S**)	3.063	2.231	162.98	139.56
	N3	O27 (**b**)	2.841	1.987	171.81	142.62
	O32	N8 (**c**)	2.835	1.976	176.32	133.58

P8 Molecule B	**Donor (D)**	**Acceptor (A)**	**D….A (Å)**	**DH….A (Å)**	**NH….O (deg)**	**N….O=C (deg)**
Intermolecular	N (13)	O (23)	2.962	2.106	172.85	177.50
Intramolecular H-bond	N (15)	O (19)	2.863	2.063	154.34	134.53
	O (27)	N (3) (**a**)	2.841	1.987	171.81	142.62

P8	Donor	Acceptor	D….A	DH….A	NH….O	N….O=C
Intramolecular	N (10)	O (13)	2.956	2.104	171.13	163.59
Intermolecular H-bond	N (8)	O (38)	2.835	1.976	176.32	133.58
	0 (19)	N (15)	2.863	2.063	154.34	134.53

Table 5: Back bone torsional variables of peptide **P9**.

Compound	residue	ϕ	θ_1	θ_2	ψ	Back bone conformation
P9 EtOAc	γVal(β-CH_2NO_2)-1	-105	64	72	172	g^+, g^+
	γVal(β-CH_2NO_2)-2	-123	51	71	-154	g^+, g^+
	γVal(β-CH_2NO_2)-3	-127	49	63	-145	g^+, g^+
	γVal(β-CH_2NO_2)-4	-110	-161	-56	175	t, g^+
P9 (m) MeOH	γVal(β-CH_2NO_2)-1	-111	50	72	-172	g^+, g^+
	γVal(β-CH_2NO_2)-2	-106	71	64	-162	g^+, g^+
	γVal(β-CH_2NO_2)-3	-102	72	69	-95	g^+, g^+
	γV(β-CH_2NO_2)-4	-99	67	74	2	g^+, g^+
P9 (e) EtOH	γV(β-CH_2NO_2)-1	-112	47	74	-170	g^+, g^+
	γV(β-CH_2NO_2)-2	-107	68	66	-160	g^+, g^+
	γV(β-CH_2NO_2)-3	-106	71	70.74	-99	g^+, g^+
	γV(β-CH_2NO_2)-4	-99	67	72	6	g^+, g^+

Table 6: Intra and Intermolecular H-bond parameters of **P9**.

P9 EtOAc	**Donor (D)**	**Acceptor (A)**	**D….A (Å)**	**DH….A (Å)**	**NH….O (deg)**	**N….O=C (deg)**
Intermolecular H-bond	N (5)	O (2)	3.067	2.253	157.55	166.28
	N (7)	O (5)	2.997	2.145	170.70	154.05
Intramolecular H-bond	N (3)	O (11) †	2.805	2.037	148.19	155.55
	O (11)	N (3) *	2.805	2.037	148.19	155.55

* Symmetry equivalent -1+x, y, z; † Symmetry equivalent 1+x, y, z

P9 $CHCl_3$/ Tol	**Donor (D)**	**Acceptor (A)**	**D….A (Å)**	**DH….A (Å)**	**NH….O (deg)**	**N….O=C (deg)**
Intermolecular	N (5)	O (2)	3.073	2.264	157.04	166.75
H-bond	N (7)	O (5)	3.016	2.166	170.26	154.35
Intramolecular	N (3)	O (11) †	2.811	2.045	147.99	156.14
H-bond	O11	N (3) *	2.811	2.045	147.99	156.14

* Symmetry equivalent -1+x, y, z; † Symmetry equivalent 1+x, y, z

P9 MeOH	Donor (D)	Acceptor (A)	D….A (Å)	DH….A (Å)	NH….O (deg)	N….O=C (deg)
Intermolecular	N (4)	O (9)	2.817	1.970	168.11	122.66
Intramolecular H-bond	O (2)	O (17)	2.725	1.906	175.62	155.38
	N (1)	O (12) *	2.877	2.070	158.41	126.05
	N (8)	0 (17)	2.858	1.999	176.83	111.51
	O (12)	N (1) †	2.877	2.070	158.41	126.05

* Symmetry equivalent 1-x, 1/2+y, 1-z; † Symmetry equivalent 1-x, -1/2+y, 1-z

P9 EtOH	Donor (D)	Acceptor (A)	D….A (Å)	DH….A (Å)	NH….O (deg)	N….O=C (deg)
Intermolecular	N (7)	O (8)	2.852	2.022	167.91	123.50
Intramolecular H-bond	O (2)	O (14) (**EtOH**)	2.748	1.953	163.19	162.37 (O….O-C)
	N (1)	O (11)*	2.638	2.000	164.53	126.22
	N (5)	O (14) (**EtOH**)	2.914	2.054	176.85	124.33 (N….O-C)
	O11	N (1)†	2.638	2.000	164.53	126.22

*Symmetry equivalent 1-x, 1/2+y, 1-z; † Symmetry equivalent 1-x, -1/2+y, 1-z

2A.3.4 Synthesis and Conformational Analysis of α, $\gamma^{3,4}$-Hybridpeptides

The results obtained from the homooligomers of β-nitromethyl substituted γ- amino acids motivated us to design **P10** and **P11** to understand the conformations of $\gamma^{3,4}$-amino acids in 1:1 α,γ-hybrid peptides. The sequences of the peptides are shown in Scheme 7. Peptide **P10** consists of both $\gamma^{3,4}$ and γ^{4}-amino acids along with Aib, while **P11** composed of alternating Aib and $\gamma^{3,4}$ amino acids. Peptides were synthesized in solution phase and pure peptides were subjected to crystallization. Single crystals of **P10** obtained from the methanol solution gave the X-ray structure as shown in the Figure 7.

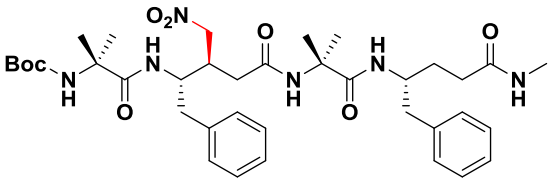

P10

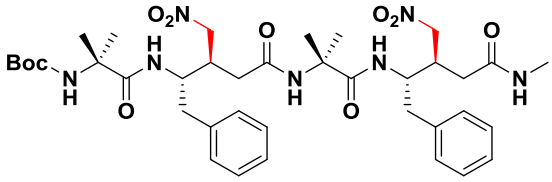

P11

Scheme 7: Sequences of α, $\gamma^{3,4}$-hybrid peptides derived from the major *anti* isomers.

The 12-helical structure of **P10** is stabilized by three intramolecular H-bonds between *i* and *i+3* residues similar to the other α,γ-hybrid peptides.[24] Both γ^{4}-Phe and $\gamma^{3,4}$-Phe adopted required *g+*, *g+* conformations along C^{γ}-C^{β} and C^{β}-C^{α} bonds to accommodate into the12-helix. The H-bond parameters and torsion angles are tabulated in the Table 7 and 8. Enormous efforts have been made to crystallize **P11** in various solvent combinations; however, it gave single crystals only in isopropanol solution. The X-ray structure of **P11** is shown in Figure 7. The 12-helical conformation of **P11** is stabilized by two 12-membered H-bonds. Analysis reveals that instead of participating into the canonical intramolecular H-bonding the terminal amide NH is involved in strong intermolecular H-bonding with the solvent isopropanol.

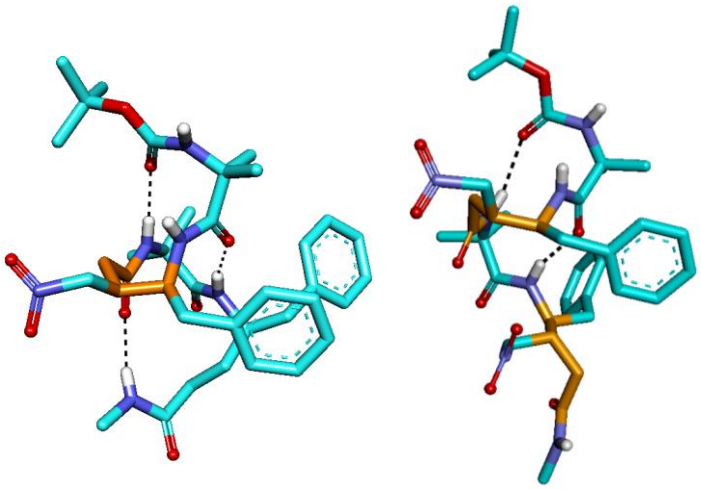

P10 **P11**

Fig 7: X-ray structures of α, $\gamma^{3,4}$-hybrid tetrapeptide 12-helices, **P10** and **P11**.

In contrast to **P10**, the nitro and the CO groups of $\gamma^{3,4}$ Phe2 in **P11** are involved in intermolecular H-bonding with NH of the $\gamma^{3,4}$ Phe2 and Boc-amide NH of the other helix. These intermolecular interactions lead to the arrangement of 12-helices into a spectacular right-handed super-helix with the pore diameter of 7.3 Å. Solvent isopropanol occupied the helical groove of the super helix in the crystal packing, suggesting its important role in peptide crystallization. A well-organized helical assembly of **P11** is shown in Figures 8. The tubular arrangement of the hybrid 12-helix, **P11**, resembles the arrangement of β-sheets in β-helix, however, through non-covalent interactions.[25] Recently, the tubular porous organic and peptide structures have attracted considerable attention due to their applications in the separation science, catalysis and nanobiotechnology.[26] We hypothesize that the tubular architecture of **P11** may serve as a new template to design soft biomaterials. In contrast, the **P10** 12- helix with single nitro amino acid did not show helical pores in single crystals, suggesting the requirement of two nitro groups for the hierarchical tubular assembly. Overall the structural analysis of heterooligomers of β-nitromethyl-substituted γ-amino acids suggested that they readily adopt helical conformations and follow the trend of other γ-peptides. In addition, helical pores observed in **P11** offer the glimpse of potential of β-nitromethyl γ-amino acids and laid the foundation for further investigation.

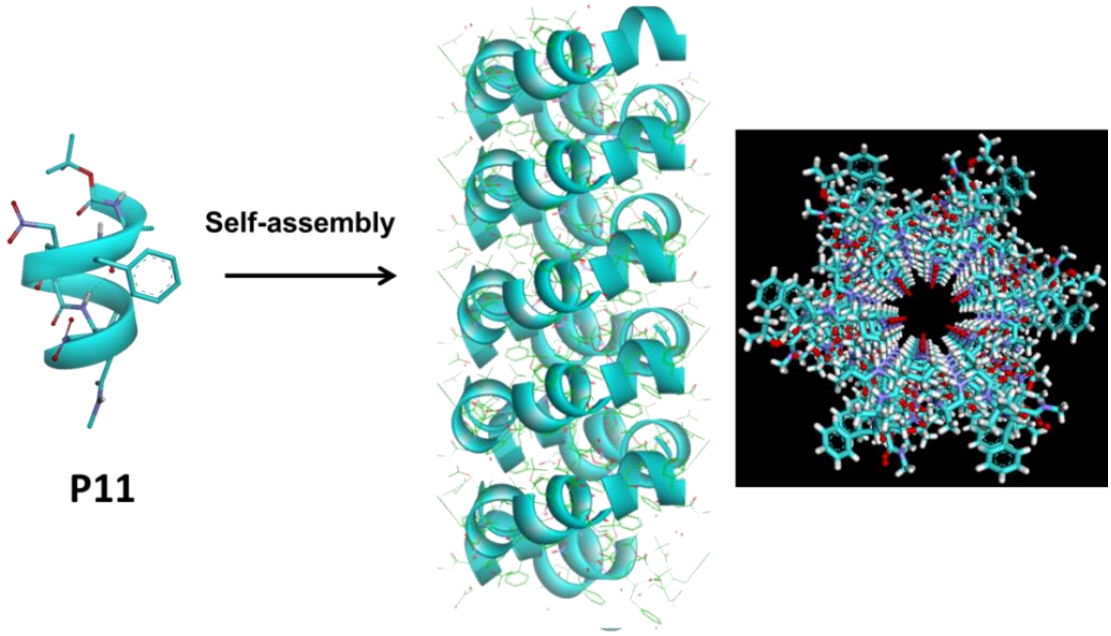

Fig 8: Hierarchical assembly of α, $\gamma^{3,4}$-hybrid 12-helix **P11** into right-handed super-helix along the b-axis and top view of the ordered self-organization of **P11** (along the c-axis).

Table 7: Back bone torsional variables of peptide **P10**.

Compound	**Residue**	ϕ	θ_1	θ_2	ψ	**Back bone conformation**
P10	Aib1	-59	-	-	-45	g^+, g^+
	γPhe(β-CH_2NO_2)-2	-121	55	63	-126	g^+, g^+
	Aib-3	-54	-	-	-37	g^+, g^+
	γPhe-4	-95	72	-170	87	g^+, t

Table 8: Intra and Intermolecular H-bond parameters of **P10**.

P10	**Donor (D)**	**Acceptor (A)**	**D……..A (Å)**	**D-H…..A (Å)**	**D-H……A (deg)**	**D…..O=C (deg)**
Intramolecular H-bonds	N (3)	O (2)	2.91	2.06	172	157
	N (4)	O (3)	2.82	1.98	166	145
	N (5)	O (6)	2.86	2.02	167	138
Intermolecular H-bonds	N (2)	O (7) *	2.67	2.09	150	151
	O (7)	N (2) ‡	2.67	2.09	150	151

† 1+x, 1+y, z; * x, 1+y, z

Table 9: Back bone torsional variables of peptide **P11**.

Compound	**Residue**	ϕ	θ_1	θ_2	ψ	**Back bone conformation**
P11	Aib1	-62	-	-	-31	g^+, g^+
	γPhe(β-CH_2NO_2)-2	-118	45	67	-129	g^+, g^+
	Aib-3	-58	-	-	-38	g^+, g^+
	γPhe(β-CH_2NO_2)-4	-118	-171	-65	-130	t, g^+

Table 10: Intra and Intermolecular H-bond parameters of **P11**.

P11	**Donor (D)**	**Acceptor (A)**	**D……..A (Å)**	**D-H…..A (Å)**	**D-H……A (deg)**	**D…..O=C (deg)**
Intra - molecular H-bonds	N (4)	O (2)	3.056	2.232	160.63	147.75
	N (5)	O (3)	2.864	2.035	161.41	143.08
Inter - molecular H-bonds	N (1)	O (6) †	2.878	2.095	151.15	117.19
	N (2)	O (4) †	3.022	2.269	146.21	154.03
	N (1)’	O (6)	2.878	2.095	151.15	117.19
	N (2)’	O (4)	3.022	2.269	146.21	154.03
	N (6)	O (15)*	2.868	2.014	171.59	122.37
	O (11)	O (7)	2.762	2.016	151.16	142.34
	O (15)	O (11)	2.757	1.950	167.89	123.35
	N (6)‡	O (15)	2.868	2.014	171.59	122.37

† Symmetry equivalent y, 1-x+y, -1/6+z; * Symmetry equivalent X, Y, -1+Z

’ Symmetry equivalent 1+x-y, x, 1/6+z ; ‡ Symmetry equivalent x, y, 1+z

2A.4. Chemistry on Nitropeptides

To understand whether β-nitromethyl substituted γ-amino acids can undergo chemical transformations similar to the nitroalkanes (Figure 1), we subjected them to selected organic transformations (Scheme 8). The transformation of β-nitromethyl group to corresponding carboxylic acid (**7**) was achieved through $NaNO_2$/AcOH oxidation.[27] The oxidation of β-nitromethyl group provided an alternative route to synthesize new 2, 3-disubstituted β-amino acids. Further, the β-nitromethyl group was transformed to oxime (**8**) using tributyl tin hydride in the presence of AIBN.[28] The transformation of 3, 4-disubstituted γ-amino acid into 3-substituted γ-amino acid (**9**) was achieved through simple catalytic hydrogenation in the presence of Pd/C.[29] In addition, 1, 3-dipolar cycloaddition product (**10**) of alkyl nitro group with phenylacetylene was achieved in presence of phenyl isocyanate under mild conditions.[30] The products of these transformations were isolated in good yields. All these reactions suggested that the nitro amino acids may serve as versatile templates to derive various β- and γ-amino acid building blocks and their utility in bioconjugations through simple organic transformations.

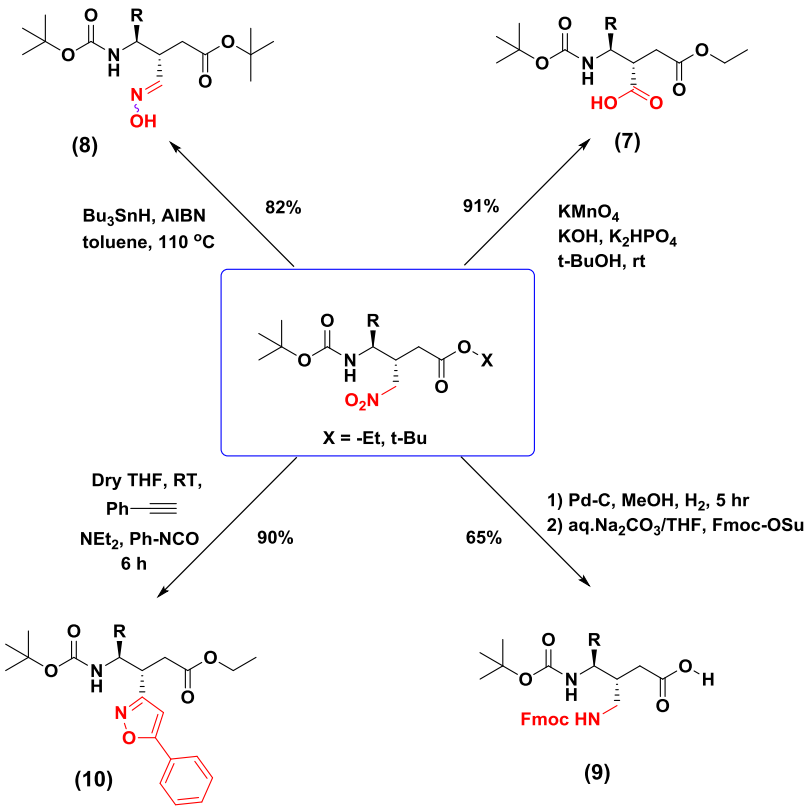

Scheme 8: Organic transformations on *N*-Boc-β-nitromethyl substituted γ-amino esters.

As a proof of concept to verify whether the nitropeptides can also undergo similar transformations as mentioned in the simple amino acid templates, we subjected **P10** to various organic transformations to derive corresponding carboxylic acid (**P12**), 1,3-dipolar cycloaddition product (**P13**) with phenylacetylene and reduction to corresponding amine (**P14**) under identical conditions. The organic transformations on hybrid peptide **P10** are shown in Scheme 9. All hybrid peptide derivatives were isolated in good yield and characterized. These results suggest that organic transformations are also possible on β-nitromethyl γ-peptides.

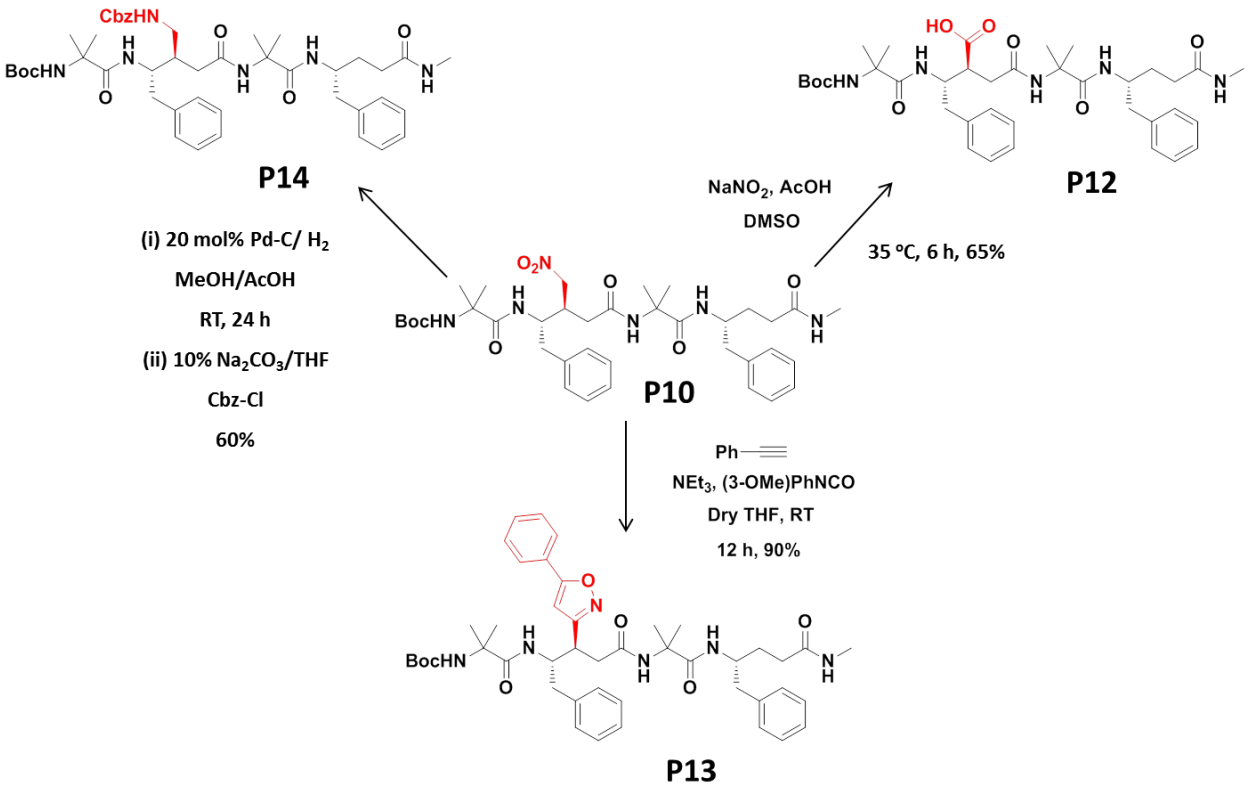

Scheme 9: Organic transformations of hybrid peptide **P10** to **P12, P13** and **P14**

2A.5 $\beta^{2,3}$-Amino Acids and Peptides

The transformation of β-nitromethyl substituted γ-amino acids to novel disubstituted β-amino acids were further explored to synthesize β-peptide **P15** to prove that organic transformations can be performed in large scale. The synthetic scheme and the sequence of **P15** are shown in Scheme 10. The peptide was synthesized in solution phase and pure peptide was subjected to crystallization. The single crystal conformation of **P15** is shown in Figure 9. Instructively, the disubstituted β-peptide adopted helical screw type conformation with 6-

membered H-bonds. Even though extensive theoretical calculations suggested stable C_6-helical conformation in β-peptides,[31] they are rarely studied in single crystals. Similar type of continuous C_6-helical β-peptides were studied with cyclic β-amino acids in solution.[32] To the best of our knowledge, this is the first report which shows stable C_6-helix of $\beta^{2,3}$-peptide in single crystals. The torsion angles and H-bond parameters of **P15** are tabulated in the Table 11 and 12. The $\beta^{2,3}$-residues displayed torsion angle values (-120°, -66°, -120°) very close to those which characterize this residue in an optimized 6-helix foldamer.[31] $\beta^{2,3}$-residue adopted a *g*+ local conformation for the θ torsion angle, facilitating formation of the (1→1) 6-membered ring H-bond and orientation of its NH towards carbonyl. Thus C6 helical conformation was formed with C=O……H–N distances in the range 2.2–2.3 Å and ∠NH….O = 125°). The structure does not have a helical topology, however resembling a ribbon. Although the ester C-terminal of **P15** was showed poor geometry of H-bonding (C=O…H–N = 2.75 Å, ∠NH….O = 95°), however, the torsion angles were found to be same as the other two residues. It is noteworthy to mention that β-nitromethyl-substituted γ-amino acids can be transformed into novel 2, 3-disubstituted β-amino acids.

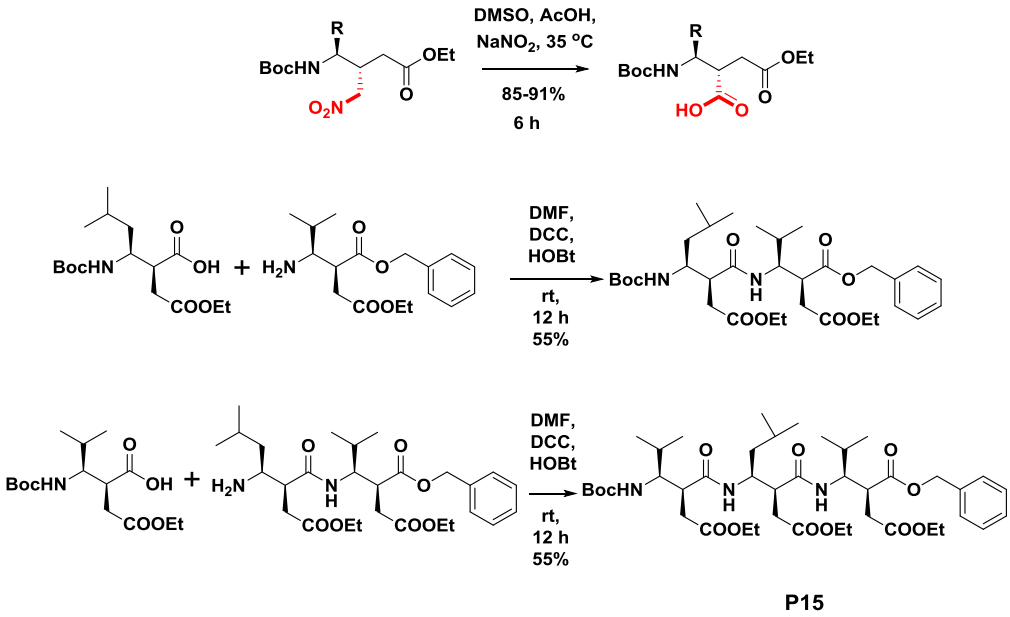

Scheme 10: Transformation of β-nitromethyl γ-amino esters into 2,3-disubstituted β-amino acids and synthesis of $\beta^{2,3}$-peptide **P15**.

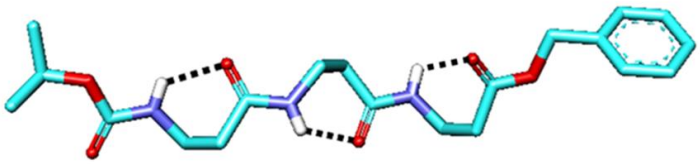

Fig 9: X-ray structure of β-peptide (**P15**) C_6-helix (Side-chains omitted for clarity).

Table 11: Back bone torsional variables (in deg) of peptide **P15**.

Residue	ϕ	θ	ψ	ω
βV	-126	-66	-126	-179
βL	-116	-66	-132	177
βV	-98	-49	-102	-
βV’	-127	-67	-126	-179
βL’	-116	-66	-132	178
βV’	-99	-48	-102	-
Average of Two molecules				
βV	-126.5 (0.5)	-66.5 (0.5)	-126 (0)	-179 (0)
βL	-116 (0)	-66.5 (0.5)	-132 (0)	177.5 (0.5)
βV	-99.5 (0.5)	-48.5 (0.5)	102 (0)	-

Table 12: Intra and Intermolecular H-bond parameters of P15.

Donor (D)	Acceptor (A)	D….A (Å)	DH….A (Å)	∠NH….O (deg)
Intra-molecular H-bond Parameters				
N1	O3	2.8	2.2	125.7
N2	O6	2.8	2.3	119.4
N3	O9	2.95	2.75	94.8
N4	O17	2.8	2.2	125.7
N5	O19	2.8	2.3	119.4
N6	O22	2.95	2.75	94.8
Inter-molecular H-bond Parameters				
N6	O4†	3.0	2.3	145.4
N6‡	O4	3.0	2.3	145.4

Symmetry operations: † 1+x, y, z; ‡ -1+x, y, z.

SECTION 2B: Synthesis and Stereochemical Analysis of thiostatines (β-sulfhydryl γ-amino acids)

2B.1 Introduction

In continuation with the nitromethane conjugate addition reactions on *E*-vinylogous amino esters, we also investigated the conjugate addition of thiols and the stereochemistry of thiol conjugate addition reaction. The reason to use thiols as nucleophiles is that it is possible to mimic the statine (β-hydroxy γ-amino acids)[33] analogues as well as modified cysteines with sulfhydryl group attached to the backbone. Recently, we reported the utility of thiostatins in the design of backbone disulfide bridged β-hairpins.[34] In contrast to the β-nitromethyl substituted γ-amino acids, β-thiol substituted γ-amino acids did not give the single crystals to determine their stereochemistry and diastereoselectivity in the thiol conjugate addition. To understand the stereochemistry of the thiol conjugate addition products, we designed and synthesized a heptapeptide composed of thiostatine and studied the stereochemistry using single crystals. To introduce thiol group into the backbone we adopted different strategy and details are given below.

2B.2 Results and Discussion

2B.2.1 Synthesis of β-sulfhydryl γ-Amino Acids

The synthesis of orthogonally protected β-thiol substituted γ-amino acids (thiostatines) is shown in Scheme 11. The starting material *tert*-butyl ester of α, β-unsaturated γ-Val(**4**) was synthesized using Wittig reaction and subjected to thioacetic acid Michael addition in the presence of DBU. Due to the self-dimerization of free thiols, we are encouraged to utilize less reactive thioacetic acid as a source of thiol in the conjugate addition. In addition, the acetyl group in thioacetic acid acts as a temporary protecting group and it can be removed through mild $NaBH_4$ reduction. The diastereomeric mixture of thioacetate conjugate addition products (**11**) were purified and subjected to the $NaBH_4$ reduction in the presence of O-nitro benzyl bromide to derive photochemically labile protecting group for free –SH (**12**) *in situ*. In contrast to the thioacetic acid conjugated addition products (**11**), the O-nitro S-benzyl *anti* (**12a**) and *syn* (**12b**) diastereoisomers (with respect to amino acid side-chain) of thiostatines were separated in 60:40

ratio through column chromatography. We utilized major diastereoisomer (**12a**) for the synthesis of **P16**. The Boc- and *tert*-butyl protecting groups were deprotected using TFA in DCM and the free amine was further protected using Fmoc- group (**13a**) and directly utilized in the solid phase synthesis.

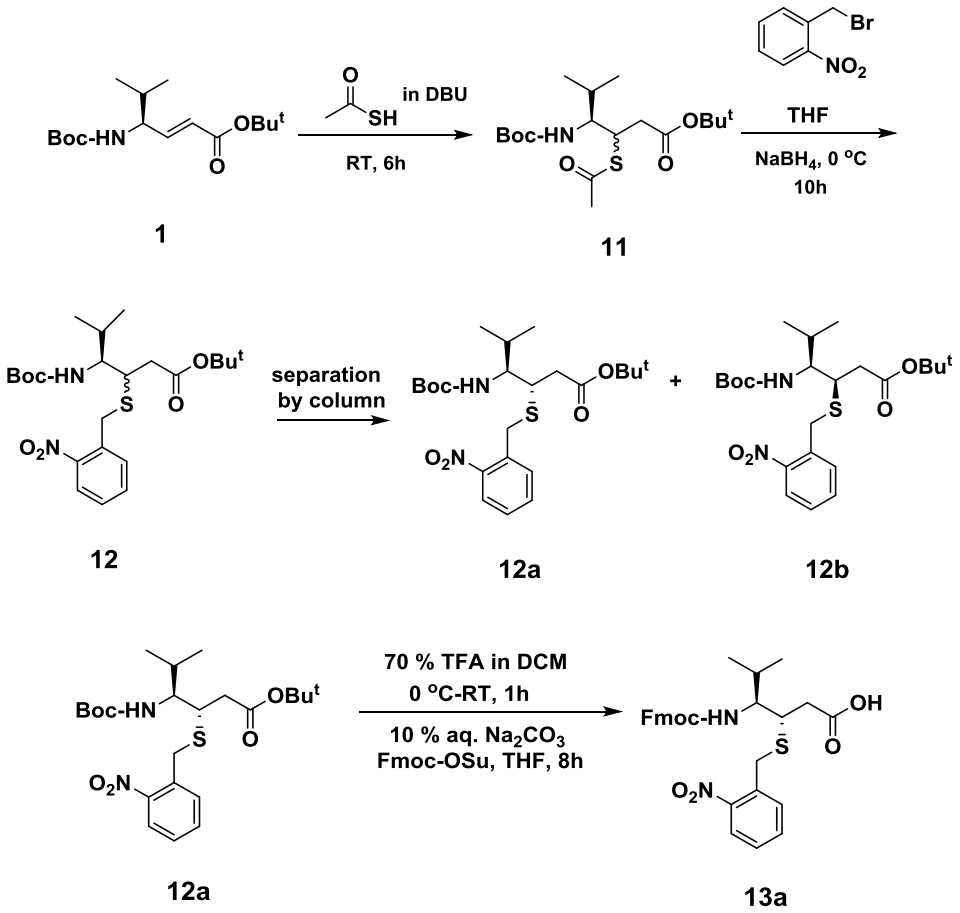

Scheme 11: Schematic representation of the synthesis of orthogonally protected thiostatine (Fmoc-γVal(β-SNB)-OH).

2B.2.2 Synthesis and Conformational Analysis of β-Sulfhydryl γ-Amino Acid in Hybrid Helix

The model peptide **P16** was synthesized using solid phase method by standard Fmoc-chemistry on Knorr amide resin at 0.2 mmol scale. All coupling reactions were performed using standard HBTU/HOBt coupling conditions. The thiostatine was incorporated at 4th position of the α,γ-

hybrid heptapeptide sequence, Ac-Aib-γPhe-^{D}Ala-(*S*,*S*)γVal(β-SNB)-Aib-γPhe-Aib-$CONH_2$. After the synthesis, the peptide **P16** was released from the resin and purified using HPLC.

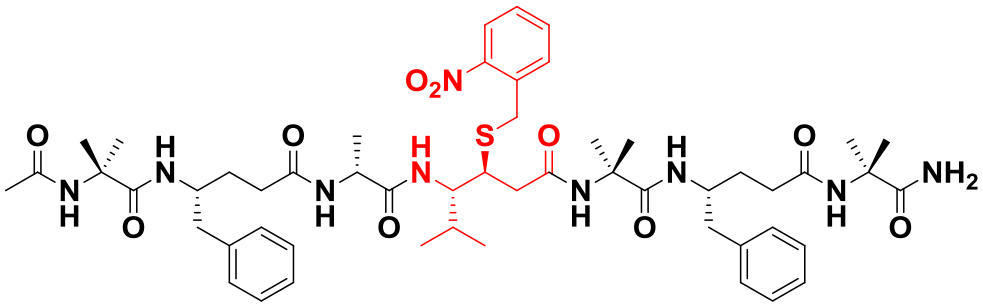

Scheme 12: Chemical structure of peptide **P16** (Ac-Aib-γPhe-^{D}Ala-(*S*,*S*)γVal(β-SNB)-Aib-γPhe-Aib-$CONH_2$).

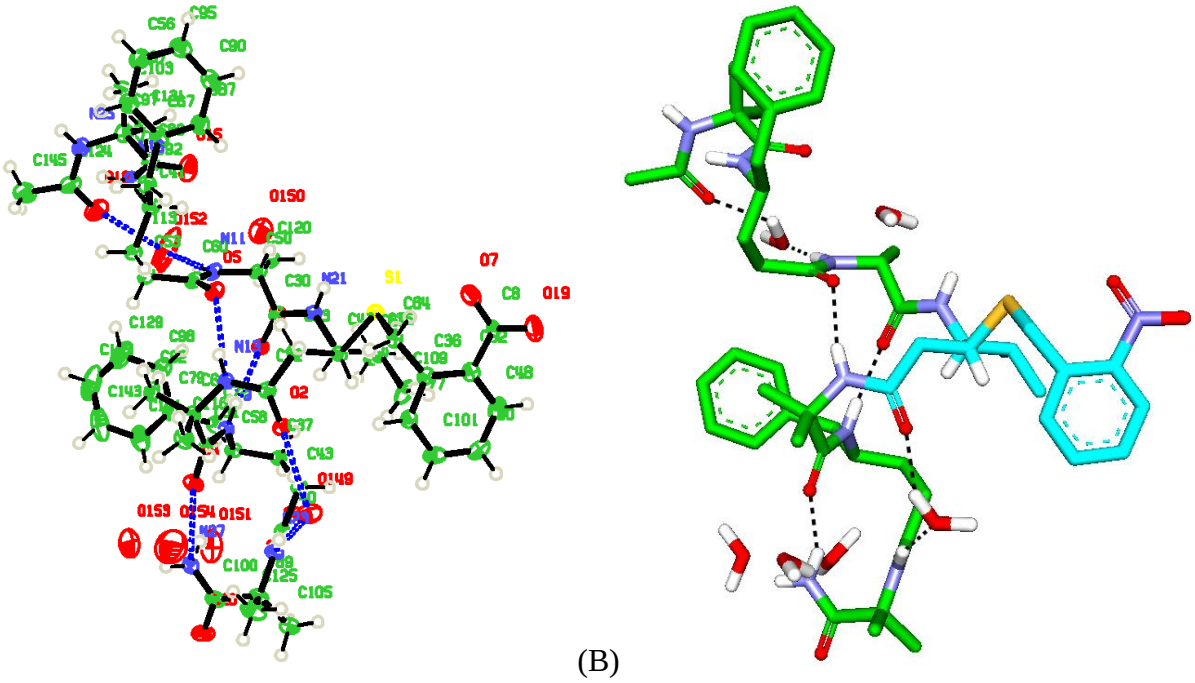

(A) (B)

Fig 10: (A) ORTEP diagram of peptide **P16** and thermal ellipsoids were drawn at 60% probability. H-bonds are shown by blue dotted lines. (B) X-ray structure of peptide **P16 (**Ac-Aib-γPhe-^{D}Ala-(*S*,*S*)γVal(β-SNB)-Aib-γPhe-Aib-$CONH_2$). H-atoms of polar atoms and β, γ C-atoms of thiostatine residue [for (*S*, *S*) stereochemistry] are shown for clarity. H-bonds are represented by dotted lines.

The peptide was subjected to crystallization to understand the stereochemistry of thiostatines. The single crystals were obtained from aqueous methanol solution and its structure is shown in Figure 10. The heptapeptide adopted distorted 12-helical conformation due to the presence of ^{D}Ala at position 3. Similar to the α,γ-hybrid 12-helix, the C-terminal 12-helix is stabilized by three intermolecular H-bonds.[24] The torsional angles and H-bond parameters are tabulated in the Tables 13 and 14. The crystal structure analysis reveals stereochemistry of thiol addition product. The stereochemistry of major product **12a** was found to be *anti* (*3S*, *4S*). More importantly, the conjugate addition of thiols followed the similar trend that was observed in the nitromethane conjugate addition to compounds **1i** and **4** (Table 1 and Scheme 4; Section 2A). This is also in good agreement with H-bond assisted nitromethane conjugate addition (Scheme 3; Section 2A). Our group is further exploring the utilization of thiostatines in the design of stable and biologically active β-hairpins and helix mimetics.

Table 13: Back bone torsional variables of peptide **P16**

Compound	**Residue**	**ϕ**	**θ1**	**θ2**	**ψ**	**ω**
P16	Aib1	-59	-	-	-36	-171
	γPhe 2	-118	68	64	-137	173
	^{D}Ala 3	60	-	-	-141	-180
	γVal(β-SNB) 4	-116	53	69	-136	-171
	Aib 5	-60	-	-	-35	-168
	γPhe 6	-114	62	64	-140	-178
	Aib 7	-62	-	-	-25	-

Table 14: Intra and Intermolecular H-bond parameters of **P16**

P16	**Donor (D)**	**Acceptor (A)**	**D……..A (Å)**	**D-H…..A (Å)**	**D-H……A (^{0})**	**D…..O=C (^{0})**
Intramolecular H-bonds	N5	O3	2.9	2.0	167	123
	N6	O4	2.9	2.1	153	146
	N8	O6	2.9	2.1	153	150
Intermolecular H-bonds	N1	O7	3.0	2.1	167	126
	O3	O9	2.8	-	-	122
	N4	O8	2.9	2.1	168	175
	O5	O11	2.8	-	-	176
	O1	O10	2.79	-	-	167
	N3	O10	2.85	1.99	176	-
	O6	O16	2.9	-	-	135

2.2 Conclusion

In conclusion, we have presented the synthesis, conformational analysis and chemical diversity of novel β-nitromethane substituted γ-amino acid homooligomers and α,γ-hybrid peptides. In addition, β-nitromethyl substituted γ-amino acids were used to construct 2,3-disubstituted β-peptide foldamers. Moreover, the alkyl nitro group can be used as an excellent intermediate to generate a variety of functional groups on peptides under mild conditions. Both $\gamma^{3,4}$ and α, $\gamma^{3,4}$-hybrid peptides showed characteristic C_{14}- and C_{12}-helical conformations, respectively. The spectacular supramolecular tubular architecture displayed by the hybrid peptide

P11 invokes further investigations in higher ordered hybrid peptides. In addition, 2, 3-disubstituted β-peptide derived from the nitro amino acids showed a notable C_6-helix signature. In comparison with other peptide foldamers, the nitropeptides showed remarkable chemical transformations. In addition, thiol conjugate addition follows the similar trend that was observed in the case of nitromethane Michael addition of dγPro (**1i**). Overall, the single crystal conformations of the $\gamma^{3,4}$-peptides, self-organized helical pore from α, $\gamma^{3,4}$-hybrid 12-helix and the transformation of alkyl nitro group into a verity of functional groups, and synthesis and the stereochemistry of thiostatines reported here can be utilized further for the construction of functional foldamers and peptidomimetics.

2.3 Experimental Section:

2.3.1 General experimental details

Column chromatography was performed on silica gel (120-200 mesh). ^{1}H NMR and ^{13}C NMR spectra were recorded on 400 MHz and on 100 MHz respectively, using residual solvent signal as internal standards ($CDCl_3$& CD_3OH). Chemical shifts (δ) reported in parts per million (*ppm*) and coupling constants (*J*) reported in Hz. Mass spectra were recorded using MALDI TOF/TOF and HRMS Electron Spray Ionization (ESI). Fluorescence measurements were performed on spectrofluorometer.

2.3.2 Synthesis procedure and characterization of compounds in Section 2A.

Crystallographic Information of Peptides

Crystal structure analysis of Boc-γLeu(β-CH_2NO_2)-COOEt (2c): Crystals were grown by slow evaporation from a solution of EtOAc. A single crystal (0.19× 0.15 × 0.12 mm) was mounted on loop with a small amount of the paraffin oil. The X-ray data were collected at 100 K temperature on a Bruker APEX(II) DUO CCD diffractometer using Mo K_α radiation (λ = 0.71073 Å), ω-scans (2θ = 56.56), for a total of 4625 independent reflections. Space group P2(1), 2(1), 2(1), a = 11.306(6), b = 31.857(16), c = 5.353(3), V = 1928.2(17) Å^3, Orthorhombic P, Z=4 for chemical formula $C_{16}H_{30}N_2O_6$, with one molecule in asymmetric unit; ρ calcd = 1.193 gcm^{-3}, μ = 0.091 mm^{-1}, F(000) = 752, R_{int}= 0.0616. The structure was obtained by direct methods using SHELXS-97.The final R value was 0.0927 (wR2 = 0.2645) 2600 observed reflections (F_0

$\geq 4\sigma$ ($|F_0|$)) and 224 variables, S = 1.161. The largest difference peak and hole were 0.920 and -0.470 eÅ^3, respectively.

Crystal structure analysis of Boc-γIleu(β-CH_2NO_2)-COOH (2b acid): Crystals were grown by slow evaporation from a solution of EtOAc and Hexane. A single crystal (0.35× 0.24 × 0.20 mm) was mounted on loop with a small amount of the paraffin oil. The X-ray data were collected at 100 K temperature on a Bruker APEX(II) DUO CCD diffractometer using Mo K_α radiation (λ = 0.71073 Å), ω-scans (2θ = 56.56), for a total of 4252 independent reflections. Space group P2(1), a = 11.226(8), b = 7.133(5), c = 12.018(9), β = 110.948(15) V= 898.7(11) Å^3, Monoclinic P, Z=2 for chemical formula $C_{14}H_{26}N_2O_6$, with one molecule in asymmetric unit; ρ calcd = 1.176 gcm^{-3}, μ = 0.092 mm^{-1}, F(000) = 344, R_{int}= 0.0345. The structure was obtained by direct methods using SHELXS-97.The final R value was 0.0441 (wR2 = 0.1012) 3359 observed reflections ($F_0 \geq 4\sigma$ ($|F_0|$)) and 205 variables, S = 1.036. The largest difference peak and hole were 0.173 and -0.239 eÅ^3, respectively.

Crystal structure analysis of Boc-γVal(β-CH_2NO_2)-γLeu(β-CH_2NO_2)-COOEt (P6): Crystals of peptide were grown by slow evaporation from a solution of EtOAc. A single crystal (0.34× 0.20 × 0.18 mm) was mounted on glass fiber with a small amount of the paraffin oil. The X-ray data were collected at 100K temperature on a Bruker APEX(II) DUO CCD diffractometer using Mo K_α radiation (λ = 0.71073 Å), ω-scans (2θ = 58.56), for a total of 5572 independent reflections. Space group P3(2) , a = 13.503(9), b = 13.503 (9), c = 14.005(10), α = 90.00, β = 90.00, γ = 120.00, V = 2211.44 Å^3, Trigonal, Z = 3, Z' = 0 for chemical formula $C_{24}H_{44}N_4O_9$, with one molecule in asymmetric unit; ρcalcd = 1.186 gcm^{-3}, μ = 0.091 mm^{-1}, F(000) = 864, R_{int} = 0.1857. The structure was obtained by direct methods using SHELXS-97. The final R value was 0.0865 (wR2 = 0.2072)1917 observed reflections ($F_0 \geq 4\sigma$ ($|F_0|$)) and 343 variables, S = 0.878. The largest difference peak and hole were 0.879 and -0.438eÅ^3, respectively. During the crystal analysis, it was observed that leucine side chain methyl carbons C_{17} and C_{18} are showing disorder due to a large difference in the vibrational behavior of atoms and therefore H-atoms attached with them are showing short intramolecular contacts due to lack of sufficient van der waals space.

Boc-γVal(β-CH_2NO_2)-γVal(β-CH_2NO_2)-COOEt (P7): Crystals of peptide were grown by slow evaporation from a solution of EtOAc. A single crystal (0.15 × 0.1 × 0.08 mm) was mounted on loop with a small amount of the paraffin oil. The X-ray data were collected at 100 K temperature on a Bruker APEX(II) DUO CCD diffractometer using Mo K_α radiation (λ = 0.71073 Å), ω-scans (2θ = 52.52), for a total of 5339 independent reflections. Space group P3 (2), a = 13.414 (11), b = 13.414 (11), c = 13.869 (11), β = 90.00, V = 2161 (3) $Å^3$, Trigonal, Z = 3 for chemical formula $C_{23}H_{42}N_4O_9$, with one molecule in asymmetric unit; ρ calcd = 1.196 gcm^{-3}, μ = 0.092 mm^{-1}, F(000) = 840, R_{int}= 0.1275. The structure was obtained by direct methods using SHELXS-97.The final R value was 0.0726 (wR2 = 0.1610) 5339 observed reflections ($F_0 \geq 4\sigma(|F_0|)$) and 333 variables, S = 1.013. The largest difference peak and hole were 0.356 and -0.368 $eÅ^3$, respectively.

Boc-γVal(β-CH_2NO_2)-γVal(β-CH_2NO_2)- γVal(β-CH_2NO_2)-COOEt (P8): Crystals of peptide were grown by slow evaporation from a solution of Ethyl acetate/ Pet-ether. A single crystal (0.1 × 0.06 × 0.08 mm) was mounted on loop with a small amount of the paraffin oil. The X-ray data were collected at 100K temperature on a Bruker APEX(II) DUO CCD diffractometer using Mo K_α radiation (λ = 0.71073 Å), ω-scans (2θ = 52.52), for a total of 13133 independent reflections. Space group P1, a = 15.4725 (13), b = 16.0538 (14), c = 16.7490 (3), β = 106.461 (2), V = 3482.3 (7) $Å^3$, Triclinic, Z = 1 for chemical formula $C_{31}H_{56}N_6O_{12}$, with three molecule in asymmetric unit; ρ calcd = 1.049 gcm^{-3}, μ = 0.081 mm^{-1}, F(000) = 1185, R_{int}= 0.0455. The structure was obtained by direct methods using SHELXS-97.The final R value was 0.0678 (wR2 = 0.1875) 24769 observed reflections ($F_0 \geq 4\sigma(|F_0|)$) and 1409 variables, S = 0.708. The largest difference peak and hole were 0.758 and -0.488 $eÅ^3$, respectively.

There is some partially occupied solvent molecule also present in the asymmetric unit. A significant amount of time was invested in identifying and refining the disordered molecule. Option SQUEEZE of program PLATON was used to correct the diffraction data for diffuse scattering effects and to identify the solvent molecule. PLATON calculated the upper limit of volume that can be occupied by the solvent to be 679.7 $Å^3$, or 19.5 % of the unit cell volume. The program calculated 106 electrons in the unit cell for the diffuse species. No data are given for the diffusely scattering species. Output of SQUEEZE reports are apended in cif file P2. The terminal atoms C101 and C110 have large displacement parameters indicating some flexibility of the terminal chains.

Boc-γVal(β-CH_2NO_2)-γVal(β-CH_2NO_2)-γVal(β-CH_2NO_2)-γVal(β-CH_2NO_2)-COOEt (P9): Crystals of peptide were grown by slow evaporation from a solution of **EtOAc**. A single crystal (0.20 × 0.15 × 0.18 mm) was mounted on loop with a small amount of the paraffin oil. The X-ray data were collected at 100 K temperature on a Bruker APEX(II) DUO CCD diffractometer using Mo K_α radiation (λ = 0.71073 Å), ω-scans (2θ = 52.52), for a total of 11806 independent reflections. Space group P 2 (1), a = 9.3190 (4), b = 23.4460 (10), c = 11.3960 (5), β = 108.4420 (7), V = 2361.9 (16) $Å^3$, Monoclinic, Z = 2 for chemical formula $C_{39}H_{70}N_8O_{15}$, with one molecule in asymmetric unit; ρ calcd = 1.154 gcm^{-3}, μ = 0.096 mm^{-1}, F(000) = 882, R_{int}= 0.0514. The structure was obtained by direct methods using SHELXS-97.The final R value was 0.0410 (wR2 = 0.0938) 10048 observed reflections ($F_0 \geq 4\sigma(|F_0|)$) and 571 variables, S = 1.001. The largest difference peak and hole were 0.433and -0.455 $eÅ^3$, respectively.

Boc-γVal(β-CH_2NO_2)-γVal(β-CH_2NO_2)-γVal(β-CH_2NO_2)-γVal(β-CH_2NO_2)-COOEt[P9 (m)]: Crystals of peptide were grown by slow evaporation from a solution of **MeOH**. A single crystal (0.11 × 0.08 × 0.06 mm) was mounted on loop with a small amount of the paraffin oil. The X-ray data were collected at 100K temperature on a Bruker APEX(II) DUO CCD diffractometer using Mo K_α radiation (λ = 0.71073 Å), ω-scans (2θ = 52.52), for a total of 9497 independent reflections. Space group P 2 (1), a = 11.601 (4), b = 16.339 (6), c = 13.508 (5), β = 103.1520 (6), V = 2493.3 (15)$Å^3$, Monoclinic, Z = 2 for chemical formula $C_{39}H_{70}N_8O_{15}$, with one molecule in asymmetric unit; ρcalcd = 1.196 gcm^{-3}, μ = 0.092 mm^{-1}, F(000) = 962, R_{int}= 0.0514. The structure was obtained by direct methods using SHELXS-97.The final R value was 0.0797 (wR2 = 0.1792) 4037 observed reflections ($F_0 \geq 4\sigma(|F_0|)$) and 592 variables, S = 0.860. The largest difference peak and hole were 0.549 and -0.438 $eÅ^3$, respectively.

Boc-γVal(β-CH_2NO_2)-γVal(β-CH_2NO_2)-γVal(β-CH_2NO_2)-γVal(β-CH_2NO_2)-COOEt [P9 (e)]: Crystals of peptide were grown by slow evaporation from a solution of **EtOH**. A single crystal (0.12 × 0.07 × 0.07 mm) was mounted on loop with a small amount of the paraffin oil. The X-ray data were collected at 100K temperature on a Bruker APEX(II) DUO CCD diffractometer using Mo K_α radiation (λ = 0.71073 Å), ω-scans (2θ = 52.52), for a total of 9465 independent reflections. Space group P 2 (1), a = 11.7666 (7), b = 16.5378 (10), c = 13.4925 (8), β = 103.3210 (10), V = 2554.9 (3)$Å^3$, Monoclinic, Z = 2 for chemical formula $C_{39}H_{70}N_8O_{15}$, with one molecule in asymmetric unit; ρcalcd = 1.068 gcm^{-3}, μ = 0.086 mm^{-1}, F(000) = 882, R_{int}= 0.0418. The structure was obtained by direct methods using SHELXS-97.The final R value was

0.0520 (wR2 = 0.1517) 7452 observed reflections ($F_0 \geq 4\sigma(|F_0|)$) and 600 variables, S = 0.665. The largest difference peak and hole were 0.522 and -0.307 eÅ^3, respectively.

Boc-Aib-γPhe(β-CH_2NO_2)-Aib-γPhe-CONHMe (P11): Crystals of peptide were grown by slow evaporation from a solution of MeOH\Tol. A single crystal (0.14 × 0.04 × 0.08 mm) was mounted on loop with a small amount of the paraffin oil. The X-ray data were collected at 100 K temperature on a Bruker APEX(II) DUO CCD diffractometer using Mo K_α radiation (λ = 0.71073 Å), ω-scans (2θ = 50.48), for a total of 36583 independent reflections. Space group P2 (1), a = 11.813 (3), b = 9.272 (2), c = 19.747 (4), β = 104.52, V = 2093.6 (8) Å^3, Monoclinic, Z = 2 for chemical formula $C_{37}H_{54}N_6O_8$ with one peptide, one methanol and one water molecules were present in an asymmetric unit; ρ (calcd) = 1.128 gcm^{-3}, μ = 0.08 mm^{-1}, F(000) = 764, R_{int}= 0.0811. The structure was obtained by direct methods using SHELXS-97. The final R value was 0.0559 (wR2 = 0.1314) 10361 observed reflections ($F_0 \geq 4\sigma(|F_0|)$) and 497 variables, S = 1.017. The largest difference peak and hole were 1.127 and -0.911 eÅ^3, respectively.

Boc-Aib-γPhe(β-CH_2NO_2)-Aib-γPhe(β-CH_2NO_2)-CONHMe (P12): Crystals of peptide were grown by slow evaporation from a solution of isopropanol. A single crystal (0.1 × 0.1 × 0.05 mm) was mounted on loop with a small amount of the paraffin oil. The X-ray data were collected at 100 K temperature on a Bruker APEX(II) DUO CCD diffractometer using Mo K_α radiation (λ = 0.71073 Å), ω-scans (2θ = 52.52), for a total of 42195 independent reflections. Space group P 61, a = 27.657(18), b = 27.657(18), c = 11.852(8), β = 90.00, V = 7835(11) Å^3, Trigonal, Z = 6 for chemical formula $C_{38}H_{55}N_7O_{10}$, 2(C_3 H_8 O), with two isopropanol molecules in asymmetric unit, ρ calcd = 1.132 gcm^{-3}, μ = 0.083 mm^{-1}, F(000) = 2864, R_{int}= 0.3425. The structure was obtained by direct methods using SHELXS-97.The final R value was 0.1189 (wR2 = 0.2095) 7400 observed reflections ($F_0 \geq 4\sigma(|F_0|)$) and 581 variables, S = 0.913. The largest difference peak and hole were 0.426 and -0.286 eÅ^3, respectively. After thorough crystallization process, we are able to get crystals in isopropanol solvent, which results in moderate quality data leads to R_{int}value above 0.25. At the same time helical packing of molecules leaves some solvent accessible voids in structure around 869 Å^3. The packing of molecules is shown in fig. S6.

Boc- βVal(CH_2COOEt)- βLeu(CH_2COOEt)- βVal(CH_2COOEt)-OBn (P15): Crystals of peptide were grown by slow evaporation from a solution of EtOH. A single crystal (0.51 × 0.11 × 0.02 mm) was mounted on loop with a small amount of the paraffin oil. The X-ray data were collected at 100 K temperature on a Bruker APEX(II) DUO CCD diffractometer using Mo

$K_\alpha$radiation (λ = 0.71073 Å), ω-scans (2θ = 57.14), for a total of 72888 independent reflections. Space group P 21, a = 11.231(2), b = 12.669 (2), c = 33.438 (6), β = 90.04 (4), V = 4757.6 (15) $Å^3$, Trigonal, Z = 4 for chemical formula C_{43} H_{69} N_3 O_{12}, with two molecules in asymmetric unit, ρ calcd = 1.145 gcm^{-3}, μ = 0.082 mm^{-1}, F(000) = 1776, R_{int}= 0.1214. The structure was obtained by direct methods using SHELXS-97.The final R value was 0.0793 (wR2 = 0.1662) 10055 observed reflections ($F_0 \geq 4\sigma(|F_0|)$) and 1059 variables, S = 0.965. The largest difference peak and hole were 1.022 and -0.386 $eÅ^3$, respectively.

General procedure for the synthesis of *N*-Boc-protected *β*-nitromethane substituted *γ*-amino ethyl esters

The *N*-Boc *α, β*-unsaturated *γ*-amino ester **1** (10.0 mmol) was dissolved in neat nitromethane (100.0 mmol). To this solution, DBU (10.0 mmol) was slowly added under N_2 atmosphere at 0 °C. Then the reaction was stirred at room temperature for about 3 hrs and the progress of reaction was monitored by TLC. After completion of the reaction, EtOAc (200 mL) was added to the reaction mixture, and washed with H_2O (3 × 80 mL), 0.5N HCl (3 × 80 mL), 10% Na_2CO_3 (3 × 80 mL) and brine (2 × 80 mL) solution, respectively. Then the organic layer was dried over anhydrous Na_2SO_4 and concentrated under reduced pressure. The crude product was subjected to silica gel column chromatography to get the pure diastereomers (**2** & **3**).

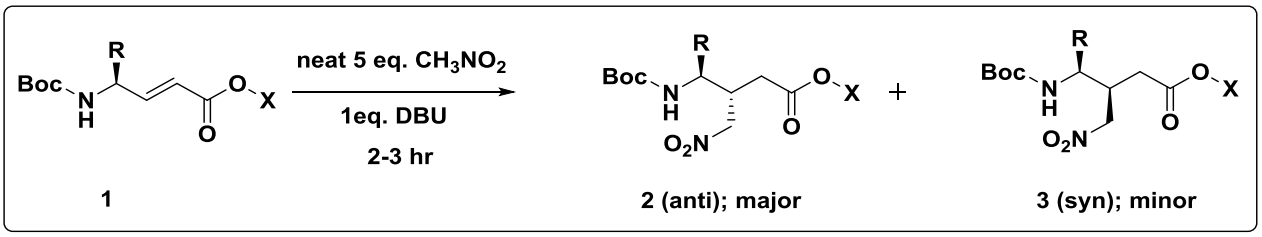

*(3R, 4S)-Ethyl-4-(tert-butoxycarbonylamino)-5-methyl-3-(nitromethyl) hexanoate (***2a***)*^{anti}

Light yellow oil (2.66 g, 80%, dr 89:11); $[\alpha]_D^{25}$ +35.0 (*c* 1.0, MeOH); The dr determined by Reverse Phase HPLC analytical C_{18} column (5 µm, 4.6 × 250 mm), flow rate 0.75 mL/min, R_t (major, **2** ^{anti}) = 33.3 min, R_t (minor, **3** ^{syn}) = 32.3 min; IR ν (cm^{-1}) 3360, 2970, 2930, 1710, 1550, 1510, 1380, 1240, 1170,1100, 1030; **^{1}H NMR** (400 MHz, $CDCl_3$) δ 4.55-4.44 (m, 2H), 4.35 (d, *J* = 10.1 Hz, 1H), 4.16 (q, *J* = 8 Hz, 2H), 3.60-3.54 (m, 1H), 2.92-2.84 (m, 1H), 2.53-2.38 (m, 2H), 1.87-1.81 (m, 1H), 1.43 (s, 9H), 1.23 (t, *J* = 8 Hz, 3H), 0.98 (d, *J* = 6.9 Hz, 6H), 0.88 (d, *J* = 6.9 Hz, 6H); **^{13}C NMR** (100 MHz, $CDCl_3$) δ 171.1, 156.3, 79.9, 76.3, 61.0, 56.9, 36.6, 34.4, 29.3, 28.3, 20.1, 16.8, 14.2; **MALDI TOF/TOF***m/z* calculated value for $C_{15}H_{27}N_2O_6$ [M+Na^+] 355.1840, found 355.1829.

*(3S,4S)-Ethyl-4-((tert-butoxycarbonyl)amino)-5-methyl-3-(nitromethyl)hexanoate(***3a***)*^{syn}**.**

Colorless oil; Yield (0.33 g, 10%); $[\alpha]_D^{25}$ -9.0 (*c* 1.0, MeOH); **IR***υ* cm^{-1} 3370, 2988, 2870, 1720, 1555, 1399, 1234, 1190, 1113, 1020 ; **^{1}H NMR** ($CDCl_3$, 400 MHz) δ 4.53-4.39 (m, 3H), 4.13 (q, *J* = 7.3 Hz, 2H) 3.51-3.45 (m, 1H), 2.98-2.90 (m, 1H), 2.47-2.30 (m, 2H), 1.77-1.69 (m, 1H), 1.4 (s, 9H), 1.25 (t, *J* = 7.1 Hz, 3H), 0.98-0.91 (m, 6H); **^{13}C NMR** ($CDCl_3$, 100 MHz) δ 172.1, 156.1, 79.7, 76.8, 61.1, 56.9, 36.1, 32.3, 30.1, 28.3, 28.1, 19.9, 18.1, 14.1; **MALDI TOF/TOF***m/z* calculated value for $C_{19}H_{28}N_2O_6$ [M+Na$^+$] 355.1840, found 355.1829.

*(3R, 4S)-Ethyl-4-(tert-butoxycarbonylamino)-3-(nitromethyl)-5-phenyl pentanoate (***2b***)*^{anti}

White solid (2.67 g, 70%, dr 80:20); *mp* 117 ^oC; $[\alpha]_D^{25}$ -114.2 (*c* 1.0, MeOH); The dr determined by isolated products**; IR***v* (cm^{-1}) 3370, 2970, 2930, 1700, 1550, 1510, 1380, 1250, 1170, 1030, 860,766; **^{1}H NMR** (400 MHz, $CDCl_3$) δ 7.23 (m, 5H), 4.54 (m, 2H), 4.34 (d, *J* = 8.24 Hz, 1H), 4.15 (q, *J* = 7.2 Hz, 2H), 3.99 (m, 1H), 2.91 (m, 2H), 2.74 (m, 1H), 2.55 (m, 2H), 1.29 (s, 9H), 1.26 (t, *J* = 7.32 Hz, 3H); **^{13}C NMR** (100 MHz, $CDCl_3$) δ 171.2, 155.6, 137.0, 129.1, 128.7, 126.9, 79.9, 76.0, 61.1, 53.1, 38.8, 38.3, 34.3, 28.2, 14.2; **MALDI TOF/TOF***m/z* value calculated for $C_{19}H_{28}N_2O_6$ [M+Na$^+$] 403.1840, found 403.1816.

*(3S, 4S)-Ethyl-4-((tert-butoxycarbonyl)amino)-3-(nitromethyl)-5-phenyl pentanoate (***3b***)*^{syn}**.**

White solid (0.67 g, 18%); mp 120 ^oC; $[\alpha]_D^{25}$ -15.0 (*c* 1.0, MeOH) ; The dr determined by isolated products; **IR***υ* (cm^{-1}) 3374, 2980, 2930, 1718, 1691, 1553, 1520, 1378, 1249, 1175, 1022, 701, 605; **^{1}H NMR** ($CDCl_3$, 400 MHz) δ 7.33-7.18 (m, 5H), 4.59-4.51(m, 3H), 4.18 (q, *J* = 7.2 Hz, 2H), 4.09 (m, 1H), 2.94-2.88(m, 1H), 2.58-2.53 (m, 2H), 1.33-1.27 (m, 12H); **^{13}C NMR** ($CDCl_3$, 100 MHz) 171.9, 155.6, 136.9, 129.0, 128.7, 126.9, 79.9, 74.7, 61.2, 52.7, 39.2, 37.7, 32.4, 29.7, 28.2, 14.2; **MALDI TOF/TOF***m/z* value calculated for $C_{19}H_{28}N_2O_6$ [M+Na$^+$] 403.1840, found 403.1816.

Experimental Procedure for the Synthesis of peptide P7:

Saponification of the ethyl ester of N-Boc- β-nitromethylγ- γamino valine acid: The Boc-NH-γVal(*β*-CH_2NO_2)-COOEt, **2a** (1.66 g, 5 mmol) was dissolved in 15 mL methanol followed by slow addition of 1N NaOH. The reaction mixture was stirred for about 4 hrs. The progress of the reaction was monitored by TLC. After completion of the reaction, methanol was evaporated under reduced pressure. Then the residue was diluted with water (60 mL), acidified (pH~ 4) with 0.5N HCl and extracted the compound with EtOAc (3 × 60 mL). The combined organic layer

was washed with 50 mL brine solution, dried over anhydrous Na_2SO_4 and concentrated under reduced pressure to get free carboxylic acid (1.37 g, 90%). The carboxylic acids were directly used for the peptide synthesis without further purification.

Deprotection of Boc-group from N-Boc- β-nitromethylγ- amino valine ethyl ester: The solution of Boc-NH-γVal(*β*-CH_2NO_2)-COOEt, **2a** (2 g, 6 mmol) in 3 mL of DCM was cooled to 0 °C in ice bath followed by addition of neat 5 mL of TFA. After completion of the reaction (~ 30 min), solvent was evaporated under reduced pressure. The residue was diluted with water and solid Na_2CO_3 was added at 0 °C until pH of the solution turned to ~10. The aqueous layer was extracted with EtOAc (3 × 50 mL). The combined organic layer was washed with 50 mL of brine solution, dried over anhydrous Na_2SO_4 and concentrated under reduced pressure to *ca*. 2 mL.

Coupling Strategy: The solution of NH_2-γVal(*β*-CH_2NO_2)-COOEt in EtOAc (2 mL) was added to the solution of Boc-γVal(*β*-CH_2NO_2)-COOH (1.37 g, 4.5 mmol) in 3 mL of DMF. Then the mixture was treated with DCC (0.93 g, 4.5 mmol) and HOBt (0.6 g, 4.5 mmol) at ice cold condition. The reaction mixture was stirred for about 12 hrs at room temperature and the completion of the reaction was monitored by TLC. After completion of the reaction, the reaction mixture was diluted with EtOAc (150 mL) and DCU was filtered through celite packed sintered funnel. Then the filtrate was washed with brine (3 × 50 mL) followed by 0.5N HCl (3 × 50 mL), 10% Na_2CO_3 (1 × 50 mL) and brine solution (1 × 80 mL). The organic layer was dried over anhydrous Na_2SO_4 and concentrated under reduced pressure. The crude product was purified by silica gel column chromatography using EtOAc/pet ether to get pure product **P7** (1.4 g, 60%).

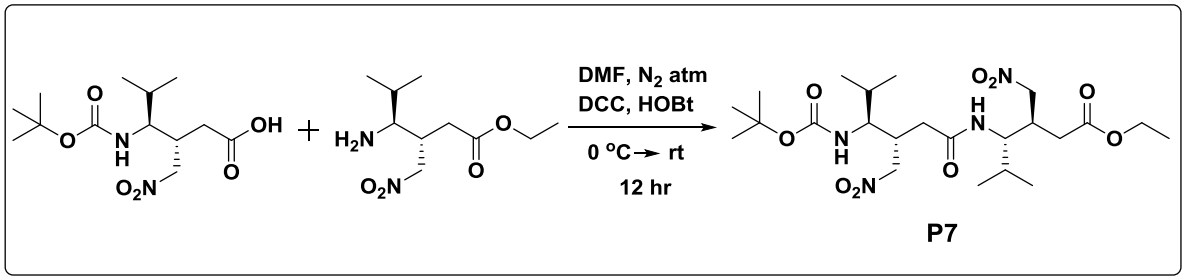

***Boc-γVal(β-CH₂NO₂)-γVal(β-CH₂NO₂)-COOEt*(P7**). Yellow solid (1.4 g, 60%); mp 120 ^oC; $[\alpha]_D^{20}$ -5.0 (*c* 1.0, MeOH); IR υ (cm^{-1}) 3427, 3254, 3062, 2964, 2950, 2564, 1742, 1642, 1554, 1461, 1295, 1253, 1166, 1033, 885, 735; ^1H NMR (400 MHz, $CDCl_3$) δ 6.31 (d, J = 10.1 Hz, 1H,

NH), 4.57 (m, 2H), 4.38 (m, 3H), 4.14 (q, J = 7.3 Hz, 2H), 3.96 (dt, J = 10.1 Hz, J = 6.6 Hz, 1H), 3.38 (td, J = 9.4 Hz, J = 3.7 Hz, 1H), 2.97 (m, 2H), 2.49 (m, 2H), 2.3 (d, J = 6.9 Hz, 2H), 1.42 (m, 11H), 1.24 (t, J = 7.1 Hz, 3H), 0.95 (m, 12H); ^{13}C NMR (100 MHz, $CDCl_3$) δ 171.2, 170.8, 157.2, 80.5, 76.0, 61.0, 58.0, 55.1, 37.2, 37.0, 36.5, 34.6, 34.0, 30.3, 29.4, 28.3, 25.6, 25.0, 20.1, 19.9, 19.5, 17.5, 14.2; MALDI TOF/TOF *m/z* calculated value for $C_{23}H_{42}N_4O_9$ [M+Na$^+$] 541.2844, found 541.2827.

Experimental Procedure for the Synthesis of Peptide P8:

Synthesis of peptide **P2** was carried out by 1+2 convergent synthesis. The **2a** carboxylic acid was subjected to the coupling reaction with free amine of dipeptide **P1** by using DCC as a coupling agent to get **P2**.

NH_2-γVal(β-CH_2NO_2)-γVal(β-CH_2NO_2)-COOEt: To the solution of dipeptide **P1** (1.0 g, 2 mmol) in DCM (2 mL) was added TFA (2 mL) slowly at 0 °C. After completion of the reaction (~30 min), TFA was evaporated under reduced pressure. Then the residue was diluted with water and solid Na_2CO_3 was added slowly at ice cold condition until the pH turned to ~10. The free amine was extracted with EtOAc (3 × 50 mL) and combined organic layer was washed with brine solution (1 × 50 mL). Then the organic layer was dried over anhydrous Na_2SO_4 and concentrated under vacuum to *ca.* 2 mL.

To the solution of Boc-NH-γVal(β-CH_2NO_2)-COOH (0.46 g, 1.5 mmol) and NH_2-γVal(β-CH_2NO_2)-γVal(β-CH_2NO_2)-COOEt(2 mL) in DMF (2 mL) was added DCC (0.3 g, 1.5 mmol) and HOBt (0.2 g, 1.5 mmol) at 0 °C. Then the reaction was stirred at room temperature for about 12 hr and progress of the reaction monitored by TLC. After completion of the reaction, EtOAc (150 mL) was added to the reaction mixture and DCU was filtered through celite packed sintered funnel. Then filtrate was washed with 0.5N HCl (3 × 50 mL), 10% Na_2CO_3 (3 × 50 mL) and brine solution (1 × 80 mL), respectively. The organic layer was dried over anhydrous Na_2SO_4 and concentrated under reduced pressure. Then crude mixture was subjected to column chromatography to get pure peptide **P8**(0.48 g, 45%).

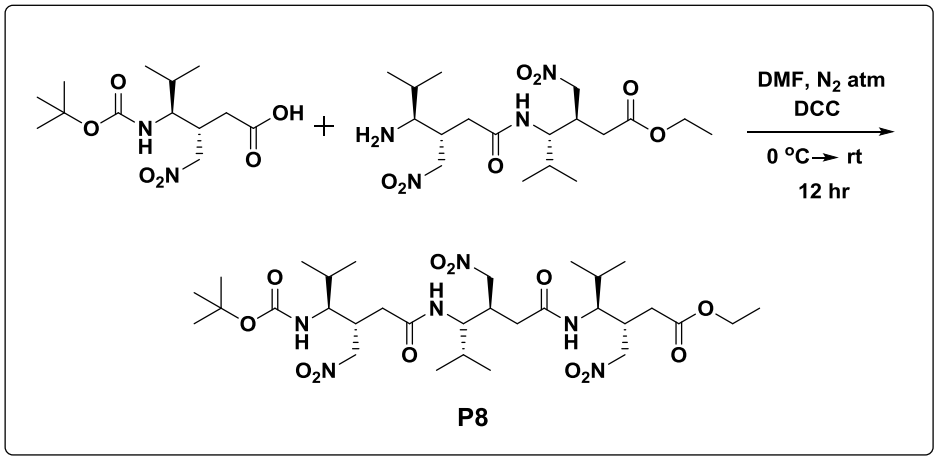

***Boc-γVal(β-CH$_2$NO$_2$)-γVal(β-CH$_2$NO$_2$)- γVal(β-CH$_2$NO$_2$)-COOEt*(P8)**: Colorless solid (0.48 g, 45%); ^{1}H NMR (400 MHz, $CDCl_3$) δ 6.82 (d, J = 9.6 Hz, 1H), 5.94 (d, J = 10.1 Hz, 1H), 4.69-4.67 (m, 2H), 4.50-4.33 (m, 5H), 4.16 (q, J = 7.1 Hz, 2H), 4.04-3.98 (m, 1H), 3.76-3.64 (m, 2H), 3.18-3.11 (m, 1H), 3.09-3.03 (m, 1H), 2.99-2.94 (m, 1H), 2.65-2.48 (m, 2H), 2.37-2.26 (m, 4H), 1.85-1.73 (m, 3H), 1.43 (s, 9H), 1.26 (t, J = 7.1 Hz, 3H), 1.07-0.91 (m, 18H); ^{13}C NMR (100 MHz, $CDCl_3$) δ 171.3, 170.9, 170.8, 157.2, 80.5, 76.0, 76.0, 75.9, 60.9, 57.0, 56.0, 54.9, 36.6, 36.5, 35.9, 35.3, 34.6, 30.8, 30.5, 29.3, 28.4, 20.3, 20.1, 20.0, 19.8, 19.6, 17.8, 14.2; HR-MS *m/z* calculated value for $C_{31}H_{56}N_6O_{12}$ [M+H$^+$] 705.4029, found 705.4036.

Experimental Procedure for the Synthesis of Peptide P9:

Peptide **P9** was synthesized by 1+3 convergent synthesis. The monomer (**2a**) acid was coupled to free amine of peptide **P8**by using DCC as a coupling agent.

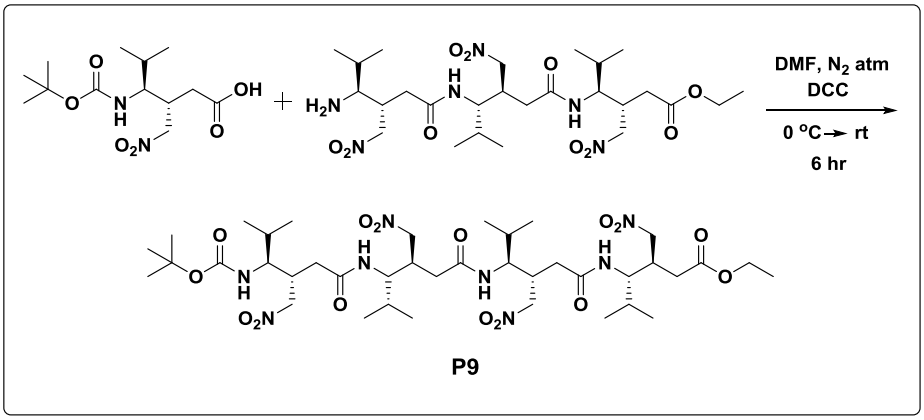

Boc-γVal(β-CH$_2$NO$_2$)-γVal(β-CH$_2$NO$_2$)- γVal(β-CH$_2$NO$_2$)- γVal(β-CH$_2$NO$_2$)-COOEt (**P9**): Colorlesss solid (0.16 g, 30%); $R_t$of the peptide **P3** = 24.3 min [Reverse phase HPLC column (C18, 5 μm, 4.6 × 250 mm column), flow rate 0.75 mL/min, mobile phase H_2O:MeOH (gradient system: B = 60% first 10 min and changed to 90% over 25 min].; ^{1}H NMR (400 MHz, $CDCl_3$) δ 7.05 (d, J = 12 Hz, 1H), 6.45 (d, J = 12 Hz, 1H), 6.04 (d, J = 12 Hz, 1H), 4.66-4.32 (m, 9H), 4.15 (q, J = 8 hz, 2H), 3.98 (m, 1H), 3.84-3.64 (m, 3H), 3.18-2.93 (m, 4H), 2.60-2.25 (m, 8H), 1.85-1.69 (m, 4H), 1.44 (s, 9H), 1.25 (t, J = 8 Hz, 3H), 1.06-0.91 (m, 24H); MALDI TOF/TOF *m/z* calculated value for $C_{39}H_{70}N_8O_{15}$ [M+H$^+$] is 891.5033, found 891.5049.

Experimental Procedure for the Synthesis of Hybrid Peptides:

Hydrolysis of ester and urethane group removal is carried out by saponification and TFA, respectively. All peptides were synthesized by standard coupling agent DCC/HOBt.

Boc-Aib-γPhe(β-CH$_2$NO$_2$)-OEt **(D):** White solid (1.2 g, 92%); ^{1}H NMR (400 MHz, $CDCl_3$) δ 7.29-7.17 (m, 5H), 6.47 (d, J = 8 Hz, 1H), 4.71-4.53 (m, 3H), 4.37 (m, 1H), 4.16 (q, J = 8 Hz, 2H), 3.05-2.74 (m, 3H), 2.68-2.47 (m, 2H), 1.42 (s, 9H), 1.31 (s, 3H), 1.27 (t, J = 8 Hz, 3H), 1.08 (s, 3H); ^{13}C NMR (100 MHz, $CDCl_3$) δ 174.7, 171.4, 155.0, 137.3, 129.1, 128.7, 126.9, 80.7, 76.0, 61.1, 36.9, 51.5, 38.9, 38.8, 34.7, 34.1, 28.4, 25.9, 25.7, 25.1, 24.8, 14.3; HRMS *m/z* calculated value for $C_{23}H_{35}N_3O_7$ [M+Na$^+$] 488.2367, found 488.2374.

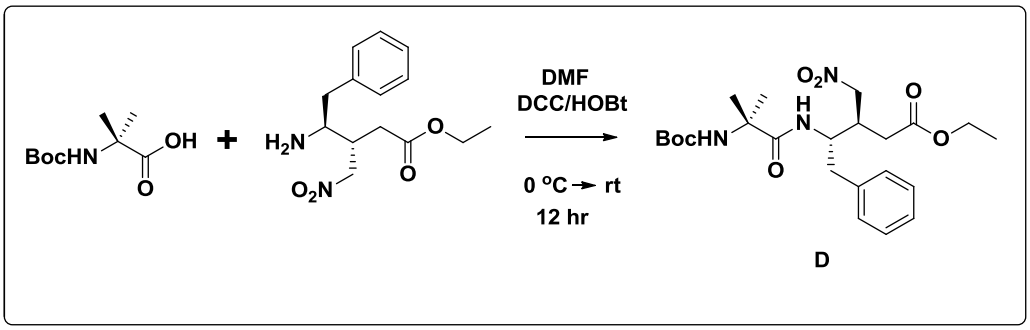

Boc-Aib-γPhe(CH$_2$NO$_2$)-Aib-γPhe-NHMe **(P10):** White solid(Yield 55%); **^{1}H NMR** (400 MHz, $CDCl_3$) *δppm* 7.56 (d, J = 8 Hz, 1H), 7.30-7.10 (m, 11H), 6.73 (d, J = 8 Hz, 1H), 4.92 (s, 1H), 4.81 (m, 1H), 4.53-4.43 (m, 2H), 4.30-4.21 (m, 1H), 2.97-2.89 (m, 3H), 2.82-2.78 (m, 4H), 2.69-2.62 (m, 2H), 2.49-2.32 (m, 4H), 2.20-2.04 (m, 2H), 1.44 (s, 9H), 1.42 (s, 3H), 1.39 (s, 3H), 1.11 (s, 3H), 0.94 (s, 3H); **^{13}C NMR** (100 MHz, $CDCl_3$) *δppm* 174.6, 174.5, 174.2, 169.3, 155.2,

139.1, 136.6, 129.5, 129.2, 128.7, 128.1, 127.3, 126.1, 81.5, 57.1, 56.8, 49.2, 49.1, 41.5, 40.1, 38.2, 35.8, 33.4, 32.6, 28.5, 28.1, 27.6, 26.4, 23.3, 23.2; **HR-MS***m/z* calculated value for $C_{37}H_{54}N_6O_8$ [M+Na$^+$] is 733.3895, observed 733.3899. R_t of the peptide is 13.6 min (C18, 5 μm, 4.6 × 250 mm column; A binary gradient H_2O (A): MeOH (B) was used as follows: B = 40% for the first 5 min, increased to 95% by 15 min and decreased to 40% by 20 min.

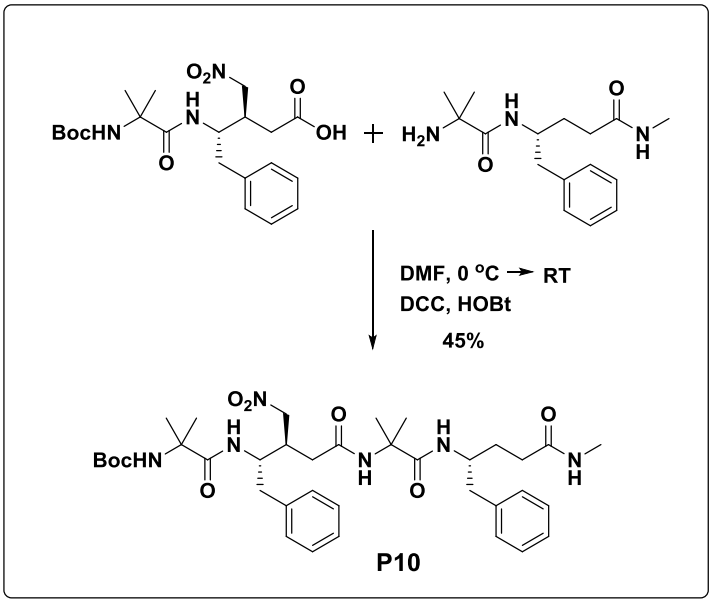

Boc-Aib-γPhe(β-CH$_2$NO$_2$)-Aib-γPhe(β-CH$_2$NO$_2$)-OEt **(T)**: White solid (0.087 g, 30%); ^{1}H NMR (400 MHz, $CDCl_3$) δ 7.78 (d, J = 8 Hz, 1H), 7.30-7.09 (m, 11H), 6.82 (d, J = 12 Hz, 1H), 5.29-4.93 (m, 2H), 4.91 (s, 1H), 4.66-4.58 (m, 2H), 4.46-4.30 (m, 2H), 4.26-4.17 (m, 2H), 3.20-3.05 (m, 2H), 3.00-2.87 (m, 3H), 2.70-2.55 (m, 3H), 2.46-2.11 (m, 2H), 1.41 (s, 9H), 1.40 (s, 3H), 1.32 (s, 3H), 1.31 (t, J = 8 Hz, 3H), 1.05 (s, 3H), 0.74 (s, 3H); ^{13}C NMR (100 MHz, $CDCl_3$) δ 174.7, 174.4, 171.0, 169.1, 155.2, 138.5, 137.4, 129.8, 129.4, 128.4, 128.1, 126.2, 81.5, 61.1, 56.9, 56.7, 50.1, 49.1, 41.4, 40.1, 38.5, 37.7, 35.8, 34.7, 28.4, 26.7, 23.3, 23.1, 14.4; HRMS *m/z* calculated value for $C_{39}H_{56}N_6O_{11}$ [M+H$^+$] 785.4085, found 785.4080.

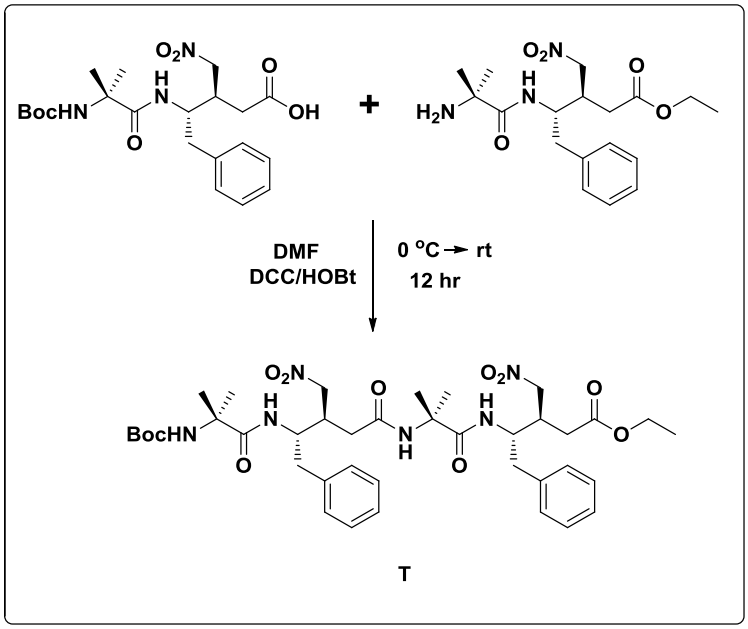

Experimental Procedure for the Synthesis of PeptideBoc-Aib-γPhe(β-CH_2NO_2)-Aib-γPhe(β-CH_2NO_2)-NHMe (P11):

Boc-Aib-γPhe(β-CH_2NO_2)-Aib-γPhe(β-CH_2NO_2)-OEt (**T**) (0.05 g, 0.064 mmol) was dissolved in 50 mL of MeOH and bubbled the solution in cold condition with methyl amine gas until there was an increase in 5 mL of volume. Then the flask was stored under N_2atm for one day at room temperature. After completion of the reaction, methanol was evaporated and the product was diluted with EtOAc (50 mL). The organic layer was washed with dil. HCl (3 × 25 mL), 25 mL of brine solution, dried over anhydrous Na_2SO_4 and concentrated under reduced pressure. The crude product was purified through RP-HPLC on C18 column using methanol/water gradient system to get pure compound **P11** (0.043 g, 90%).

***Boc-Aib-γPhe(β-CH_2NO_2)-Aib-γPhe(β-CH_2NO_2)-NHMe* (P11)**: White solid (0.043 g, 90%); ^{1}H NMR (400 MHz, $CDCl_3$) δ 7.63 (d, J = 8 Hz, 1H), 7.29-7.09 (m, 11H), 6.82 (d, J = 8 Hz, 1H), 6.74 (d, J = 4 Hz, 1H), 4.98 (s, 1H), 4.96-4.85 (m, 2H), 4.63-4.37 (m, 4H), 3.11-2.91 (m, 6H), 2.84 (d, J = 4 Hz, 1H), 2.89-2.16 (m, 6H), 1.43 (s, 9H), 1.39 (s, 3H), 1.36 (s, 3H), 1.09 (s, 3H), 0.90 (s, 3H); HRMS *m/z* calculated value for $C_{38}H_{55}N_7O_{10}$ [M+H$^+$] 770.4088, found 770.4080. R_t of the peptide is 13.4 min (C18, 5 µm, 4.6 × 250 mm column; A binary gradient H_2O (A): MeOH (B) was used as follows: B = 40% for the first 5 min, increased to 95% by 15 min and decreased to 40% by 20 min.

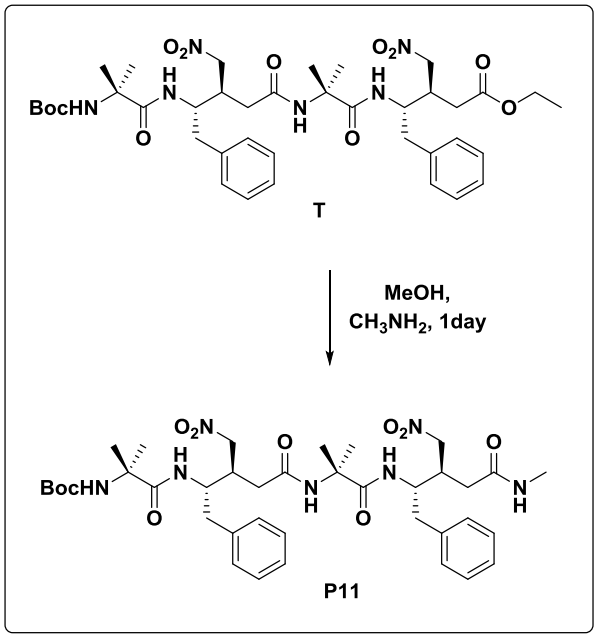

Chemistry on Nitropeptides:

Procedure for the synthesis of β-amino acids Boc-γLeu(β-COOH)-COOEt (7)*:*

The Boc-γLeu(β-CH_2NO_2)-COOEt (2 mmol) in t-BuOH (8 mL) at ~25 ^oC was treated with aqueous buffer KOH (0.5 M in KOH and 1.25 M in K_2HPO_4, 3 mL). The mixture was stirred for 2 min and then aqueous $KMnO_4$ (0.5 M, 4mL) was added with slight cooling to maintain the temperature at ~25 ^oC. After stirring for another 60 min, saturated Na_2SO_3 (~ 5 mL) was added with cooling. The mixture was adjusted to pH ~3 with 1N HCl and the resulting solution was extracted with EtOAc (3x 25 mL). The combined organic layer dried over anhydrous Na_2SO_4 and evaporated under reduced pressure to yield 95 % (1.9 mmol) the acid.

(2S, 3S)-3-(tert-butoxycarbonylamino)-2-(2-ethoxy-2-oxoethyl)-4-methylpentanoic acid* [Boc-γLeu(β-COOH)-COOEt] (7):** White colour solid; Yield 95%; mp 111-113 °C; **IRν* (cm^{-1}) 3381, 3212, 2975, 2933, 2873, 1475, 1490, 1521, 1370, 1241, 1162, 1026, 846, 607; **^{1}H NMR** (DMSO-d_6, 400 MHz) δ 12.39 (bs, 1H), 6.77 (d, J = 9.2 Hz, 1H), 4.07-3.99 (m, 2H), 3.95-3.88 (m, 1H), 2.90-2.84 (m, 1H), 2.45-2.43 (m, 2H), 1.58-1.47 (m, 1H), 1.37(s, 9H), 1.16 (t, J = 7.1 Hz); **^{13}C NMR** (DMSO-d_6, 100 MHz) δ 174.28, 172.52, 155.70, 78.30, 60.44, 49.29, 46.27, 31.16, 28.72, 24.88, 23.87, 21.07, 14.57 ; **MALDI TOF/TOF***m/z* value for $C_{15}H_{27}NO_6$**[M+ Na^+]** 354.1887 (calcd), 354.1888 (observed).

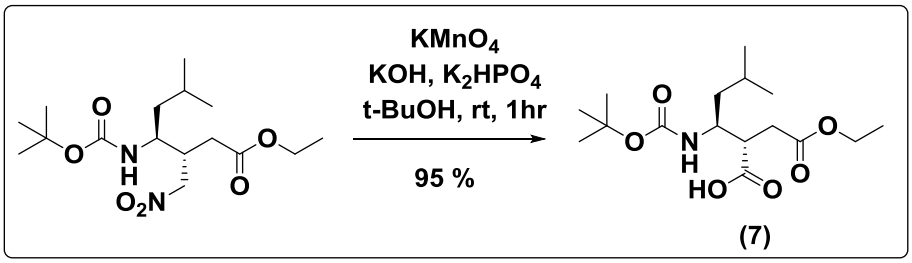

Procedure for the synthesis of β-amino acids Boc-γLeu(β-CH=NOH)-COO^{t}Bu (8)*:*

A solution of Bu_3SnH (0.2 mL, 0.75 mmol) and AIBN (0.033 g, 0.2 mmol) in toluene (0.2 mL) was added to a r.t solution of the Boc-γVal(*β*-CH_2NO_2)-O^{t}Bu (0.18 g, 0.5 mmol) in toluene (0.2 mL). The resulting mixture was immersed in a 110 ^oC oil bath and stirred for 5 hr. Additional AIBN (0.033 g, 0.2 mmol) was then added, and the reaction mixture was stirred for additional 3 h. It was then cooled to RT and concentrated under vacuum. The crude product was purified by silica gel chromatography to get 88% desired product.

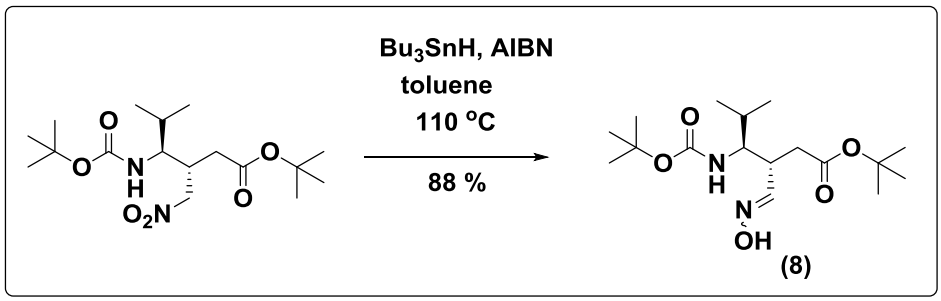

(3S, 4S)-tert-butyl 4-(tert-butoxycarbonylamino)-3-((hydroxyimino)methyl)-5-methylhexanoate: White color solid; yield 88%; mp 125-127 °C; **IR** *v* (cm^{-1}) 3384, 3310, 2971, 1690, 1546, 1371, 1283, 1162, 1088, 1046, 937, 682; **^{1}H NMR** ($CDCl_3$, 400 MHz) *δ* 7.56 (bs, 1H, -OH), 7.43 (d, *J* = 6.4 Hz, 1H, *H*-C=N-OH), 4.65 (d, *J* = 10.5 Hz, 1H, NH), 3.51-3.45 (m, 1H), 3.10-3.03 (m, 1H), 2.47-2.44 (m, 2H), 1.77-1.65 (m, 1H), 1.44 (s, 9H, Boc), 1.43 (s, ^{t}Bu), 0.99-0.91 (m, 6H); **^{13}C NMR** ($CDCl_3$, 100 MHz) *δ* 171.09, 156.13, 151.17, 80.97, 79.32, 58.16, 38.08, 36.82, 31.23, 28.45, 28.13, 20.01, 19.09 ; **MALDI TOF/TOF** *m/z* value for $C_{17}H_{32}N_2O_5$ **[M+Na$^+$]** 367.2203 (calcd), 367.2200 (observed).

Procedure for the synthesis of β-amino acids Boc-γLeu(β-CH_2NHFmoc)-COO^{t}Bu (9)*:*

The Boc-γLeu(*β*-CH_2NO_2)-COOEt (0.28 g, 1mmol) and 20% (w/w) Pd-C were dissolved in EtOH (10 mL) in a RB contained magnetic bar under nitrogen atmosphere and stirred for 8 hr under H_2 gas atmosphere provided by balloon. The progress of reaction was monitored by TLC.

After completion of the reaction filtered the Pd-C through sintered funnel and evaporated EtOH to get our desired amino acid. Residue was dissolved in 15 mL of water and the pH was adjusted to ~11 by slow addition of Na_2CO_3. The solution of Fmoc-OSu (0.337 g, 1 mmol) in THF added slowly. The reaction stirred for overnight. After completion of the reaction, reaction mixture acidified with 2N HCl and aqueous layer extracted with EtOAc (3x 30 mL). The combined organic layer was washed with brine and dried over anhydrous Na_2SO_4. The crude product was purified by silica gel chromatography to get 65 % (0.7 mmol) pure product.

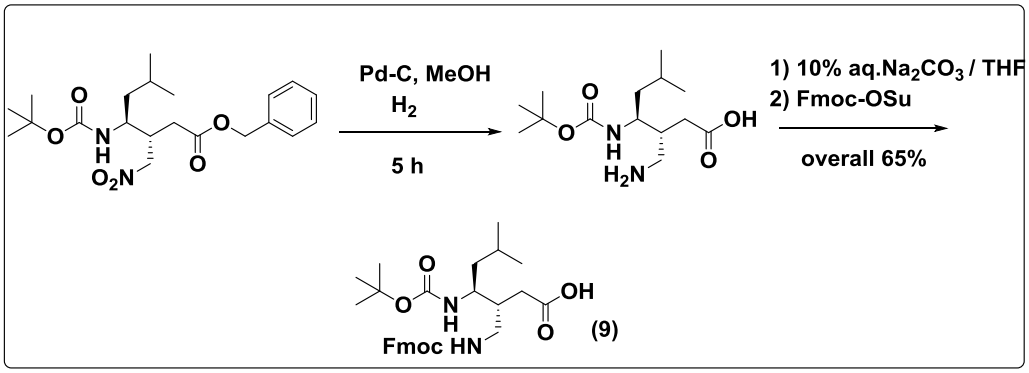

(3R, 4S)-3-((((9H-fluoren-9-yl)methoxy)carbonylamino)methyl)-4-(tert-butoxycarbonylamino)-6-methylheptanoic acid: Light yellowish oil; Overall yield 65 %; **IR** ν cm^{-1} ; **^{1}H NMR** (DMSO-d_6, 400MHz) δ 12.02 (bs, 1H, -COOH), 7.90-7.30 (m, 8H, aromatic), 6.6 (d, J = 9.6 Hz, 1H, NH), 4.27-4.21 (m, 3H), 4.05-4.00 (m, 1H), 3.70-3.66 (m, 1H), 3.13-2.74 (m, 2H), 2.21-2.06 (m, 2H), 1.58-1.50 (m, 1H), 1.37 (s, 9H), 0.86-0.79 (m, 6H); **^{13}C NMR** (DMSO-d_6, 100 MHz) δ 176.80, 156.40, 143.06, 139.91, 137.92, 130.03, 129.90, 120.55, 110.30, 78.03, 51.09, 43.99, 41.91, 34.24, 28.71, 24.88, 24.02, 21.91, 14.59; **MALDI TOF/TOF** *m/z* value for $C_{29}H_{38}N_2O_6$ **[M+Na$^+$]** 533.2322 (calcd), 532.2300 (observed).

Procedure for the synthesis of β-amino acids Boc-γLeu(β-phenyloxazole)-COO^{t}Bu (10)*:*

To the dry THF (2 mL) solution of Boc-NH-γPhe(CH_2NO_2)-OEt (0.38 g, 1mmol), phenylacetylene (0.55 mL, 5 mmol) and phenylisocyanate (0.55 mL, 5 mmol) were added. Triethylamine (0.42 mL, 3 mmol) was added to the above solution drop wise at room temperature and stir the reaction for 6 h. After completion of the reaction, urea (by product) was filtered out through celite using EtOAc (50 mL). Filtrate was washed with 5% HCl (3 × 20 mL), 10% Na_2CO_3 (3 × 20 mL), brine solution (3 × 20 mL) and dried over anhydrous Na_2SO_4. The crude product was purified by silica gel chromatography to get 90% (0.9 mmol) pure product.

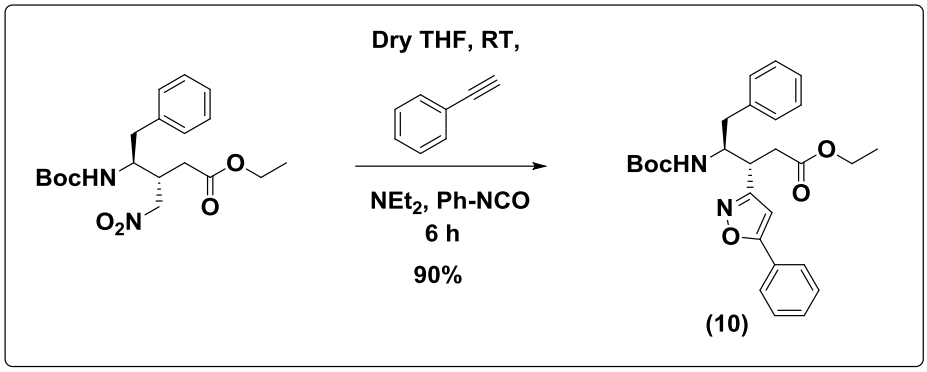

(3S, 4S)-ethyl 4-((tert-butoxycarbonyl)amino)-5-phenyl-3-(5-phenylisoxazol-3-yl)pentanoate: Colorless solid; Yield 90%; mp 99-101 °C; IR ν cm^{-1} 3395, 2970, 2925, 2861, 1731, 1690, 1590, 1508, 1448, 1378, 1254, 1169, 1030, 944, 914, 850, 764, 693, 586, 496; **^{1}H NMR** ($CDCl_3$, 400 MHz) δ 7.79 (m, 2H), 7.51-7.45 (m, 3H), 7.30-7.17 (m, 6H), 6.42 (s, 1H), 5.28 (d, J = 8 Hz, 1H), 4.33-4.26 (m, 1H), 4.12-4.03 (m, 2H), 3.54-3.50 (m, 1H), 2.88-2.67 (m, 4H), 1.39 (s, 9H), 1.18 (t, J = 8 Hz, 3H); **^{13}C NMR** (100 MHz, CDCl3) δ 171.1, 169.8, 164.2, 155.8, 138.0, 137.4, 130.5, 130.0, 129.3, 129.2, 128.6, 127.4, 126.7, 126.0, 120.8, 100.8, 79.5, 60.8, 54.0, 40.3, 37.4, 36.9, 28.5, 14.2; **HR-MS** *m/z* value calculated for $C_{27}H_{32}N_2O_5$ **[M+H$^+$]** 464.2311, observed 464.2359.

Procedure for the synthesis of Boc-Aib-γPhe(β-COOH)-Aib-γPhe-NHMe (P12):

To the DMSO (0.3 mL) solution of peptide **P10**(10 mg, 0.014 mmol), $NaNO_2$ and AcOH were added. Stir the reaction mixture at 35 °C for 12 h. After completion of the reaction, crude mixture diluted with MeOH and directly subjected to reverse phase HPLC purification using MeOH/H_2O as a gradient system to get 65% (6.3 mg, 0.009 mmol) pure peptide **P12**.

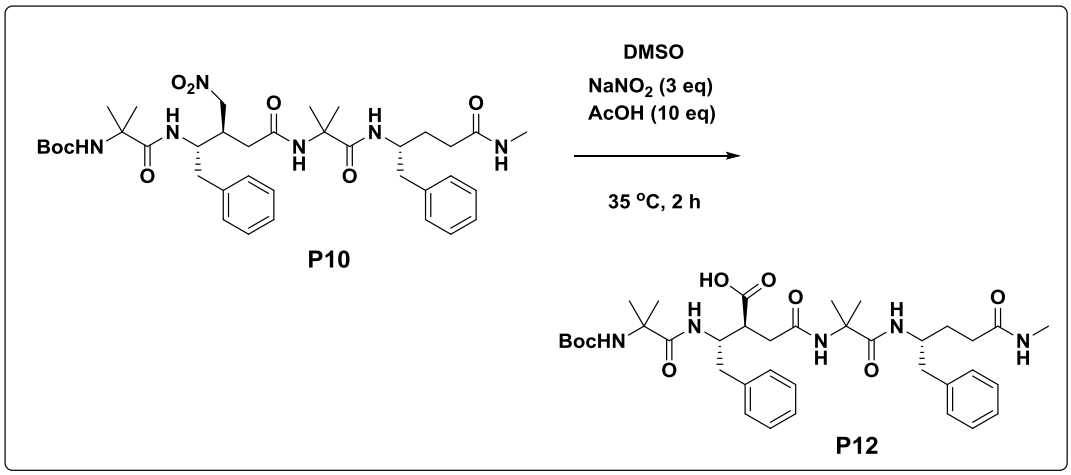

Boc-Aib-γPhe(β-COOH)-Aib-γPhe-NHMe (P12): White solid(Yield 65%); **^{1}H NMR** (400 MHz, $CDCl_3$) *δppm* 7.75 (d, *J* = 8 Hz, 1H), 7.64 (s, 1H), 7.40 (d, *J* = 8 Hz, 1H), 7.38 (d, *J* = 8 Hz, 1H), 7.24-7.09 (m, 11H), 5.15 (s, 1H), 4.27-4.16 (m, 2H), 2.87-2.59 (m, 10H), 2.42-2.31 (m, 4H), 1.45 (s, 3H), 1.42 (s, 9H), 1.35 (s, 3H), 1.14 (s, 3H), 0.96 (s, 3H); **^{13}C NMR** (100 MHz, $CDCl_3$) *δppm* 189.2, 188.8, 175.9, 175.8, 174.6, 155.3, 139.0, 137.2, 129.6, 128.5, 128.1, 126.9, 126.1, 81.1, 57.1, 56.7, 49.7, 49.1, 45.0, 41.2, 40.7, 36.2, 32.9, 29.9, 28.5, 28.2, 27.1, 26.7, 23.7, 23.5, 23.0; **HR-MS** *m/z* calculated value for $C_{37}H_{53}N_5O_8$ [M+Na$^+$] 718.3786, observed 718.3794. R_t of the peptide is 13.6 min (C18, 5 µm, 4.6 × 250 mm column; A binary gradient H_2O (A): MeOH (B) was used as follows: B = 40% for the first 5 min, increased to 95% by 15 min and decreased to 40% by 20 min.

Procedure for the synthesis of Boc-Aib-γPhe(β-phenylisoxazole)-Aib-γPhe-NHMe (P13): To the dry THF (1 mL) solution of **P10** (10 mg, 0.014 mmol), phenylacetylene (7.0 µL, 0.065 mmol) and 3-methoxyphenylisocyanate (8.5 µL, 0.065 mmol) were added. Triethylamine (9.0 µL, 0.065 mmol) was added to the above solution at room temperature and stir the reaction for 12 h. After completion of the reaction, evaporated the THF and then crude product was purified by HPLC using MeOH/H_2O as a gradient system to get 70% (7.8 mg, 0.0098 mmol) pure product.

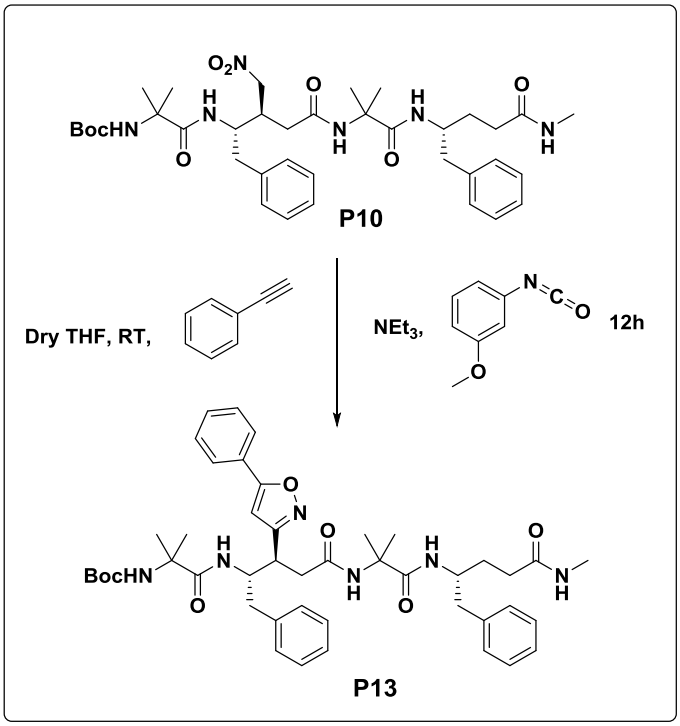

Boc-Aib-γPhe(β-phenylisoxazole)-Aib-γPhe-NHMe (P13): White solid(Yield 70%); **^{1}H NMR** (400 MHz, $CDCl_3$) *δppm* 7.81-7.78 (m, 2H), 7.72 (d, *J* = 8 Hz, 1H), 7.52-7.40 (m, 4H), 7.24-7.03 (m, 10H), 6.91-6.8 (m, 1H), 6.38 (s, 1H),5.07 (s, 1H), 4.51-4.45 (m, 1H), 4.33-4.26 (m, 1H), 3.65-3.59 (m, 2H), 2.87-2.70 (m, 6H), 2.63-2.57 (m, 1H), 2.53-2.45 (m, 1H), 2.39-2.26 (m, 3H), 2.17-2.10 (m, 2H), 1.51 (s, 3H), 1.39 (s, 9H), 1.39 (s, 3H), 1.21 (s, 3H), 0.94 (s, 3H); **^{13}C NMR** (100 MHz, $CDCl_3$) *δppm* 174.5, 170.2, 165.1, 155.2, 139.3, 137.3, 130.8, 129.6, 129.5, 129.3, 128.5, 128.0, 126.9, 126.0, 115.6, 100.4, 81.1, 56.9, 49.4, 41.5, 40.7, 39.6, 38.5, 33.3, 32.9, 28.5, 28.3, 27.6, 26.4, 23.3, 23.1; **HR-MS***m/z* calculated value for $C_{45}H_{58}N_6O_7$ [M+Na$^+$] 817.4259, observed 817.4270. R_t of the peptide is 16.1 min (C18, 5 µm, 4.6 × 250 mm column; A binary gradient H_2O (A): MeOH (B) was used as follows: B = 40% for the first 5 min, increased to 95% by 15 min and decreased to 40% by 20 min.

Procedure for the synthesis of Boc-Aib-γPhe(β-CH$_2$NHCbz)-Aib-γPhe-NHMe (P14): The peptide **P10** (0.1 g, 0.14 mmol) and 20% (w/w) Pd-C were dissolved in MeOH/AcOH(1:1, 5 mL) and stirred for 8 hr under H_2 atmosphere. After completion of the reaction, Pd-C is filtered through sintered funnel and evaporated MeOH/AcOH under reduced pressure to get peptide free amine. The free amine was further dissolved in 5 mL of THF and 5 mL of 10% Na_2CO_3 was added slowly. The solution of Cbz-Cl (20 µL, 0.14 mmol) in THF (2 mL) added slowly to the reaction mixture and stirred at room temperature for about 5h. After completion of the reaction, reaction mixture acidified with 1N HCl and extracted with EtOAc (3x 30 mL). The combined organic layer was washed with brine and dried over anhydrous Na_2SO_4. The crude product was purified by reverse phase HPLC to get 60 % (57 mg, 0.084 mmol) pure product.

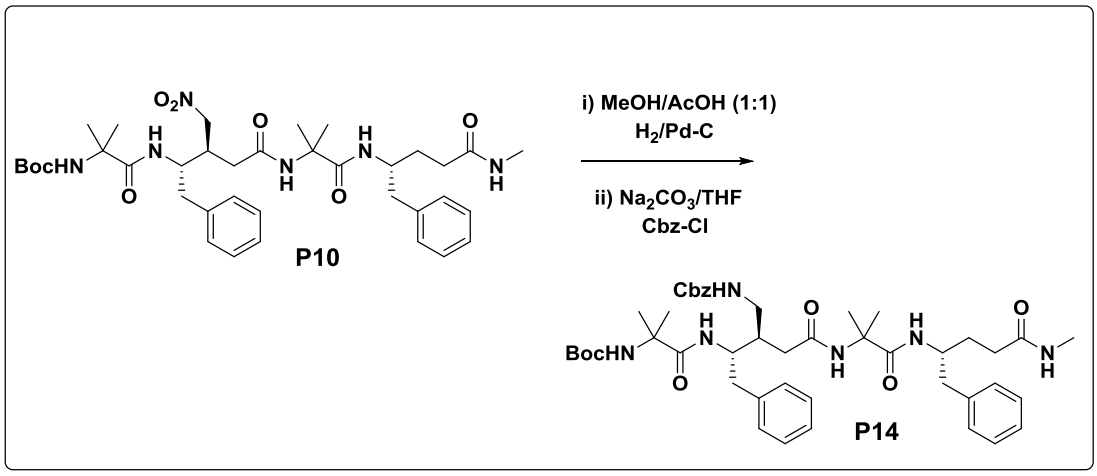

Boc-Aib-γPhe(β-CH_2NHCbz)-Aib-γPhe-NHMe (P14): White solid (Overall yield 60%); **^{1}H NMR** ($CDCl_3$, 400 MHz) δ 7.84 (S, 1h), 7.68 (d, J = 8Hz, 1H), 7.36 (m, 5H), 7.24-7.08 (m, 12H), 6.67 (d, J = 8Hz, 1H), 5.15 (m, 3H), 4.73 (s, 1H), 4.17 (m, 2H), 2.77 (m, 5H), 2.60 (m, 1H), 2.33 (m, 4H), 2.03 (m, 2H), 1.42 (s, 9H), 1.37 (s, 3H), 1.36 (s, 3H), 1.13 (s, 3H), 0.96 (s, 3H); **^{13}C NMR** ($CDCl_3$, 150.99 MHz) 176.0, 174.9, 174.4, 171.9, 155.2, 154.9, 138.7, 137.7, 136.1, 129.3, 129.1, 128.6, 128.4, 128.4, 128.4, 128.0, 126.7, 126.0, 80.8, 67.2, 56.8, 56.4, 50.1, 49.4, 41.0, 40.9, 39.5, 36.4, 32.4, 32.2, 28.3, 28.3, 27.4, 27.1, 26.6, 23.5, 23.3; **HR-MS***m/z* calculated value for $C_{45}H_{62}N_6O_8$ [M+H$^+$] 815.4707, found 815.4719.R_t of the peptide is 10.6 min (C18, 5 μm, 4.6 × 250 mm column; A binary gradient H_2O (A): MeOH (B) was used as follows: B = 40% for the first 5 min, increased to 95% by 15 min and decreased to 40% by 20 min.

Procedure for the Synthesis of β^{2,3}-peptides:

Beta amino acids were synthesized using above mentioned protocol. Hydrolysis of ester and removal of urethane group of β-amino acids are carried out by saponification and TFA, respectively. Tri peptide was synthesized by 1+2 convergent synthesis using standard coupling agent DCC/HOBt.

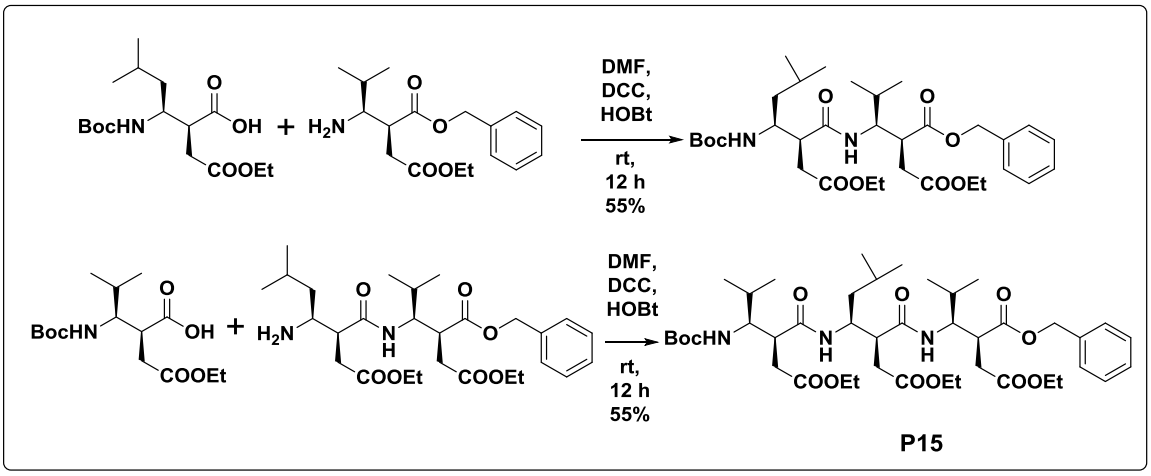

***Boc- βVal(CH_2COOEt)- βVal(CH_2COOEt)- βVal(CH_2COOEt)-OBn* (P15)**: White solid (Yield-55%); Retention time t_R = 13.5 min; **^{1}H NMR** (400 MHz, $CDCl_3$) δ 7.40-7.32 (m, 5H), 6.57 (d, J = 12 Hz, 1H), 6.03 (d, J = 12 Hz, 1H), 5.17 (q, J = 12 Hz, 2H), 4.17-4.07 (m, 7H), 3.83 (td, J = 12 Hz, J = 4 Hz, 1H), 3.75 (d, J = 4 Hz, 1H), 3.41-3.28 (m, 2H), 3.00 (m, 1H), 2.81 (m, 1H),

2.73-2.44 (m, 6H), 1.68-1.58 (m, 2H), 1.54-1.47 (m, 1H), 1.42 (s, 9H), 1.26-1.18 (m, 9H), 1.04-0.79 (m, 18H); **^{13}C NMR** (100 MHz, $CDCl_3$) δ 173.7, 173.7, 173.6, 171.9, 171.1, 156.8, 135.4, 128.8, 128.7, 128.5, 79.4, 67.2, 61.3, 61.1, 60.9, 58.3, 55.8, 48.8, 44.7, 43.2, 43.1, 42.9, 42.1, 36.0, 35.5, 35.4, 32.4, 31.8, 28.6, 25.0, 22.6, 22.4, 20.4, 20.0, 19.9, 19.4, 14.3; **HR-MS***m/z* calculated value for $C_{43}H_{69}N_3O_{12}$ [M+Na$^+$] 842.4773 and observed 842.4777.

2.3.3. Synthesis procedure and characterization of compounds in Section 2B.

Crystal data analysis of Ac-Aib-*γ*Phe-Aib-(*3S, 4S*)-*γ*Val(*β*-SNB)-Aib-*γ*Phe-Aib-CONH$_2$ (P16): Crystals were grown by slow evaporation from a solution of aqueous methanol. A single crystal (0.1 × 0.08 × 0.02 mm) was mounted on loop with a small amount of the paraffin oil. The X-ray data were collected at 100K temperature on a Bruker APEX DUO CCD diffractometer using Mo K_α radiation (λ = 0.71073 Å), ω-scans (2θ = 56.90), for a total of 20903 independent reflections. Space group P 1, a = 9.19 (11), b = 12.59 (14), c = 13.69 (16), β = 77.53 (3), V = 1499.6 (3) Å^3, triclinic, Z = 1 for chemical formula C_{54} H_{75} N_8 O_{10} S, 6(O), with one molecule in an asymmetric unit; ρ calcd. = 1.245 gcm^{-3}, μ = 0.125 mm^{-1}, F (000) = 552, R_{int} = 0.0338. The final R value was 0.0492 (wR2 = 0.1388) 11235 observed reflections ($F_0 \geq 4\sigma$ ($|F_0|$)) and 722 variables, S = 0.967. The structure was obtained by direct methods using SHELXS-97. All non-hydrogen atoms were refined anisotropically. The hydrogen atoms were fixed geometrically in the idealized position and refined in the final cycle of refinement as riding over the atoms to which they are bonded.

Synthesis of Thiostatins from (*E*)-*α, β*-Unsaturated *γ*-Aminoacids

In 50 mL RB flask, Boc-dγVal-O^{t}Bu (**1**, 1.49 g, 5mmol) was treated with mixture of DBU (0.228 g, 1.5mmol) and thioacetic acid (2.28 g, 30 mmol). The reaction mixture was vigorously stirred for another 6h. The progress of reaction was monitored by the TLC. After the completion of reaction, the thioacetic acid was evaporated under reduced pressure and residue was dissolved in 70 mL of ethyl acetate. The organic layer was treated 5 % aqueous HCl (3 × 30 mL), 5 % aqueous Na_2CO_3 (3 × 30 mL) and brine (1 × 30 mL). The organic layer was dried over anhydrous Na_2SO_4 and evaporated under reduced pressure. The diastereomeric mixture of Boc-*γ*Val*β*-(SAc)-O^{t}Bu (**2**) was obtained after column chromatography in 70 % (1.3 g) yield.

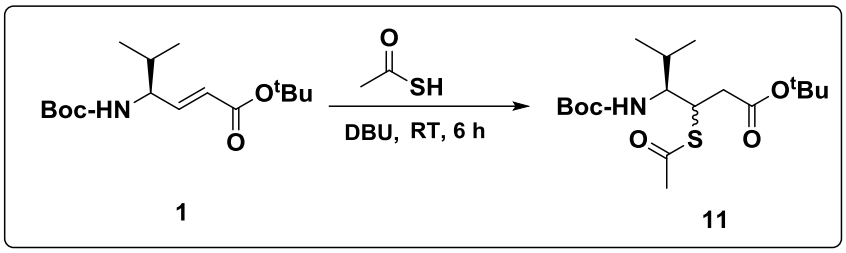

The diastereomeric mixture of Boc-γValβ-(SAc)-O^{t}Bu (**2**, 1.3 g, 3.4 mmol) was dissolved in THF (25 mL). To this, *ortho*-nitro benzyl bromide (3.74 g, 17 mmol) was added. The reaction mixture was cooled to 0 °C and treated with $NaBH_4$ (1.29 g, 34 mmol) in water (4 mL). The reaction was allowed to stir for another 12 h. After completion of reaction, the excess $NaBH_4$ was quenched with 5 % aqueous HCl and the solvent THF was evaporated under reduced pressure. Then the residue was dissolved in ethyl acetate (75 mL) washed with brine, dried over anhydrous $Na_2SO_4$and concentrated under reduced pressure to get crude diastereomeric mixture of Boc-γValβ(S-ONB)O^{t}Bu. The crude product was purified through silica gel column chromatography using 5 % ethyl acetate in petroleum ether to get pure diastereomers (**3a** and **3b**) in 40 % yield (0.64 g).

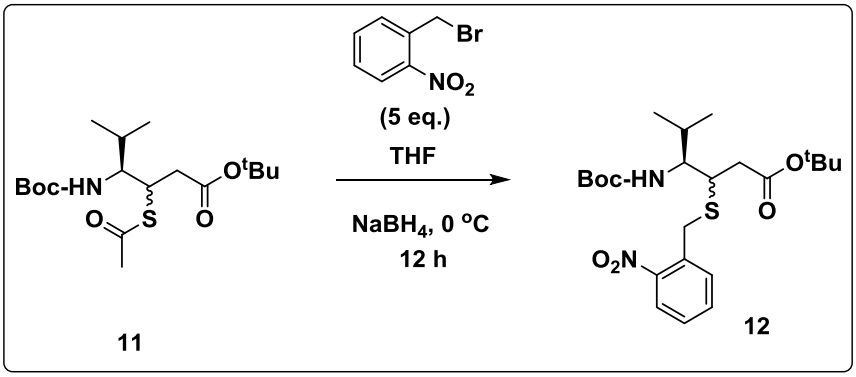

Procedure for synthesis of Fmoc-γValβ(S-ONB)-OH

The pure diastereomerBoc-γValβ(S-ONB)O^{t}Bu (**3a**, 0.384 g, 0.8 mmol) was dissolved in DCM (3 mL). The solution was cooled to 0 °C and to this added TFA (3mL).The reaction mixture was stirred for another 1h at RT. After completion of the reaction, solvent DCM and TFA were evaporated under reduced pressure and residue was co-evaporated with DCM (three times). Then the residue was dissolved in 10 % aqueous Na_2CO_3 (10 mL) and added THF (3mL). To this reaction mixture Fmoc-OSu (0.276 g, 0.8 mmol) in THF (5 mL) was added. The reaction

mixture was stirred for another 8h. After the completion of reaction, solvent THF was evaporated and residue was treated with 5 % aqueous HCl to make pH~2. Then the aqueous layer was extracted with ethyl acetate (30 mL × 3) and the combined organic layer was washed with brine solution (50 mL). The combined organic layer was dried over anhydrous Na_2SO_4 and concentrated under reduced pressure to get Fmoc-*γ*Val*β*-(S-ONB)-OH (**4a**, 0.394 g) in 90 % yield, which was used for solid phase peptide synthesis without further purification.

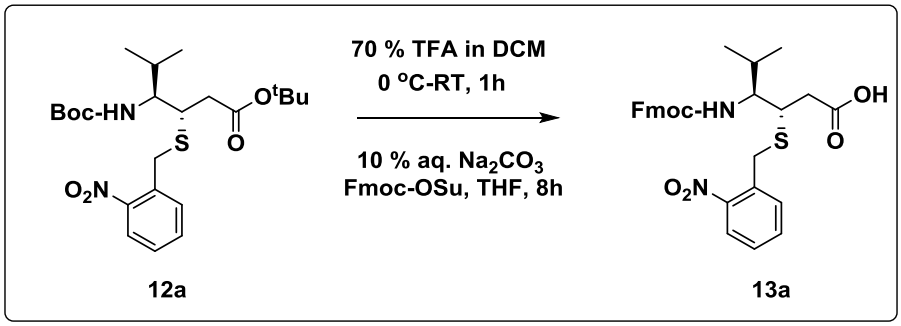

(3R, 4S)-tert-Butyl 4-((tert-butoxycarbonyl)amino)-5-methyl-3-((2nitrobenzyl)thio)hexanoate (Boc-γValβ-(S-ONB)O^{t}Bu) ***(12a);*** Gummy oil (0.384 g, 24 %) ^{1}H NMR (400 MHz, $CDCl_3$)*δ* 7.97 (d, *J* = 8.4 Hz, 1H), 7.56-7.49 (m, 2H), 7.43-7.39 (m, 1H), 4.45 (d, *J* = 10.8 Hz, 1H), 3.57-3.51 (m, 1H), 3.09-3.01 (m, 1H), 2.65-2.47 (m, 2H), 2.13-2.08 (m, 1H), 1.45 (s, 9H), 1.42 (s, 9H); ^{13}C NMR (100 MHz, $CDCl_3$) 171.4, 158.0, 148.6, 133.9, 132.9, 128.2, 125.3, 81.0, 79.2, 60.8, 57.6, 43.8, 39.5, 32.4, 28.9, 28.3, 28.0, 20.3, 16.0; HRMS (ESI)*m/z*calcd. for $C_{23}H_{36}N_2O_6S$ [M + Na] is 491.2192, found 491.2236.

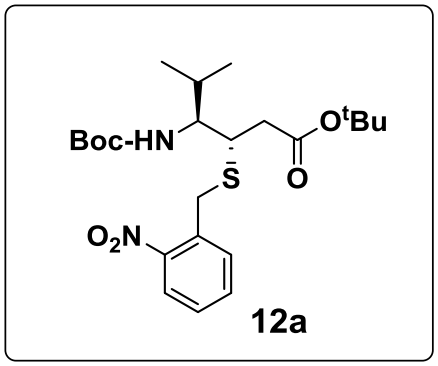

(3S, 4S)-tert-Butyl 4-((tert-butoxycarbonyl)amino)-5-methyl-3-((2nitrobenzyl)thio)hexanoate (Boc- γValβ-(S-ONB)O^{t}Bu) ***(12b)****;* Gummy oil (0.256 g, 16 %) ^{1}H NMR (400 MHz, $CDCl_3$)δ7.97 (d, *J* = 7 Hz, 1H), 7.57-7.50 (m, 2H), 7.44-7.40 (m, 1H), 4.44 (d, *J* = 8 Hz, 1H), 3.39-3.34 (m, 1H), 3.29-3.25 (m, 1H), 2.67-2.53 (m, 2H), 1.69-1.61 (m, 1H), 1.46 (s, 9H), 1.41 (s,9H); ^{13}CNMR (100 MHz, $CDCl_3$)δ 171.0, 155.9, 148.6, 134.0, 133.07, 128.3, 125.4, 80.9, 79.1, 60.36, 59.7, 44.8, 41.3, 33.7, 28.2, 28.0, 19.7, 19.1; HRMS (ESI)*m/z*calcd. for $C_{23}H_{36}N_2O_6S$ [M + Na] is 491.2192, found 491.2226.

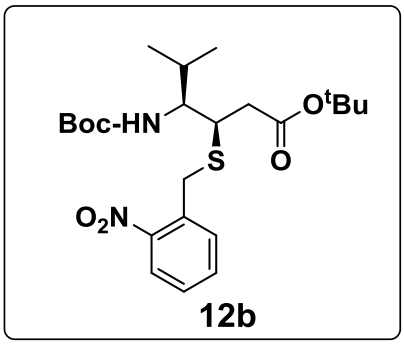

Procedure for the solid phase synthesis of heptapeptide P16:

Peptide was synthesized at 0.2 mmol scales on Knorr-Amide resin using standard Fmoc-chemistry. HBTU/HOBt was used as coupling agents. Reaction times for deprotections and couplings were 30 min and 1 h, respectively. The final amine was capped with acetyl group using Ac_2O/Py. After completion of the synthesis, peptide was cleaved from resin using 15 mL of TFA in an aluminum foil wounded round bottom flask. After the completion of cleavage, the resin was filtered and washed with 3 mL TFA. The cleavage mixture was evaporated under reduced pressure to give gummy product. Peptides were further recrystallized using cold diethyl ether and purified through reverse phase HPLC on C_{18} column using MeOH/H_2O gradient. Homogeneity of peptides was further confirmed using analytical C_{18} column in same MeOH/H_2O gradient system. The mass of peptides were confirmed by MALDI TOF/TOF.

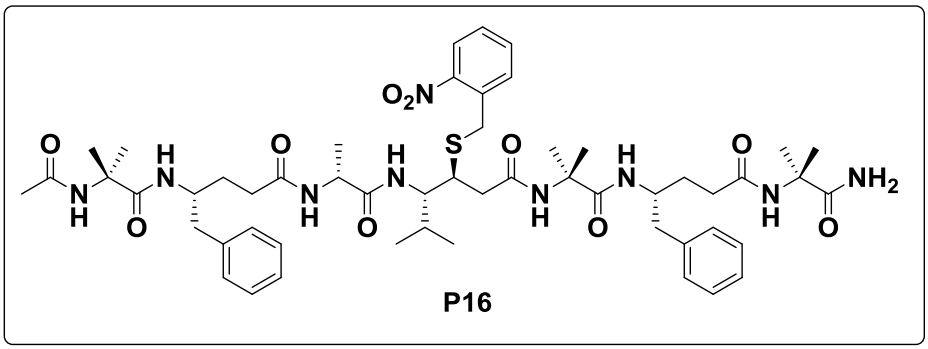

2.4 References

1. (a) Abel, A. *Advances in Amino Acid Mimetics and Peptidomimetics*. JAI: Stanford, Vol. 2. **1999**. (b) Kazmierski, W. M. *Methods in Molecular Medicine: Peptidomimetic protocols* Humana: Totowa, NJ, **1999**. (c) Seebach, D.; Beck, A. K.; Bierbaum, D. J. *Chem. Biodiv*. **2004**, *1*, 1111. (d) Horne, W. S.; Gellman, S. H. *Acc. Chem. Res*. **2008**, *41*, 1399. (e) Cheng, R. P.; Gellman, S. H.; DeGrado, W. F. *Chem. Rev*. **2001**, *101*, 3219. (f) Vasudev, P. G.; Chatterjee, S.; Shamala, N.; Balaram, P. *Chem Rev*. **2011**, *111*, 657. (g) Price, J. L.; Horne, W. S.; Gellman, S. H. *J. Am. Chem. Soc.* **2010**, *132*, 12378. (h) Schramm, P.; Sharma, G. V. M.; Hofmann, H. –J. *Biopolymers* **2010**, *94*, 279.
2. (a) Williams, P. G.; Moore, R. E.; Paul, V. J. *J. Nat. Prod*. **2003**, *66*, 1356. (b) Simmons, T. L.; Nogle, L. M.; Media, J.; Valeriote, F .A.; Mooberry, S. L.; Gerwick, W. H. *J. Nat. Prod.* **2009**, *72*, 1011. (c) Golakoti, T.; Yoshida, W. Y.; Chaganty, S.; Moore, R. E. *Tetrahedron* **2000**, *56*, 9093. (d) Maibaum, J.; Rich, D. H. *J. Org. Chem*. **1988**, *53*, 869. (e) Linington, R. G.; Clark, B. R.; Trimble, E. E.; Almanza, A.; Uren, L. –D.; Kyle, D. E.; Gerwick, W. H. *J. Nat. Prod.* **2009**, *72*, 14. (f) Nieman, J. A.; Coleman, J. E.; Wallace, D. J.; Piers, E.; Lim, Y.; Roberge, M.; Andersen, R. J. *J. Nat. Prod*. **2003**, *66*, 183.
3. (a) Sill, G. J. *Curr. Opin. Pharmacol*. **2006**, *6*, 108. (b) Silverman, R. B. *Angew. Chem., Int. Ed.* **2008**, *47*, 3500.
4. Seebach, D.; Hook, D. F.; Glattli, A. *Biopolymers (Peptide Science)* **2006**, *84*, 23.
5. (a) Seebach, D.; Brenner, M.; Rueping, M.; Jaun, B. *Chem. -Eur. J.* **2002**, *8*, 573. (b) Basuroy, K.; Dinesh, B.; Madhusudana Reddy, M. B.; Chandrappa, S.; Raghothama, S.;

Shamala, N.; Balaram, P. *Org. Lett*. **2013**, *15*, 4866. (c) Vasudev, P. G.; Chatterjee, S.; Shamala, N.; Balaram, P. *Acc. Chem. Res*. **2009**, *42*, 1628.

6. (a) Appella, D. H.; Christianson, L. A.; Karle, I. L.; Powell, D. R.; Gellman, S. H. *J. Am. Chem. Soc.* **1996**, *118*, 13071.(b) Choi, S. H.; Guzei, I. A.; Spencer, L. C.; Gellman, S. H. *J. Am. Chem. Soc.* **2010**, *132*, 13879.
7. Jadhav, S. V.; Gopi, H. N. *Chem. Commun*. **2013**, *49*, 9179.
8. (a) Mali, S. M.; Bandyopadhyay, A.; Jadhav, S. V.; Ganesh Kumar, M.; Gopi, H. N. *Org. Biomol. Chem*. **2011**, *9*, 6566. (b) Bandyopadhyay, A.; Mali, S. M.; Lunawat, P.; Raja, K. M. P.; Gopi, H. N. *Org. Lett*. **2011**, ***13***, 4482. (c) Bandyopadhyay, A.; Gopi, H. N. *Org. Lett*. **2012**, *14*, 2770. (d) Ganesh Kumar, M.; Benke, S. N.; Raja, K. M. P.; Gopi, H. N. *Chem. Comm*., **2015**, *51*, 13397. (e) Hagihara, M.; Anthony, N. J.; Stout, T. J.;Clardy, J.; Schreiber, S. L. *J. Am. Chem. Soc.* **1992**, *114*, 6568.
9. Plummer, J. S.; Emery, L. A.; Stier, M. A.; Suto, M. J. *Tetrahedron Lett*. **1993**, *34*, 7529.
10. (a) Ono, N. *The Nitro Group in Organic Synthesis*, Wiley-VCH, New York, 2001. (b) Luzzio, F. A. *Tetrahedron* **2001**, *57*, 915. (c) Ballini, R.; Bosica, G.; Fiorini, D.; Palmieri, A.; Petrini, M. *Chem. Rev*. **2005**, *105*, 933. (d) Barrett, A. G. M.; Graboski, G. G. *Chem. Rev*. **1986**, *86*, 751. (e) Breuer, E.; Aurich, H. G.; Nielsen, A. *Nitrones, Nitronates&Nitroxides, The chemistry of functional groups* S. Patai, Ed.; J. Wiley & Sons: New York, 1992.
11. (a) Perlmutter,P. *Conjugate Addition Reactions in Organic Synthesis*, Pergamon: Oxford, **1992**. P.339. (b) Christoffers, J.; Baro, A. *Angew. Chem., Int. Ed*. **2003**, *42*, 1688. (c) Alexakis, A.; Benhaim, C. *Eur. J. Org. Chem*. **2002**, 3221. (d) Tsogoeva, S. B. *Eur. J. Org. Chem*. **2007**, 1701. (e) Kireev, A. S.; Manpadi, M.; Kornienko, A. *J. Org. Chem.* **2006**, *71*, 2630. (f) Hanessian, S.; Ma, J.; Wang, W. *J. Am. Chem. Soc.* **2001**, *123*, 10200 (g) Yamamoto, Y.; Chounan, Y.; Nishii, S.; Ibuka, T.; Kitahara, H. *J. Am. Chem. Soc.* **1992**, *114*, 7652. (h) Asao, N.; Shimada, T.; Sudo, T.; Tsukada, N.; Yazawa, K.; Gyoung, Y. S.; Uyehara, T.; Yamamoto, Y. *J. Org. Chem.* **1997**, *62*, 6274. (i) Sewald, N.; Hiller, K. D.; K¨orner, M.; Findeisen, M. *J. Org. Chem.* **1998**, *63*, 7263. (j) Cailleau, T.; Cooke, J. W. B.; Davies, S. G.; Ling, K. B.; Naylor, A.; Nicholson, R. L.; Price, P. D.; Roberts, P. M.; Russell, A. J.; Smith, A. D.; Thomson, J. E. *Org. Biomol. Chem.* **2007**, *5*, 3922.

12. (a) Plummer, J. S.; Emery, L. A.; Stier, M. A.; Suto, M. J. *Tetrahedron Lett*. **1993**, *34*, 7529. (b) Kimura, Y.; Aarashi, S.; Takahashi, M.; Hayakawa, I. *Chem. Pharm. Bull.* **1994**, *42*, 1442. (c) Ohtake, N.; Yamada, K.; Mano, E.; Okamoto, O.; Ushijima, R.; Nakagawa, S. *J. Antibiot*. **1997**, *50*, 567. (d) Hanessian, S.; Buckle, R.; Bayrakdarian, M. *J. Org. Chem.* **2002**, *67*, 3387. (e) Beylin, V.; Boyles, D. C.; Curran, T. T.; Macikenas, D.; Parlett IV, R. V.;Vrieze, D. *Org. Process Res. Dev.* **2007**, *11*, 441.
13. (a) Mali,S. M.; Bandyopadhyay, A.; Jadhav, S. V.; Ganesh Kumar, M.; Gopi, H. N. *Org. Biomol. Chem*. **2011**, *9*, 6566. (b) Bandyopadhyay, A.; Mali, S. M.; Lunawat, P.; Raja, K. M. P.; Gopi, H. N. *Org. Lett*. **2011**, *13*, 4482. (c) Bandyopadhyay, A.; Gopi, H. N. *Org. Lett*. **2012**, *14*, 2770.
14. (a) Ocejo, M.; Vicario, J. L.; Badia, D.; Carrillo, L.; Reyes, E. *Synlett*. **2005**, 2110. (b) Jadhav, S. V.; Bandyopadhyay, A.; Benke, S. N.; Mali, S. M.; Gopi, H. N. *Org. Biomol. Chem.* **2011**, *9*, 4182.
15. Dorigo, A. E.; Pratt, D. W.; Houk, K. N. *J. Am. Chem. Soc.* **1987**, *109*, 6591.
16. Wiberg, K. B.; Martin, E. *J. Am. Chem. Soc*. **1985,** *107*, 5035.
17. Brownstein, S.; Dunogues, J.; Lindsay, D.; Ingold, K. U. *J. Am. Chem. Soc*. **1977**, *99*, 2073.
18. Vasudev, P. G.; Shamala, N.; Ananda, K.; Balaram, P. *Angew. Chem., Int. Ed. Engl*. **2005**, *44*, 4972.
19. (a) Matthews, B. W. *Macromolecules* **1972**, *5*, 818. (b) Milner-White, E. J. *J. Mol. Biol*. **1990**, *216*, 385.
20. Vasudev, P. G.; Shamala, N.; Ananda, K.; Balaram, P. *Angew. Chem., Int. Ed.* **2005**, *44*, 4972.
21. (a) Basuroy, K.; Dinesh, B.; Madhusudana Reddy, M. B.; Chandrappa, S.; Raghothama, S.; Shamala, N.; Balaram, P. *Org. Lett*. **2013**, *15*, 4866. (b) Vasudev, P. G.; Chatterjee, S.; Shamala, N.; Balaram, P. *Acc. Chem. Res*. **2009**, *42*, 1628. (c) Seebach, D.; Brenner, M.; Rueping, M.; Jaun, B. *Chem. -Eur. J.* **2002**, *8*, 573. (d) Jadhav, S. V.; Gopi, H. N. *Chem. Commun*. **2013**, *49*, 9179.
22. Basuroy, K.; Dinesh, B.; Madhusudana Reddy, M. B.; Chandrappa, S.; Raghothama, S.; Shamala, N.; Balaram, P. *Org. Lett*. **2013**, *15*, 4866.

23. (a) Barlow, D. J.; Thornton, J. M. *J. Mol. Biol*. **1988**, *201*, 601. (b) Karle, I. L.; Balaram, P. *Biochemistry* **1990**, *29*, 6747.
24. (a) Bandyopadhyay, A.; Gopi, H. N. *Org. Lett*. **2012**, *14*, 2770. (b) Bandyopadhyay, A.; Jadhav, S. V.; Gopi, H. N. *Chem. Commun*. **2012**, *48*, 7170.
25. (a) Leinala, E. K.; Davies, P. L.; Jia, Z. *Structure* **2002**, *10*, 619. (b) Jurnak, F.; Yoder, M. D.; Pickersgill, R.; Jenkins, J. *Curr. Opin. Struct. Biol*. **1994**, *4*, 802.
26. (a) Bong, D. T.; Clark, T. D.; Granja, J. R.; Ghadiri, M. R. *Angew. Chem., Int. Ed.* **2001**, *40*, 988. (b) Shimizu, T.; Masuda, M.; Minamikawa, H. *Chem. Rev*. **2005**, *105*, 1401. (c) Percec, V.; Dulcey, A. E.; Balagurusamy, V. S. K.; Miura, Y.; Smidrkal, J.; Peterca, M.; Nummelin, S.; Edlund, U.; Hudson, S. D.; Heiney, P. A.; Duan, H.; Magonov, S. N.; Vinogradov, S. A. *Nature* **2004**, *430*, 764. (d) Yan, X.; Zhu, P.; Li, J. *Chem. Soc. Rev*. **2010**, *39*, 1877. (e) Kim, J. H.; Lee, M.; Lee, J. S.; Park, C. B. *Angew. Chem., Int. Ed*. **2012**, *51*, 517. (f) Montenegro, J.; Ghadiri, M. R.; Granja, J. R. *Acc. Chem. Res*. **2013**, *46*, 2955.(g) Jadhav, S. V.; Misra, R.; Singh, S. K.; Gopi, H. N. *Chem. Eur. J.***2013**, *19*, 16256.
27. (a) Savilles-Stones, E. A.; Lindell, S. D. *Synlett* **1991**, 591. (b) Matt, C.; Wagner, A.; Mioskowski, C. *J. Org. Chem*. **1997**, *62*, 234.
28. Pham-Huu, D-P.; Petruová, M.; BeMiller, J. N.; Petru, L. *Synlett*. **1998**, 1319.
29. Figueras, F.; Coq. B. *J. Mol. Catal. A: Chem*. **2001**, *173*, 223.
30. Duffy, J. L.; Kurth, M. J. *J. Org. Chem*. **1994**, *59*, 3783.
31. Gunther, R.; Hofmann, H. J. *Helv. Chim. Acta* **2002**, *85*, 2149.
32. (a) Rua, F.; Boussert, S.; Parella,T.; Diez-Perez,I.; Branchadell, V.; Giralt, E.; Ortuno, R. M. *Org. Lett*. **2007,***9*, 3643. (b) Torres, E.; Gorrea, E.; Burusco, K. K.; Da Silva, E.; Nolis, P.; Rua, F.; Boussert, S.; Diez-Perez, I.; Dannenberg, S.; Izquierdo, S.; Giralt, E.; Jaime, C.; Branchadell, V.; Ortuno, R. M. *Org. Biomol. Chem.* **2010**, *8*, 564.
33. Bandyopadhyay, A.; Malik, A.; Ganesh Kumar, M.; Gopi, H. N. *Org. Lett*., **2014**, *16*, 294-297.
34. Ganesh Kumar, M.; Mali, S. M.; Raja, K. M. P.; Gopi, H. N. *Org. Lett*., **2015**, *17*, 230.

2.5 Appendix I: Characterization Data of Synthesized Compounds

Designation	Description	Page
Boc-(*S*, *S*)γVal(β-CH_2NO_2)-OEt (**2a**)	^{1}H NMR (400 MHz)	128
Boc-(*R*, *S*)γVal(β-CH_2NO_2)-OEt (**3a**)	^{1}H NMR (400 MHz)	128
Boc-(*S*, *S*)γPhe(β-CH_2NO_2)-OEt (**2b**)	^{1}H NMR (400 MHz)	129
Boc-(*R*, *S*)γPhe(β-CH_2NO_2)-OEt (**3b**)	^{1}H NMR (400 MHz)	129
Boc-γVal(β-CH_2NO_2)-γVal(β-CH_2NO_2)-OEt (**P7**)	^{1}H NMR (400 MHz)	130
Boc-γVal(β-CH_2NO_2)-γVal(β-CH_2NO_2)-γVal(β-CH_2NO_2)-OEt (**P8**)	^{1}H NMR (400 MHz)	130
Boc-γVal(β-CH_2NO_2)-γVal(β-CH_2NO_2)-γVal(β-CH_2NO_2)-γVal(β-CH_2NO_2)-OEt (**P9**)		131
Boc-Aib-γPhe(β-CH_2NO_2)-Aib-γPhe-OEt (**P10**)	^{1}H NMR (400 MHz)	131
Boc-Aib-γPhe(β-CH_2NO_2)-Aib γPhe(β-CH_2NO_2)-OEt (**P11**)	^{1}H NMR (400 MHz)	132
Boc-Aib-γPhe(β-COOH)-Aib-γPhe-OEt (**P12**)	^{1}H NMR (400 MHz)	132
Boc-Aib-γPhe(β-CH=NOH)-Aib-γPhe-OEt (**P13**)	^{1}H NMR (400 MHz)	133
Boc-Aib-γPhe(β-CH_2NH_2)-Aib-γPhe-OEt (**P14**)	^{1}H NMR (400 MHz)	133
Boc-Aib-γPhe(β-phenyloxazolyl)-Aib-γPhe-OEt (**P15**)	^{1}H NMR (400 MHz)	134
Boc-(*S*, *S*)γVal(β-SNB)-O^{t}Bu (**12a**)	^{1}H NMR (400 MHz)	134
Boc-(*R*, *S*)γVal(β-SNB)-O^{t}Bu (1**2b**)	^{1}H NMR (400 MHz)	135

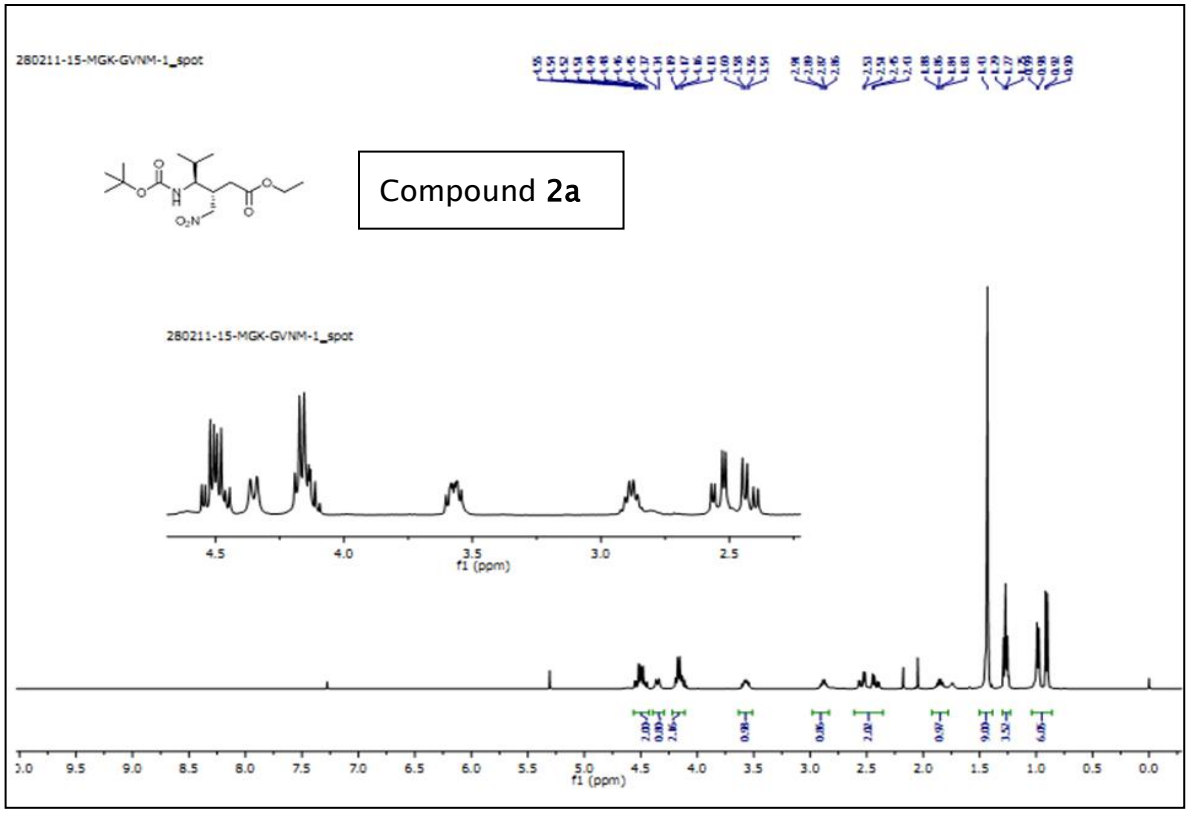
280211-15-MGK-GVNM-1_spot
Compound 2a
280211-15-MGK-GVNM-1_spot
f1 (ppm)
f1 (ppm)

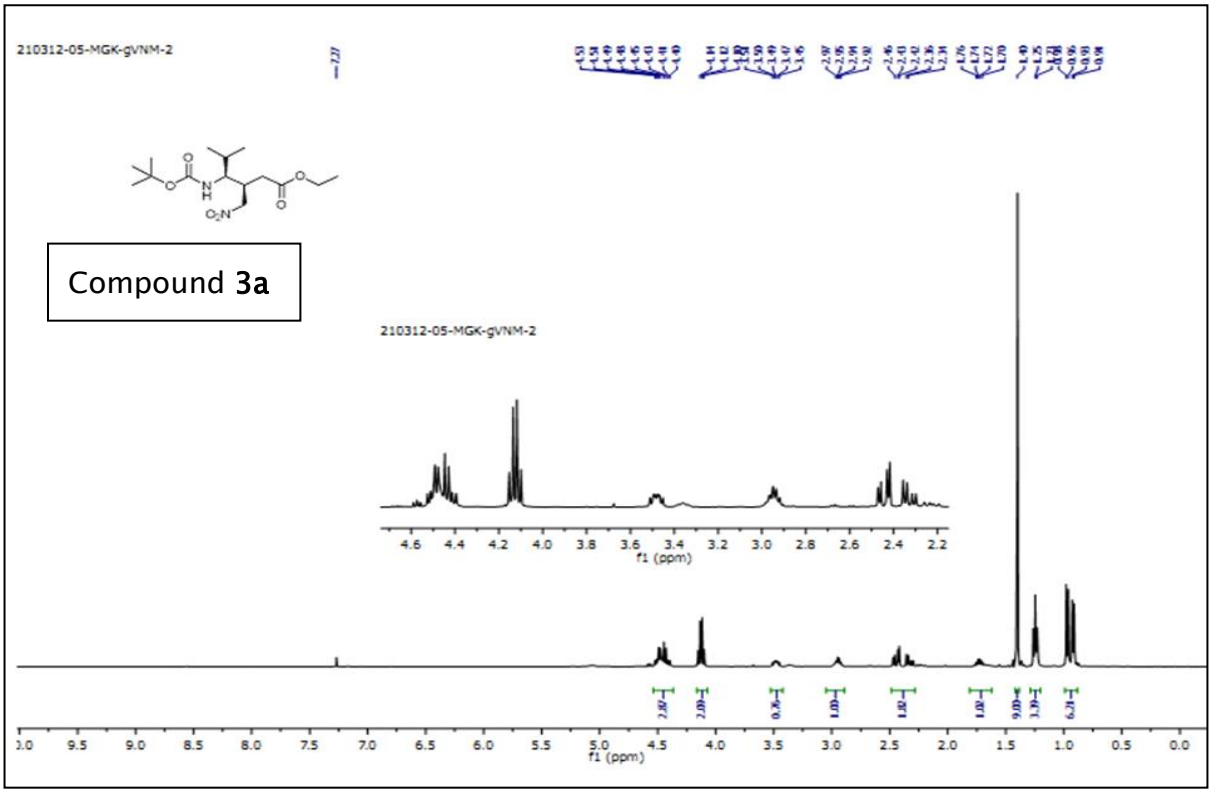
210312-05-MGK-gVNM-2
Compound 3a
210312-05-MGK-gVNM-2
f1 (ppm)
f1 (ppm)

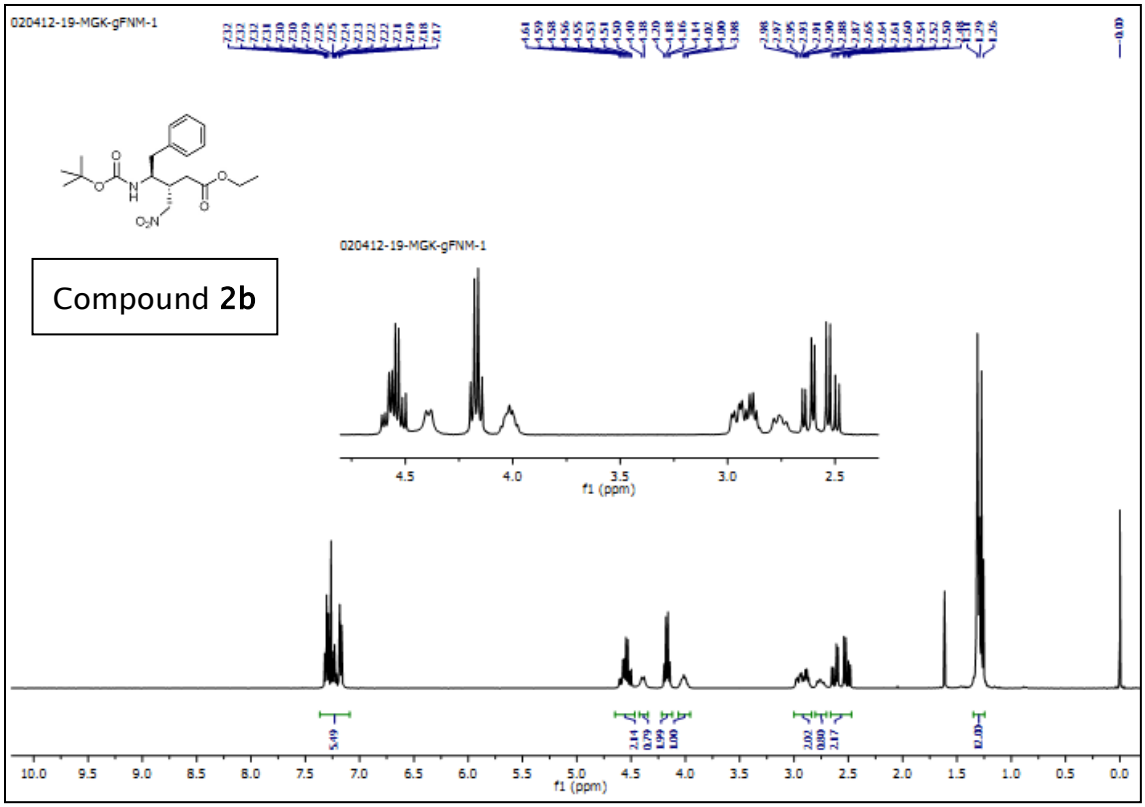
020412-19-MGK-gFNM-1
Compound 2b
020412-19-MGK-gFNM-1
f1 (ppm)

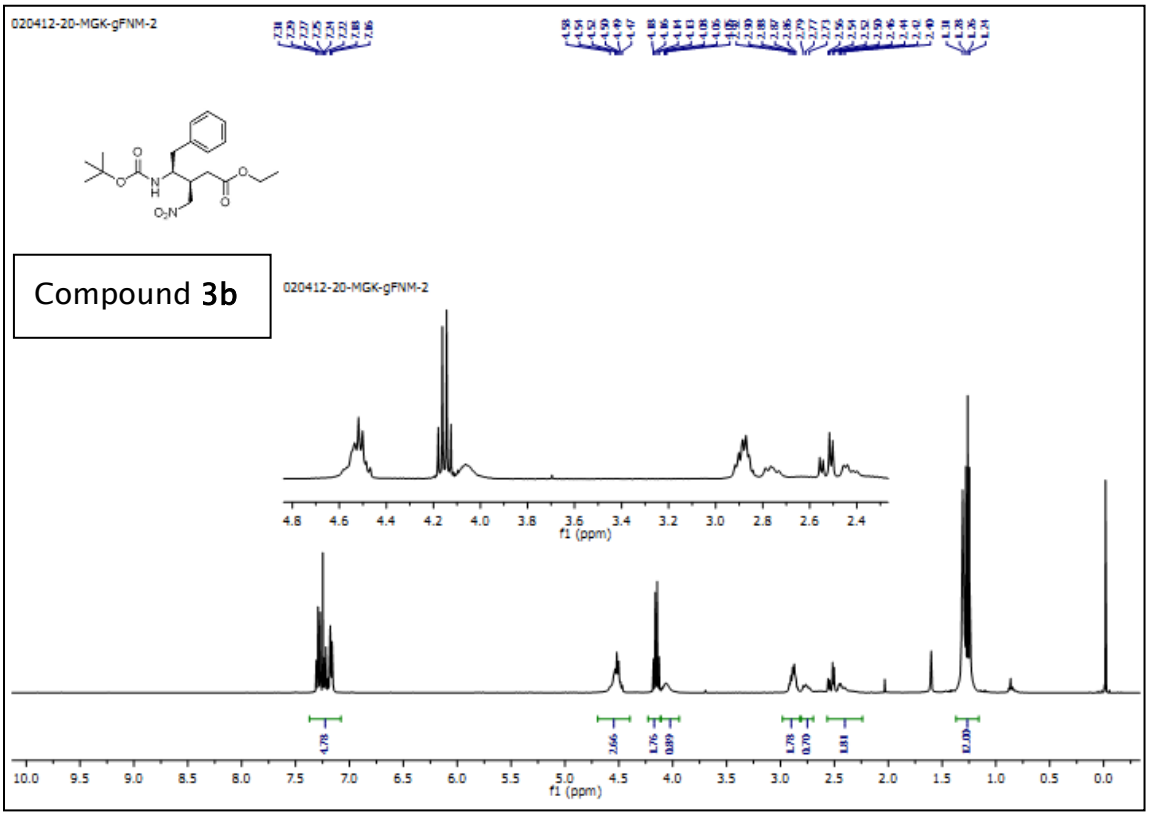
020412-20-MGK-gFNM-2
Compound 3b
020412-20-MGK-gFNM-2
f1 (ppm)

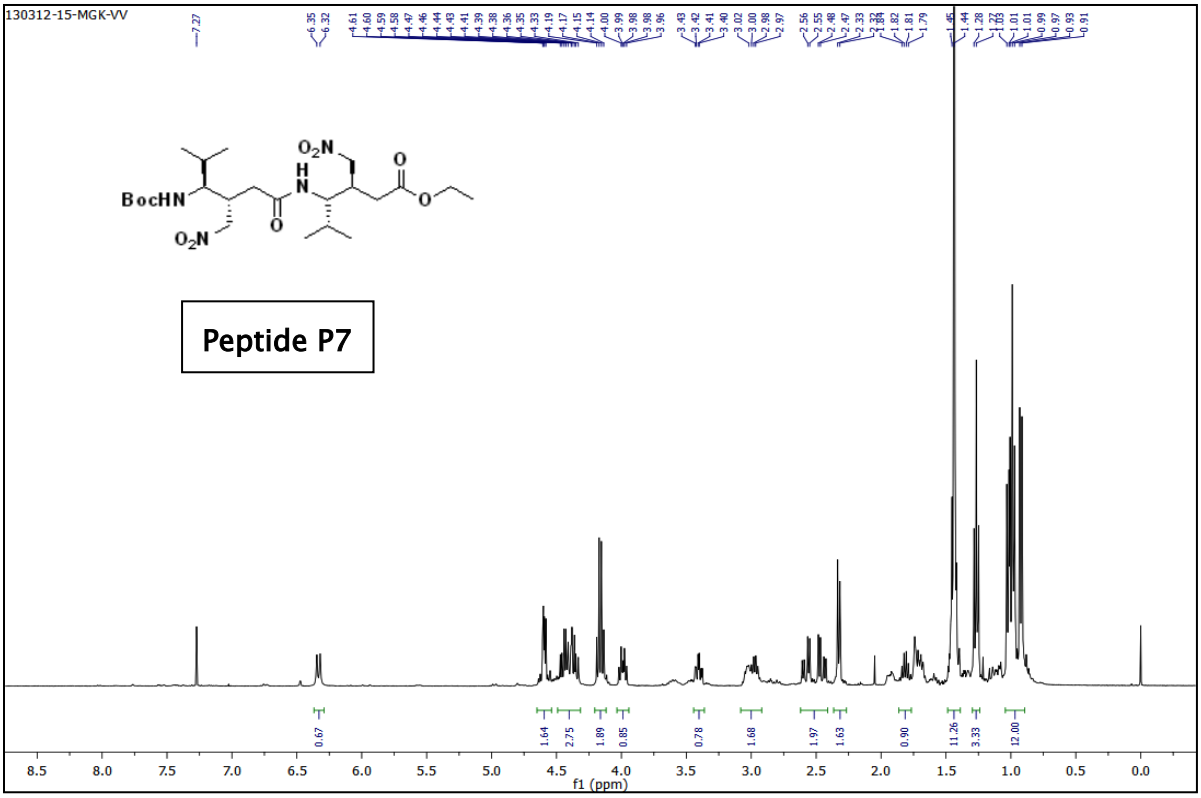
130312-15-MGK-VV
BocHN
O_2N
H
N
O
O
O_2N
O
O
Peptide P7
f1 (ppm)

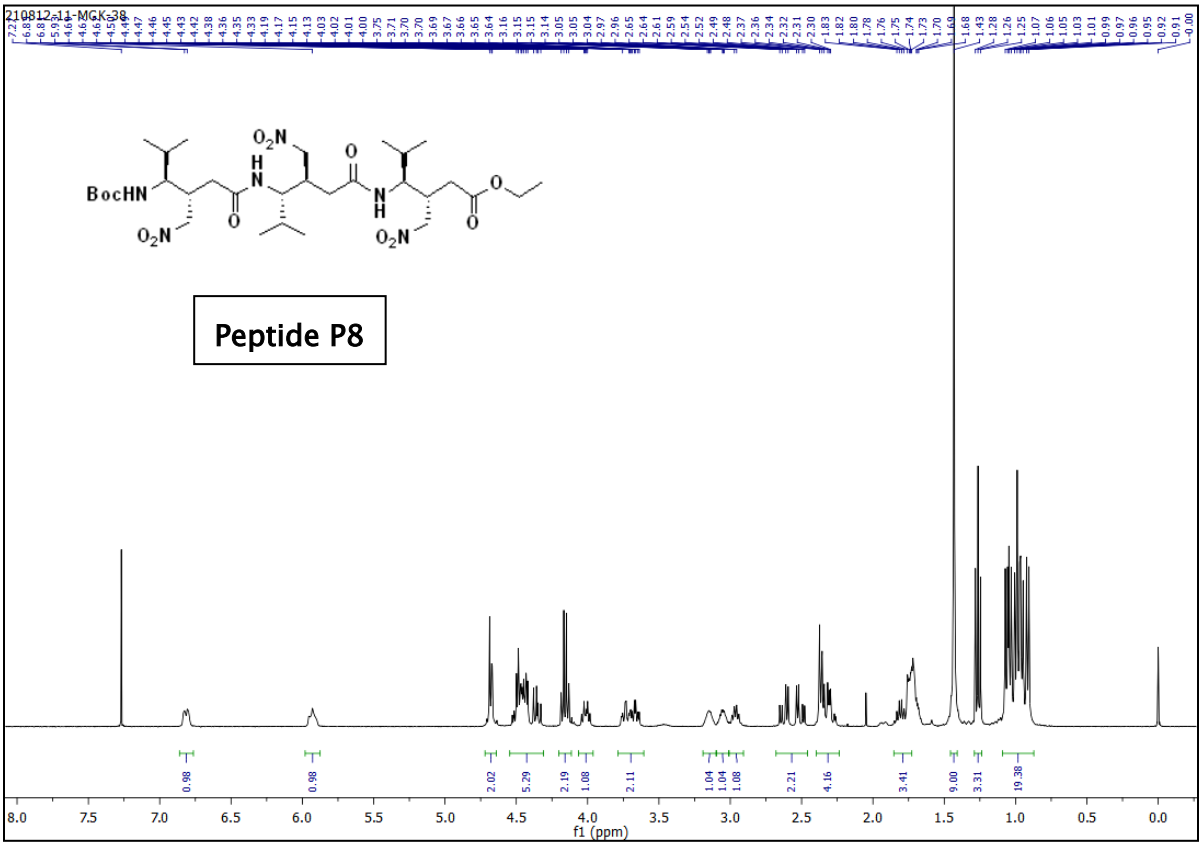
210812-11-MGK-38
BocHN
O_2N
H
N
O
O
O_2N
N
H
O_2N
O
O
Peptide P8
f1 (ppm)

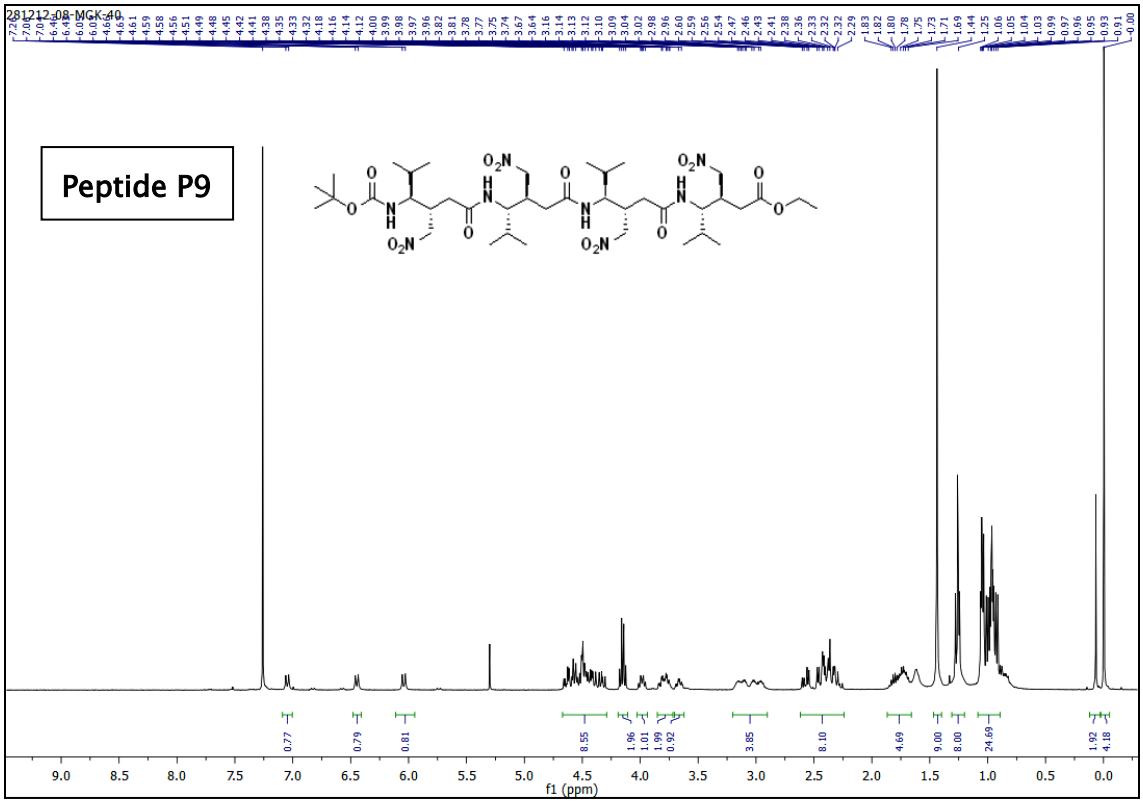
281212-08-MGK-40
Peptide P9
f1 (ppm)

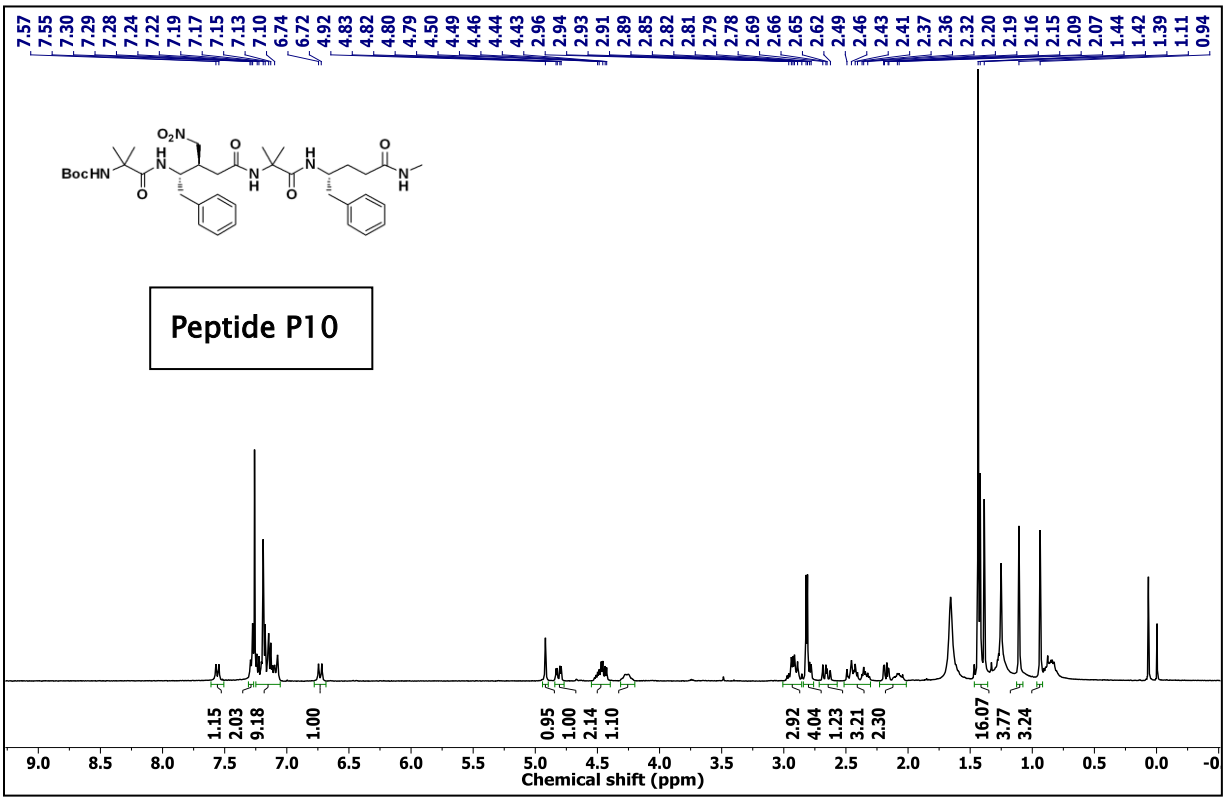
Peptide P10
Chemical shift (ppm)

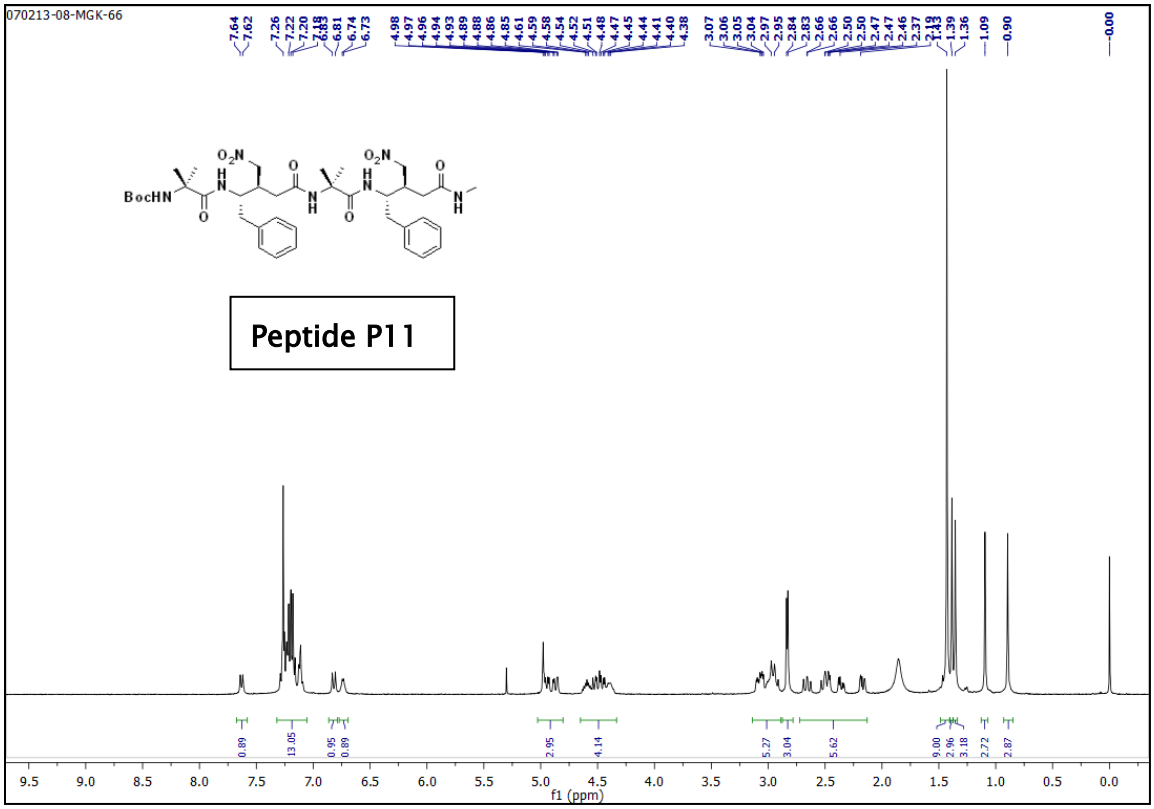
070213-08-MGK-66
Peptide P11
f1 (ppm)

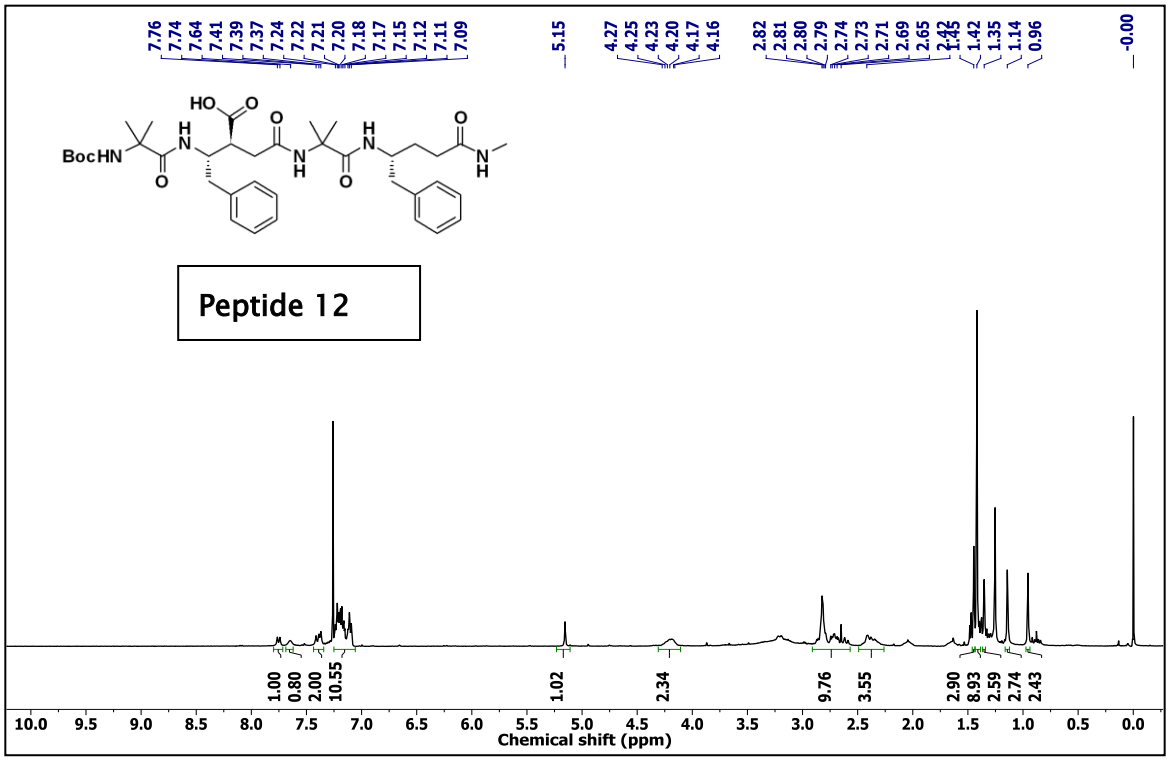
Peptide 12
Chemical shift (ppm)

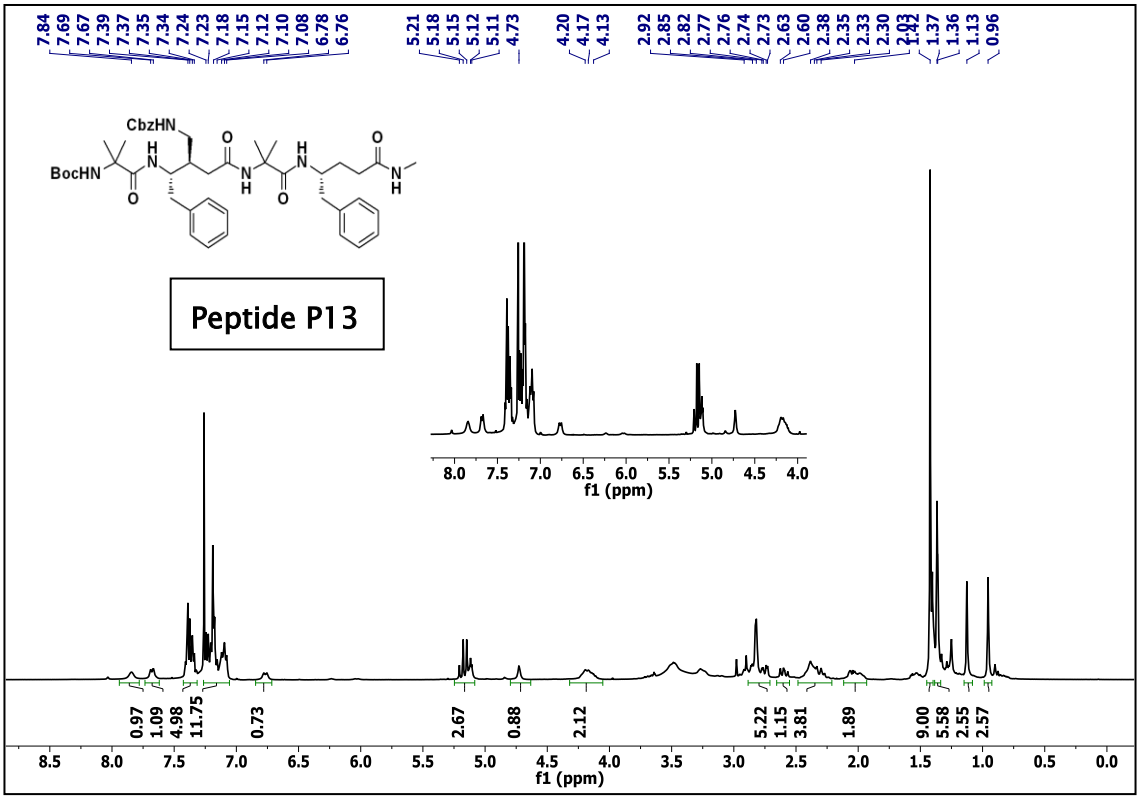
Peptide P13
CbzHN
BocHN
f1 (ppm)

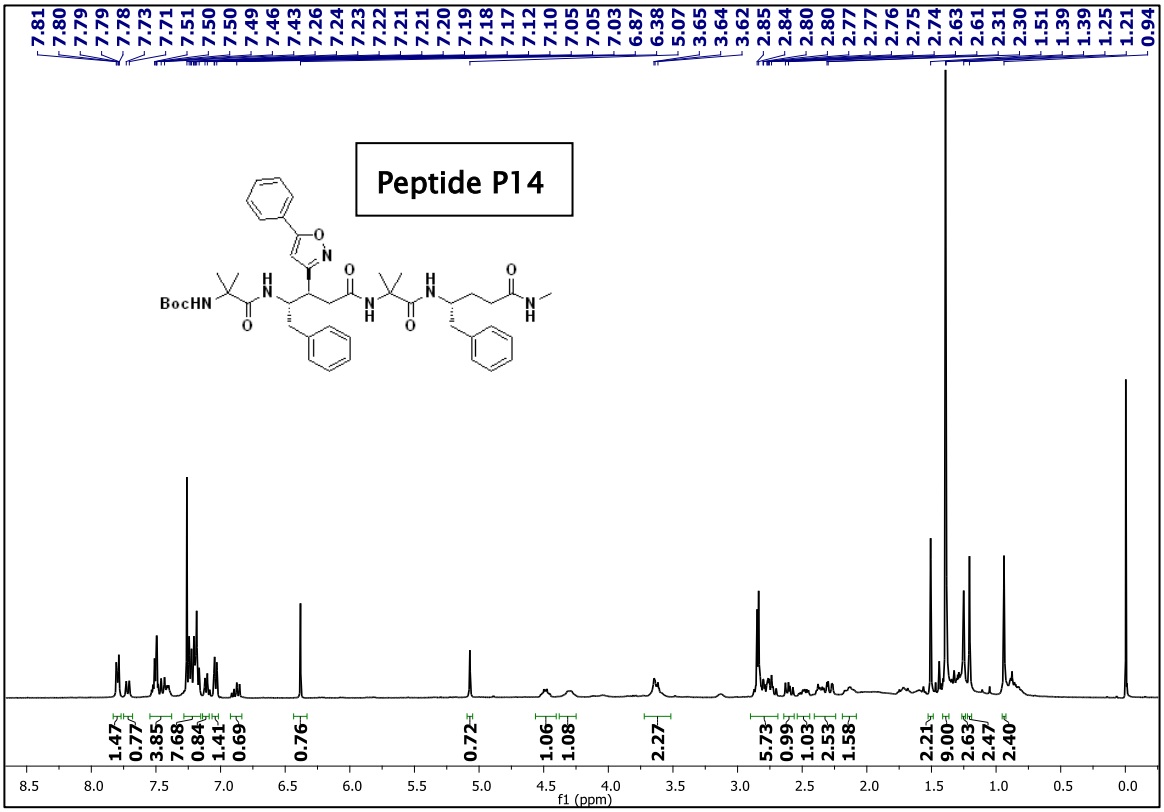
Peptide P14
BocHN
f1 (ppm)

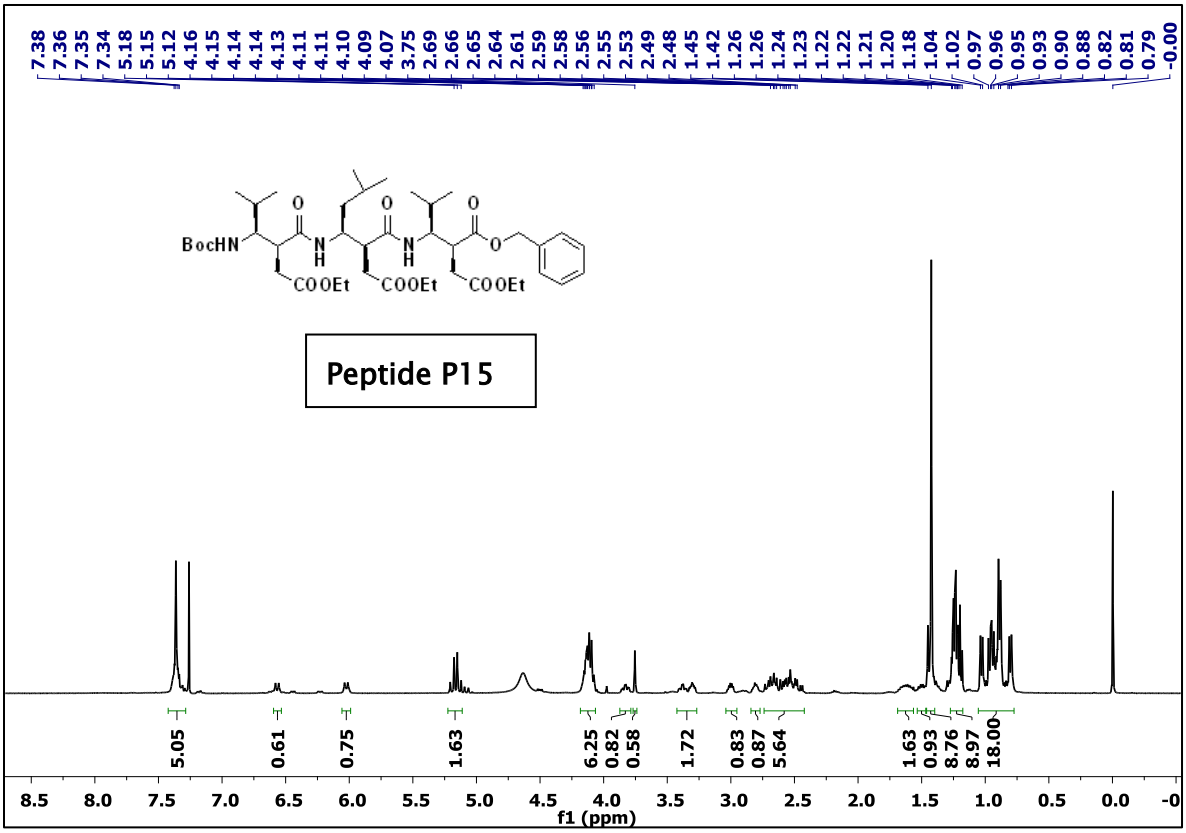
Peptide P15
BocHN
COOEt
f1 (ppm)

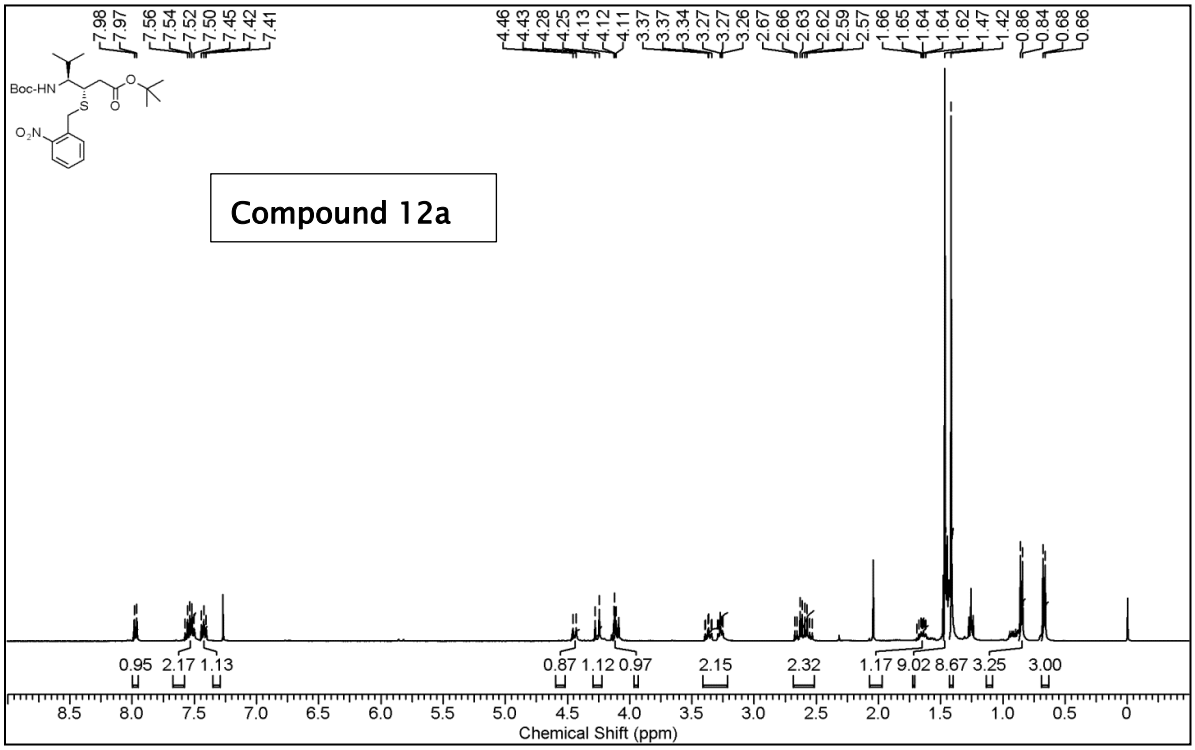
Compound 12a
Boc-HN
Chemical Shift (ppm)

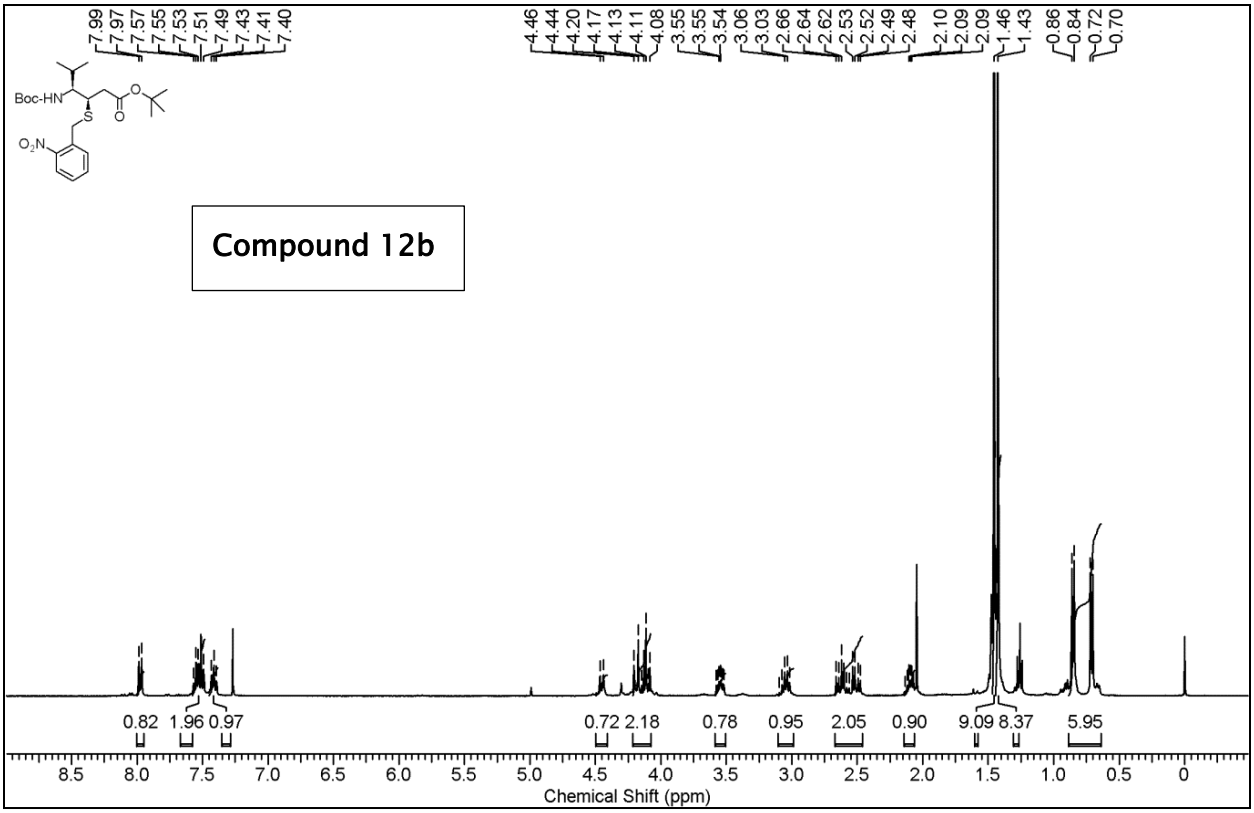
Compound 12b
Boc-HN
S
O
O
O_2N
7.99 7.97 7.57 7.55 7.53 7.51 7.49 7.43 7.41 7.40
4.46 4.44 4.20 4.17 4.13 4.11 4.08
3.55 3.55 3.54 3.06 3.03 2.66 2.64 2.62 2.53 2.52 2.49 2.48 2.10 2.09 2.09
1.46 1.43
0.86 0.84 0.72 0.70
0.82 1.96 0.97
0.72 2.18 0.78 0.95 2.05 0.90 9.09 8.37 5.95
8.5 8.0 7.5 7.0 6.5 6.0 5.5 5.0 4.5 4.0 3.5 3.0 2.5 2.0 1.5 1.0 0.5 0
Chemical Shift (ppm)

Chapter 3

Peptide Foldamers with Heterogeneous Backbone: Utilization of *Z*-Vinylogous Amino Acids in the Design of α, γ-Hybrid Helices

3.1 Introduction

The well-defined, three dimensional structures of proteins are crucial for their diverse functions in all living systems. This universal feature of proteins has created enormous interest in chemists to build protein like structures from the oligomers of unnatural amino acid building blocks and organic templates.[1] As described in Chapters 1 and 2, β- and γ-peptides are among the most extensively studied unnatural oligomers. Despite the backbone conformational freedom, these β- and γ-peptides spontaneously fold into well-defined structures and adopted protein like folding properties.In addition, the hybrid peptides with the combination of αβ, αγ and βγ amino acid residues displayed a variety of helical structures with different H-bonding patterns.[2-9] The γ-residues with two additional backbone carbon atoms further offer flexibility in the design of foldamers. Indeed, many bacteria including *Bacillus anthracis* produces γ-amino acid polymer, poly-γ-glutamate, for their survival at high salt concentrations as well as for virulence.[10] Several years back Rydon proposed the left-handed helical signature of poly-γ-glutamate with larger C_{17} and C_{19} H-bond pseudocycles.[11] Oligomers of γ-amino acids with and without side-chains displayed a variety of well-defined folded structures. In their pioneering work, Seebach and Hanessian independently showed the well-defined 14-helical organizations from homooligomers of γ^4, $\gamma^{2,4}$ and $\gamma^{2,3,4}$ alkyl substituted amino acids.[3] Further, Balaram and colleagues reported helices and β-turns using γ^4 and $\gamma^{3,3}$-amino acids (gabapentin).[4] Contemporarily, Gellman and colleagues reported a variety of helical structures from γ- and hybrid γ-peptides from the constrained cyclic γ-amino acids.[6] Sharma and colleagues utilized 4-substituted carbo amino acids to derive helical foldamers.[7] In addition to the oligomers with amide linkages, Guichard and colleagues demonstrated the utility of urea bonds in the design of γ-peptide foldamers with additional H-bonds.[8] Besides these synthetic γ-amino acids, Schreiber and colleagues have showed the extended sheet type of structures from the peptides composed of naturally occurring non-ribosomal (*E*)-α,β-unsaturated γ-amino acids.[12] In continuation, Hofmann and colleagues reported a variety of helical structures with H-bonded pseudocycles from (*E)*- and (*Z)*-vinylogous amino acids through theoretical calculations.[13] Strikingly, (*E)*-vinylogous oligomers adopt helical conformations with larger H-bond pseudocycles (C_{19}, C_{22} and C_{27}), whereas *Z*-vinylogous peptides prefer stable C_7- and C_9-helices through nearest neighbor interactions. Recently, Maillard and coworkers have shown that γ-peptides containing thiazole-based γ-amino

acids, which are similar to *Z*-vinylogous amino acids adopted C_9 helices in homooligomers.[14] Grison *et al*. and others also reported *cis*-vinylog turn and α-turn mimetics using *Z*-vinylogous amino acids.[15]

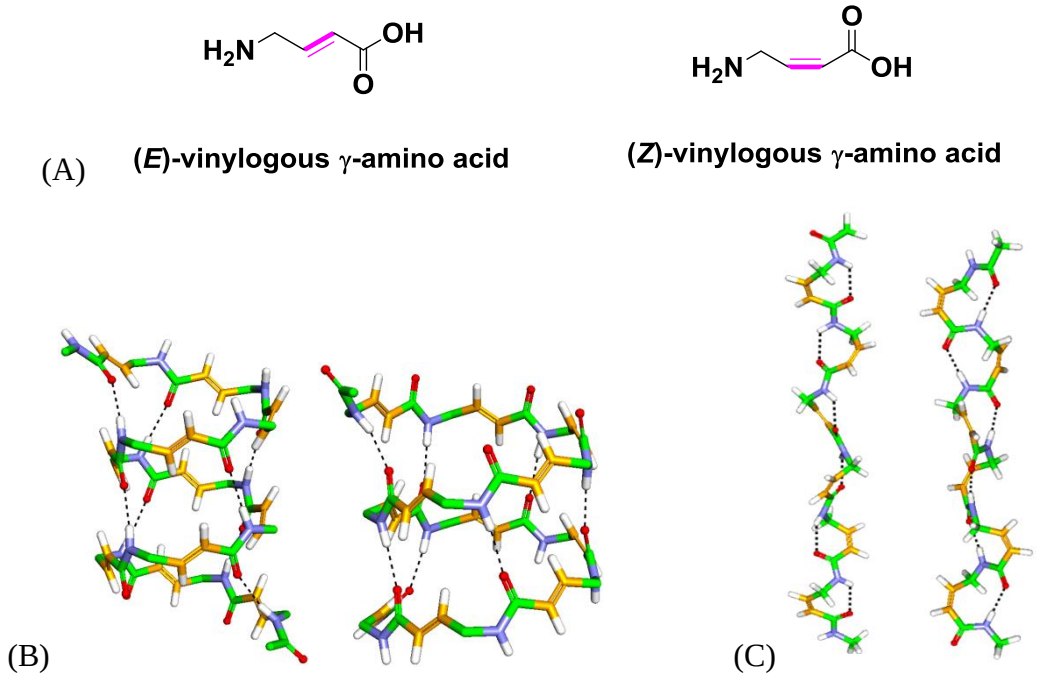

Fig 1: (A) Chemical structures of (*E*)- and (*Z*)-vinylogous γ-amino acids. Most stable C22- and C27-helices of (*E*)-vinylogous-peptide hexamers (B) and C7- and C9- helices of (*Z*)-vinylogous-peptide hexamers (C). Coordinates of the model structures are taken from *ref*.13.

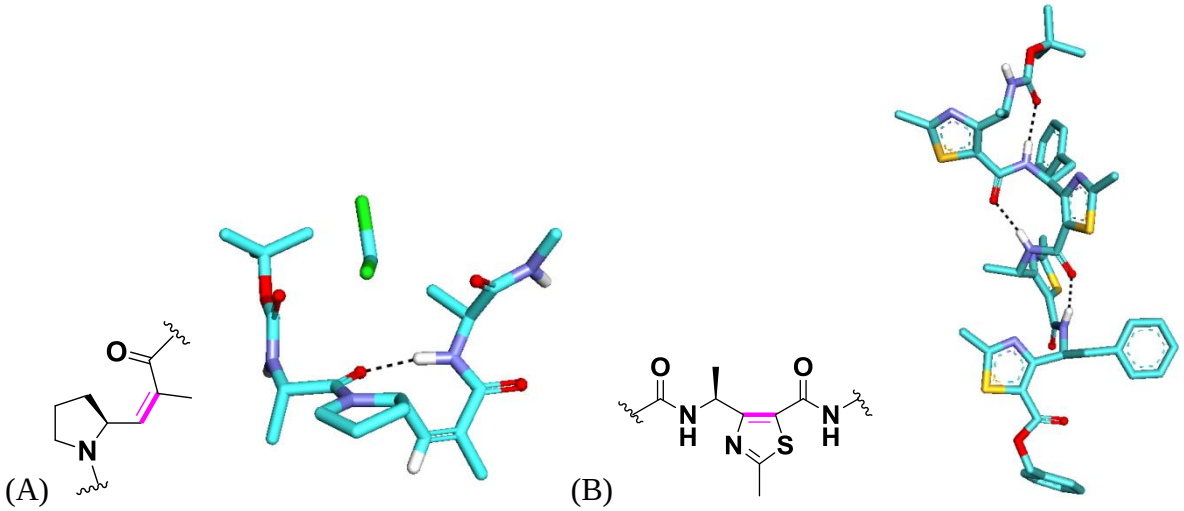

Fig 2: (A) X-ray structure of cis-Vinylog turn in dipeptide and (B) C_9-helical structure of Thiazole based γ-amino acid tetramer. Crystallographic data have been taken from *ref*. 14 and 15a.

3.2 Aim and Rationale of the Present Work

We have been interested in the design of folded architectures constructed from conformationally constrained α, β-unsaturated γ-amino acids. In the previous chapters, we have demonstrated the utilization of conformationally restricted conjugated double bonds in the design of miniature β-meanders and helix-turn-helix type of mimetics. In addition, we also showed the utility of *E*-vinylogous amino esters as Michael acceptors to derive β- and γ-peptide foldamers.[16-18] Moreover, we illustrated the direct transformation of unsaturated hybrid peptides into helical foldamers using catalytic hydrogenation.[16] The conformational studies suggested that *E*-vinylogous amino acids promote the extended β-sheets type of structures. In addition, we showed in Chapter 1 that these amino acids can be used to bend the helix rather than accommodating into the helix. We anticipate that insertion of conjugated double bonds into helical structures would greatly enhance their utility for further functionalization. Designed helical peptides may be used as inhibitors for various protein-protein interactions as well as to create peptide nanotubes.[19] We envisioned that instead of β-sheet promoting *E*-vinylogous amino acids, *Z*-vinylogous amino acids can be incorporated into the helical structures without affecting their overall helix folding. As we have been interested in the design of hybrid peptide foldamers composed of α- and γ-amino acids, we sought to investigate the conformations of *Z*-vinylogous residues in hybrid peptides. In this Chapter, we are reporting the design, synthesis and crystal conformations of various hybrid peptide helices composed of single and multiple *Z*-vinylogous amino acids. In addition, hybrid peptides also provide an opportunity to understand the conformational properties of *cis* double bonds in acyclic systems.

3.3 Results and Discussion

3.3.1 Synthesis of (Z)-α, β-Unsaturated γ-Amino acids

We utilized Witting-Horner reaction to synthesize *Z*-vinylogous amino acids. The schematic representation of synthesis is shown in Scheme 1.[20] The Wittig-Horner ylide was generated *in situ* by treating alkyl ester of 2-(diphenoxyphosphoryl)acetate with NaI and DBU. The *in situ* generated ylide was further treated with Boc-amino aldehyde. We standardized the reaction using both ethyl and *tert*-butyl esters of 2-(diphenoxyphosphoryl)acetate. The coupling reaction between the ylide and the N-Boc-amino aldehyde gave both *cis* and *trans* products in the ratio of

approximately 80:20, respectively. Both *E*- and *Z*- isomers were separated using column chromatography. The stereochemistry of the double bonds was confirmed using ^{1}H NMR. In addition, we also obtained the single crystals of major isomer **2d** and its X-ray structure and torsional angles are shown in Figure 3. In order to reduce the synthetic steps, we continued with *tert*-butyl esters of N-Boc protected *Z*-vinylogous amino acids. The N-Boc and *tert*-butyl ester of the major *cis* isomers were deprotected using 50% TFA in DCM in a single step and the free amine obtained after the deprotection of Boc- group was further protected with solid phase compatible Fmoc group. The Fmoc-protected *Z*-vinylogous amino acids were isolated in excellent yields and directly used for the solid phase synthesis without further purification.

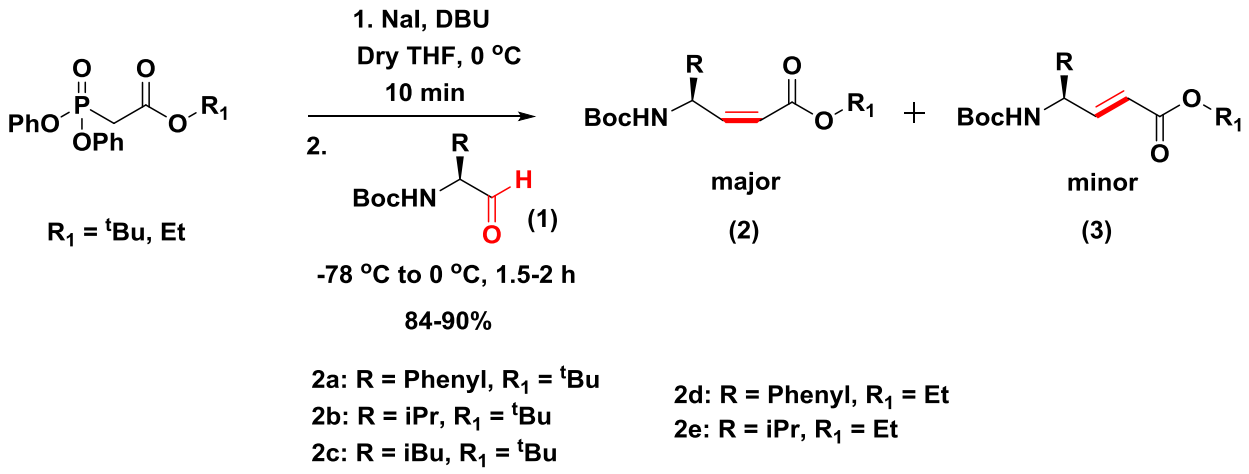

Scheme 1: Synthesis of (*Z*)-α, β-Unsaturated γ-Amino acids using Wittig-Horner Reaction.

(A)

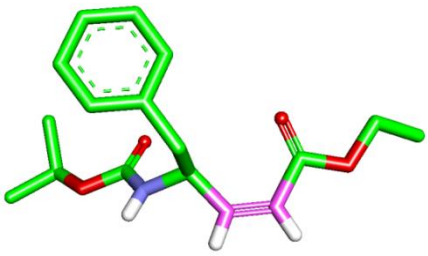

(B)

2d	ϕ	θ_1	θ_2	ψ
(Z)-dγPhe	-122	150	1	-174

Fig 3: (A) X-ray structure of compound **2d** and (B) Torsional variables (in deg) of compound **2d**.

3.3.2 Incorporation of (*Z*)-α, β-Unsaturated γ-Amino acids in α, γ-Hybrid Helix: Synthesis and Conformational Analysis

In order to understand whether *Z*-vinylogous amino acids (*Z*-dγX) can be accommodated into the helix, we designed α,γ-hybrid peptide **P1** from the previously reported (our own group) α,γ-hybrid peptide 12-helix (Model peptide: **M**).[21] Peptide **P1** consists of a single *Z*-vinylogous amino acid along with other γ^4-amino acids with alternating α-amino acid, Aib. The sequences of **P1** and model peptide **M** is shown in Scheme 2. Peptide **P1** was synthesized by solid phase method on Rink amide resin using standard Fmoc- chemistry. The coupling reactions were performed using HBTU coupling reagent. The crude peptide was purified using reverse phase HPLC on C_{18} column and pure peptide was subjected to crystallization in various solvent combinations to understand its unambiguous conformation.

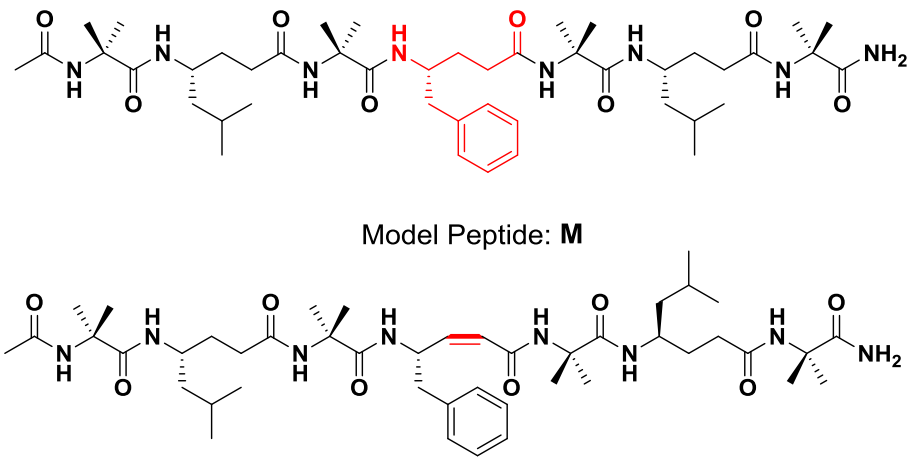

Scheme 2: Sequences of α, γ-hybrid model peptide (**M**) and peptide **P1**.

Single crystals of **P1** were obtained from the slow evaporation of peptide solution in aqueous methanol and its X-ray structure is shown in Figure 4A. Instructively, crystal structure analysis suggests that the peptide adopted a right handed 12-helix conformation. Both saturated γ-amino acids γLeu2 and γLeu6 have adopted *gauche*$^+$, *gauche*$^+$ (g^+, g^+) conformation along C^γ-C^β and C^β-C^α bonds in the helix. As anticipated, *Z*-dγPhe4 nicely accommodated into the 12-helix, however, without adopting the backbone conformations of saturated γ-amino acids. The backbone conformations of γ-residues can be measured by introducing two additional torsional

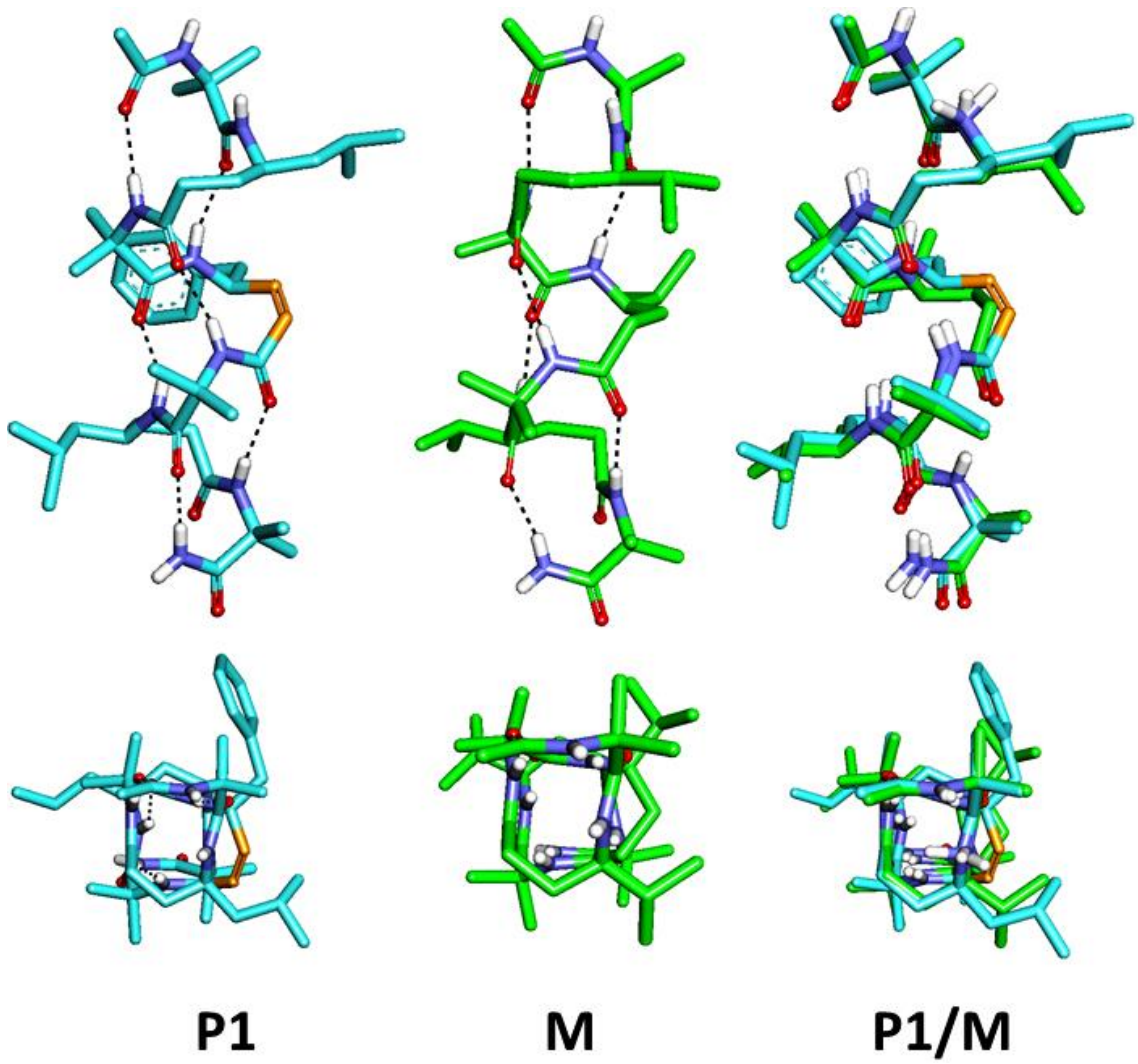

(A) (B) (C)

Fig 4: (A) X-ray structure of Peptide **P1**, (B) X-ray structure of model peptide **M** and (C) Overlay of Peptides **P1** and **M** (double bond highlighted in orange color).

variables θ_1 and θ_2 along with ϕ and ψ. The θ_1 and θ_2 generally attain the value $\approx \pm 60°$ in saturated γ-residues. The torsional angle θ_2 in *Z*-vinylogous residue is expected to take torsional value close to 0°. As predicted, θ_2 in Z-dγPhe4 arrive at the value -2°. In order to accommodate *Z*- vinylogous residue into the helix, both torsional variables θ_1 and ψ attained the unusual values +94° and -79°, respectively. However, torsion angle ϕ was found to be -122°, which is similar to that of saturated γ^4-amino acids in 12-helix. These results suggested that it is not necessary that θ_1 and θ_2 should adopt g^+, g^+ conformation for the γ-residues to accommodate into the helix.

Similar to peptide **M**, **P1** also stabilized by six intramolecular H-bonds existed between the residues *i* and *i+3*. Further the superposition of **P1** and **M** shown in Figure 4C, suggested an excellent backbone correlation between the two peptides. The torsional values and H-bond parameters of **P1** are tabulated in Table 3 and 4, respectively.

3.3.3 Design, Synthesis and Conformational Analysis of Peptides P2-P5

In order to understand whether residues other than ZdγPhe can be accommodated into the helix, we designed hybrid peptides, **P2** and **P3**, containing ZdγVal and ZdγLeu, respectively (Scheme 3). Peptides were synthesized similar to **P1** and pure peptides were subjected to crystallization in various solvent combinations to understand their unambiguous conformations. Both **P2** and **P3** gave X-ray quality single crystals from the slow evaporation of peptide solution in aqueous methanol and their crystal structures are shown in Figure 5. Both **P2** and **P3** adopted right handed 12-helical conformations. Similar to the 1:1 alternating α,γ-hybrid heptapeptides, both the structures are stabilized by six intramolecular H-bonds between *i* and *i+3* residues. Akin to *Z*-dγPhe, θ_1 of *Z*-dγVal and Z-dγLeu attained +105° and +98°, respectively. The ψ values of *Z*-dγVal and *Z*-dγLeu were found to be -74° and -82° which are consistent with ψ values of *Z*-dγPhe in **P1**. The torsion angles of all Z-vinylogous residues are tabulated in Tables 5 and 7.

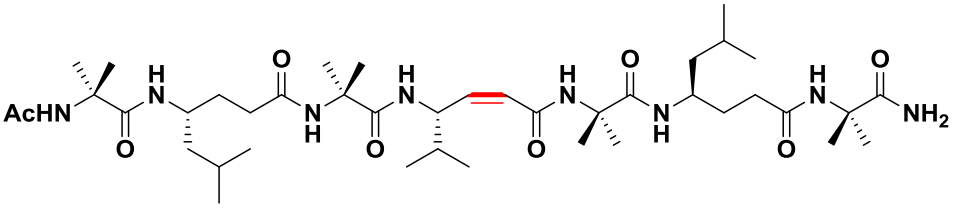

P2

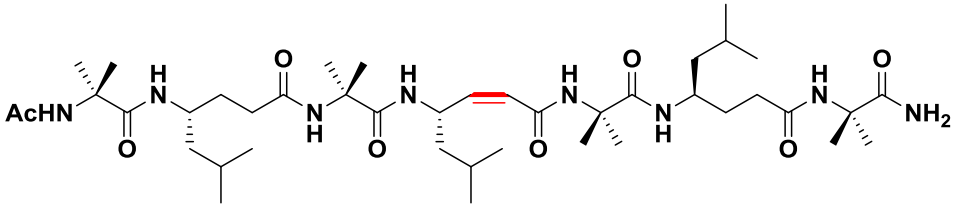

P3

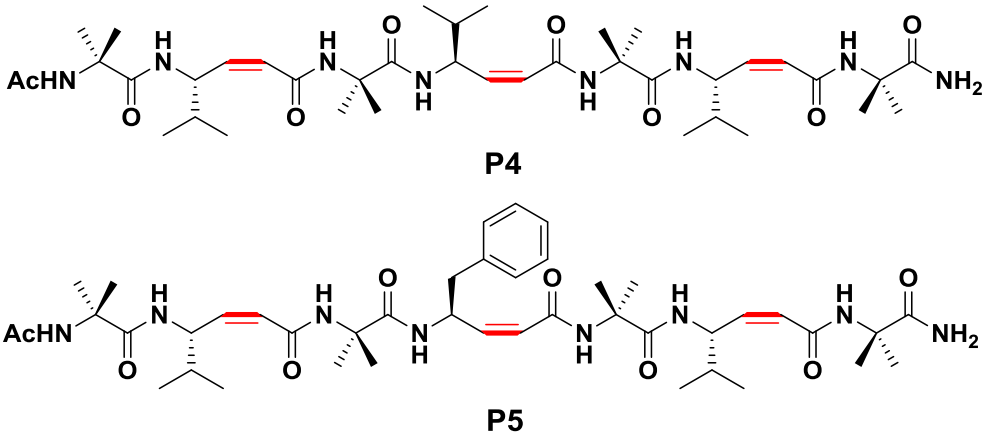

Scheme 3: Sequences of *Z*-vinylogous γ-amino acids contained α, γ-hybrid peptides **P2-P5**.

To verify whether multiple vinylogous amino acids can be accommodated into the 12-helix, we designed **P4** and **P5** with 1:1 alternating α- and *Z*-vinylogous residues (Scheme 3). Peptide **P4** is composed of alternating Aib and Z-dγVal, while **P5** consists of Z-dγVal and Z-dγPhe along with alternating Aib. Both the peptides were synthesized on solid phase and purified. Various attempts were made to get single crystals of **P4** and **P5**. The X-ray quality single crystals of these peptides were obtained from the solution of aqueous methanol and their X-ray structures are shown in Figure 6.

In a sharp contrast to the unusual planar structure displayed by the 1:1 alternating α- and *E*-vinylogous residues reported earlier,[16c] peptides **P4** and **P5** adopted right handed 12-helical conformations similar to the α,γ-hybrid peptides containing saturated γ^4-amino acids. The 12-helical structures are stabilized by six intramolecular H-bonds between the residues *i* and *i+3*. The torsional angles of **P4** and **P5** are tabulated in Tables 9 and 11, respectively. The H-bond parameters of **P4** and **P5** are tabulated in the Tables 10 and 12, respectively. Analysis of the crystal structure of **P4** reveals that the torsional angles θ_1 and ψ in all three Z-vinylogous residues in the helix attained the average values 99± 3° and -79±7°, respectively. Similarly, **P5** with different *Z*-vinylogous residues also showed the 12-helical structure. Both θ_1 and ψ in **P5** attained the values 103±2° and -75±1°, respectively. The torsion angle ϕ attained the anticlinal conformation similar to the saturated γ^4-residues in 12-helix.[22] The 12-helix structure in both the

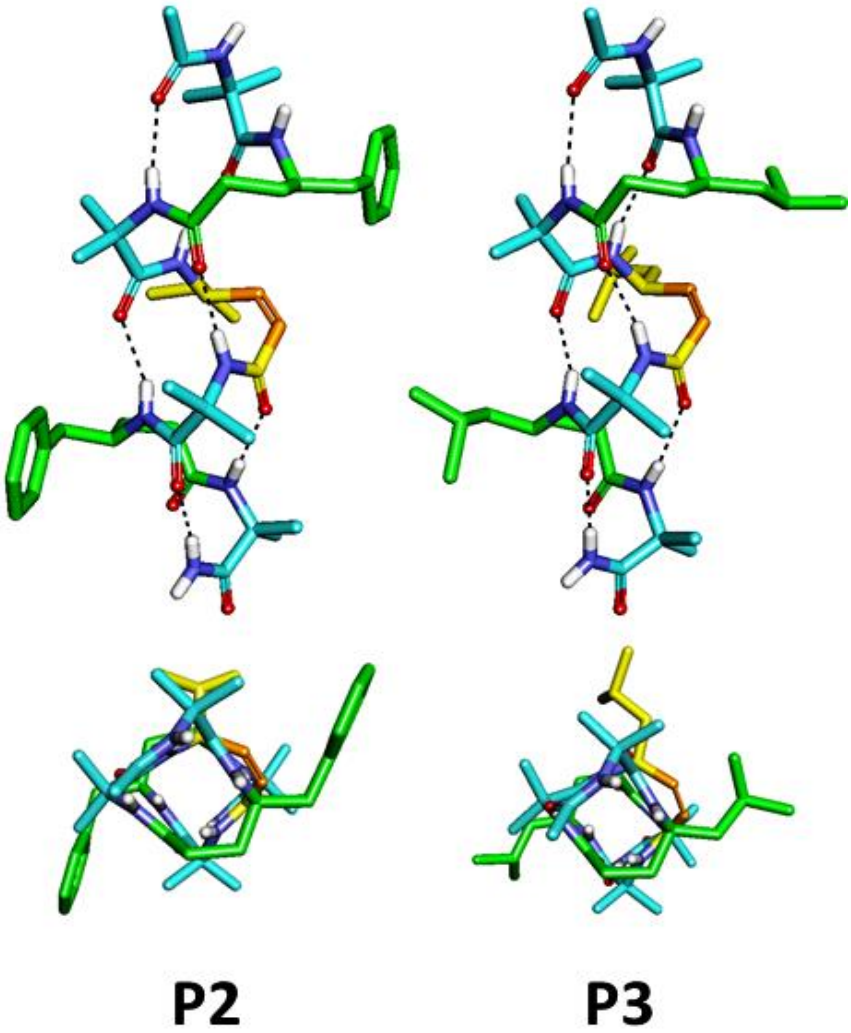

Fig 5: X-ray structures of peptide **P2** and **P3**

peptides is stabilized by six intermolecular H-bonds. The additional interesting feature in all Z-vinylogous helices (**P1**-**P5**) is that the structures are also stabilized by a weak C-H---π interactions between γ-H of *i* and conjugated double bonds of *i+2* residues (Figure 7). The distances of the C-H---π interactions are within the limits of the standard C-H---π interactions (Table 1).[23]

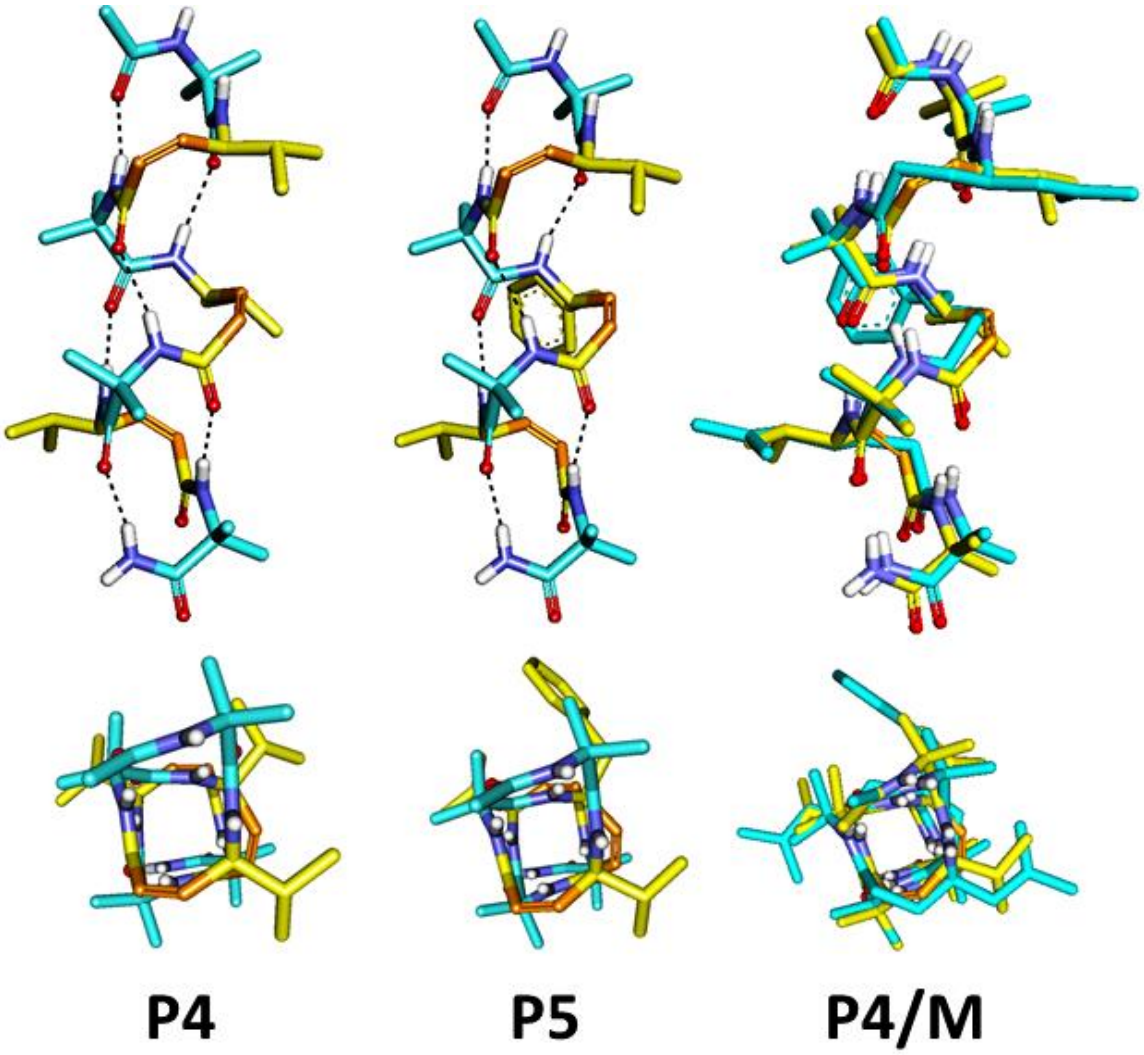

(A) (B)

Fig 6: (A) X-ray structure of Peptide **P4** and **P5**, (B) Overlay of Peptides **P4** and **M** (double bond highlighted in orange color).

Examination of the all crystal structures revealed that the Aib residues adopted right handed helical conformations by having average ϕ and ψ value -56±6° and -44±6°, respectively. Overall, these results suggests that *Z*-vinylogous residues can be accommodated into the 12-helix without deviating overall folding of the helix.

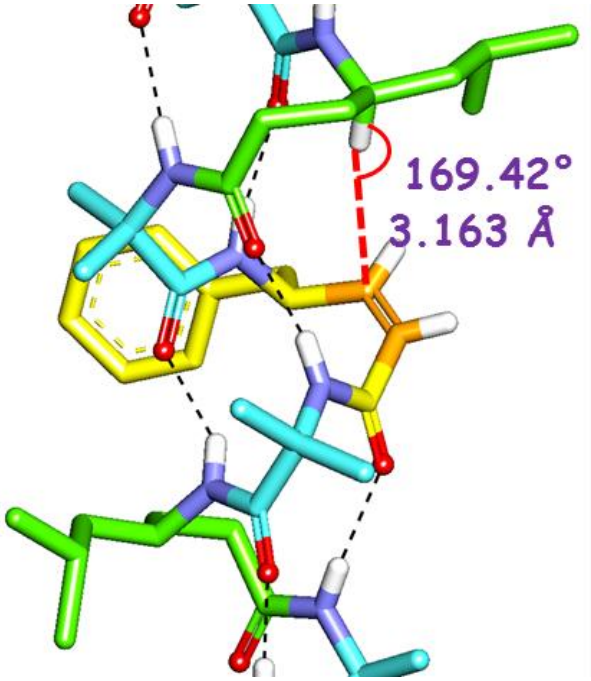

Fig 7: X-ray structures of Peptide **P1** where CH---π interaction shown in red dotted lines.

Table 1: CH-π interaction parameters of peptides **P1**-**P5**.

Peptide	**Donor (D)**	**Acceptor (A)**	**D….A (Å)**	**DH….A (Å)**	**NH….O (deg)**
P1	C7	C27	4.13	3.16	169
P2	C53	C72	3.88	2.91	168
P3	C7	C24	3.78	2.85	159
P5	C7	C22	4.17	3.24	158
	C18	C33	4.09	3.16	158
P6	C7	C23	4.14	3.26	151
	C18	C34	4.01	3.07	161

Table 2: Comparison of torsional angles between *Z*-dγX and γX residues

α, γ – hybrid 12-Helix	ϕ	θ_1	θ_2	ψ	***Ref.***
Balaram and Our lab (Chiral γ^4 - amino acid)	-125	52	61	-118	5c, 25
Balaram's lab (Achiral γ^4 - amino acid)	-132	53.6	59.9	-112	5b
Hoffmann's prediction (γ^4 - amino acid)	123	-53	-63	126	14
Gellman lab $\gamma^{2,3,4}$ - amino acid	143	-56	-52	111	7a
Gellman $\gamma^{2,3}$ - amino acid	-129	56	56	-121	7c
Our Lab (*S, S*) – (β-hydroxyl γ-amino acid)	-114	53 (173)	60 (168)	-122	25c
Our Lab (*R, S*) –(β-hydroxyl γ-amino acid)	-115	54	63 (-170)	-140	25c
Our Lab (*S, S*) – (β-nitromethyl γ-amino acid)	-112	61	63	-174	20
Present Work: Z-vinylogous - γ^4 - amino acid	**-119^0**	**101^0**	**0^0**	**78^0**	-

Table 3: Torsional Angle Parameters of **P1**

α, γ - hybrids	ϕ	θ_1	θ_2	ψ	ω
Aib 1	-61	-	-	-39	-176
γLeu 2	-122	49	63	-123	-173
Aib 3	-53	-	-	-40	-178
z-γPhe 4	-122	95	-2	-79	-167
Aib 5	-59	-	-	-38	-167
γLeu 6	-141	54	56	-108	-180
Aib 7	-56	-	-	-51	-

Table 4: Hydrogen Bond Parameters of **P1**

Intramolecular H-bonds

Donor (D)	**Acceptor (A)**	**D….A (Å)**	**DH….A (Å)**	**NH….O (deg)**
N3	O1	2.90	2.04	177
N4	O2	2.82	2.00	158
N5	O3	2.87	2.03	165
N6	O4	2.83	2.06	149
N7	O5	3.00	2.15	173
N8	O6	2.80	1.95	171

Intermolecular H-bonds

Donor (D)	**Acceptor (A)**	**D….A (Å)**	**DH….A (Å)**	**NH….O (deg)**
N1	O7†	2.87	2.03	164
N2	O8†	2.83	2.06	149
N1‡	O7	2.87	2.03	164
N2‡	O8	2.83	2.06	149

Symmetry operations: † x, y, -1+z; ‡ x, y, 1+z

Table 5: Torsional Angle Parameters of **P2**

α, γ - hybrids	ϕ	θ_1	θ_2	ψ	ω
Aib 1	-60	-	-	-45	-
γPhe 2	-	50	66	-	-
Aib 3	-53	-	-	-39	173
z-γVal 4	-	106	-0	-74	-
Aib 5	-61	-	-	-43	-
γPhe 6	-	53	63	-	-
Aib 7	-59	-	-	-44	-

Table 6: Hydrogen Bond Parameters of **P2**

Intramolecular H-bonds

Donor (D)	**Acceptor (A)**	**D….A (Å)**	**DH….A (Å)**	**NH….O (deg)**
N3	O1	2.89	2.03	178
N4	O2	2.82	2.00	159
N5	O3	3.03	2.20	162
N6	O4	2.89	2.14	146
N7	O5	2.97	2.11	173
N8	O6	2.79	1.96	160

Intermolecular H-bonds

Donor (D)	**Acceptor (A)**	**D….A (Å)**	**DH….A (Å)**	**NH….O (deg)**
N1	O7†	2.88	2.03	171
N2	O8†	2.99	2.17	159
N1‡	O7	2.88	2.03	171
N2‡	O8	2.99	2.17	159
O3	O23	2.67	-	-
N5	O22	2.40	2.23	90.5
O6	O19	3.00	-	-
O3	O22	2.85	-	-

Symmetry operations: † 1+x, y, z; ‡ -1+x, y, z

Table 7: Torsional Angle Parameters of P3

α,γ - hybrids	ϕ	θ_1	θ_2	ψ	ω
Aib 1	-62	-	-	-41	-178
γLeu 2	-	51	65	-	-177
Aib 3	-50	-	-	-49	180
z-γLeu 4	-	98	-4	-83	-167
Aib 5	-61	-	-	-38	-175
γLeu 6	-	52	58	-	-177
Aib 7	-51	-	-	-51	-

Table 8: Hydrogen Bond Parameters of **P3**

Intramolecular H-bonds

Donor (D)	**Acceptor (A)**	**D….A (Å)**	**DH….A (Å)**	**NH….O (deg)**
N3	O1	3.07	2.23	165
N4	O2	2.85	2.00	168
N5	O3	2.85	2.00	167
N6	O4	2.87	2.07	154
N7	O5	3.02	2.17	170
N8	O6	2.86	2.00	174

Intermolecular H-bonds

Donor (D)	**Acceptor (A)**	**D….A (Å)**	**DH….A (Å)**	**NH….O (deg)**
N1	O7†	2.83	1.98	167
N2	O8†	2.93	2.13	154
N1‡	O7	2.83	1.98	167
N2‡	O8	2.93	2.13	154
O1	O9	2.84	2.04	163
O9	O10†	2.74	-	-

Symmetry operations: † -1+x, y, z; ‡ 1+x, y, z

Table 9: Torsional Angle Parameters of **P4**

α,γ-hybrids	ϕ	θ_1	θ_2	ψ	ω
Aib 1	-53	-	-	-43	177
z-γVal 2	-	95	4	-73	-
Aib 3	-54	-	-	-47	174
z-γVal 4	-	101	3	-86	-
Aib 5	-57	-	-	-43	175
z-γVal 6	-	102	2	-77	-
Aib 7	-57	-	-	-52	-

Table 10: Hydrogen Bond Parameters of **P4**

Intramolecular H-bonds

Donor (D)	**Acceptor (A)**	**D….A (Å)**	**DH….A (Å)**	**NH….O (deg)**
N3	O1	2.83	1.99	165
N4	O2	2.97	2.11	173
N5	O3	2.88	2.04	169
N6	O4	2.85	2.03	157
N7	O5	2.95	2.10	171
N8	O6	2.81	1.97	166

Intermolecular H-bonds

Donor (D)	**Acceptor (A)**	**D….A (Å)**	**DH….A (Å)**	**NH….O (deg)**
N1	O7[†]	2.87	2.02	165
N2	O8[†]	2.90	2.11	152
N1[‡]	O7	2.87	2.02	165
N2[‡]	O8	2.90	2.11	152

Table 11: Torsional Angle Parameters of **P5**

α, γ - hybrids	ϕ	θ_1	θ_2	ψ	ω
Aib 1	-56	-	-	-41	172
z-γVal 2	-123	104	-0	-77	-171
Aib 3	-51	-	-	-53	176
z-γPhe 4	-116	102	-2	-74	-175
Aib 5	-51	-	-	-47	172
z-γVal 6	-114	105	1	-74	-173
Aib 7	-61	-	-	-50	-

Table 12: Hydrogen Bond Parameters of **P5**

Intramolecular H-bonds

Donor (D)	**Acceptor (A)**	**D….A (Å)**	**DH….A (Å)**	**NH….O (deg)**
N3	O1	2.97	2.12	168
N4	O2	2.90	2.06	167
N5	O3	2.93	2.09	166
N6	O4	2.86	2.03	164
N7	O5	3.06	2.22	165
N8	O6	2.84	2.00	168

Intermolecular H-bonds

Donor (D)	Acceptor (A)	D….A (Å)	DH….A (Å)	NH….O (deg)
N1	O7†	2.95	2.10	168
N2	O8†	2.89	2.09	153
N1‡	O7	2.95	2.10	168
N2‡	O8	2.89	2.09	153

Symmetry operations: † -1+x, y, -1+z; ‡ 1+x, y, 1+z

3.4 Comparison of α, γ-Hybrid Helices containing (*E*)-α, β-Unsaturated γ-Amino acids and (*Z*)-α, β-Unsaturated γ-Amino acids

Careful analysis of the local conformations of *Z*-vinylogous residues in the helices as well as in the monomer single crystals revealed very interesting features of conjugated double bonds. In general, conjugation favors the planar structure of α, β-unsaturated carbonyl group. The α, β-unsaturated carbonyl group in the monomer attained the planar structure with local *s-cis* conformation. The choice for the *s-trans* or *s-cis* over the other depends on the steric interactions of substituents in the conjugated system. The structural analysis of various *E*-vinylogous residues and peptides revealed that amides and peptides preferred *s-cis* conformations while ethyl and methyl esters preferred *s-trans* conformation to avoid 1, 3-allyic strain and maintained the planarity along the α,β-unsaturated carbonyl group.[16] In a sharp contrast, the *cis* double bonds in the hybrid helices **P1-P5** deviated away from the planarity with the carbonyl groups inferring that they are not in conjugation. They adopted neither *s-trans* nor *s*-cis conformations. The local torsion angle (C^{β}-C^{α}-C-O = 105°) reveals that the C=C double bonds are almost perpendicular to the carbonyl group suggesting no π-conjugation (Figure 8), which is unusual property of α, β-unsaturated carbonyl group. The deviation from planarity of *Z*-vinylogous residues in the helix may be dictated by the strength of the intramolecular H-bonds existed in helical structure.

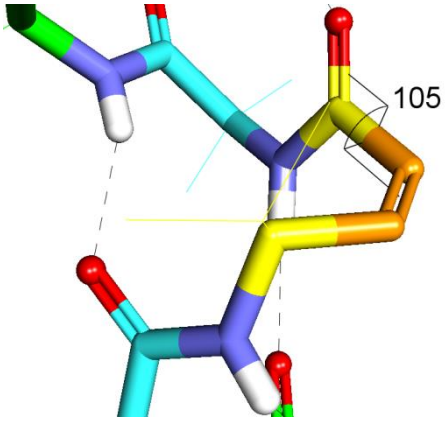

Fig 8: X-ray structure of peptide **P2** depicting no π-conjugation between C=C and C=O (C^{β}-C^{α}-C-O = 105°).

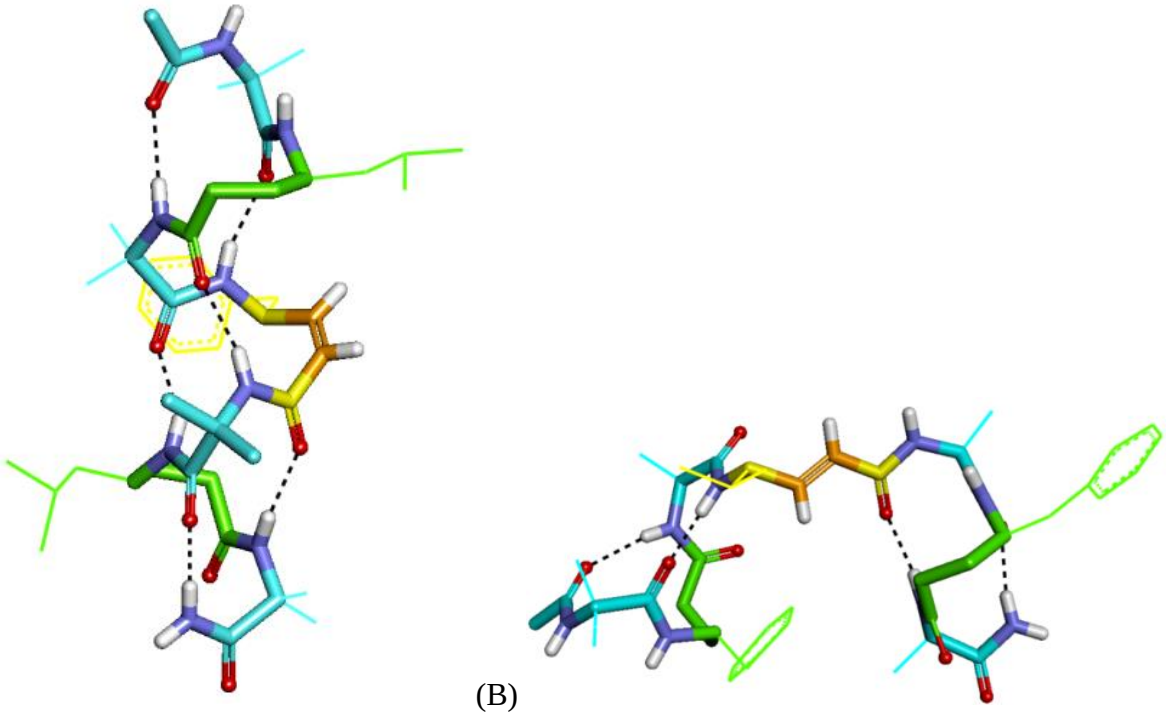

Fig 9: (A) X-ray structure of Peptide Ac-Aib-γLeu-Aib-ZdγPhe-Aib-γLeu-Aib-NH_2 (**P1**) and (B) X-ray structure of Peptide Ac-Aib-γPhe-Ala-EdγVal-Aib-γPhe-Aib-NH_2 (**P5** from Chapter 1).

The remarkable results obtained from this Chapter and from the Chapter1 provided an excellent opportunity to compare the conformational properties of *Z*- and *E*-vinylogous amino acids and their utility in the design of hybrid peptides. Results suggested that *Z*-vinylogous amino acids

can be readily accommodated into the helix, while selective insertion of *E*-vinylogous amino acids into helix leads to bending of the helix into two halves (helix-loop-helix type, Figure 9). Even in the highly strained bend structures, double bond and carbonyl group were retained their π-conjugation by adopting local *s-cis* conformation. In contrast, the Z-vinylogous amino acids lost their π-conjugation while accommodating into the helix. The double bonds and the carbonyl groups of Z-vinylogous residues adopted neither *s-cis* nor *s-trans* conformation in the helix. Overall, these results suggested that it is easy to break π-conjugation in the *Z*-α, β-unsaturated carbonyl groups compared to the *E*-α, β-unsaturated carbonyl compounds. The conformational properties of these amino acids may also influence their chemical reactivity; however, they are yet to be investigated.

3.5 Conclusions

In conclusion, we presented the synthesis and utilization of *Z*-vinylogous amino acids in the design of hybrid peptide foldamers. Results suggested that Z-vinylogous residues can be readily accommodated into the 12-helix, without any deviation from the overall folding of the helix. It has been proved in various examples that the saturated γ-residues preferred gauche conformation along C^{γ}-C^{β}(θ_1) and C^{β}-C^{α}(θ_2) bonds and anticlinal conformations along N-C^{γ}(ϕ) and C^{α}-C'(ψ) bonds. In contrast, Z-vinylogous residues adopted entirely different torsional values for θ_1, θ_2 and ψ, however, still participated in 12-helix. These results suggested the structural plasticity of 12-helical structures. In comparison with *E*-vinylogous residues, Z-vinylogous residues are more flexible and easy to accommodate into the helix with loss of π-conjugation between the double bond and the carbonyl group. In addition, any acyclic α, β-unsaturated carbonyl systems preferred to adopt either *s-cis* or *s-trans* conformation, however, the conformations displayed by the *Z*-vinylogous residues are quite unusual. We are speculating that these conformational factors may also influence their chemical reactivity towards electrophiles and nucleophiles.

3.6 Experimental Section

General Experimental Details:

All amino acids, diphenylphosphite, TFA, *tert*-butylbromoacetate, DBU, NaI, HBTU, HOBt, LAH, NMP and Knorr-Amide resin were commercially available. DCM, DMF, ethyl acetate and petether (60-80 °C) have used after distillation. THF was dried over sodium and distilled immediately prior to use. Column chromatography was performed on silica gel (120-200 mesh). Final peptides were purified on reverse phase HPLC (C_{18} column, MeOH/H_2O 60:40-95:5 as gradient with flow rate 3.00 mL/min). ^{1}H spectra were recorded on 500 MHz (or ^{13}C on 125 MHz) and 400 MHz (or ^{13}C on 100 MHz) using residual solvents as internal standards ($CDCl_3$ δ_H 7.26 ppm, δ_C 77.3 ppm and CD_3OD δ_H 3.31 ppm, δ_C 49.0 ppm). Chemical shifts (δ) reported in *ppm* and coupling constants (J) in Hz.

Crystallographic Information of Peptides:

Crystal structure analysis of Ac-U-γL-U-zdγF-U-γL-U-NH$_2$ (P1): Crystals of peptide were grown by slow evaporation from a solution of aqueous methanol. A single crystal (0.24 × 0.09 × 0.12 mm) was mounted on loop with a small amount of the paraffin oil. The X-ray data were collected at 100K temperature on a Bruker APEX (II) DUO CCD diffractometer using Mo K_α radiation (λ = 0.71073 Å), ω-scans (2θ = 57.62), for a total of 16653 independent reflections. Space group P21, a = 14.987(13), b = 10.674(9), c = 16.027(14), β = 101.600(13), V = 2512 (4) Å^3, Monoclinic C, Z = 2 for chemical formula $C_{45}H_{74}N_8O_8$, with one molecule in asymmetric unit; ρ calcd = 1.131 gcm^{-3}, μ = 0.078 mm^{-1}, F (000) = 928, R_{int}= 0.1635. The structure was obtained by direct methods using SHELXS-97.The final R value was 0.0861 (wR2 = 0.1237) 6558 observed reflections ($F_0 \geq 4\sigma$ ($|F_0|$)) and 558 variables, S = 1.225. The largest difference peak and hole were 0.339 and -0.361 eÅ^3, respectively.

Crystal structure analysis of Ac-U-γF-U-zdγV-U-γF-U-NH$_2$ (P2): Crystals of peptide were grown by slow evaporation from a solution of aqueous methanol. A single crystal (0.4 × 0.1 × 0.18 mm) was mounted on loop with a small amount of the paraffin oil. The X-ray data were collected at 100K temperature on a Bruker APEX (II) DUO CCD diffractometer using Mo K_α radiation (λ = 0.71073 Å), ω-scans (2θ = 56.58), for a total of 94183 independent reflections. Space group P21, a = 16.284(5), b = 18.044(6), c = 17.846(6), β = 91.586(8), V = 5241 (3) Å^3,

Monoclinic C, Z = 4 for chemical formula $C_{47}H_{70}N_8O_8$, 3(O), with three water molecules in asymmetric unit; ρ calcd = 1.17 gcm^{-3}, μ = 0.084 mm^{-1}, F (000) = 2310, R_{int}= 0.1892. The structure was obtained by intrinsic methods using SHELXS-97.The final R value was 0.1009 (wR2 = 0.2163) 25705 observed reflections ($F_0 \geq 4\sigma$ ($|F_0|$)) and 1211 variables, S = 1.015. The largest difference peak and hole were 1.179 and -0.506 $eÅ^3$, respectively.

Crystal structure analysis of Ac-U-γF-U-zdγL-U-γF-U-NH_2 (P3): Crystals of peptide were grown by slow evaporation from a solution of aqueous methanol. A single crystal (0.4 × 0.1 × 0.18 mm) was mounted on loop with a small amount of the paraffin oil. The X-ray data were collected at 100K temperature on a Bruker APEX(II) DUO CCD diffractometer using Mo K_α radiation (λ = 0.71073 Å), ω-scans (2θ = 57.60), for a total of 44241 independent reflections. Space group P21, a = 16.086(16), b = 8.774(9), c = 18.544(19), β = 90.076(16), V = 2613 (5) $Å^3$, Monoclinic C, Z = 2 for chemical formula $C_{42}H_{76}N_8O_8$, 2(CH_4O)), with two methanol molecules in asymmetric unit; ρ calcd = 1.125 gcm^{-3}, μ = 0.08 mm^{-1}, F(000) = 968, R_{int}= 0.4105. The structure was obtained by intrinsic methods using SHELXS-97.The final R value was 0.1447 (wR2 = 0.2790) 12101 observed reflections ($F_0 \geq 4\sigma$($|F_0|$)) and 578 variables, S = 1.14. The largest difference peak and hole were 0.645 and -0.697 $eÅ^3$, respectively.

Crystal structure analysis of Ac-U-zdγV-U-zdγV-U-zdγV-U-NH_2 (P4): Crystals of peptide were grown by slow evaporation from a solution of aqueous methanol. A single crystal (0.21 × 0.09 × 0.04 mm) was mounted on loop with a small amount of the paraffin oil. The X-ray data were collected at 100K temperature on a Bruker APEX (II) DUO CCD diffractometer using Mo K_α radiation (λ = 0.71073 Å), ω-scans (2θ = 50.00), for a total of 52207 independent reflections. Space group P21, a = 16.282(11), b = 16.024(11), c = 18.094(12), β = 111.192(12), V = 4402 (2) $Å^3$, Monoclinic C, Z = 4 for chemical formula $C_{39}H_{66}N_8O_8$, with one molecule in asymmetric unit; ρ calcd = 1.194 gcm^{-3}, μ = 0.084 mm^{-1}, F (000) = 1720, R_{int}= 0.3242. The structure was obtained by intrinsic methods using SHELXS-97.The final R value was 0.1046 (wR2 = 0.2002) 13991 observed reflections ($F_0 \geq 4\sigma$ ($|F_0|$)) and 1021 variables, S = 0.968. The largest difference peak and hole were 0.327 and -0.384 $eÅ^3$, respectively.

Crystal structure analysis of Ac-U-zdγV-U-zdγF-U-zdγV-U-NH_2 (P5): Crystals of peptide were grown by slow evaporation from a solution of MeOH/EtOAc. A single crystal (0.24 × 0.05 × 0.1 mm) was mounted on loop with a small amount of the paraffin oil. The X-ray data were

collected at 100K temperature on a Bruker APEX (II) DUO CCD diffractometer using Mo K_α radiation (λ = 0.71073 Å), ω-scans (2θ = 57.30), for a total of 30273 independent reflections. Space group P21, a = 10.101(11), b = 18.11(2), c = 14.706(16), β = 99.027(18), V = 2633 (5) $Å^3$, Monoclinic C, Z = 2 for chemical formula $C_{43}H_{66}N_8O_8$, with one molecule in asymmetric unit; ρ calcd = 1.038 gcm^{-3}, μ = 0.072 mm^{-1}, F(000) = 888, R_{int}= 0.2833. The structure was obtained by intrinsic methods using SHELXS-97.The final R value was 0.1324 (wR2 = 0.3013) 12862 observed reflections ($F_0 \geq 4\sigma$ ($|F_0|$)) and 533 variables, S = 0.725. The largest difference peak and hole were 0.327 and -0.384 $eÅ^3$, respectively.

There is some partially occupied solvent molecule also present in the asymmetric unit. A significant amount of time was invested in identifying and refining the disordered molecule. Option SQUEEZE of program PLATON was used to correct the diffraction data for diffuse scattering effects and to identify the solvent molecule. PLATON calculated the upper limit of volume that can be occupied by the solvent to be 463.3 $Å^3$, or 17.5% of the unit cell volume. The program calculated 194 electrons in the unit cell for the diffuse species. No data are given for the diffusely scattering species. Outputs of SQUEEZE report are appended in cif file P5.

Procedure for synthesis of Ethyl/t-Butyl Diphenylphosphonoacetate:[22]

To a solution of diphenylphosphite (10 mmol) in DCM (10 mL) were added ethyl/t-Butyl bromoacetate (10 mmol) and then triethylamine (14 mmol) at 0 °C. After stirring for 15 min at 0 °C, the mixture was stirred for 1 h at RT. Then reaction was quenched with H_2O and extracted with EtOAc-hexane (3:1) (3× 30 mL). Then, the extract was washed with water (3× 30 mL) followed by brine (2 × 30 mL) and dried over anhydrous Na_2SO_4 and concentrated to pale yellow residue. The crude product was purified by column chromatography to get pure desired product in 65-80% yield.

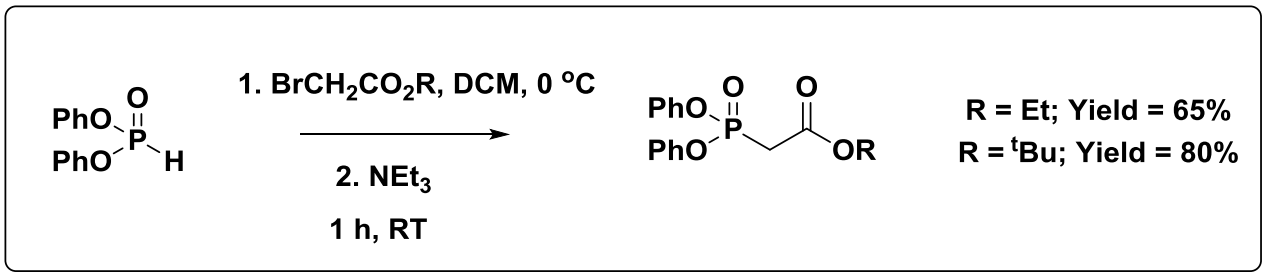

General procedure for synthesis of Ethyl/ tert-butyl ester of Boc-NH-(*Z*)-α, β-Unsaturated γ-amino acids:[22]

A freshly prepared solution of *tert*-butyl 2-(diphenoxyphosphoryl)acetate (**1**) (5 mmol) in THF (40 mL) was treated with NaI (6 mmol) and DBU (5 mmol) at 0 °C for 10 min. After the mixture was cooled to -78 °C, amino aldehyde 2 (5 mmol) was added. After 10 min, the resulting mixture was warmed to 0 °C over 1.5-2 h. The reaction was quenched with saturated NH_4Cl, followed by extraction with EtOAc (3 × 50 mL) and combined organic layer was washed with brine solution (2 × 50 mL). The crude mixture was subjected to silica column chromatography to get desired product in 85-90% yield.

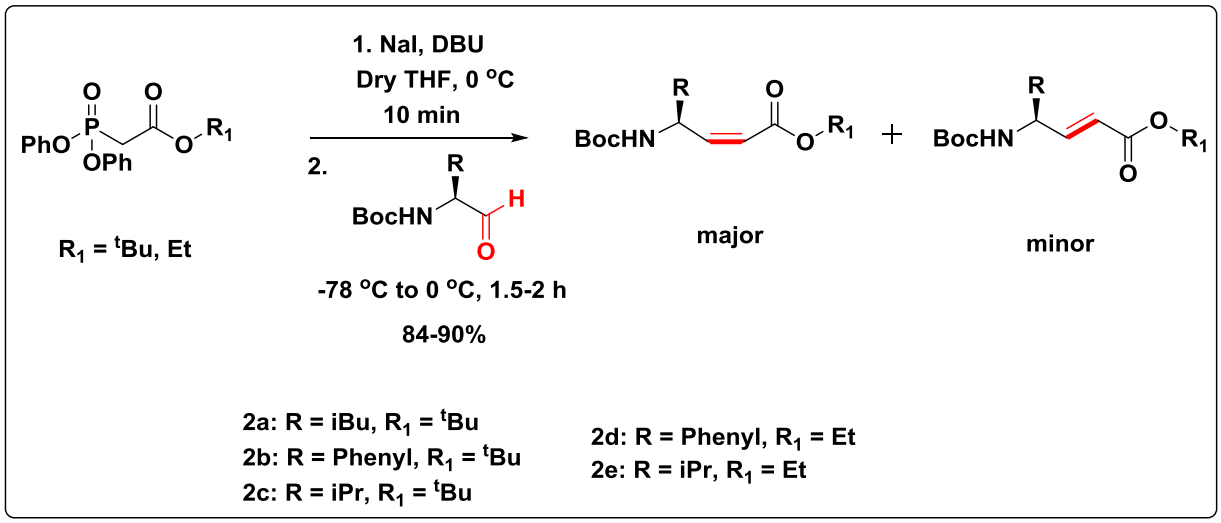

General procedure for the synthesis of Fmoc-(*Z*)-α, β-Unsaturated γ-amino acids: The *tert*-Butyl ester of (*Z*)-α, β-Unsaturated γ-amino acid (3 mmol) was dissolved in 3 mL of DCM and then 5 mL of TFA was added to the reaction mixture at 0 °C. After 1 h, TFA was removed under *vacuum*. Residue was dissolved in 10 mL of water and adjusted pH to ~8 by addition of solid Na_2CO_3. The solution of Fmoc-OSu (2.7 mmol) in 10 mL of THF was added slowly to the reaction mixture and stirred overnight at RT. After completion of the reaction, the reaction mixture was acidified with 1N HCl under cold condition and extracted with ethyl acetate (3× 50 mL). The combined organic layer was washed with brine solution, dried over anhydrous Na_2SO_4 and concentrated under reduced pressure to give white solid product of Fmoc-(Z)-α, β-Unsaturated γ-amino acids in 72-80% yields. They were directly used for solid phase peptide synthesis without further purification.

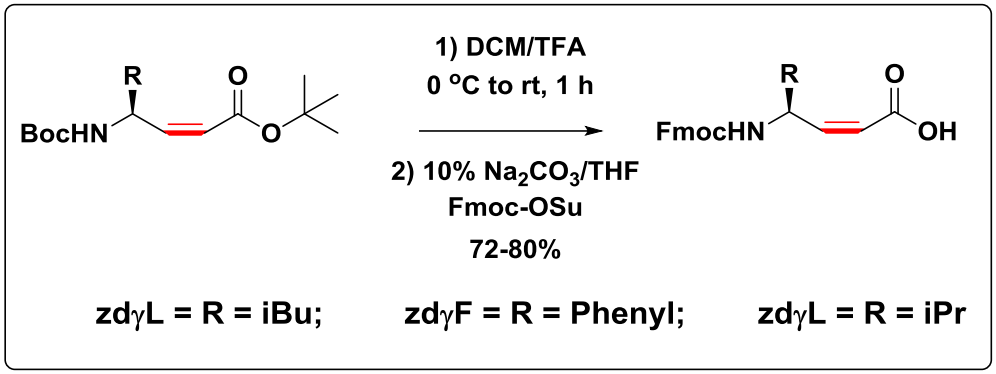

(S,Z)-tert-butyl 4-((tert-butoxycarbonyl)amino)-5-phenylpent-2-enoate: White solid (88%; *dr* 94.5:6.5); The *dr* determined by ^{1}H NMR; ^{1}H NMR (400 MHz, $CDCl_3$) δ 7.32-7.21 (m, 5H), 6.81 (minor *E*-isomer, dd, *J* = 16 Hz, *J* = 5 Hz), 5.79 (minor *E*-isomer, dd, *J* = 16 Hz, *J* = 4 Hz), 6.05 (bs, 1H), 5.73 (d, *J* = 12 Hz, 1H), 5.31 (m, 1H), 4.80 (s, 1H), 2.98-2.88 (m, 2H), 1.49 (s, 9H), 1.38 (s, 9H); ^{13}C NMR (100 MHz, $CDCl_3$) δ 165.3, 155.4, 148.3, 137.5, 129.7, 128.5, 126.7, 121.9, 80.8, 50.3, 40.6, 28.5, 28.3; HR-MS *m/z* calculated value for $C_{20}H_{29}NO_4$ is 347.2097 and observed 347.2081.

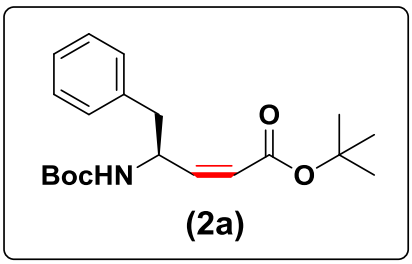

(*S,Z)-tert-butyl 4-((tert-butoxycarbonyl)amino)-5-methylhex-2-enoate (**2b**)*: White solid (90%,*dr* 91:9); The *dr* determined by ^{1}H NMR;^{1}H NMR (400 MHz, $CDCl_3$) δ6.73 (minor *E*-isomer, dd, *J* = 16 Hz, *J* = 4 Hz), 5.96 (bs, 1H), 5.74 (d, J = 12 Hz, 1H), 5.82 (minor *E*-isomer, dd, *J* = 16 Hz, *J* = 4 Hz), 4.89 (bs, 2H), 1.94 (m, 1H), 1.49 (s, 9H), 1.42 (s, 9H), 0.92 (m, 6H); ^{13}C NMR (100 MHz, $CDCl_3$) δ 165.3, 155.4, 146.8, 122.4, 80.7, 79.1, 53.8, 32.6, 28.4, 28.2, 19.1, 17.9; HR-MS *m/z* calculated value for $C_{16}H_{29}NO_4$ is 299.2097 and observed 299.2062.

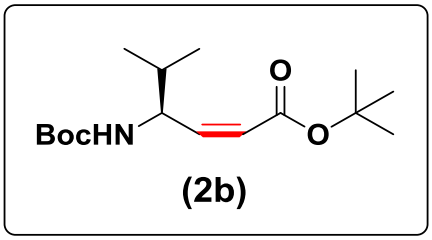

(S,Z)-tert-butyl 4-((tert-butoxycarbonyl)amino)-6-methylhept-2-enoate ***(2c)***: White solid (84%,*dr* 90:10); The *dr* determined by ^{1}H NMR; ^{1}H NMR (400 MHz, $CDCl_3$) δ 6.66 (minor *E*-isomer, dd, *J* = 16 Hz, *J* = 5 Hz), 5.96 (br, 1H),5.77 (minor *E*-isomer, dd, *J* = 16 Hz, *J* = 4 Hz), 5.64 (d, *J* = 8 Hz, 1H), 5.04 (br, 1H), 4.84 (br, 1H), 1.63 (m, 1H), 1.46 (s, 9H), 1.40 (s, 9H), 1.35 (m, 2H), 0.94 (d, *J* = 4 Hz, 3H), 0.91 (d, *J* = 4 Hz, 3H); ^{13}C NMR (100 MHz, $CDCl_3$) δ 165.4, 155.3, 148.5, 121.7, 80.7, 79.2, 47.5, 43.7, 28.5, 28.3, 24.9, 23.3, 22.2; HR-MS *m/z* calculated value for $C_{17}H_{31}NO_4$ is 313.2253 and observed 313.2277.

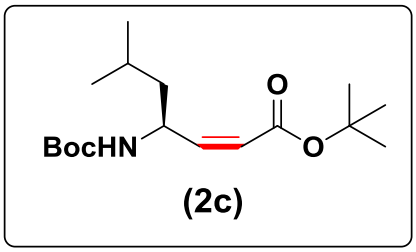

ethyl (S,Z)-4-((tert-butoxycarbonyl)amino)-5-phenylpent-2-enoate ***(2d)***: White solid (83%, *dr* 90:10);^{1}H NMR (400 MHz, $CDCl_3$) δ 7.27 (m, 5H), 6.20 (bs, 1H), 5.83 (d, *J* = 12 Hz, 1H), 5.34 (m, 1H), 4.77 (bs, 1H), 4.19 (q, *J* = 8 Hz, 2H), 2.97 (m, 2H), 1.37 (s, 9H), 1.30 (t, *J* = 8 Hz, 3H); ^{13}C NMR (100 MHz, $CDCl_3$) δ 165.9, 155.4, 150.3, 129.7, 128.6, 126.8, 120.0, 60.4, 50.7, 40.3, 28.4, 14.4; HR-MS *m/z* calculated value for $C_{18}H_{25}NO_4$ is 319.1784 and observed 319.1791.

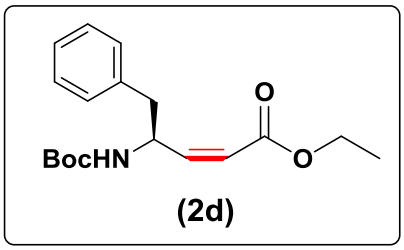

ethyl(S,Z)-4-((tert-butoxycarbonyl)amino)-5-methylhex-2-enoate ***(2e)***: White solid (88%, *dr* 85:15);^{1}H NMR (400 MHz, $CDCl_3$) δ 6.06 (bd, *J* = 8 Hz, 1H), 5.83 (d, *J* = 12 Hz, 1H), 4.95 (m,

1H), 4.87 (s, 1H), 4.18 (q, J = 8 Hz, 2H), 1.96 (m, 1H), 1.42 (s, 9H), 1.29 (t, J = 8 Hz, 3H), 0.93 (m, 6H); ^{13}C NMR (100 MHz, $CDCl_3$) δ 166.0, 155.6, 149.2, 120.7, 79.4, 60.4, 54.0, 32.7, 28.5, 19.3, 18.1, 14.4; HR-MS *m/z* calculated value for $C_{14}H_{25}NO_4$ is 271.1784 and observed 271.1790.

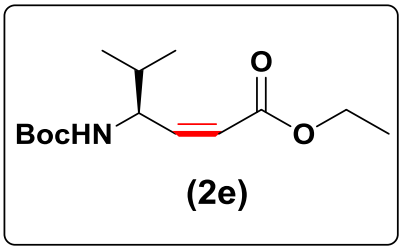

General procedure for sold phase synthesis of peptides P1-P5:

Peptides were synthesized at 0.2 mmol scales on Knorr-Amide resin using standard Fmoc-chemistry. HBTU/HOBt was used as coupling agents. Reaction times for deprotections and couplings were 30 min and 1 h, respectively. The final amine was capped with acetyl group using Ac_2O/Py. After completion of the synthesis, peptides were cleaved from resin using 15 mL of TFA. After the completion of cleavage, the resin was filtered and washed with 3 mL TFA. The cleavage mixture was evaporated under reduced pressure to give gummy product. Peptides were further recrystallized using cold diethyl ether and purified through reverse phase HPLC on C_{18} column using MeOH/H_2O gradient. Homogeneity of peptides was further confirmed using analytical C_{18} column in same MeOH/H_2O gradient system. The mass of peptides were confirmed by MALDI TOF/TOF.

Characterization data of peptides:

Peptide P1:

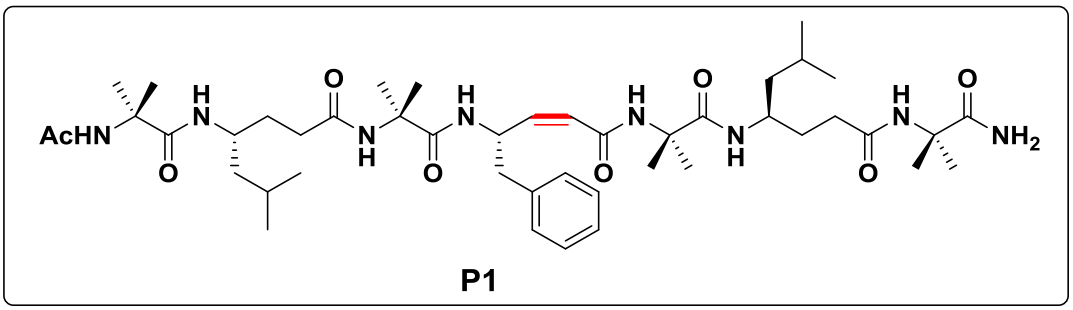

^{1}H NMR (500 MHz, Methanol-d_3) δ 8.36 (s, 1H), 8.29 (d, 2H), 8.23 (s, 1H), 7.96 (s, 1H), 7.91 (d, J = 10 Hz, 1H), 7.76 (s, 1H), 7.44-7.12 (m, 6H), 6.99 (s, 1H), 5.98 (dd, J = 10 Hz, J = 10 Hz, 1H), 5.87 (d, J = 10 Hz, 1H), 3.94 (m, 2H), 2.96 (m, 2H), 2.41 (m, 2H), 2.01 (m, 7H), 1.66 (m, 1H), 1.53-1.45 (m, 21H), 1.30 (s, 3H), 1.26 (m, 1H), 1.17 (m, 1H), 1.06 (s, 3H), 0.94 (m, 5H), 0.86 (m, 7H); HR-MS *m/z* calculated value for $C_{45}H_{74}N_8O_8$ [M+H$^+$] is 855.5708 and observed 855.5720.

Peptide P2:

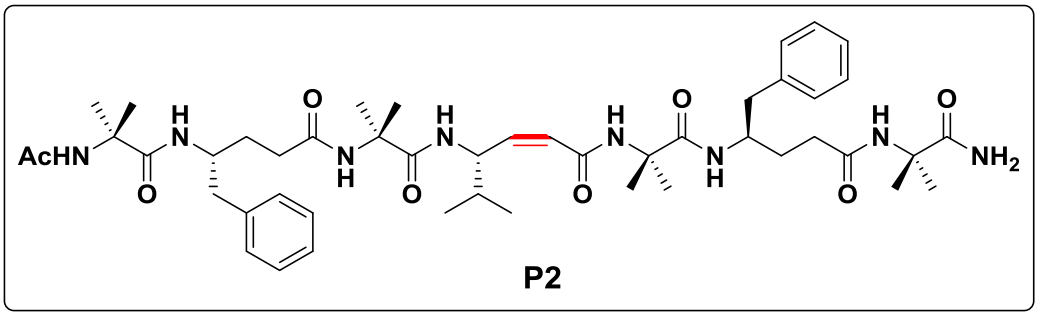

^{1}H NMR (400 MHz, Methanol-d_3) δ 8.40 (d, J = 8 Hz, 1H), 8.29 (d, J = 8 Hz, 1H), 8.25 (s, 2H), 7.96 (s, 1H), 7.88 (s, 1H), 7.53 (d, J = 8 Hz, 1H), 7.27-7.12 (m, 10H), 6.75 (s, 1H), 5.85 (d, J = 12 Hz, 5.69 (t, J = 12 Hz, 1H), 4.64 (bs, 1H), 4.11 (m, 1H), 2.78 (m, 3H), 2.39 (m, 2H), 2.10 (m, 3H), 1.99 (s, 3H), 1.79-1.54 (m, 2H), 1.49 (s, 3H), 1.45 (bs, 6H), 1.43 (s, 3H), 1.35 (s, 3H), 1.34 (s, 3H), 1.26 (s, 3H), 1.10 (s, 3H), 0.91 (d, J = 8 Hz, 3H), 0.85 (d, J = 3H); HR-MS *m/z* calculated value for $C_{47}H_{70}N_8O_8$ [M+H$^+$] is 875.5400 and observed 875.5411.

Peptide P3:

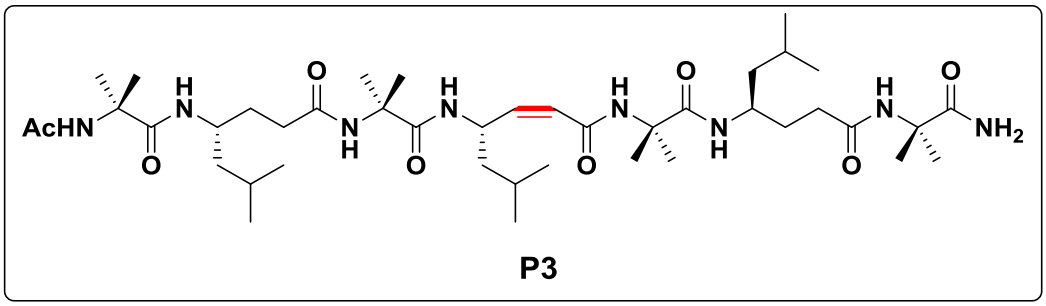

^{1}H NMR (400 MHz, Methanol-d_3) δ 8.34 (s, 1H), 8.30 (d, J = 8 Hz, 1H), 8.28 (d, J = 8 Hz, 1H), 8.24 (s, 1H), 7.94 (s, 1H), 7.85 (d, J = 8 Hz, 1H), 7.80 (s, 1H), 7.37 (d, J = 8 Hz, 1H), 6.71 (s,

1H), 5.80 (m, 2H), 3.93 (m, 2H), 2.44 (m, 2H), 2.03 (s, 1H), 1.98 (s, 3H), 1.93 (m, 3H), 1.73 (m, 2H), 1.59 (m, 3H), 1.58 (s, 3H), 1.47-1.44 (m, 18H), 1.41 (s, 3H), 1.37 (s, 1H), 1.24 (m, 3H), 0.90 (m, 24H); HR-MS *m/z* calculated value for $C_{42}H_{76}N_8O_8$ [M+H$^+$] is 821.5824 and observed 821.5825.

Peptide P4:

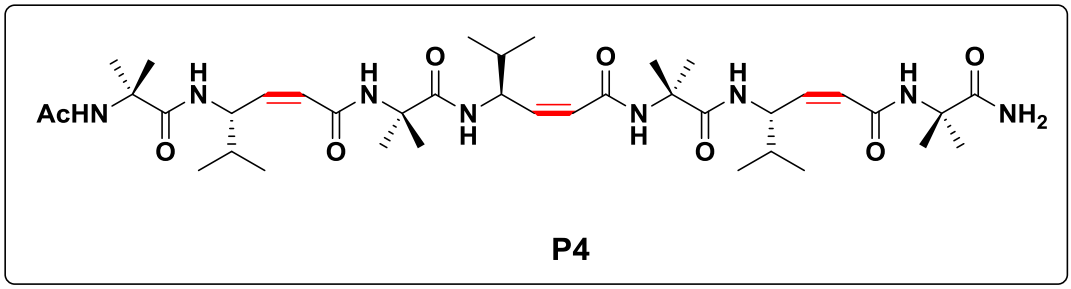

^{1}H NMR (400 MHz, DMSO-d_6) δ 8.14 (s, 1H), 8.03 (s, 1H), 7.97 (s, 1H), 7.90 (s, 1H), 7.80 (s, 1H), 7.79 (d,J = 8 Hz, 2H), 7.58 (d, J = 8 Hz, 1H), 7.19 (s, 1H), 6.78 (s, 1H), 5.84 (m, 3H), 5.71 (m, 3H), 4.95 (m, 1H), 4.68 (m, 2H), 1.82 (s, 3H), 1.77 (m, 3H), 1.39-1.23 (m, 24H), 0.95-0.78 (m, 18H); HR-MS *m/z* calculated value for $C_{39}H_{66}N_8O_8$ [M+H$^+$] is 775.5082 and observed 775.5092.

Peptide P5:

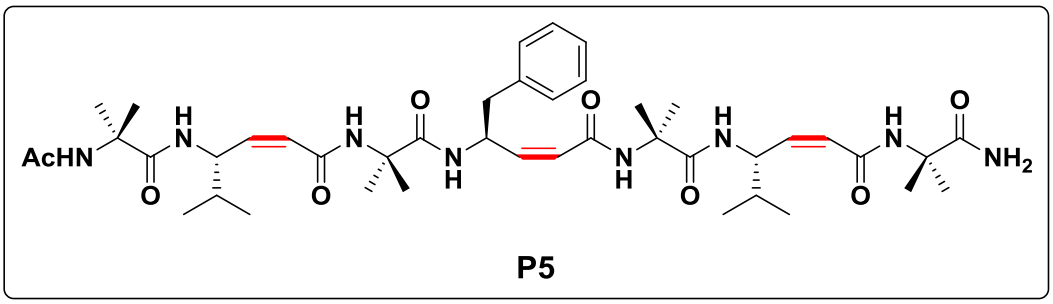

^{1}H NMR (500 MHz, Methanol-d_3) δ 8.44 (s, 1H), 8.35 (d, J = 10 Hz, 1H), 8.27 (bs, 2H), 8.16 (bs, 2H), 7.81 (s, 1H), 7.71 (d, J = 10 Hz, 1H), 7.31 (d, J = 10 Hz, 2H), 7.20 (m, 3H), 2.94 (m, 1H), 1.94 (m, 3H), 1.75 (m, 2H), 1.54 (s, 2H), 1.52 (s, 3H), 1.46 (m, 16H), 1.36 (s, 3H), 1.28 (s, 3H), 1.24 (s, 3H), 0.96-0.83 (m, 16H); HR-MS *m/z* calculated value for $C_{43}H_{66}N_8O_8$ [M+H$^+$] is 823.5082 and observed 823.5083.

3.7 References

1. (a) Gellman, S. H. *Acc. Chem. Res*. **1998**, *31*, 173. (b) Hill, D. J.; Mio, M. J.; Prince, R. B.; Hughes, T. S.; Moore, J. S. *Chem. Rev*. **2001**, *101*, 3893. (c) Cheng, R. P.; Gellman, S. H.; DeGrado, W. F. *Chem. Rev*. **2001**, *101*, 3219. (d) Venkatraman, J.; Shankaramma, S. C.; Balaram, P. *Chem. Rev*. **2001**, *101*, 3131. (e) Seebach, D.; Beck, A. K.; Bierbaum, D. J. *Chem. Biodiversity* **2004**, 1, 1111. (f) Goodman, C. M.; Choi, S.; Shandler, S.; DeGrado, W. F. *Nat. Chem. Biol*. **2007**, *3*, 252. (g) Hecht, S.; Huc, I. *Foldamers: Structure, Properties and Applications*; Wiley-VCH: Weinheim, **2007**. (h) Seebach, D.; Gardiner, J. *Acc. Chem. Res*. **2008**, *41*, 1366. (i) Horne, W. S.; Gellman, S. H. *Acc. Chem. Res*. **2008**, *41*, 1399. (j) Cummings, C. G.; Hamilton, A. D. *Curr. Opin. Chem. Biol*. **2010**, *14*, 341. (k) Vasudev, P. G.; Chatterjee, S.; Shamala, N.; Balaram, P. *Chem. Rev*. **2011**, *111*, 657. (l) Pilsl, L. K. A.; Reiser, O. *Amino Acids* **2011**, *41*, 709. (m) Martinek, T. A.; Fülöp, F. *Chem. Soc. Rev*. **2012**, *41*, 687.
2. (a) Seebach, D.; Abele, S.; Gademann, K.; Jaun, B. *Angew. Chem., Int. Ed*. **1999**, *38*, 1595. (b) Seebach, D.; Schreiber, V. J.; Abele, S.; Daura, X.; Gunsteren, F. W. *Helv. Chim. Acta* **2000**, *83*, 34. (c) Hetenyi, A.; Mandity, I. M.; Martinek, T. A.; Toth, G. K.; Fulop, F. *J. Am. Chem. Soc*. **2005**, *127*, 547. (d) Appella, D. H.; Christianson, L. A.; Klein, D. A.; Powell, D. R.; Huang, X. L.; Barchi, J. J.; Gellman, S. H. *Nature* **1997**, *387*, 381. (e) Rua, F.; Boussert, S.; Parella, T.; Diez-Perez, I.; Branchadell, V.; Giralt, E.; Ortuno, R. M. *Org. Lett*. **2007**, *9*, 3643. (f) Mandity, I. M.; Weber, E.; Martinek, T. A.; Olajos, G.; Toth, G. K.; Vass, E.; Fulop, F. *Angew. Chem., Int. Ed*. **2009**, *48*, 2171. (g) Petersson, E. J.; Schepartz, A. *J. Am. Chem. Soc*. **2008**, *130*, 821. (h) Giuliano, M. W.; Horne, W. S.; Gellman, S. H. *J. Am. Chem. Soc*. **2009**, *131*, 9860. (i) Choi, S. H.; Guzei, I. A.; Spencer, L. C.; Gellman, S. H. *J. Am. Chem. Soc*. **2010**, *132*, 13879. (j) Price, J. L.; Horne, W. S.; Gellman, S. H. *J. Am. Chem. Soc*. **2010**, *132*, 12378. (k) Legrand, B.; Andre, C.; Moulat, L.; Wenger, E.; Didierjean, C.; Aubert, E.; Averlant-Petit, M. C.; Martinez, J.; Calmes, M.; Amblard, M. *Angew. Chem., Int. Ed*. **2014**, *53*, 13131.(l) Sharma, G. V.; Yadav, T. A.; Marumudi, K.; Thodupunuri, P.; Reddy, P. P.; Kunwar, A. C. *Chem.-Asian J*. **2014**, *9*, 3153.
3. (a) Hintermann, T.; Gademann, K.; Jaun, B.; Seebach, D. *Helv. Chim. Acta* **1998**, *81*, 893. (b) Hanessian, S.; Luo, X.; Schaum, R.; Michnick, S. *J. Am. Chem. Soc*. **1998**, *120*, 8569.

4. (a) Vasudev, P. G.; Shamala, N.; Ananda, K.; Balaram, P. *Angew. Chem., Int. Ed*. **2005**, *44*, 4972. (b) Chatterjee, S.; Vasudev, P. G.; Raghothama, S.; Ramakrishnan, C.; Shamala, N.; Balaram, P. *J. Am. Chem. Soc*. **2009**, *131*, 5956. (c) Basuroy, K.; Dinesh, B.; Shamala, N.; Balaram, P. *Angew. Chem., Int. Ed*. **2012**, *51*, 8736. (d) Basuroy, K.; Dinesh, B.; Reddy, M. B. M.; Chandrappa, S.; Raghothama, S.; Shamala, N.; Balaram, P. *Org. Lett*. **2013**, *15*, 4866. (e) Basuroy, K.; Dinesh, B.; Shamala, N.; Balaram, P. *Angew. Chem., Int. Ed*. **2013**, *52*, 3136. (f) Reddy, M. B. M.; Basuroy, B.; Chandrappa, S.; Dinesh, B.; Basavalingappa, V.; Venkatesha, M. A.; Balaram, P. *New. J. Chem*. **2015**, *39*, 3319.
5. Jones, C. R.; Qureshi, M. K. N.; Truscott, F. R.; Hsu, S. T. D.; Morrison, A. J.; Smith, M. D. *Angew. Chem., Int. Ed*. **2008**, *47*, 7099.
6. (a) Guo, L.; Chi, Y. G.; Almeida, A. M.; Guzei, I. A.; Parker, B. K.; Gellman, S. H. *J. Am. Chem. Soc*. **2009**, *131*, 16018. (b) Guo, L.; Almeida, A. M.; Zhang, W.; Reidenbach, A. G.; Choi, S. H.; Guzei, I. A.; Gellman, S. H. *J. Am. Chem. Soc*. **2010**, *132*, 7868. (c) Guo, L.; Zhang, W.; Guzei, I. A.; Spencer, L. C.; Gellman, S. H. *Org. Lett*. **2012**, *14*, 2582. (d) Fisher, B. F.; Guo, L.; Dolinar, B. S.; Guzei, I. A.; Gellman, S. H. *J. Am. Chem. Soc*. **2015**, *137*, 6484. (e) Liu, R.; Chen, X.; Falk, S. P.; Mowery, B. P.; Karlsson, A. J.; Weisblum, B.; Palecek, S. P.; Masters, K. S.; Gellman, S. H. *J. Am. Chem. Soc*. **2014**, *136*, 4333.
7. Sharma, G V. M.; Chandramouli, N.; Choudhary, M.; Nagendar, P.; Ramakrishna, K. V. S.; Kunwar, A. C.; Schramm, P.; Hofmann, H. –J. *J. Am. Chem. Soc*. **2009**, *131*, 17335.
8. (a) Pendem, N.; Nelli, Y. R.; Douat, C.; Fischer, L.; Laguerre, M.; Ennifar, E.; Kauffmann, B.; Guichard, G. *Angew. Chem., Int. Ed*. **2013**, *52*, 4147. (b) Fremaux, J.; Dolain, C.; Kauffmann, B.; Clayden, J.; Guichard, G. *Chem. Commun*. **2013**, *49*, 7415.
9. (a) Guo, L.; Almeida, A. M.; Zhang, W.; Reidenbach, A. G.; Choi, S. H.; Guzei, I. A.; Gellman, S. H. *J. Am. Chem. Soc*. **2010**, *132*, 7868. (b) Sawada, T.; Gellman, S. H. *J. Am. Chem. Soc*. **2011**, *133*, 7336. (c) Shin, Y. –H.; Mortenson, D. E.; Satyshur, K. A.; Forest, K. T.; Gellman, S. H. *J. Am. Chem. Soc*. **2013**, *135*, 8149. (d) Sharma, G. V. M.; Thodupunuri, P.; Sirisha, K.; Basha, S. J.; Gurava Reddy, P.; Sarma, A. V. S. *J. Org. Chem*. **2014**, *79*, 8614.
10. Candela, T.; Fouet, A. *Mol. Microbiol*. **2006**, *60*, 1091.
11. Rydon, H. N. *J. Chem. Soc.*, **1964**, 1328.
12. Hagihara, M.; Schreiber, S. L. *J. Am. Chem. Soc*. **1992**, *114*, 6570.

13. (a) Baldauf, C.; Gunther, R.; Hofmann, H. –J. *Helv. Chim. Acta* **2003**, *86*, 2573. (b) Baldauf, C.; Gunther, R.; Hofmann, H. –J. *J. Org. Chem*. **2005**, *70*, 5351.
14. Mathieu, L.; Legrand, B.; Deng, C.; Vezenkov, L.; Wenger, E.; Didierjean, C.; Amblard, M.; Averlant-Petit, M. –C.; Masurier, N.; Lisowski, V.; Martinez, J.; Maillard, L. T. *Angew. Chem., Int. Ed*. **2013**, *52*, 6006.
15. (a) Grison, C.; Coutrot, P.; Ge´neve, S.; Didierjean, C.; Marraud, M. *J. Org. Chem*. **2005**, *70*, 10753. (b) Grison, C.; Ge´neve, S.; Halbin, E.; Coutrot, P. *Tetrahedron* **2001**, *57*, 4903. (c) Krishna, Y.; Sharma, S.; Ravi, A. S.; Koley, D. *Org. Lett*. **2014**, *16*, 2084.
16. (a) Mali, S. M.; Bandyopadhyay, A.; Jadhav, S. V.; Ganesh Kumar, M.; Gopi, H. N. *Org. Biomol. Chem.* **2011**, *9*, 6566. (b) Bandyopadhyay, A.; Mali, S. M.; Lunawat, P.; Raja, K. M. P.; Gopi, H. N. *Org. Lett*. **2011**, *13*, 4482. (c) Bandyopadhyay, A.; Gopi, H. N. *Org. Lett*. **2012**, *14*, 2770. (d) Ganesh Kumar, M.; Benke, S. N.; Raja, K. M. P.; Gopi, H. N. *Chem. Comm*. **2015**, *51*, 13397.
17. Ganesh Kumar, M.; Mali, S. M.; Raja, K. M. P.; Gopi, H. N. *Org. Lett*. **2015**, *17*, 230.
18. Ganesh Kumar, M.; Gopi, H. N. *Org. Lett*. **2015**, *17*, 4738.
19. Jadhav, S. V.; Misra, R.; Gopi, H. N. *Chem. - Eur. J*. **2014**, *20*, 16523.
20. Ando, K. *et al*. *J. Org. Chem*. **2000**, *65*, 4745.
21. Jadhav, S. V.; Misra, R.; Singh, S. K.; Gopi, H. N. *Chem. Eur. J*. **2013**, *19*, 16256.
22. Plevin, M. J.; Bryce, D. L.; Boisbouvier, J. *Nat. Chem*. **2010**, *2*, 466.
23. (a) Bandyopadhyay, A.; Gopi, H. N. *Org. Lett*. **2012**, *14*, 2770. (b) Jadhav, S. V.; Bandyopadhyay, A.; Gopi, H. N. *Org. Biomol. Chem*. **2013**, *11*, 509. (c) Bandyopadhyay, A.; Malik, A.; Ganesh Kumar, M.; Gopi, H. N. *Org. Lett*. **2014**, *16*, 294.
24. Plevin, M. J.; Bryce, D. L.; Boisbouvier, J. *Nat. Chem*. **2010**, *2*, 466.

3.8 Appendix I: Characterization Data of Synthesized Compounds

Designation	Description	Page
Boc-Z-dγPhe-O^{t}Bu (**2a**)	^{1}H NMR (400 MHz)	171
Boc-Z-dγVal-O^{t}Bu (**2b**)	^{1}H NMR (400 MHz)	171
Boc-Z-dγLeu-O^{t}Bu (**2c**)	^{1}H NMR (400 MHz)	172
Boc-Z-dγPhe-OEt (**2d**)	^{1}H NMR (400 MHz)	172
Boc-Z-dγVal-OEt (**2e**)	^{1}H NMR (400 MHz)	173
Ac-Aib-γLeu-Aib-zdγPhe-Aib-γLeu-Aib-NH_2 (**P1**)	^{1}H NMR (400 MHz)	173
Ac-Aib-γPhe-Aib-zdγVal-Aib-γPhe-Aib-NH_2 (**P2**)	^{1}H NMR (400 MHz)	174
Ac-Aib-γLeu-Aib-zdγLeu-Aib-γLeu-Aib-NH_2 (**P3**)	^{1}H NMR (400 MHz)	175
Ac-Aib-zdγVal-Aib-zdγVal-Aib-zdγVal-Aib-NH_2 (**P4**)	^{1}H NMR (400 MHz)	176
Ac-Aib-zdγVal-Aib-zdγPhe-Aib-zdγVal-Aib-NH_2 (**P5**)	^{1}H NMR (400 MHz)	177

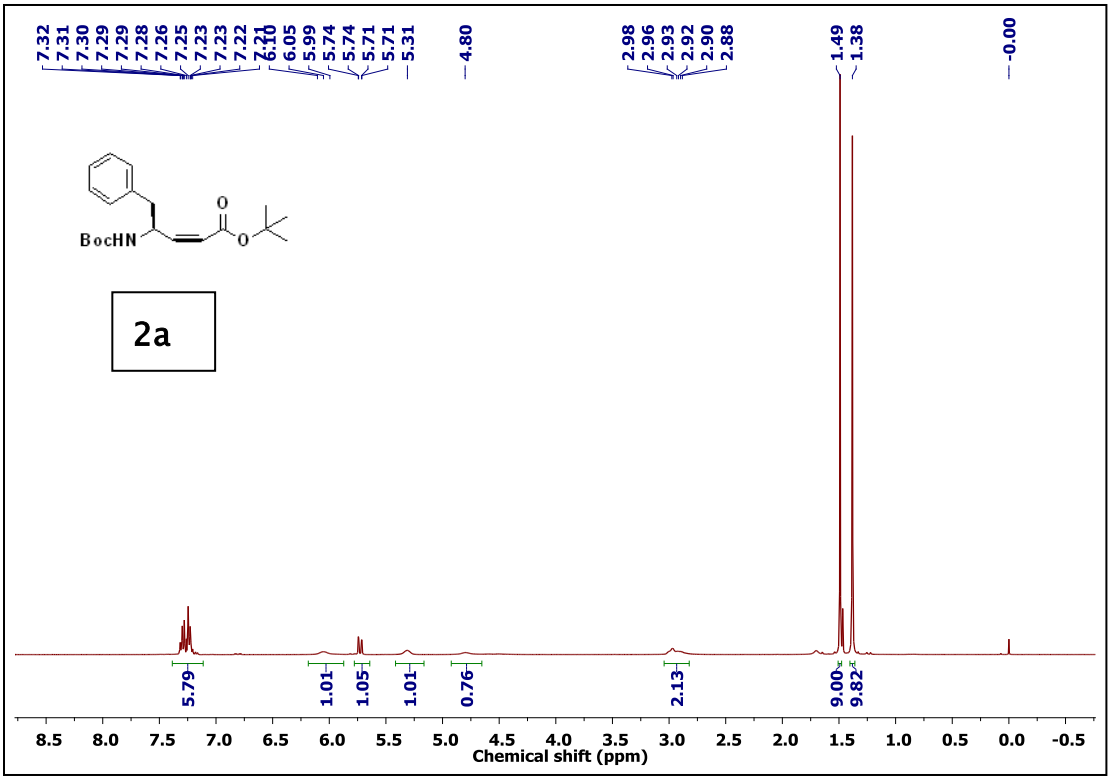
7.32
7.31
7.30
7.29
7.29
7.28
7.26
7.25
7.23
7.23
7.22
6.10
6.05
5.99
5.74
5.74
5.71
5.71
5.31
4.80
2.98
2.96
2.93
2.92
2.90
2.88
1.49
1.38
-0.00
BocHN
O
O
2a
5.79
1.01
1.05
1.01
0.76
2.13
9.00
9.82
8.5 8.0 7.5 7.0 6.5 6.0 5.5 5.0 4.5 4.0 3.5 3.0 2.5 2.0 1.5 1.0 0.5 0.0 -0.5
Chemical shift (ppm)

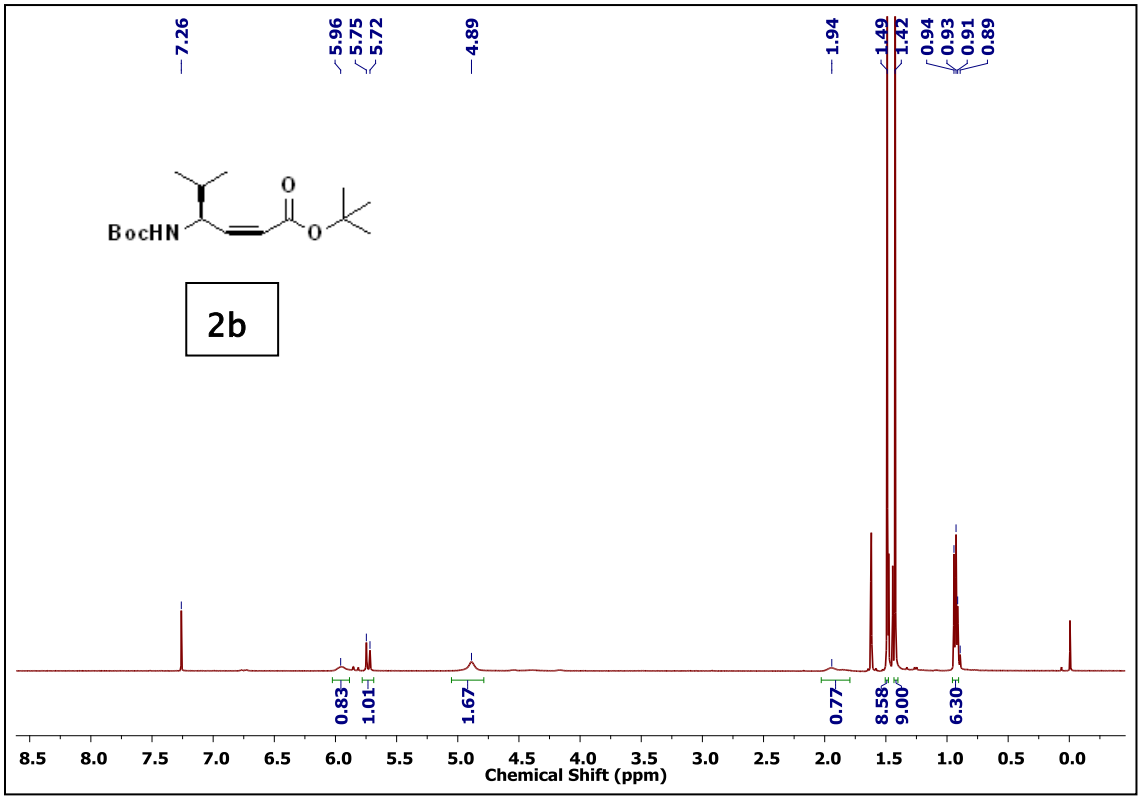
7.26
5.96
5.75
5.72
4.89
1.94
1.49
1.42
0.94
0.93
0.91
0.89
BocHN
O
O
2b
0.83
1.01
1.67
0.77
8.58
9.00
6.30
8.5 8.0 7.5 7.0 6.5 6.0 5.5 5.0 4.5 4.0 3.5 3.0 2.5 2.0 1.5 1.0 0.5 0.0
Chemical Shift (ppm)

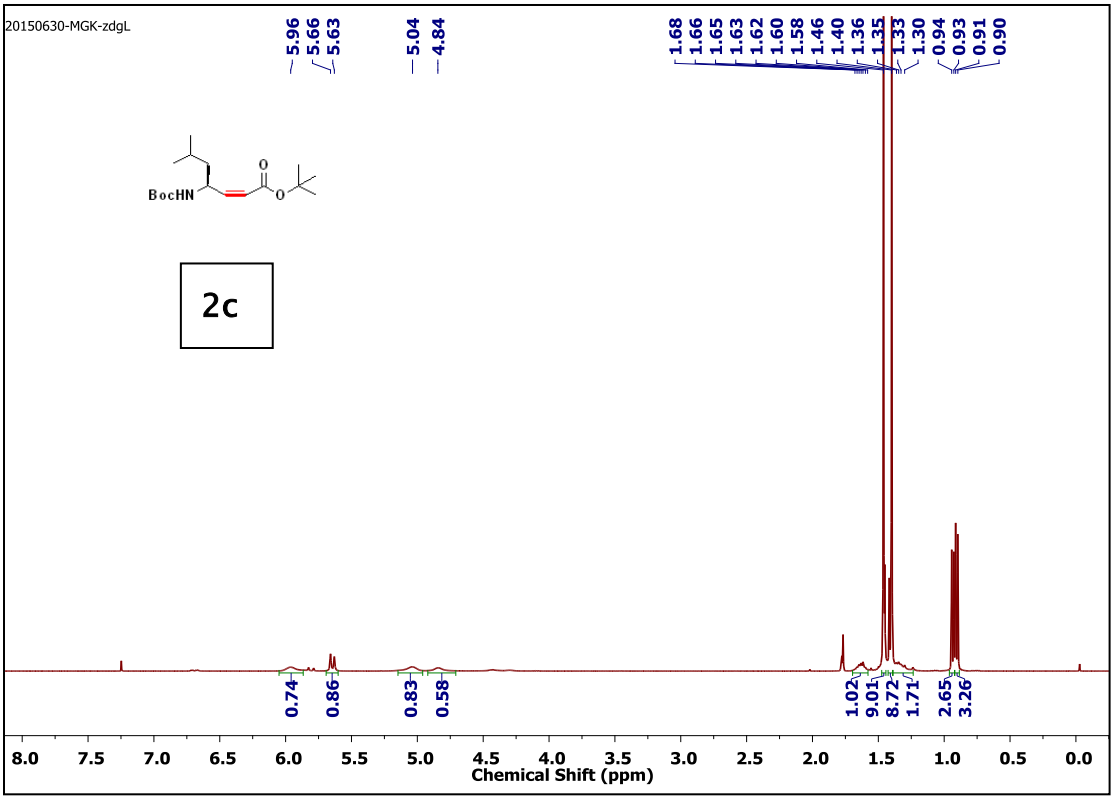
20150630-MGK-zdgL
5.96
5.66
5.63
5.04
4.84
1.68
1.66
1.65
1.63
1.62
1.60
1.58
1.46
1.40
1.36
1.35
1.33
1.30
0.94
0.93
0.91
0.90
BocHN
O
O
2c
0.74
0.86
0.83
0.58
1.02
9.01
8.72
1.71
2.65
3.26
8.0 7.5 7.0 6.5 6.0 5.5 5.0 4.5 4.0 3.5 3.0 2.5 2.0 1.5 1.0 0.5 0.0
Chemical Shift (ppm)

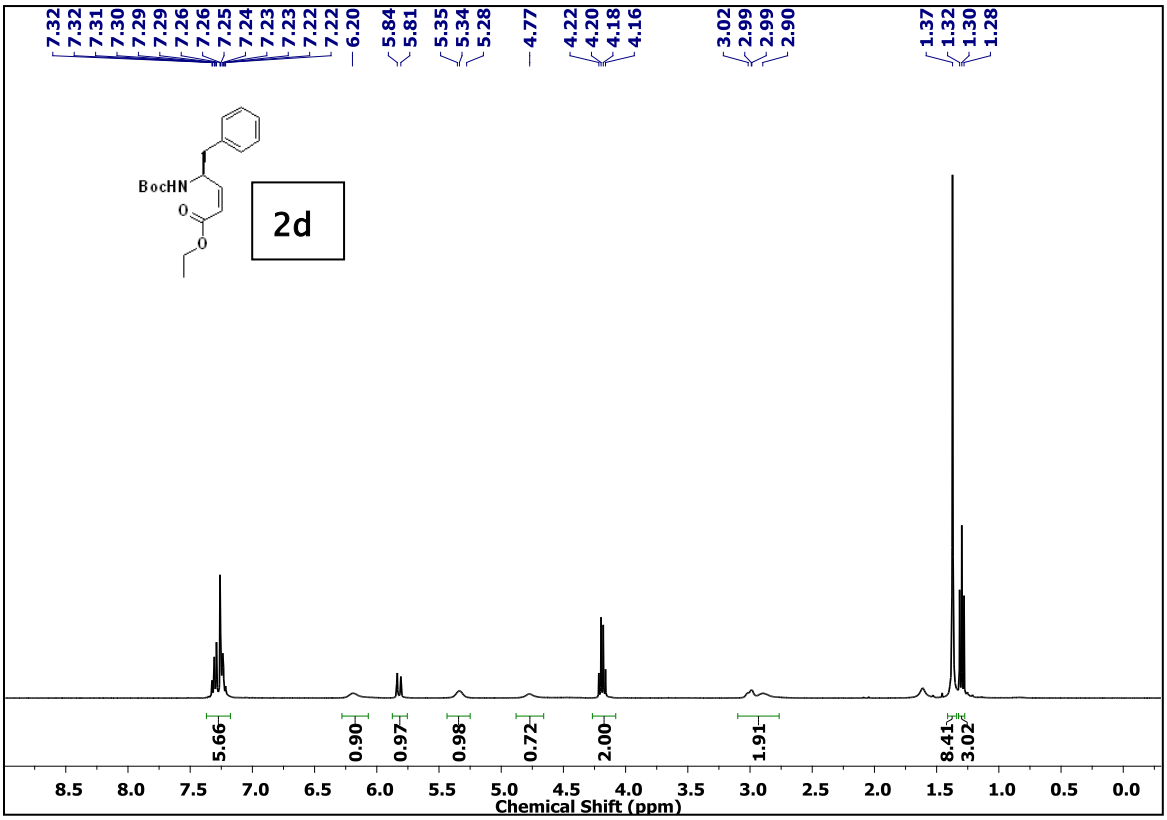
7.32
7.32
7.31
7.30
7.29
7.29
7.26
7.26
7.25
7.24
7.23
7.23
7.22
7.22
6.20
5.84
5.81
5.35
5.34
5.28
4.77
4.22
4.20
4.18
4.16
3.02
2.99
2.99
2.90
1.37
1.32
1.30
1.28
BocHN
O
O
2d
5.66
0.90
0.97
0.98
0.72
2.00
1.91
8.41
3.02
8.5 8.0 7.5 7.0 6.5 6.0 5.5 5.0 4.5 4.0 3.5 3.0 2.5 2.0 1.5 1.0 0.5 0.0
Chemical Shift (ppm)

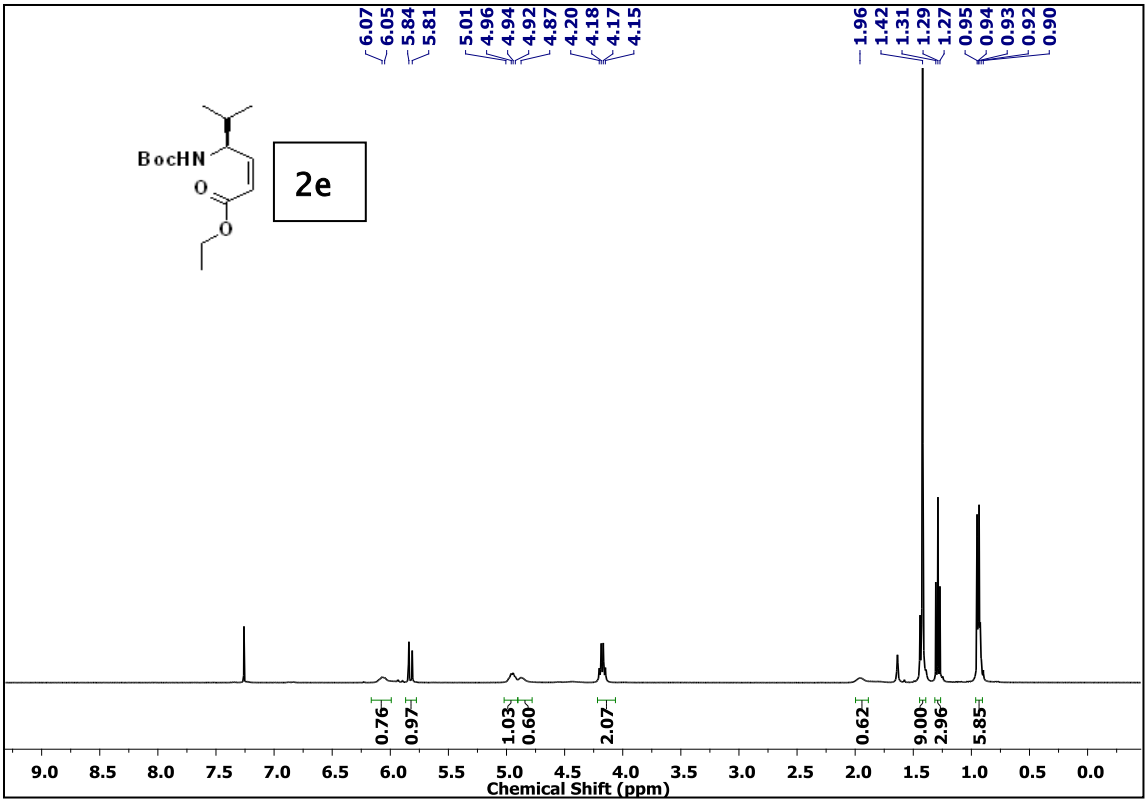
BocHN
O
O
2e
6.07
6.05
5.84
5.81
5.01
4.96
4.94
4.92
4.87
4.20
4.18
4.17
4.15
1.96
1.42
1.31
1.29
1.27
0.95
0.94
0.93
0.92
0.90
0.76
0.97
1.03
0.60
2.07
0.62
9.00
2.96
5.85
9.0 8.5 8.0 7.5 7.0 6.5 6.0 5.5 5.0 4.5 4.0 3.5 3.0 2.5 2.0 1.5 1.0 0.5 0.0
Chemical Shift (ppm)

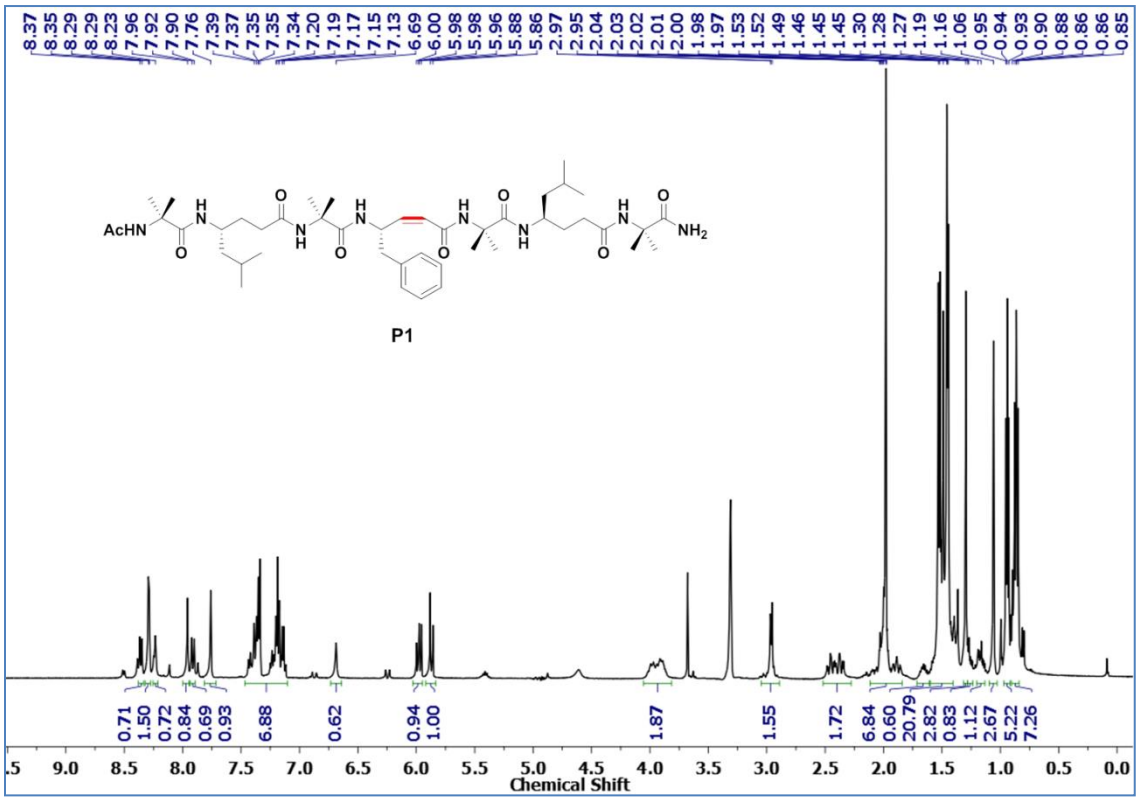
AcHN
NH2
P1
0.71
1.50
0.72
0.84
0.69
0.93
6.88
0.62
0.94
1.00
1.87
1.55
1.72
6.84
0.60
20.79
2.82
0.83
1.12
2.67
5.22
7.26
9.0 8.5 8.0 7.5 7.0 6.5 6.0 5.5 5.0 4.5 4.0 3.5 3.0 2.5 2.0 1.5 1.0 0.5 0.0
Chemical Shift

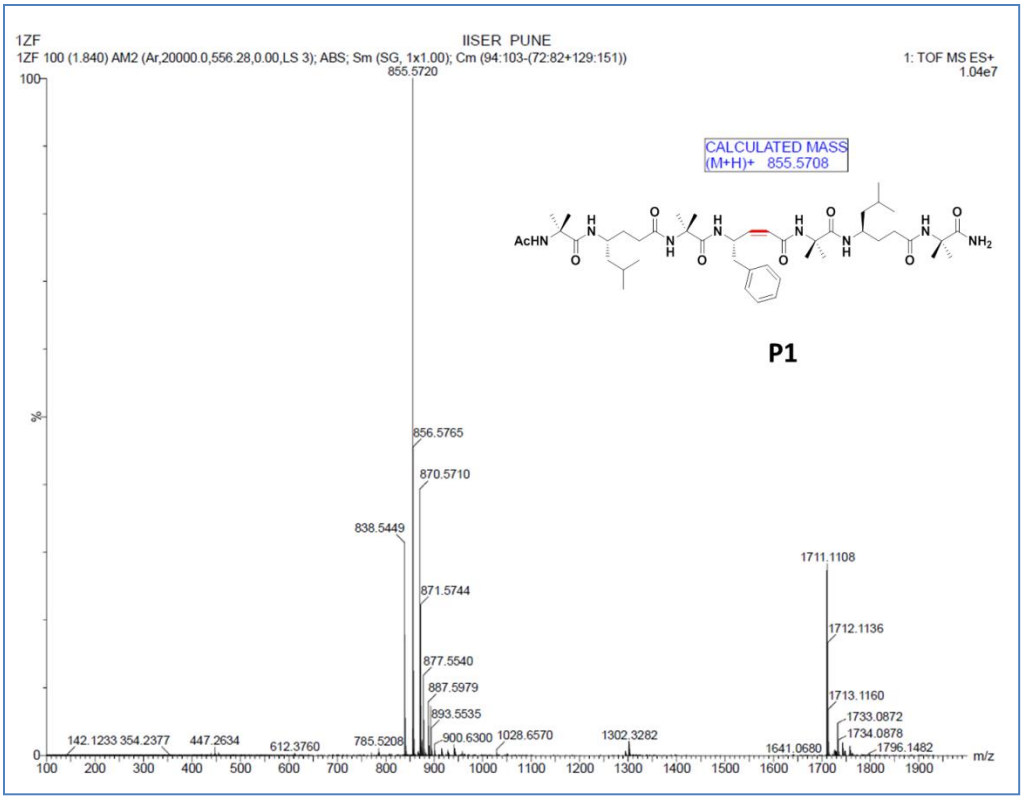
1ZF
IISER PUNE
1ZF 100 (1.840) AM2 (Ar,20000.0,556.28,0.00,LS 3); ABS; Sm (SG, 1x1.00); Cm (94:103-(72:82+129:151))
1: TOF MS ES+
1.04e7
CALCULATED MASS
(M+H)+ 855.5708
P1
855.5720
856.5765
870.5710
838.5449
871.5744
877.5540
887.5979
893.5535
900.6300
1028.6570
1302.3282
1711.1108
1712.1136
1713.1160
1733.0872
1734.0878
1796.1482
1641.0680
142.1233
354.2377
447.2634
612.3760
785.5208
m/z

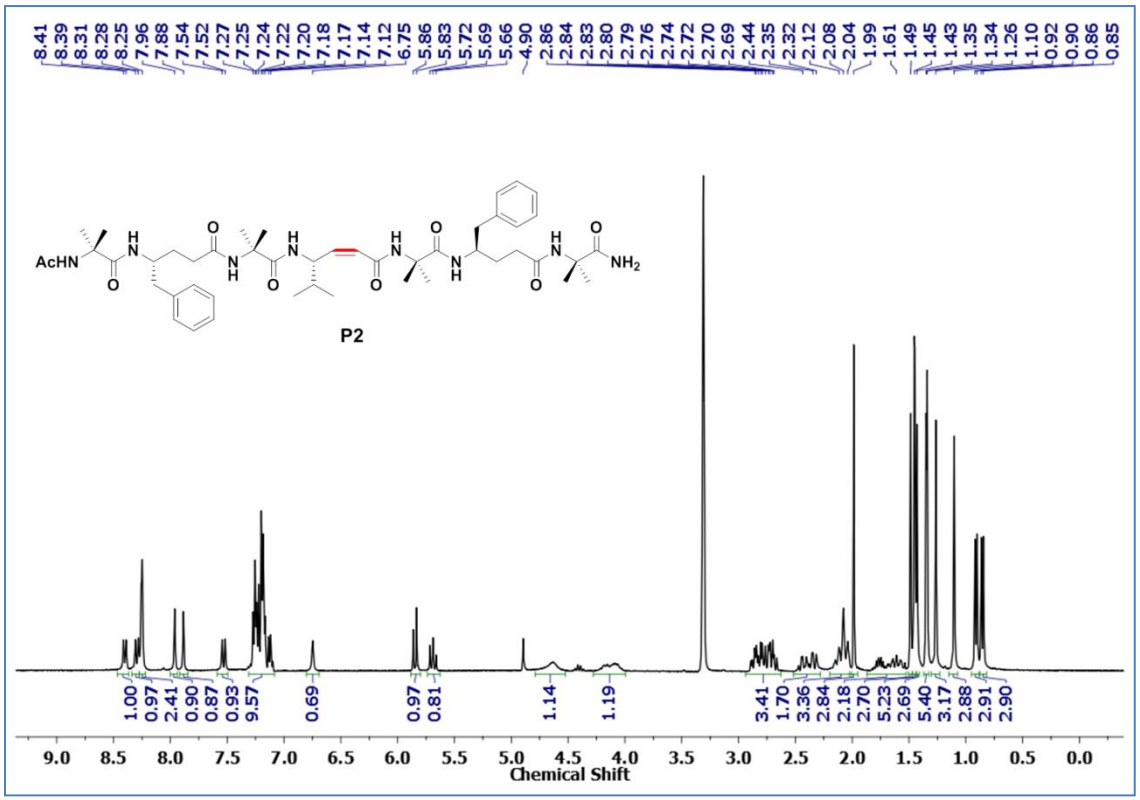
P2
Chemical Shift

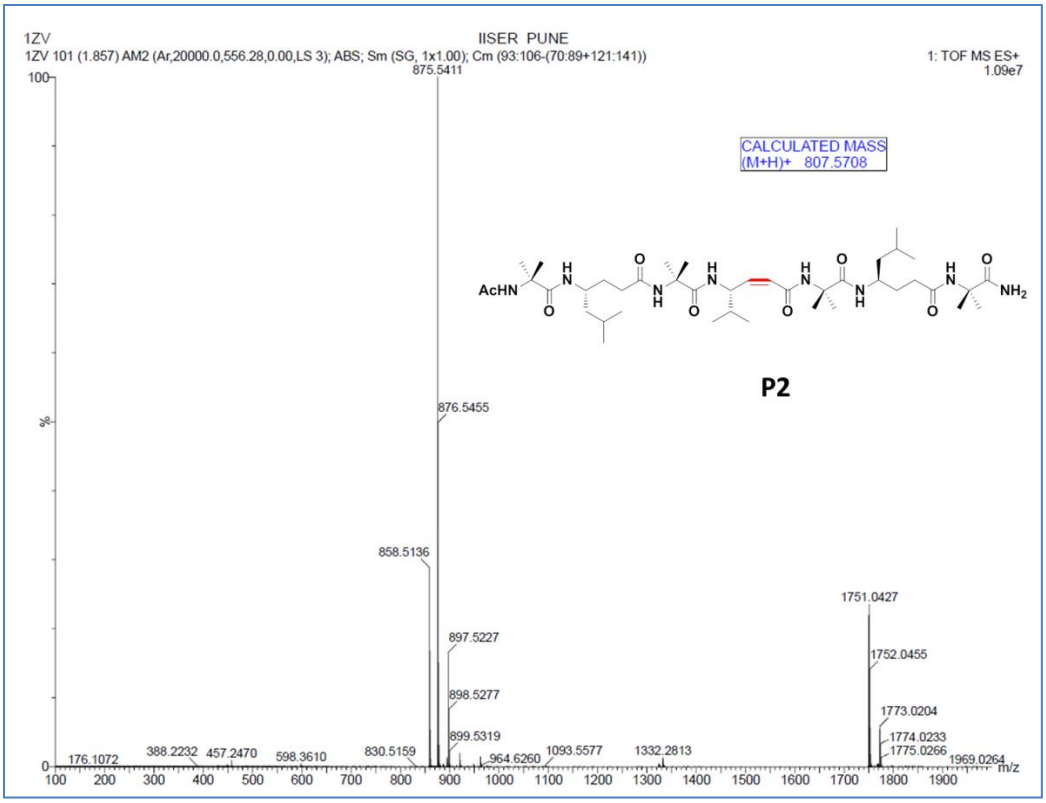
1ZV
IISER PUNE
1ZV 101 (1.857) AM2 (Ar,20000.0,556.28,0.00,LS 3); ABS; Sm (SG, 1x1.00); Cm (93:106-(70:89+121:141))
1: TOF MS ES+
1.09e7
CALCULATED MASS
(M+H)+ 807.5708
P2
875.5411
876.5455
858.5136
897.5227
898.5277
899.5319
1751.0427
1752.0455
1773.0204
1774.0233
1775.0266
1969.0264
176.1072
388.2232
457.2470
598.3610
830.5159
964.6260
1093.5577
1332.2813
m/z

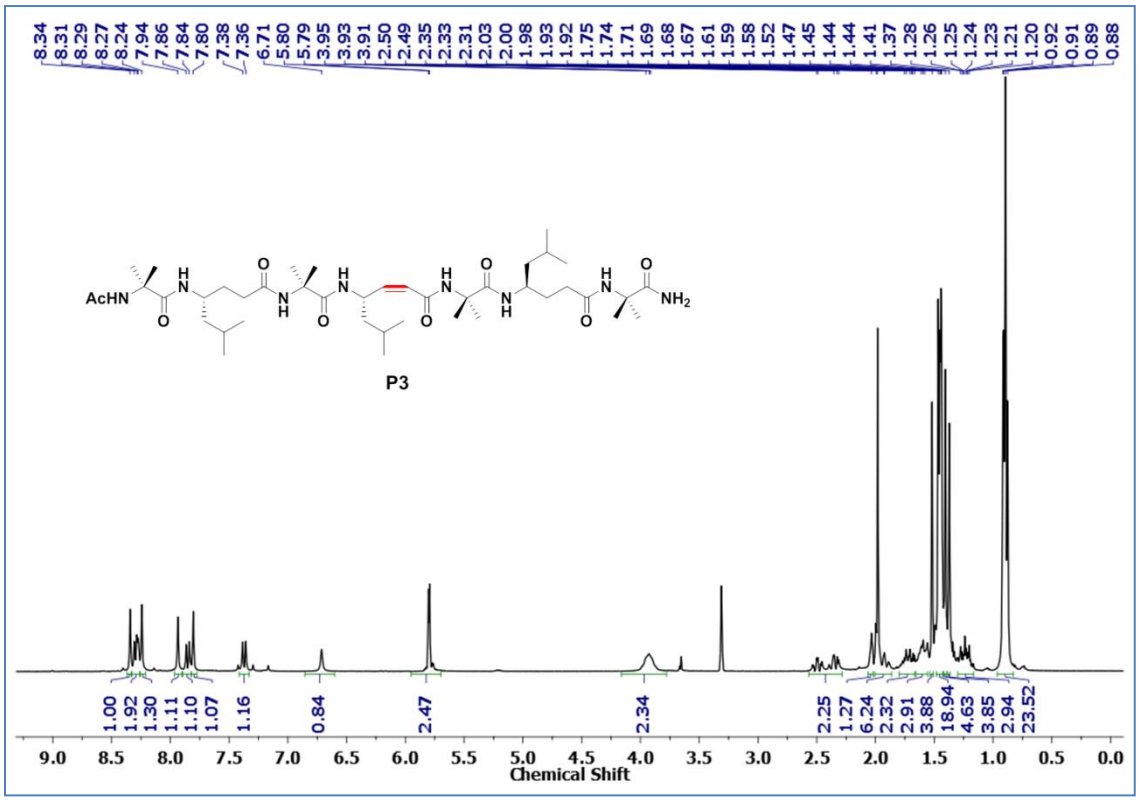
P3
Chemical Shift

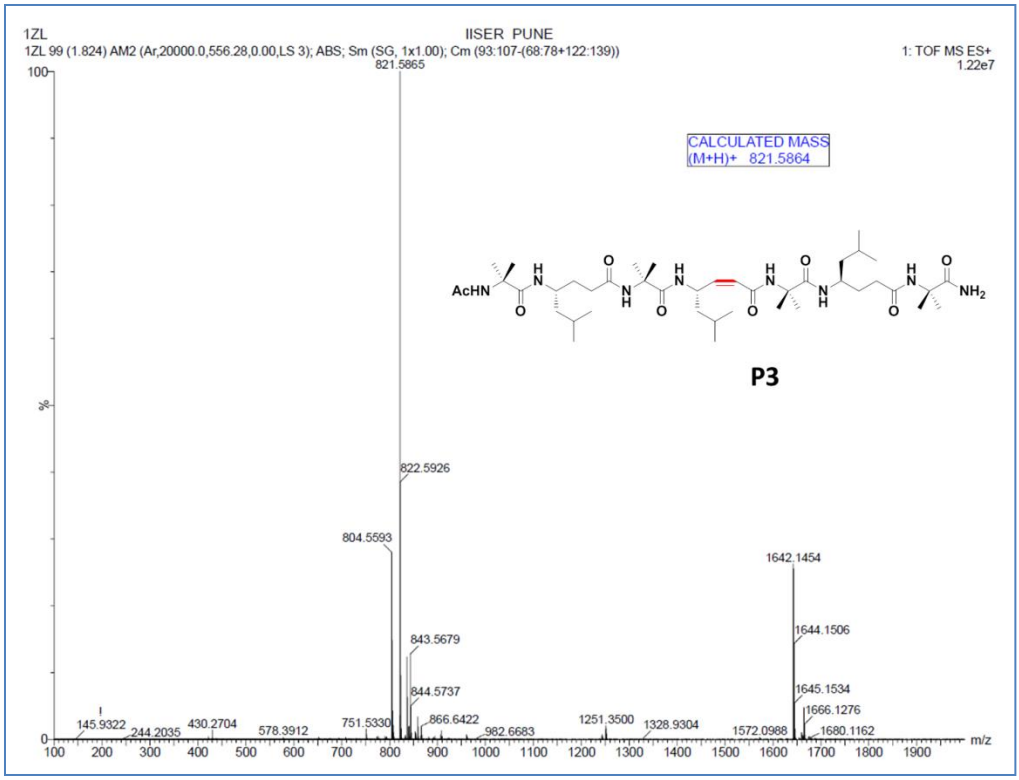
1ZL
IISER PUNE
1ZL 99 (1.824) AM2 (Ar,20000.0,556.28,0.00,LS 3); ABS; Sm (SG, 1x1.00); Cm (93:107-(68:78+122:139))
1: TOF MS ES+
1.22e7
CALCULATED MASS
(M+H)+ 821.5864
P3
821.5865
822.5926
804.5593
843.5679
844.5737
1642.1454
1644.1506
1645.1534
1666.1276
1680.1162
145.9322
244.2035
430.2704
578.3912
751.5330
866.6422
982.6683
1251.3500
1328.9304
1572.0988
m/z

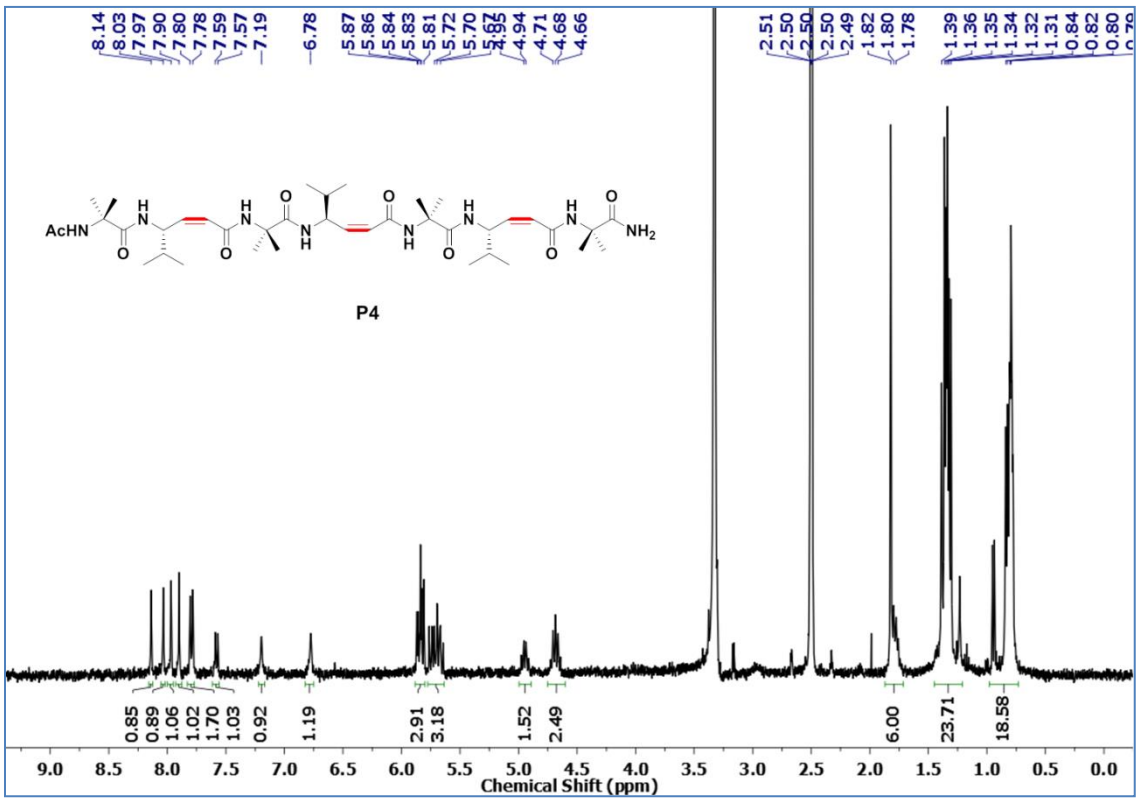
P4
Chemical Shift (ppm)

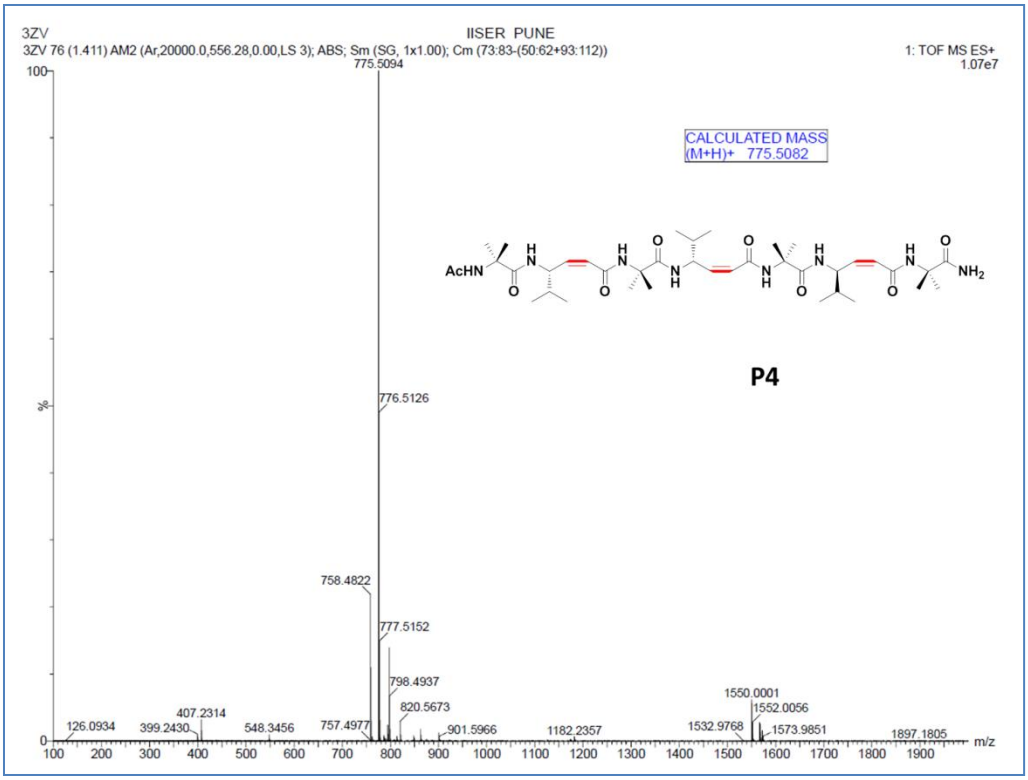
3ZV
IISER PUNE
3ZV 76 (1.411) AM2 (Ar,20000.0,556.28,0.00,LS 3); ABS; Sm (SG, 1x1.00); Cm (73:83-(50:62+93:112))
1: TOF MS ES+
1.07e7
CALCULATED MASS
(M+H)+ 775.5082
P4
775.5094
776.5126
758.4822
777.5152
798.4937
820.5673
1550.0001
1552.0056
1573.9851
1532.9768
1897.1805
901.5966
1182.2357
757.4977
548.3456
407.2314
399.2430
126.0934
m/z

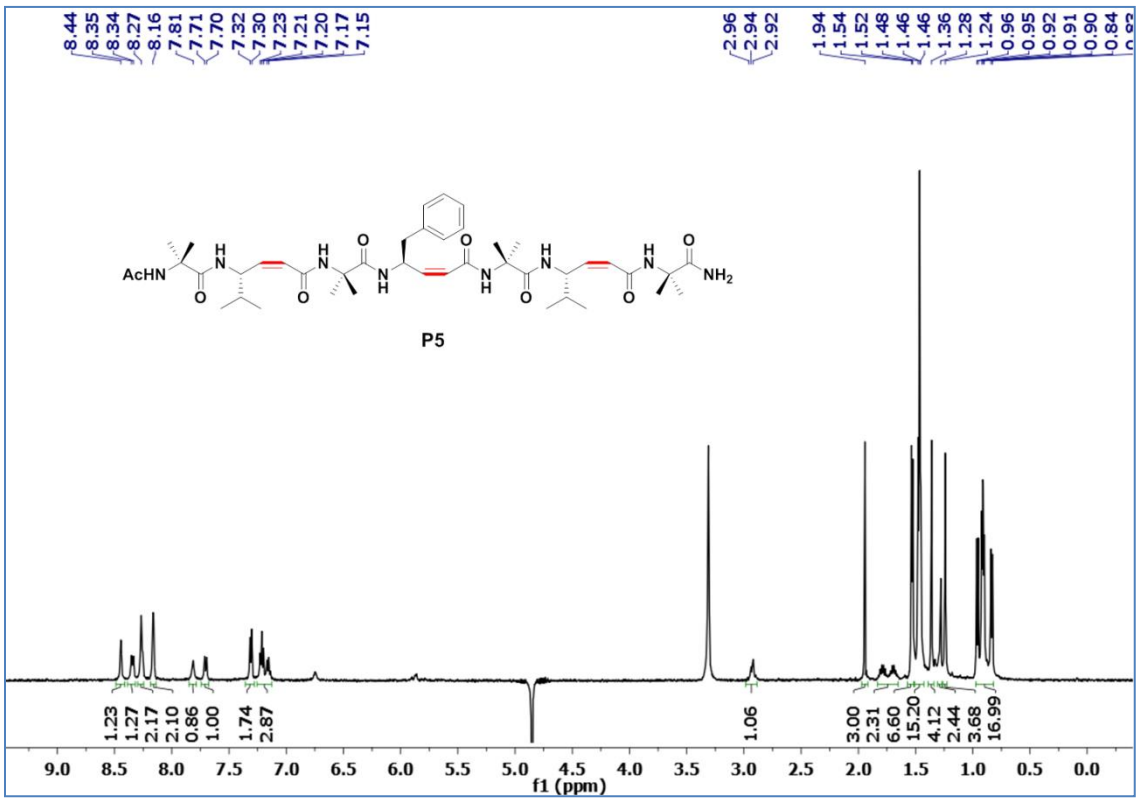
P5
f1 (ppm)

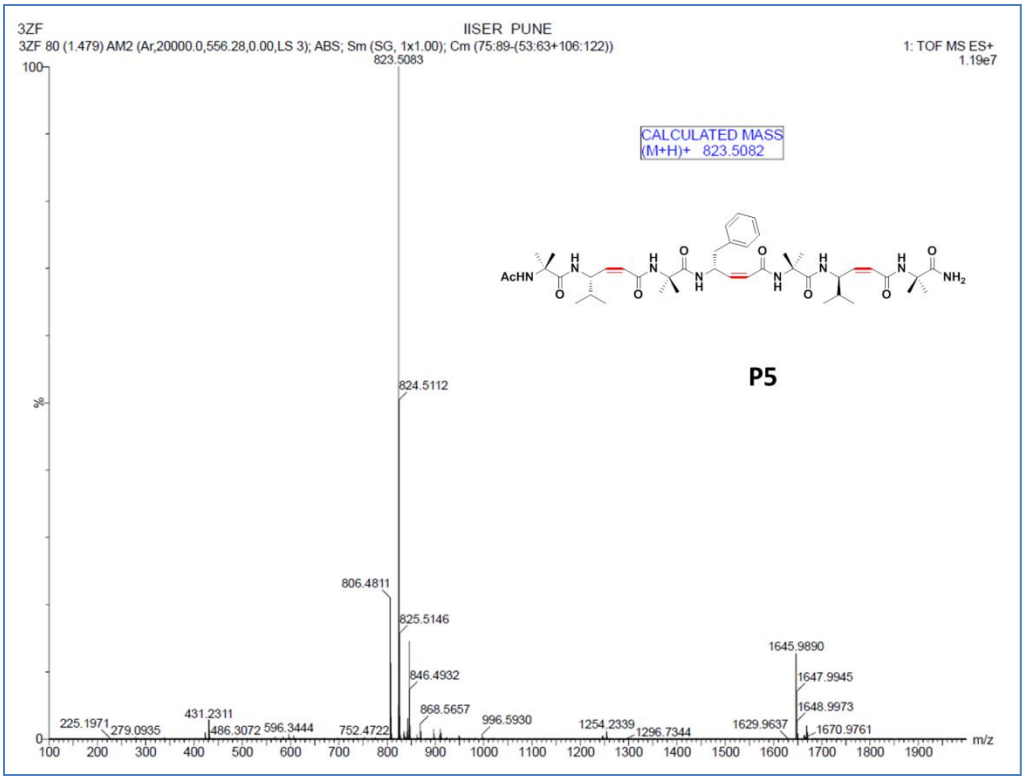
3ZF
IISER PUNE
3ZF 80 (1.479) AM2 (Ar,20000.0,556.28,0.00,LS 3); ABS; Sm (SG, 1x1.00); Cm (75:89-(53:63+106:122))
1: TOF MS ES+
1.19e7
CALCULATED MASS
(M+H)+ 823.5082
P5
823.5083
824.5112
806.4811
825.5146
846.4932
868.5657
996.5930
1645.9890
1647.9945
1648.9973
1670.9761
1629.9637
1254.2339
1296.7344
752.4722
596.3444
486.3072
431.2311
279.0935
225.1971
m/z

Chapter 4

Unprecedented Rearrangement in (*E*)-Vinylogous Amides through α, β→β, γ Double Bond Migration

4.1 Introduction

Mimicking protein or peptide structures using synthetic molecules is very attractive from the perspective of medicinal chemistry.[1] Enormous efforts have been made in the literature to design peptidomimetics either by modifying the existing structures of peptides with unnatural amino acids,[2, 3] cyclization of linear peptides,[4] organic templates bearing amino acid side-chains[5] or small molecules from *de novo* design.[6] A variety of unnatural amino acids that mimic α-amino acid side-chains such as peptoids, β-peptides and γ-peptides have been exploited to design peptidomimetics. Their structural properties and analogy with protein structures have been discussed in the previous Chapters 1 to 3. We have been engaging in the synthesis and conformational analysis of foldamers composed of a naturally occurring α, β-unsaturated γ-amino acids[7] and some of the these results have been presented in the previous Chapters. This Chapter is focusing on some of the accidental results that were observed during the course of our investigation on the structural properties of *E*-vinylogous amino acids. Here, we are presenting the migration of double bonds from α, β→β, γ in the hybrid peptides and the rearrangement of N-protected α, β-unsaturated γ-amino acid amides into γ-lactams through multiple double bond migrations mediated by a base.

4.2 Aim and Rationale of the Present Work

In addition to the β-sheets and β-hairpin structures, recently we reported the unusual planer structures of 1:1 alternating Aib and *E*-vinylogous residues.[7e] By using *E*-vinylogous residues we also successfully mimicked the supersecondary structures like β-meanders and helix-turn-helix motifs.[7d] In continuation, we anticipated that it may be possible to generate new folded architectures in hybrid peptides composed of stereochemically constrained proline, which is not ideally suited for the design of either α-helix or β-sheet,[8] and *E*-vinylogous residues. In this context, we have designed and synthesized a hybrid hexapeptide (**P**) composed of 1:1 alternating proline and *E*-vinylogous residues. The sequence of the peptide is shown in Figure 1.

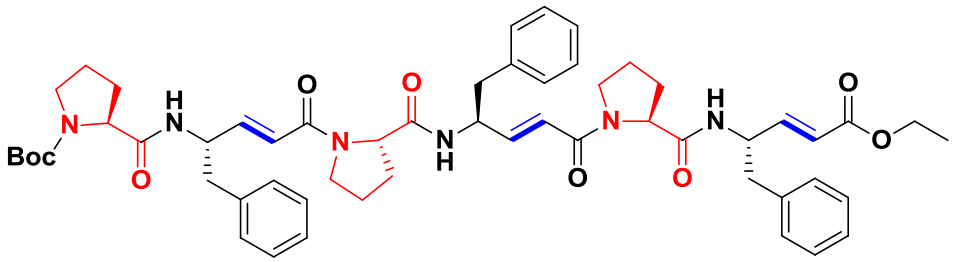

P

Fig 1: Structure of hexapeptide Boc-Pro-dγPhe-Pro-dγPhe-Pro-dγPhe-OEt (**P**).

4.3 Results and Discussion

4.3.1 Synthesis of Boc-Pro-dγPhe-Pro-dγPhe-Pro-dγPhe-OEt Hexapeptide (P)

In order to isolate good amount of pure peptide **P**, we used solution phase strategy for the synthesis. The schematic representation of the synthesis is shown in Scheme 2. The dipeptide Boc-Pro-dγPhe-OEt (**P1**) obtained after the coupling reaction between Boc-Pro and free amine of dγPhe-OEt using DCC/HOBt (Scheme 1) was purified and subjected for the tetrapeptide (**P2**) synthesis using 2+2 condensation strategy. In addition, **P1** also gave X-ray quality single crystals and its X-ray structure is shown in Figure 2. Interestingly, X-ray analysis revealed that it adopted a reverse turn type conformation, however, without any intramolecular H-bonds. The torsional variables are tabulated in Table 1. Further, reverse turn type of conformation displayed by **P1** motivated us to synthesize tetra and hexapeptides anticipating that they may yield ribbon type of conformation. Tetrapeptide, Boc-Pro-dγPhe-Pro-dγPhe-OEt (**P2**) was synthesized by 2+2 convergent synthesis involving Boc-Pro-dγPhe-COOH (**P1-A**) and NH_2-Pro-dγPhe-OEt (**P1-B**) (Scheme 2). The Boc group was deprotected using 50% TFA in DCM and 1N NaOH in THF was used for the saponification of ethyl ester. Similar to the dipeptide the coupling reaction was performed using DCC/HOBt coupling conditions. The pure peptide **P2** was subjected to hexapeptide (**P**) synthesis using 4+2 condensation strategy. The ethyl ester of tetrapeptide (**P2**) was hydrolyzed using 1N NaOH in THF solution and 50% TFA was used for Boc-deprotection of dipeptide (**P1**). Similar to **P1** and **P2**, the final coupling reaction was performed using DCC/HOBt coupling reagents (Scheme 3). The crude hexapeptide **P** was purified through reverse phase HPLC on C_{18} column using MeOH/H_2O gradient system. The pure peptide was subjected to 2D NMR and crystallization to understand its conformation.

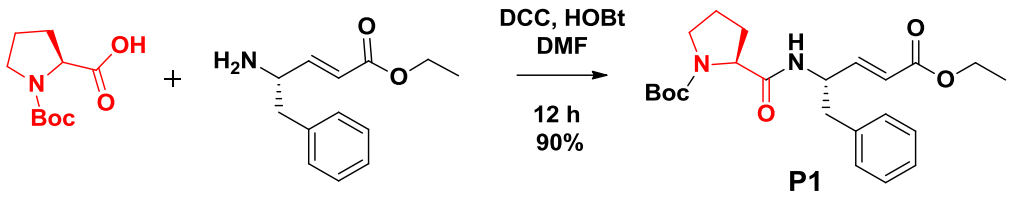

Scheme 1: Synthesis of dipeptide **P1.**

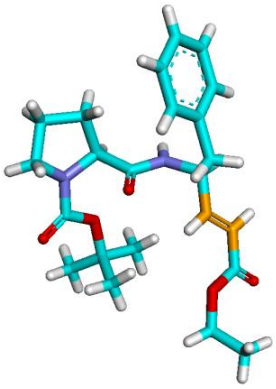

Fig 2: X-ray structure of dipeptide **P1**.

Table 1: Torsional parameters (in deg) of peptide **P1**

P1	ϕ	θ_1	θ_2	ψ	ω
Pro	-52	-	-	151	76
dγPhe	69	121	176	-10	-

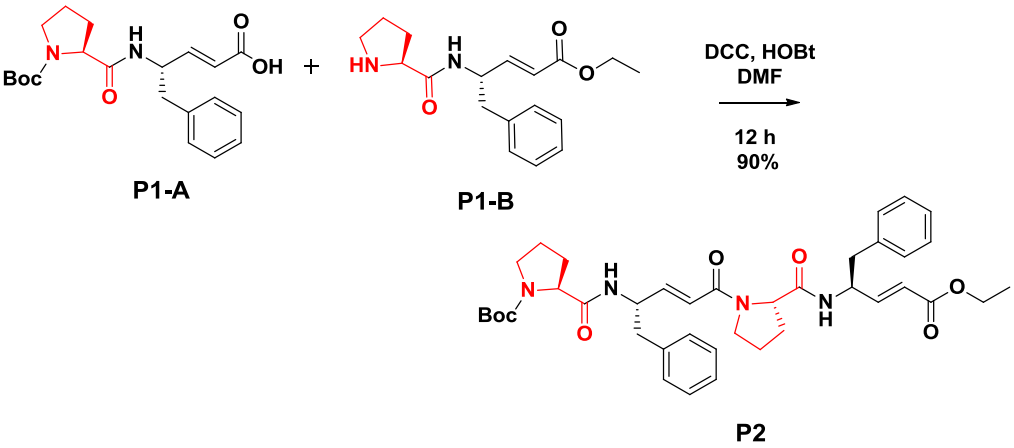

Scheme 2: Synthesis of tetrapeptide **P2.**

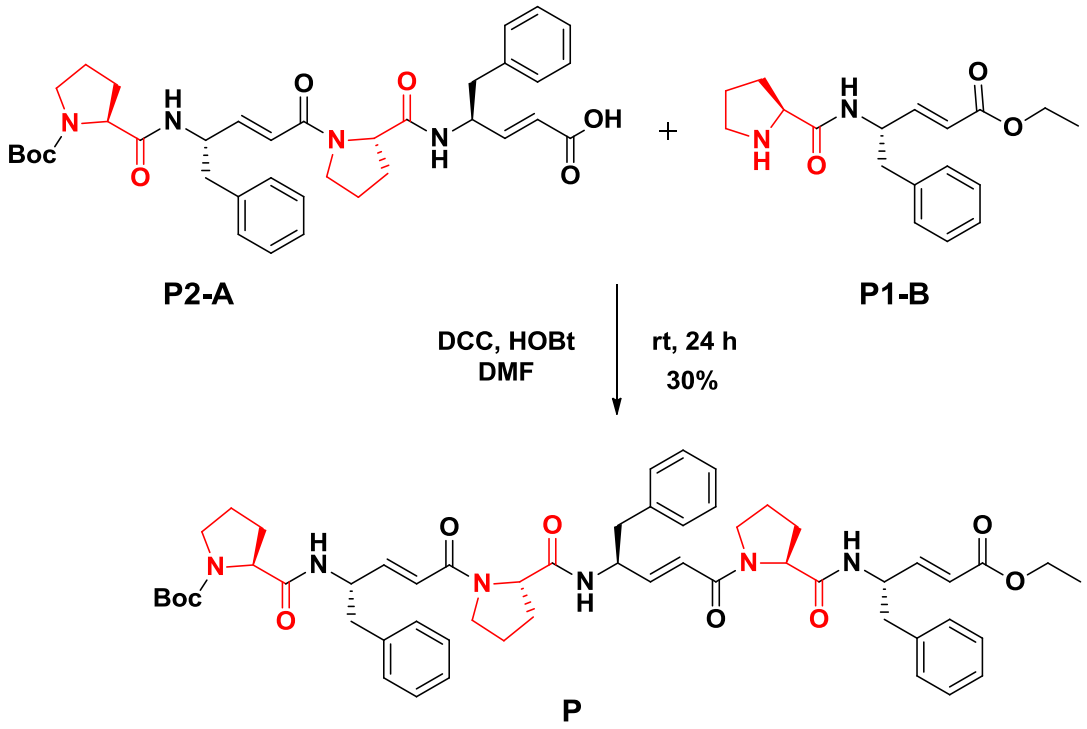

Scheme 3: Synthesis of hexapeptide (**P**).

4.3.2 Unusual α, β → β, γ Double Bond Migration in Hybrid Peptide

Due to presence of three proline residues, we find it difficult to analyze ^{1}H NMR as well as 2D NMR (TOCSY and ROESY) of hexapeptide **P**. As we find it difficult to analyze its solution structure, we made enormous efforts to crystallize peptide **P** from various solvent combinations. Finally, we are able to get the X-ray quality single crystals from aqueous methanol solution. The X-ray structure of **P** is shown in Figure 3A.

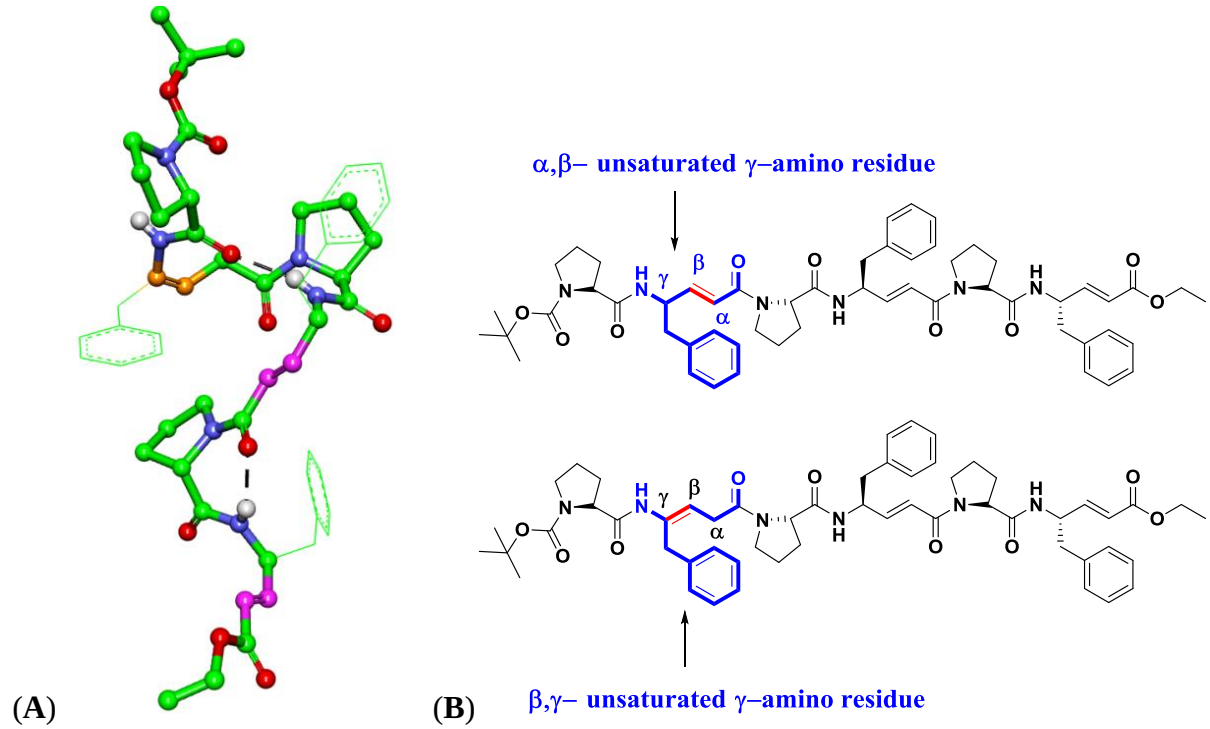

Fig 3: (**A**) X-ray structure of peptide **P** and (**B**) Chemdraw structure of peptide **P**.

Table 2: Torsional parameters of peptide **P**

Pro-dγPhe Hexapeptide (P)	ϕ	θ_1	θ_2	ψ	ω
Pro	-65	-	-	-42	-162
dγPhe	-61	**-1**	**111**	-149	-176
Pro	-77	-	-	-8	177
dγPhe	-94	-6	-175	169	-170
Pro	-88	-	-	61	-173
dγPhe	-115	0	177	178	-

Table 3: Hydrogen bond parameters of peptide **P**

Donor (D)	**Acceptor (A)**	**D….A (Å)**	**DH….A (Å)**	**NH….O (deg)**
N4	O3	2.88	2.06	158
N6	O6	2.8	2.06	148
N2	O5’	2.86	2.19	134
O5	N2’	2.86	2.19	134

In a sharp contrast to the unusual planar structure of hybrid peptide composed of 1:1 alternating Aib and *E*-vinylogous residues,[7e] a quick glance of the X-ray structure of **P** reveals that the hybrid peptide adopted a novel 12/7 mixed helix. Although, proline is known as helical breaker in α-peptide sequences,[8] we are surprised to see the accommodation of proline into the helix. The torsional angles of proline are tabulated in Table 2. All three prolines attained different torsional values. Detailed inspection of the crystal structure revealed an unexpected α, β → β, γ double bond migration in dγPhe2 of **P** (Figure 3B). Surprised by this unusual double bond migration, we searched for the literature precedents. Though there are not many synthetic examples delineating double migration in unconjugated systems available in the literature, however, α, β → β, γ double bond migration is an important key step in biosynthesis of many polyketides and antibiotic natural products.[9] Recently Schaberle and colleagues showed the double bond migration in biosynthesis of corallopyronin A (Figure 4).[9] Using NMR and high-resolution MS measurements they proved the role of a dehydratase that responsible for the migration of double bonds.

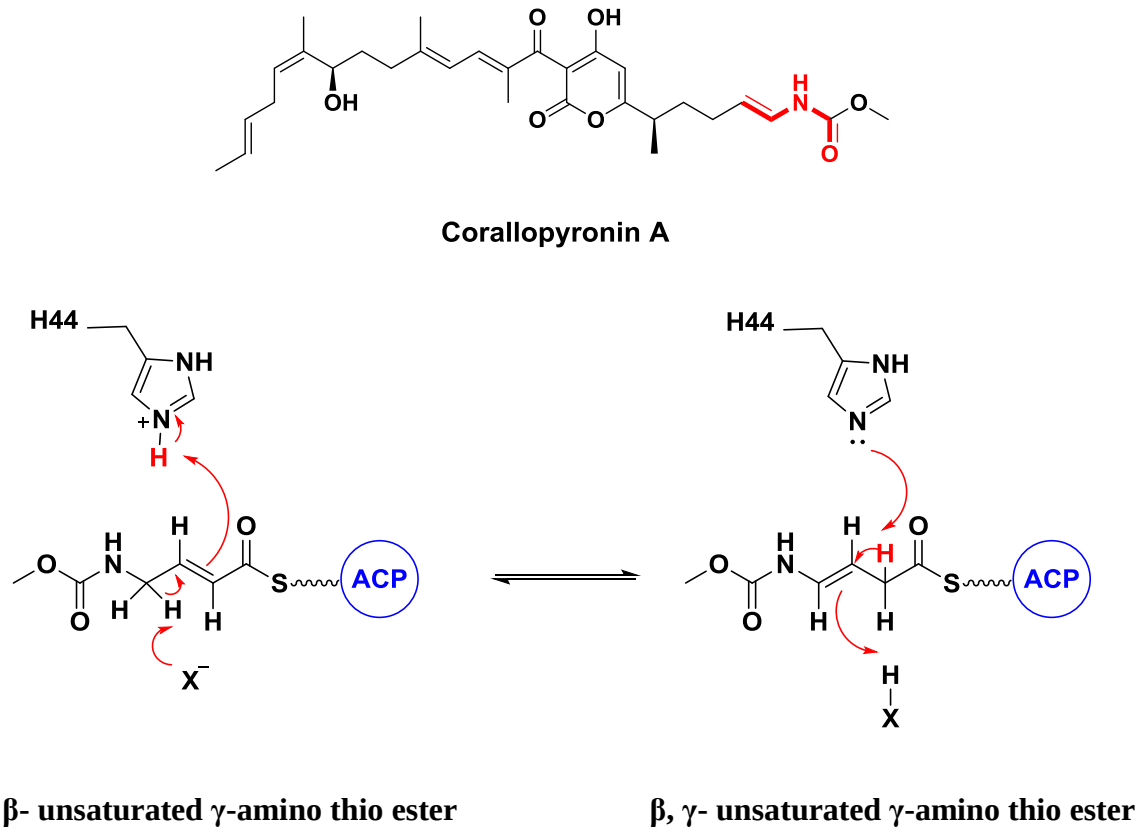

Fig 4: Proposed mechanism for double bond migration in biosynthesis of corallopyronin A.

Inspired by nature's way of double bond migration in the biosynthesis of antibiotics, we sought to investigate the mechanism of unusual α, β → β, γ double bond migration in the hexapeptide **P**. We speculated that similar to the enzyme dehydratase mediated double bond migration, the basic reaction conditions used in the saponification of the tetrapeptide might have been played a role in the double bond migration during the synthesis of peptide **P**. To test our hypothesis, we resynthesized the tetrapeptide ethyl ester **P2** and subjected for the ester hydrolysis using 1N NaOH. In order to isolate pure peptide we re-esterified with MeI/K_2CO_3 to get peptide **P3** (Scheme 4). Crude peptide **P3** was subjected to RP-HPLC purification and characterized by ^{1}H NMR (Figure 5).

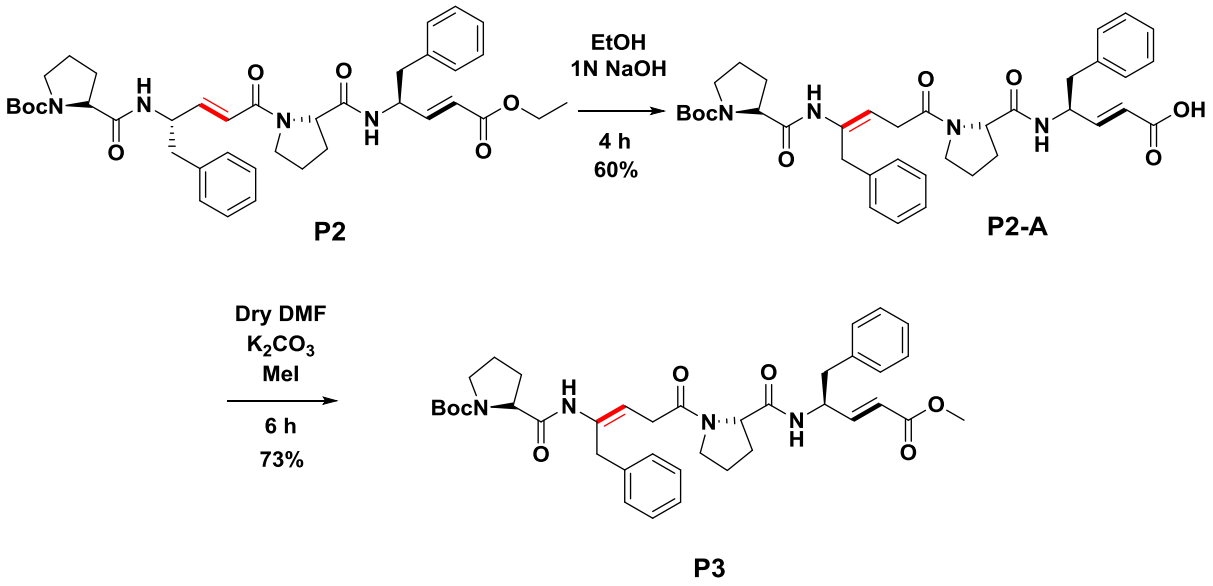

Scheme 4: Hydrolysis and re-esterification of tetrapeptide **P2**

Surprising results were obtained from ^{1}H NMR studies. Indeed, **P3** showed the double bond migration from α, β to β, γ position. Details of double bond migration in **P2** and **P3** are shown in Figure 5. These results confirm that the role of alkali in the migration of double bonds. Further, these results support the base mediated double bond migration in corallopyronin A by dehydratase.[9]

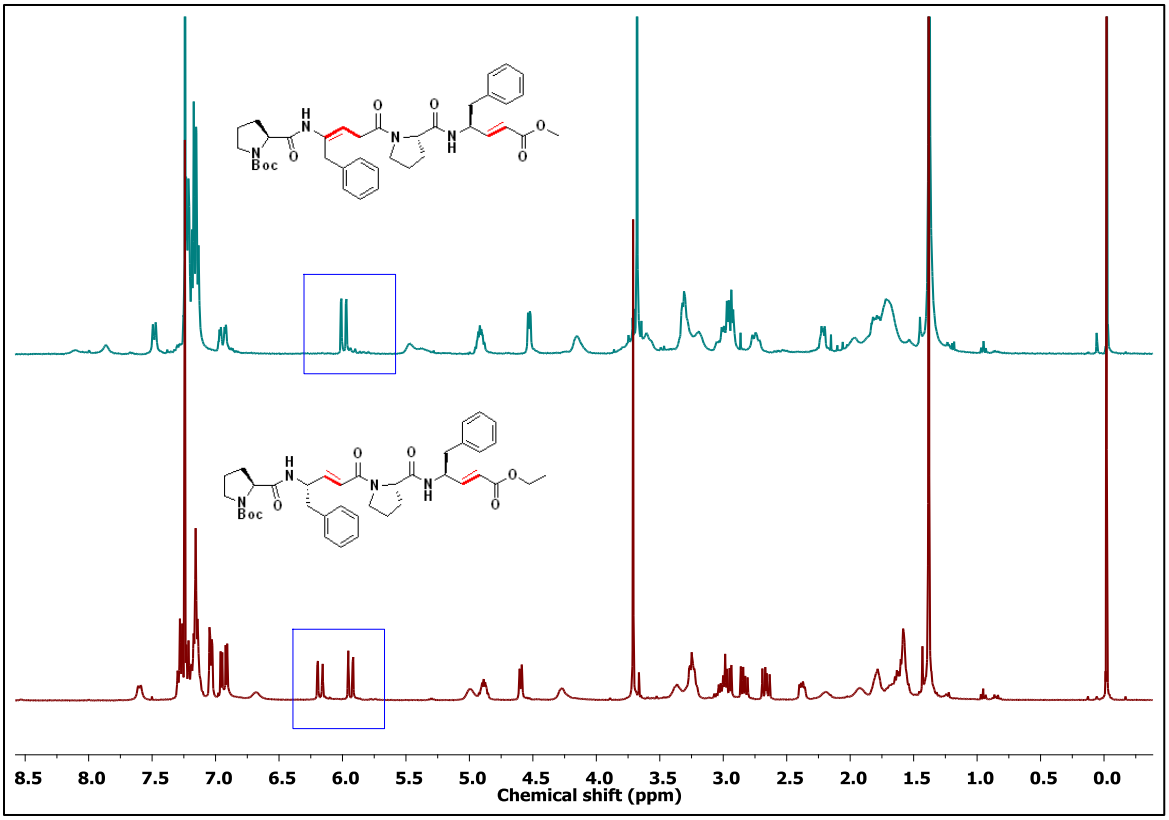

Fig 5: Double bond migration in peptide **P3**.

4.4 Unprecedented Rearrangement in α, β-Unsaturated γ-Amino Acid Amides

Double bond migration in the base hydrolysis of the tetrapeptide **P2** motivated us to investigate this novel double bond migration in simple α, β-unsaturated γ-amino esters. As we have been using simple *E*-vinylogous esters, we never observed this double bond migration in monomers. However, we subjected ethyl ester of Boc-dγPhe for the saponification and re-esterified the acid similar to the **P3**. ^{1}H NMR results suggests that there is no migration of double bond. We hypothesized that as ester hydrolysis is more facile process than the double bond migration, simple systems may prefer the hydrolysis. In addition, carboxylate anion formed during the hydrolysis may create difficulty to generate another negative charge in the system. Based on these results, we hypothesized that instead of simple esters if we do the same reaction on amides it may be possible to observe the double bond migration. To test our hypothesis, we synthesized N-Boc (*E*)-α, β-unsaturated γ-phenylalanine benzyl amide (Scheme 5) as a model system, and subjected to the base treatment under identical conditions as of **P2** using 1N NaOH

in THF solution. The reaction mixture was stirred for about 48 hrs and the reaction mixture was extracted with ethyl acetate. We were able to isolate only 40% of the product after the aqueous work-up and subjected to ^{1}H NMR. Surprisingly, we observed the formation of γ-lactam instead of double bond migrated product. The schematic representation of the reaction is shown in Scheme 5. The γ-lactam product was further confirmed by single crystal X-ray structure. The structure is shown in Figure 6.

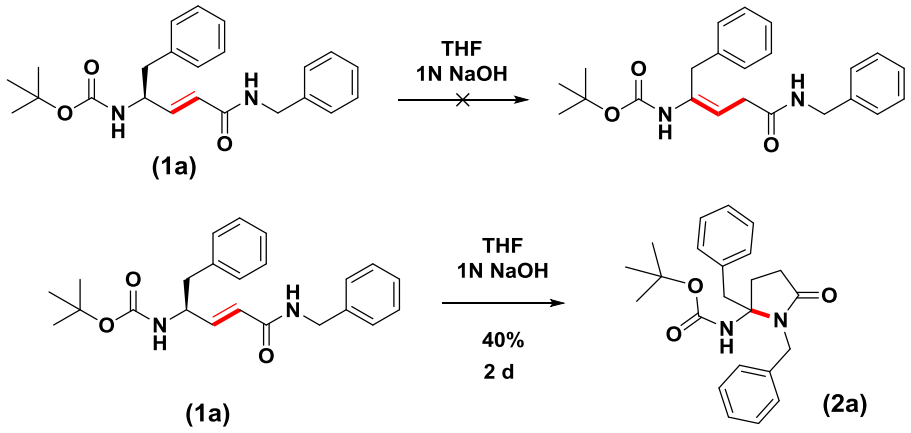

Scheme 5: Synthesis of γ-lactam from α, β-unsaturated γ-amino amides

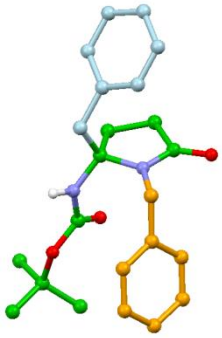

Fig 6: X-ray structure of compound **2a**.

The remarkable feature of this transformation is that it is possible to introduce various amino acids side-chains on to the single γ-lactam. This unprecedented novel rearrangement with great simplicity motivated us to investigate substrate specificity as well as to improve the yield of the rearrangement product. In addition, we anticipate that this kind of molecules may find applications in the design of various protein-protein interaction inhibitors (PPI's inhibitors). As we isolated only 40% yield in the transformation of **1a** to **2a**, we tried various bases and organic

solvents to improve the yield of γ-lactam formation. The list of bases and organic solvents tried in the transformation of **1a** to **2a** is given in the Table 3. Out of all organic and inorganic bases in the Table 3, complete transformation of **1a** to **2a** was achieved within 12 h in dry THF solution using KO^{t}Bu as a base (Scheme 6). After the standardization, we screened various *E*-vinylogous amides to confirm substrate specificity (Table 4). The list of *E*-vinylogous amides and corresponding γ-lactams is given in Table 4. Out of all the compounds, we were able to get the single crystals for the compounds **2b**, **2e** and **2f**. The X-ray crystal structures of these molecules are shown in Figure 7. It should be noted that all γ-lactams isolated in the rearrangement are racemic mixtures.

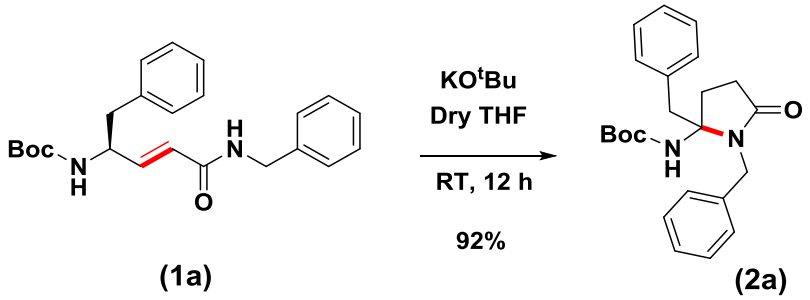

Scheme 6: Synthesis of γ-lactams from α, β-unsaturated γ-amino amides using KO^{t}Bu as a base.

Table 3: Solvents and bases screened for the formation of γ-lactam from α, β-unsaturated γ-phenylalanine benzyl amide.

Base	Solvent	Completion	Time
LiOH	THF	-	2 d
NaOH	THF	40 %	2 d
CsOH	THF/DMF	50%	2 d
DBU	THF/DCM	-	2d
n-BuLi	THF	-	1 d
KO^{t}Bu	THF	100%	12 h

Table 4: List of γ-lactams generated from α, β-unsaturated γ-amino amide.

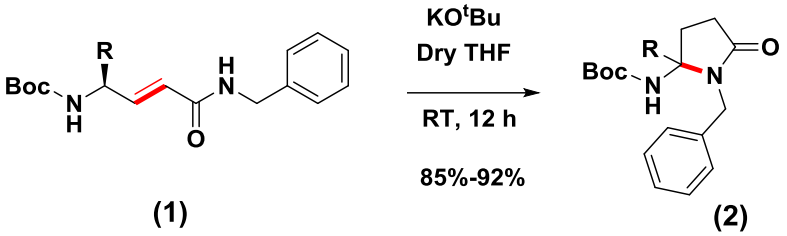

S. No	1	2	% Yield
a	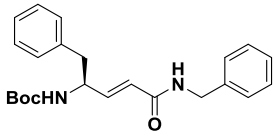	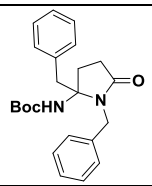	92
b	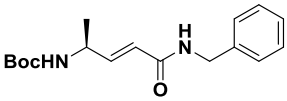	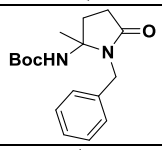	85
c	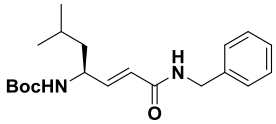	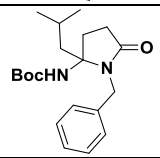	75
d	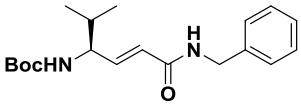	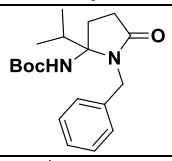	90
e	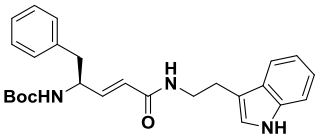	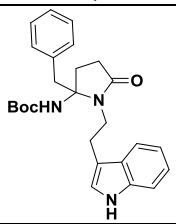	85
f	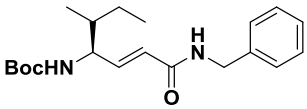	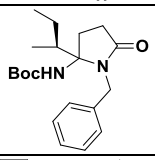	90
g	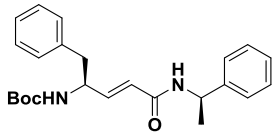	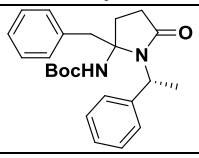	77

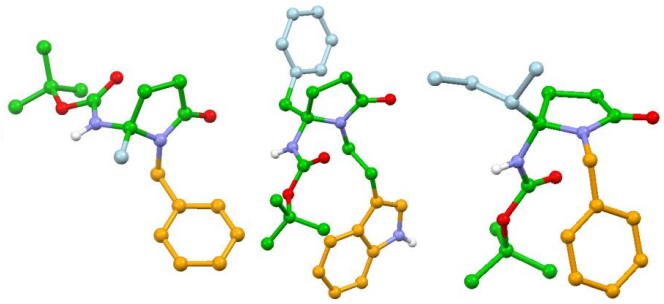

(2b) **(2e)** **(2f)**

Fig 7: X-ray structure of compounds 2b, 2e and 2f.

Based on the double bond migration in the peptides and γ-lactam formation in the monomers, we proposed the plausible mechanism for the formation of γ-lactams as shown in Scheme 7. We hypothesized that there is a possibility of two double bond migrations during the γ-lactam formation starting from *E*-vinylogous amides. We speculated that similar to the dehydratase, base abstracts the γ-proton from *E*-vinylogous amides which leads to the formation of β, γ-double bond migrated product **A**. Further, the double migrated product transformed to imide **B** in the presence of a base. Finally, this imide undergoes conjugate addition type reaction with deprotonated C-terminal amide, which leads to the formation of γ-lactam (**2**).

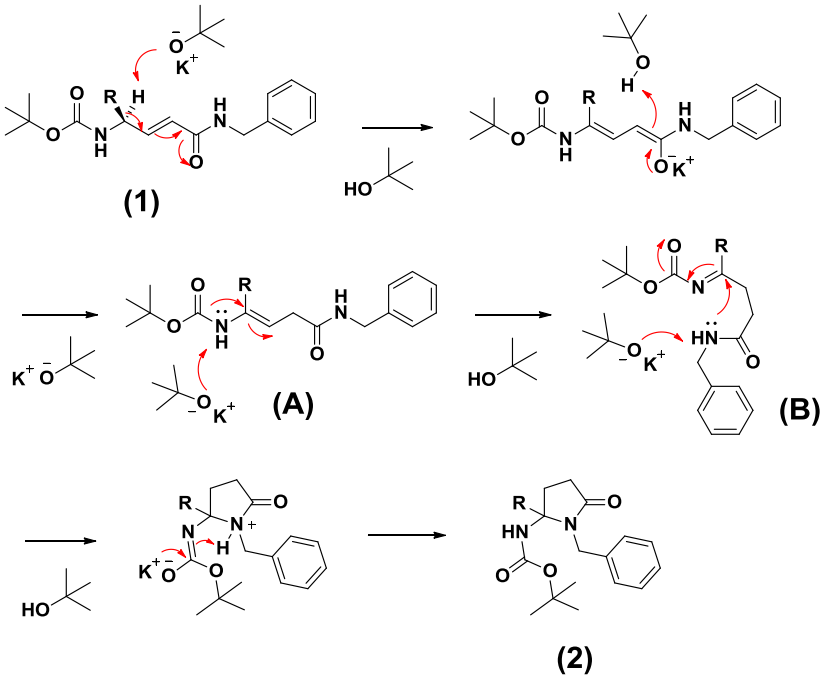

Scheme 7: Plausible mechanism for the formation of γ-lactams from α, β-unsaturated γ-amides.

We further speculated that in the case of **P** or **P3,** the C-terminal is an imide bond rather an amide bond and it is not possible to create negative charge on the imide, so the reaction stops at one double bond migration that is α, β →β, γ. In case of other C-terminal amides such as **2 (a-g)**, it is possible to achieve two double bond migrations and eventually γ-lactams. Presently, we are investigating the biological activities of these lactams as well as the detailed mechanism of the reaction.

4.5 Future Perspective

We foresee that these γ-lactams may be utilized as small molecule peptidomimetics since all amino acid side chains can be incorporated in a simple γ-lactam (Figure 8). Due to their structural integrity they can be explored as various PPI inhibitors. For example, three residues of p53 enzyme (Phe, Typ, Leu) are known as epitopes which helps to bind hDM2. Through this rearrangement, it is possible to introduce all these three side chains on simple γ-lactam and may be tested for its inhibitory activity against p53-hDM2 interactions.

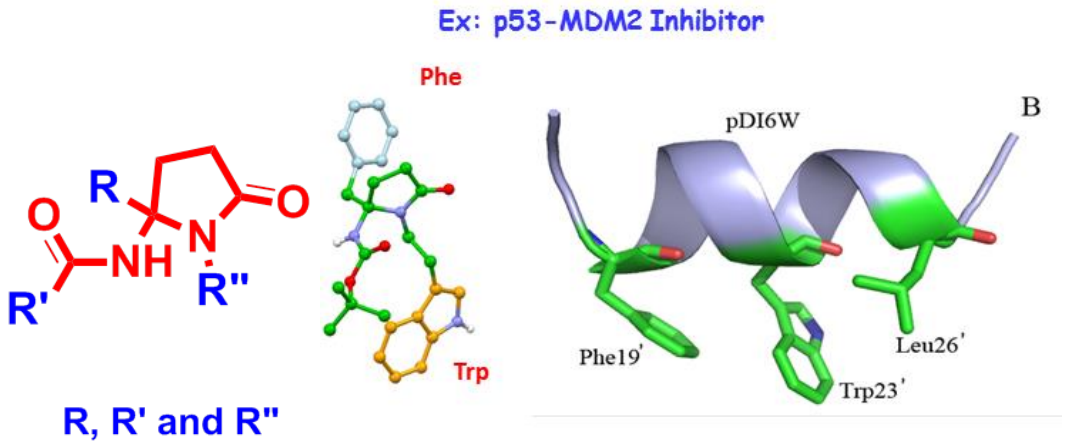

Fig 8: Small molecule peptidomimetics.

4.6 Conclusions

In conclusion, we have demonstrated the α, β → β, γ double bond migration in peptides followed by a novel rearrangement in α,β-unsaturated γ-amino acid amides. The α, β → β, γ double bond migration observed in peptide **P** was found to be very similar to corallopyronin A polyketide biosynthesis. To the best of our knowledge this is the first report where the double

bond migrated intermediate was trapped, isolated and characterized. Unlike in peptides, the *E*-vinylogous amide monomer units showed remarkable γ-lactams formation under identical conditions. The novel rearrangement and the γ-lactam may find potential applications in the drug discovery. The major advantage of this rearrangement is that it is possible to introduce various amino acids side chains on the γ-lactam in a single step. We are currently exploring the γ-lactams in the design of protein-protein interaction inhibitors. In addition to this we are also investigating the how to achieve stereo selectivity in the rearrangement and the detailed mechanism of the rearrangement. Overall, naturally occurring *E*-vinylogous amino acids not only serving as templates for the construction of various protein secondary and supersecondary structures but also served as templates to synthesize γ-lactams.

4.7 Experimental Section

Crystallographic Information

Crystal structure analysis of Boc-Pro-dγPhe-OEt (P1): Crystals of peptide were grown by slow evaporation from a solution of EtOAc. A single crystal (0.45× 0.35 × 0.30 mm) was mounted on loop with a small amount of the paraffin oil. The X-ray data were collected at 100K temperature on a Bruker APEX DUO CCD diffractometer using Mo K_α radiation (λ = 0.71073 Å), ω-scans (2θ = 58.56), for a total of 4937 independent reflections. Space group C2, a = 46.223(4), b = 6.3410(5), c = 7.5718(6), α= 90.00, β= 97.948(2), γ= 90.00, V=2198.0(3)$Å^3$, Monoclinic C, Z=4 for chemical formula $C_{23}H_{32}N_2O_5$, with one molecule in asymmetric unit; ρcalcd =1.259gcm^{-3}, μ= 0.088mm^{-1}, F(000)= 896, R_{int}= 0.0191. The structure was obtained by direct methods using SHELXS-97. The final R value was 0.038 (wR2=0.1011) 4721 observed reflections ($F_0 \geq 4\sigma(|F_0|)$) and 275 variables, S = 1.056. The largest difference peak and hole were 0.283 and -0.212e$Å^3$, respectively.

Boc-Pro-dγPhe-Pro-dγPhe-Pro-dγPhe-OEt (P3): Crystals of peptide were grown by slow evaporation from a solution of aqueous methanol. A single crystal (0.15 × 0.1 × 0.05 mm) was mounted on loop with a small amount of the paraffin oil. The X-ray data were collected at 100K temperature on a Bruker APEX(II) DUO CCD diffractometer using Mo K_α radiation (λ = 0.71073 Å), ω-scans (2θ = 50.00), for a total of 34755 independent reflections. Space group P212121, a = 9.923(2), b = 16.088(4), c = 32.891(8), β = 90.00, V = 5251(2) $Å^3$, Orthorhombic,

Z = 4 for chemical formula C55 H68 N6 O9, with one molecule in asymmetric unit; ρcalcd = 1.211gcm^{-3}, μ = 0.083 mm^{-1}, F(000) = 2044, R_{int}= 0.0719. The structure was obtained by intrinsic methods using SHELXS-97.The final R value was 0.0526 (wR2 = 0.1274) 11452 observed reflections ($F_0 \geq 4\sigma(|F_0|)$) and 635 variables, S = 0.883. The largest difference peak and hole were 0.518 and -0.352eÅ^3, respectively.

General Experimental Details:

All amino acids, diphenyl phosphite, TFA, *tert*-butyl bromoacetate, LAH and DMF are commercially available. DCM, DMF, ethyl acetate and pet ether (60-80 °C) have used after distillation. THF was dried over sodium and distilled immediately prior to use. Column chromatography was performed on silica gel (120-200 mesh). Final peptides were purified on reverse phase HPLC (C_{18} column, MeOH/H_2O 60:40-95:5 as gradient with flow rate 3.00 mL/min). ^{1}H spectra were recorded on 500 MHz (or ^{13}C on 125 MHz) and 400 MHz (or ^{13}C on 100 MHz) using residual solvents as internal standards ($CDCl_3$ δ_H 7.26 ppm, δ_C 77.3 ppm and CD_3OD δ_H 3.31 ppm, δ_C 49.0 ppm). Chemical shifts (δ) reported in ppm and coupling constants (J) reported in Hz.

Crystallographic Informations:

Crystal structure analysis of Boc-Pro-dγPhe-OEt (P1): Crystals of peptide were grown by slow evaporation from a solution of EtOAc. A single crystal (0.45× 0.35 × 0.30 mm) was mounted on loop with a small amount of the paraffin oil. The X-ray data were collected at 100K temperature on a Bruker APEX DUO CCD diffractometer using Mo K_α radiation (λ = 0.71073 Å), ω-scans (2θ = 58.56), for a total of 4937 independent reflections. Space group C2, a = 46.223(4), b = 6.3410(5), c = 7.5718(6), α= 90.00, β= 97.948(2), γ= 90.00, V= 2198.0(3)Å^3, Monoclinic C, Z=4 for chemical formula C_{23} H_{32} N_2 O_5, with one molecule in asymmetric unit; ρ calcd = 1.259gcm^{-3}, μ= 0.088mm^{-1}, F(000)= 896, R_{int}= 0.0191. The structure was obtained by direct methods using SHELXS-97. The final R value was 0.038 (wR2= 0.1011) 4721 observed reflections ($F_0 \geq 4\sigma$ ($|F_0|$)) and 275 variables, S = 1.056. The largest difference peak and hole were 0.283 and -0.212eÅ^3, respectively.

Boc-Pro-dγPhe-Pro-dγPhe-Pro-dγPhe-OEt (P): Crystals of peptide were grown by slow evaporation from a solution of aqueous methanol. A single crystal (0.15 × 0.1 × 0.05 mm) was

mounted on loop with a small amount of the paraffin oil. The X-ray data were collected at 100K temperature on a Bruker APEX(II) DUO CCD diffractometer using Mo K_α radiation (λ = 0.71073 Å), ω-scans (2θ = 50.00), for a total of 34755 independent reflections. Space group P212121, a = 9.923(2), b = 16.088(4), c = 32.891(8), β = 90.00, V = 5251(2) $Å^3$, Orthorhombic, Z = 4 for chemical formula C55 H68 N6 O9, with one molecule in asymmetric unit; ρcalcd = 1.211gcm^{-3}, μ = 0.083 mm^{-1}, F (000) = 2044, R_{int} = 0.0719. The structure was obtained by intrinsic methods using SHELXS-97. The final R value was 0.0526 (wR2 = 0.1274) 11452 observed reflections ($F_0 \geq 4\sigma$ ($|F_0|$)) and 635 variables, S = 0.883. The largest difference peak and hole were 0.518 and - 0.352 e$Å^3$, respectively.

General procedure for the Synthesis of Boc-N- α, β-unsaturated γ-amino esters:

Boc-α, β-unsaturated γ-amino esters: *N*-Boc-Amino aldehyde (10 mmol) was dissolved in 30 mL of dry THF followed by Wittig ylide (11 mmol) was added at RT. Reaction mixture was stirred for about 5 h at RT. Completion of the reaction was monitored by TLC. After completion, solvent was evaporated and the crude product was purified by column chromatography using EtOAc/pet ether to get (88%) of pure product.

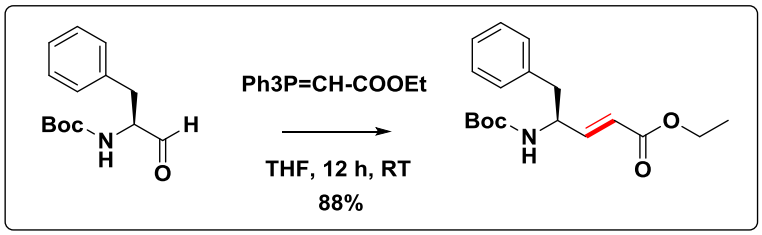

(*S*, *E*)-ethyl 4-((tert-butoxycarbonyl)amino)-5-phenylpent-2-enoate: White powder solid; Yield 88%; ^{1}H NMR (400 MHz, $CDCl_3$) δ 7.30-7.14 (m, 5H), 6.89 (dd, *J* = 16 Hz, *J* = 4 Hz, 1H), 5.84 (dd, *J* = 16 Hz, *J* = 2 Hz, 1H), 4.59 (b, 1H), 4.16 (q, *J* = 7 Hz, 2H), 2.88 (m, 2H), 1.37 (s, 9H), 1.25 (t, *J* = 7.1 Hz, 3H); ^{13}C NMR (100 MHz, $CDCl_3$) δ 166.3, 155.2, 147.6, 136.4, 129.4, 128.6, 126.9, 121.1, 79.9, 60.5, 52.3, 40.9, 28.3, 14.2; MALDI TOF/TOF *m/z* calculated value for $C_{18}H_{25}NO_4$ [M+Na$^+$] 342.1676 and observed 342.1657.

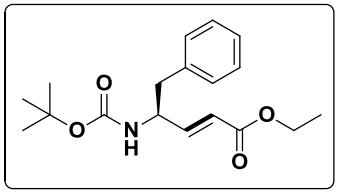

General procedure for the Synthesis of Peptide P1 and P2:

Dipeptide and hexapeptide were prepared by conventional solution-phase fragment condensation strategy. Deprotections were performed with trifloroacetic acid and saponification for *N*- and *C*-termini respectively. Couplings were carried out using N, N'-dicyclohexylcarbodiimide (DCC) and 1-hydroxybenzotriazole (HOBt) in DMF. Dipeptide was synthesized using Boc-Pro-OH and NH_2-dγPhe-OEt. Tetrapeptide was synthesized by 2+2 condensation strategy involving Boc-Pro-dγPhe-COOH and NH_2-Pro-dγPhe-OEt. All peptides were purified by RP-HPLC using MeOH/H_2O system.

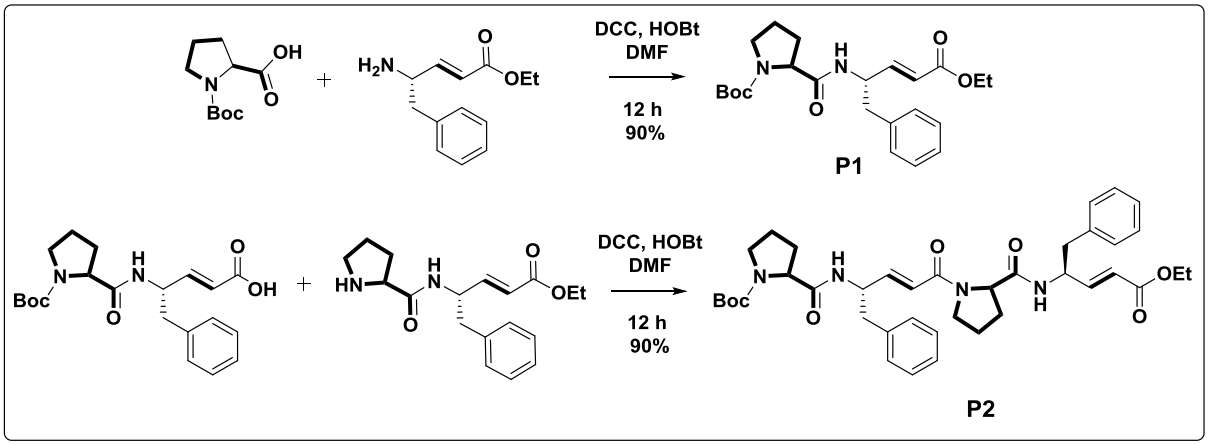

Boc-Pro-dγPhe-COOEt (P2): White colour solid; yield 90%; ^{1}H NMR (500 MHz, $CDCl_3$) δ 7.16 (m, 5H, aromatic), 6.93 (d br, *J*=14.6 Hz, 1H, β-vinyl -CH), 5.89 (dd, *J*=15.6 Hz, *J*=1.5 Hz, 1H, α-vinyl -CH), 4.94 (m br, 1H, -γ dgF-CH), 4.12-4.23 (m, 3H, pro-CH & -OCH_2 of dgF), 2.7-3.35 (m, 4H, CH_2 of pro & ω CH_2 of dgF), 1.63-2.20 (m, 4H, -CH_2-CH_2- of pro), 1.42 (s, 9H, ^{t}Bu), 1.23 (t, *J*=7 Hz, 3H, CH_3 of dgF); ^{13}C NMR (100 MHz, CDCL3) δ 171.99, 166.07, 147.05, 136.43,129.10, 128.66, 127.03, 121.17, 81.25, 80.73, 61.42, 60.49, 60.07, 50.39, 47.10, 40.25,

34.02, 30.97, 28.39, 25.02, 25.02, 23.15, 14.25. MALDI TOF/TOF *m/z* value for - $C_{23}H_{32}N_2O_5$ $[M + Na]^+$ 439.22 (cacld) & 439.17 (observed).

Boc-Pro-dγPhe-Pro-dγPhe-OEt (P2): ^{1}H NMR (400 MHz, $CDCl_3$) δ 7.63 (d, 1H), 7.32-7.16 (m, 8H), 7.05 (m, 2H), 6.95 (dd, *J* = 16 Hz, J = 4 Hz, 1H), 6.70 (s, 1H), 6.19 (dd, *J* = 16 Hz, *J* = 2 Hz, 1H), 5.95 (dd, *J* = 16 Hz, J = 4 Hz, 1H), 5.01 (s, 1H), 4.91 (m, 1H), 4.62 (d, *J* = 4 Hz, 1H), 4.29 (bs, 1H), 4.18 (q, *J* = 4 Hz, 2H), 3.40-3.21 (m, 4H), 3.02-2.64 (m, 3H), 2.39 (m, 1H), 2.20 (bs, 1H), 1.96 (bs, 3H), 1.80 (m, 2H), 1.64-1.55 (m, 3H), 1.40 (s, 9H), 1.28 (t, *J* = 8 Hz, 3H); HRMS *m/z* calculated value for $C_{39}H_{50}N_4O_7$ $[M+Na^+]$ is 709.3572 and observed 709.3590.

Synthesis of Hexapeptide Boc-Pro-dγPhe-Pro-dγPhe-Pro-dγPhe-OEt (P3):

Hexapeptide (P3) was synthesized b 4+2 condensation strategy involving Boc-Pro-dγPhe- Pro-dγPhe-COOH and NH_2-Pro-dγPhe-OEt.

Saponification of the ethyl ester of peptide P2: The Boc-Pro-dγPhe-Pro-dγPhe-COOEt (**P2**) (1.4 g, 2 mmol) was dissolved in 10 mL ethanol followed by 1N NaOH (0.16 mg, 4 mmol) was added slowly to the solution. The reaction mixture was stirred for about 4 h. The progress of the reaction was monitored by TLC. After completion of the reaction, ethanol was evaporated under reduced pressure. Then the residue was diluted with water (60 mL), acidified (pH~ 4) with 0.5N HCl and extracted the compound with EtOAc (3 × 60 mL). The combined organic layer was washed with 50 mL brine solution, dried over anhydrous Na_2SO_4 and concentrated under reduced pressure to get free carboxylic (**P2-A**) acid (1.18 g, 90%). The carboxylic acids were directly used for the peptide synthesis without further purification.

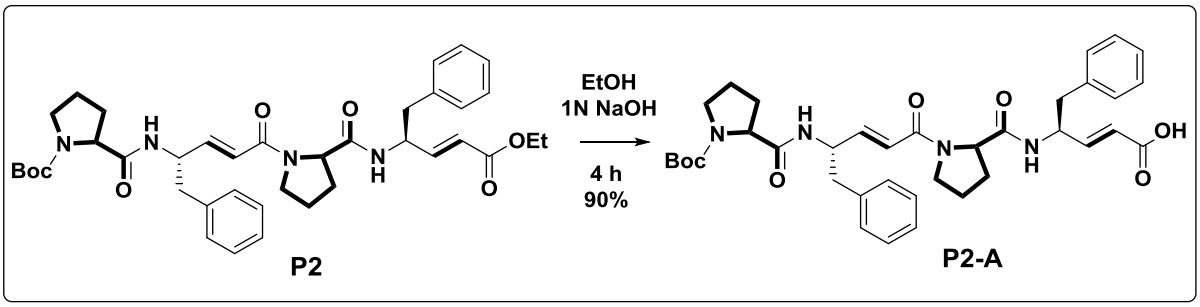

Deprotection of Boc-group from N-Boc- β-nitromethylγ- amino valine ethyl ester: The solution of Boc-Pro-dγPhe-COOEt (**P1**) (1.04 g, 2.5 mmol) in 3 mL of DCM was cooled to 0 °C

in ice bath followed by addition of neat 5 mL of TFA. After completion of the reaction (~ 30 min), solvent was evaporated under reduced pressure. The residue was diluted with water and solid Na_2CO_3 was added at 0 °C until pH of the solution turned to ~10. The aqueous layer was extracted with EtOAc (3 × 50 mL). The combined organic layer was washed with 50 mL of brine solution, dried over anhydrous Na_2SO_4 and concentrated under reduced pressure to *ca*. 2 mL of dipeptide amine **P1-N**.

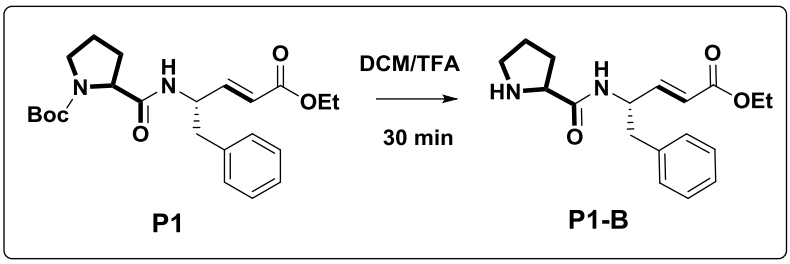

Coupling Strategy: The solution of NH-Pro-dγPhe-COOEt (**P1-N**) in EtOAc (2 mL) was added to the solution of Boc-Pro-dγPhe-Pro-dγPhe-COOH (**P2-A**) (1.18 g, 1.8 mmol) in 3 mL of DMF. Then the mixture was treated with DCC (0.37 g, 1.8 mmol) and HOBt (0.24 g, 1.8 mmol) at ice cold condition. The reaction mixture was stirred for about 24 h at room temperature and the completion of the reaction was monitored by TLC. After completion of the reaction, the reaction mixture was diluted with EtOAc (150 mL) and DCU was filtered through celite packed sintered funnel. Then the filtrate was washed with brine (3 × 50 mL) followed by 0.5N HCl (3 × 50 mL), 10% Na_2CO_3 (1 × 50 mL) and brine solution (1 × 80 mL). The organic layer was dried over anhydrous Na_2SO_4 and concentrated under reduced pressure. The crude product was purified by RP-HPLC using MeOH/H_2O system to get pure product **P** (0.52 g, 30%).

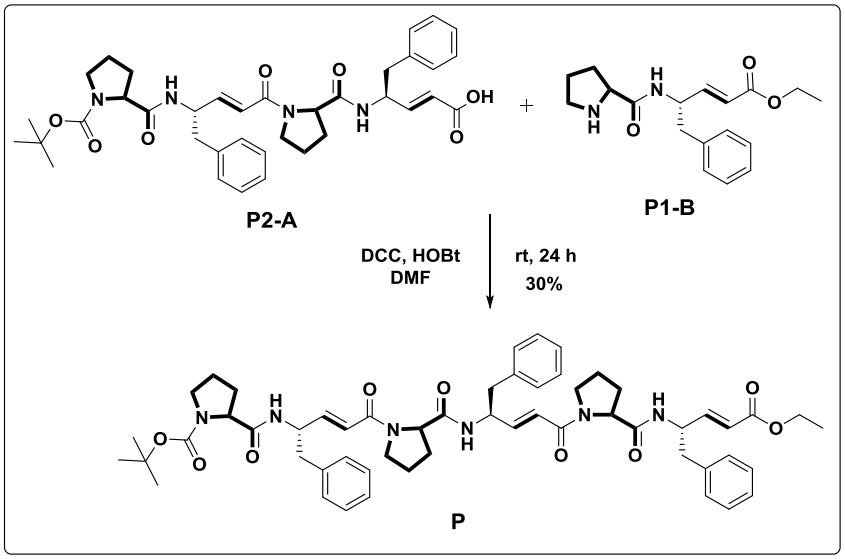

Procedure for the synthesis of tetrapeptide P4:

To the 1 mL dry DMF solution of peptide P2-A (0.65 g, 1 mmol), K_2CO_3 (0.14 g, 1 mmol) and MeI (63 µL, 1 mmol) were added at RT and stirred the reaction for 6 h. After completion of the reaction, mixture was diluted with EtOAc (150 mL) and washed with 0.5N HCl (3 × 50 mL), 10% Na_2CO_3 (1 × 50 mL) and brine solution (1 × 50 mL). The organic layer was dried over anhydrous Na_2SO_4 and concentrated under reduced pressure. The crude product was purified by column chromatography to get pure product **P3** (0.47 g, 70%).

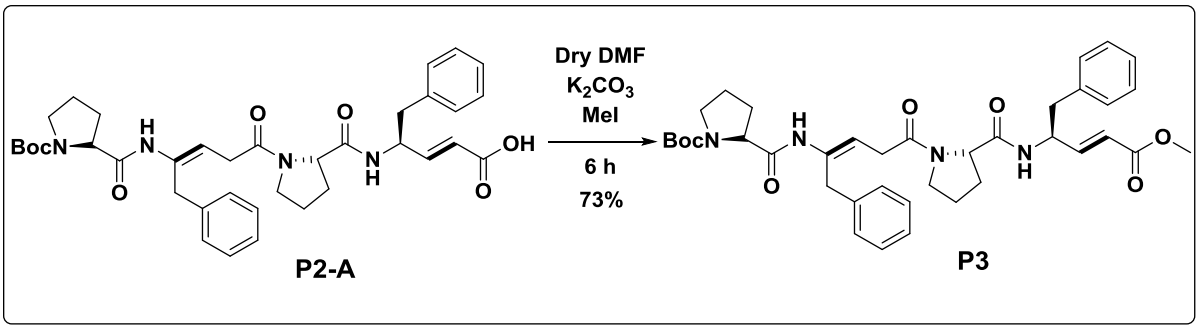

General procedure for the synthesis of α,β-unsaturated γ-amino amides:

Saponification of the ethyl ester of α, β-unsaturated γ-amino acids **(1)***:* The Boc-dγXaa-OEt (**1**) (5 mmol) was dissolved in 10 mL ethanol followed by 1N NaOH (10 mmol) was added slowly to the solution. The reaction mixture was stirred for about 4 h. The progress of the reaction was monitored by TLC. After completion of the reaction, ethanol was evaporated under reduced

pressure. Then the residue was diluted with water (60 mL), acidified (pH~ 4) with 0.5N HCl and extracted the compound with EtOAc (3 × 60 mL). The combined organic layer was washed with 50 mL brine solution, dried over anhydrous Na_2SO_4 and concentrated under reduced pressure to get free carboxylic acid.

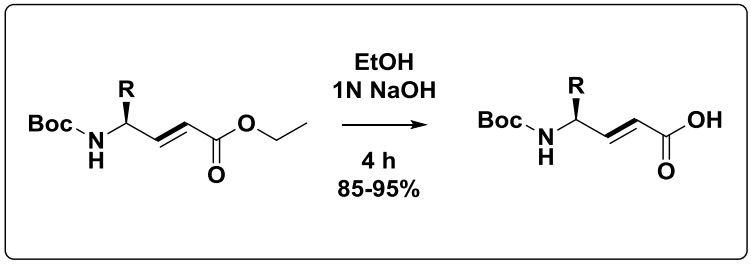

Coupling Strategy: To the 3 mL DMF solution of Boc-dγXaa-COOH (**2**) (3 mmol) diisopropylethylamine (3 mmol), benzylamine (3 mmol) were added. Then the mixture was treated with HBTU (3 mmol) at ice cold condition. The reaction mixture was stirred for about 12 h at room temperature. After completion of the reaction, the reaction mixture was diluted with EtOAc (150 mL) and washed with 0.5N HCl (3 × 50 mL), 10% Na_2CO_3 (1 × 50 mL) and brine solution (1 × 80 mL) respectively. The organic layer was dried over anhydrous Na_2SO_4 and concentrated under reduced pressure. The crude product was purified by column chromatography using DCM/EtOAc system to get pure products **3**.

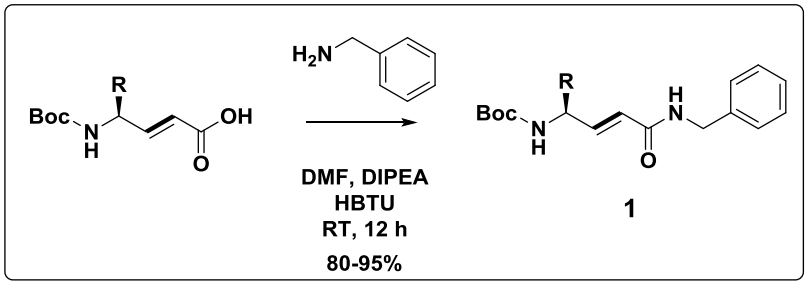

General procedure for the synthesis of γ-lactams from α,β-unsaturated γ-amino amides:

To the dry THF solution of α, β-unsaturated γ-amino amide (**3**, 2 mmol), t-BuOK (6 mmol, 3 eq) was carefully added under N_2 atmosphere and stirred the reaction for overnight at RT or refluxed for 4-5 h. After the completion of reaction, (monitored by TLC) water (30 mL) was added and the reaction mixture was extracted with EtOAc (30 mL × 3) and the combined organic layers were washed with brine (30 mL × 2), dried with Na_2SO_4 and concentrated under reduced

pressure. The product was purified by column chromatography to get pure desired product in 75-92% yields.

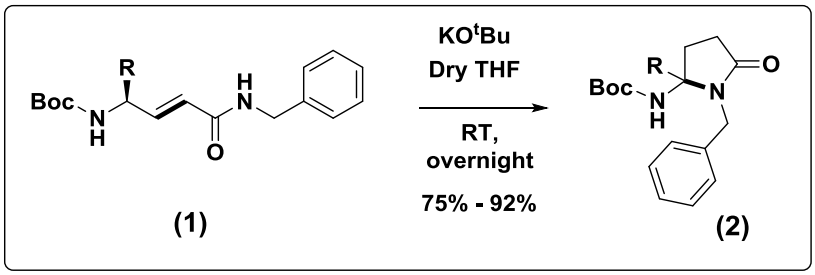

Characterization of compounds 1 and 2:

1. (*S, E*)-*tert-butyl (5-(benzylamino)-5-oxo-1-phenylpent-3-en-2-yl)carbamate* (**1a**):

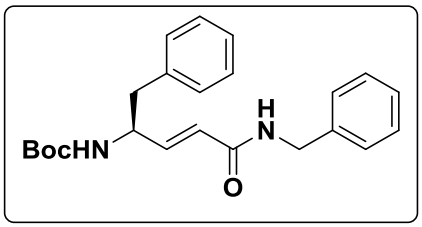

White solid, Yield 95%; ^{1}H NMR (400 MHz, DMSO-d_6) δ 8.56 (t, J = 8 Hz, 1H), 7.33-7.17 (m, 10H), 7.12 (d, J = 12 Hz, 1H), 6.62 (dd, J = 16 Hz, J = 4 Hz, 1H), 5.97 (d, J = 16 Hz, 1H), 4.30 (m, 3H), 2.83-2.70 (m, 2H), 1.31 (s, 9H); **^{13}C NMR** (100 MHz, DMSO-d_6) δ 164.6, 155.0, 143.1, 139.5, 138.4, 129.2, 128.7, 128.3, 128.1, 127.3, 126.8, 126.2, 123.3, 77.8, 52.7, 42.1, 28.2; **HR-MS** *m/z* value calculated for $C_{23}H_{28}N_2O_3$ is 380.2100, observed 380.2122.

2. *(S, E)-tert-butyl (5-(benzylamino)-5-oxopent-3-en-2-yl)carbamate* (**1b**):

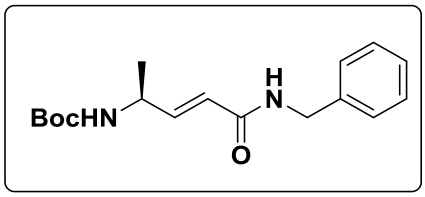

White solid, Yield 83%; ^{1}H NMR (400 MHz, DMSO-d_6) δ 7.34-7.25 (m, 5H), 6.74 (dd, J = 15.4 Hz, J = 5.2 Hz, 1H), 6.10 (bs, 1H), 5.88 (d, 1H, J = 12 Hz), 4.63 (bs, 1H), 4.48 (d, 2H, J = 8 Hz), 4.34 (m, 1H), 1.43 (s, 9H), 1.24 (d, 3H, J = 8 Hz); ^{13}C NMR (100 MHz, DMSO-d_6) δ 165.6,

155.1, 145.5, 138.2, 128.8, 128.0, 127.6, 122.6, 79.8, 47.2, 43.8, 28.5, 20.7; HRMS *m/z* value calculated for $C_{17}H_{24}N_2O_3$ is 304.1787, found 304.1790.

3. (*S*, *E*)-*tert-butyl (1-(benzylamino)-6-methyl-1-oxohept-2-en-4-yl)carbamate* (**1c**):

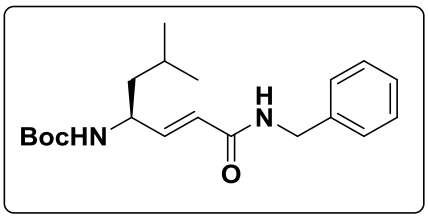

White solid, Yield 83%; ^{1}H NMR (400 MHz, DMSO-d_6) δ 8.55 (t, J = 8 Hz, 1H), 7.33-7.23 (m, 5H), 7.00 (d, J = 8 Hz, 1H), 6.52 (dd, J = 12 Hz, J = 4 Hz, 1H), 5.97 (d, J = 16 Hz, 1H), 4.31 (m, 2H), 4.11 (m, 1H), 1.57 (m, 1H), 1.38 (s, 9H), 1.26 (m, 1H), 0.87 (d, J = 4 Hz, 6H); ^{13}C NMR (100 MHz, DMSO-d_6) δ 164.7, 155.1, 143.9, 139.5, 128.7, 128.3, 127.7, 127.4, 126.8, 122.9, 77.7, 49.3, 42.9, 42.1, 28.3, 24.3, 22.7, 21.9; HRMS *m/z* value calculated for $C_{20}H_{30}N_2O_3$ is 346.2256, observed 346.2262.

4. (*S*, *E*)-*tert-butyl (6-(benzylamino)-2-methyl-6-oxohex-4-en-3-yl)carbamate* (**1d**):

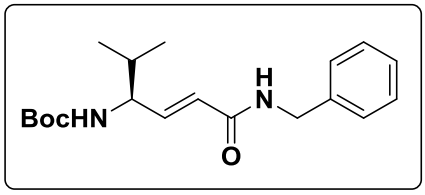

White solid, Yield 88%; ^{1}H NMR (400 MHz, DMSO-d_6) δ 8.54 (t, J = 8 Hz, 1H), 7.33-7.21 (m, 5H), 7.01 (d, J = 12 Hz, 1H), 6.55 (dd, J = 16 Hz, J = 4 Hz, 1H), 5.98 (d, J = 16 Hz, 1H), 4.31 (m, 2H), 3.85 (m, 1H), 1.72 (m, 1H), 1.38 (s, 9H), 0.83 (m, 6H); ^{13}C NMR (100 MHz, DMSO-d_6) δ 164.7, 155.3, 142.0, 139.5, 128.3, 127.4, 126.8, 124.3, 77.7, 57.0, 40.1, 38.3, 31.9, 28.3, 19.1, 18.7; HR-MS *m/z* value calculated for $C_{19}H_{28}N_2O_3$ is 332.2100, observed 332.2130.

5. (*S*,*E*)-*tert-butyl(5-((2-(1H-indol-3-yl)ethyl)amino)-5-oxo-1-phenylpent-3-en-2-yl) carbamate* (**1e**):

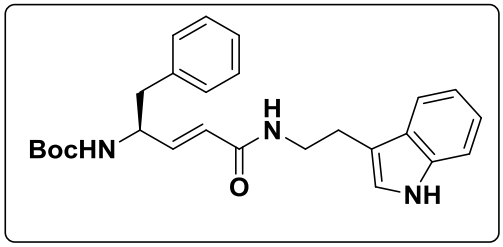

Brown color solid, Yield 80%; ^{1}H NMR (400 MHz, DMSO-d_6) δ 10.81 (s, 1H), 8.16 (t, J = 8 Hz, 1H), 7.52 (d, J = 8 Hz, 1H), 7.34-6.95 (m, 12 H), 6.58 (dd, J = 16 Hz, J = 4 Hz, 1H), 5.90 (d, J = 16 Hz, 1H), 4.29 (m, 1H), 3.38 (m, 2H), 2.78 (m, 4H), 1.31 (s, 9H); ^{13}C NMR (100 MHz, DMSO-d_6) δ 164.6, 154.9, 142.4, 138.4, 136.2, 129.2, 128.1, 127.2, 126.1, 123.6, 122.6, 120.9, 118.2, 111.8, 111.4, 77.7, 52.7, 28.2, 25.2; HRMS *m/z* value calculated for $C_{26}H_{31}N_3O_3$ is 433.2365, observed 433.2369.

6. *tert-butyl ((4S, 5S, E)-1-(benzylamino)-5-methyl-1-oxohept-2-en-4-yl)carbamate* (1**f**):

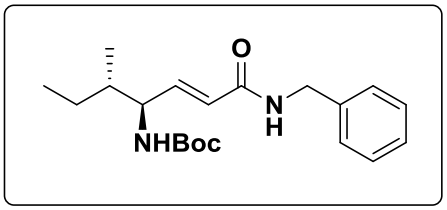

White solid, Yield 89%; ^{1}H NMR (400 MHz, DMSO-d_6) δ 8.55 (t, J = 8 Hz, 1H), 7.33-7.04 (m, 5H), 7.05 (d, J = 8 Hz, 1H), 6.53 (dd, J = 16 Hz, J = 8 Hz, 1H), 5.97 (d, J = 16 Hz, 1H), 4.32 (m, 2H), 3.93 (m, 1H), 1.49 (m, 1H), 1.38 (s, 9H), 1.08 (m, 1H), 0.82 (m, 6H); ^{13}C NMR (100 MHz, DMSO-d_6) δ 164.6, 155.2, 141.7, 139.5, 128.3, 127.4, 126.8, 124.4, 77.7, 55.6, 42.2, 38.3, 28.3, 25.2, 15.4, 11.2; HRMS *m/z* value calculated for $C_{20}H_{30}N_2O_3$ is 346.2256, observed 346.2257.

7. *tert-butyl ((S, E)-5-oxo-1-phenyl-5-(((R)-1-phenylethyl)amino)pent-3-en-2-yl)carbamate* (**1g**):

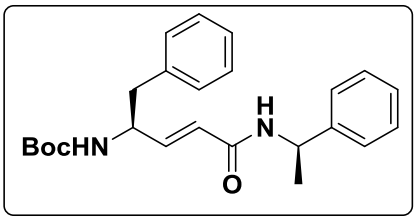

White solid, Yield 81%; ^{1}H NMR (400 MHz, DMSO-d_6) δ 7.34-7.52 (m, 10H), 6.78 (d, 1H, J = 16 Hz), 5.78 (d, 2H, J = 16 Hz), 5.20-5.11 (m, 1H), 4.55 (s, 2H), 2.91-2.83 (m, 2H), 1.49 (d, 3H, J = 8 Hz), 1.38 (s, 9H); ^{13}C NMR (100 MHz, DMSO-d_6) δ 164.4, 155.2, 143.6, 143.1, 136.7, 129.6, 128.8, 128.6, 127.5, 126.9, 126.4, 123.7, 79.9, 52.5, 49.0, 41.2, 38.7, 28.4, 23.6, 21.8.; HRMS *m/z* value calculated for $C_{24}H_{30}N_2O_3$ is 394.2256, found 394.2264.

8. *tert-butyl (1,2-dibenzyl-5-oxopyrrolidin-2-yl)carbamate* (**2a**):

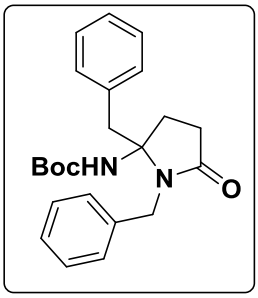

Colorless solid, Yield 92%; ^{1}H NMR (400 MHz, $CDCl_3$) δ 7.41 (d, 2H, J = 8 Hz), 7.33-7.24 (m, 6H), 7.09 (d, 2H, J = 4 Hz), 4.92 (s, 1H), 4.61 (s, 2H), 3.06-2.95 (m, 2H), 2.51-2.48 (m, 1H), 2.33-2.27 (m, 2H), 1.92-1.86 (m, 1H), 1.32 (s, 9H); ^{13}C NMR (100 MHz, $CDCl_3$) δ 175.5, 153.5, 138.4, 134.4, 130.3, 128.9, 128.7, 128.4, 127.6, 127.4, 77.8, 44.4, 43.4, 30.0, 29.6, 28.3; HRMS *m/z* value calculated for $C_{23}H_{28}N_2O_3$ is 380.2100, found 380.2144.

9. *tert-butyl (1-benzyl-2-methyl-5-oxopyrrolidin-2-yl)carbamate* (**2b**):

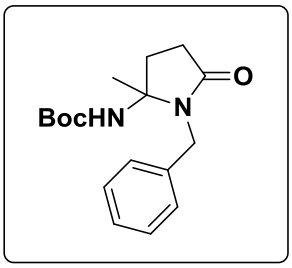

Colorless solid, Yield 85%; ^{1}H NMR (400 MHz, $CDCl_3$) δ 7.29-7.20 (m, 5H), 4.89 (bs, 1H), 4.60 (d, 1H, J = 12 Hz), 4.27 (d, 1H, J = 12 Hz), 2.81 (bs, 1H), 2.55-2.40 (m, 2H), 2.08-2.01 (m, 1H), 1.37 (s, 9H), 1.33 (s, 3H); ^{13}C NMR (100 MHz, $CDCl_3$) δ 175.5, 153.4, 138.6, 128.6, 127.9, 127.2, 80.1, 74.8, 42.5, 32.6, 29.8, 28.6, 28.4; HRMS *m/z* value calculated for $C_{17}H_{24}N_2O_3$ is 305.1860, found 305.1897.

10. *tert-butyl (1-benzyl-2-isobutyl-5-oxopyrrolidin-2-yl)carbamate* (**2c**):

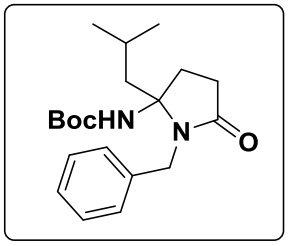

Pale yellow thick liquid, Yield 75%; ^{1}H NMR (400 MHz, $CDCl_3$) δ 7.29-7.12 (m, 5H), 4.79 (bs, 1H), 4.33 (bs, 2H), 2.75 (m, 1H), 2.45-2.08 (m, 3H), 1.61 (m, 1H), 1.36 (m, 2H), 1.25 (s, 9H), 0.89-0.73 (m, 6H); ^{13}C NMR (100 MHz, $CDCl_3$) δ ; 175.8, 156.6, 137.2, 136.4, 128.5, 127.3, 110.1, 79.8, 43.7, 29.1, 28.4, 26.8, 23.6, 21.3; HRMS *m/z* value calculated for $C_{26}H_{31}N_3O_3$ is 346.2256, observed 346.2260.

11. *tert-butyl (1-benzyl-2-isopropyl-5-oxopyrrolidin-2-yl)carbamate* (**2d**):

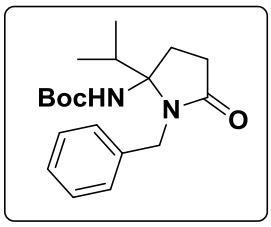

Colorless solid, Yield 90%; ^{1}H NMR (400 MHz, $CDCl_3$) δ 7.34-7.20 (m, 5H), 4.85 (s, 1H), 4.43-4.23 (m, 2H), 2.87-2.84 (m,1H), 2.35-1.98 (m, 4H), 1.31 (s, 9H), 0.96 (d, 3H, J = 8 Hz), 0.61 (bs, 3H).; ^{13}C NMR (100 MHz, $CDCl_3$) δ 176.2, 153.4, 138.2, 128.7, 128.5, 127.8, 127.2, 80.6, 79.7, 43.7, 42.7, 40.9, 35.6, 34.5, 30.0, 29.8, 28.3, 24.1, 18.3, 16.7, 15.8.; HRMS *m/z* value calculated for $C_{19}H_{28}N_2O_3$ is 332.2100, observed 332.2121.

12. *tert-butyl (1-(2-(1H-indol-3-yl)ethyl)-2-benzyl-5-oxopyrrolidin-2-yl)carbamate* (**2e**):

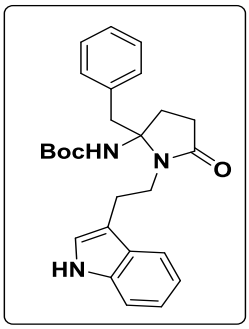

Brown color solid, Yield 85%; ^{1}H NMR (400 MHz, $CDCl_3$) δ 7.41 (d, J = 8 Hz, 2H), 7.33-7.24 (m, 8H), 7.08 (m, 2H), 4.92 (s, 1H), 4.61 (s, 2H), 3.01 (m, 2H), 2.48 (m, 1H), 2.31 (m, 2H), 1.90 (m, 1H), 1.32 (s, 9H); ^{13}C NMR (100 MHz, $CDCl_3$) δ 175.5, 138.4, 134.4, 130.3, 128.9, 128.7, 128.4, 127.6, 127.4, 77.8, 44.4, 43.4, 30.0, 29.6, 28.3; HRMS *m/z* value calculated for $C_{26}H_{31}N_3O_3$ is 433.2365, observed 433.2361.

13. *tert-butyl (1-benzyl-2-((S)-sec-butyl)-5-oxopyrrolidin-2-yl)carbamate* (**2f**):

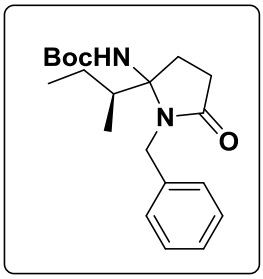

Pale yellow solid, Yield 90%; ^{1}H NMR (400 MHz, $CDCl_3$) δ 7.38-7.16 (m, 10H), 4.85 (bs, 1H) (major), 4.73 (bs, 1H) (minor), 4.52-4.41 (m, 2H) (major), 4.16 (m, 2H) (minor), 2.36-2.17 (m, 4H) (major), 2.06 (m, 2H) (minor), 1.85 (m, 2H) (minor), 1.59 (m, 2H), 1.35 (bs, 9H) (major), 1.28 (bs, 9H) (minor), 1.10 (m, 2H) (minor), 0.93 (m, 6H) (major), 0.65 (bs, 2H) (minor), 0.46 (bs, 2H) (minor); HRMS *m/z* value calculated for $C_{20}H_{30}N_2O_3$ is 346.2256, observed 346.2261.

14. *Compound* (**2g**):

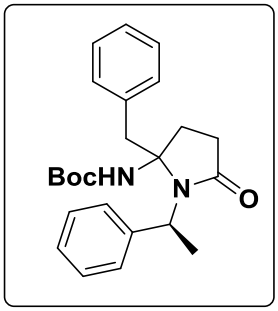

Pale yellow solid, Yield 77%; ^{1}H NMR (400 MHz, $CDCl_3$) δ 7.62-6.98 (m, 10H), 5.11 (s, 1H, Boc-N*H*, major), 4.93 (Boc-N*H*, minor) 4.64 (q, *J* = 8 Hz, 1H), 3.04-2.59 (m, 3H), 2.37-2.19 (m, 4H), 1.88 (d, *J* = 8 Hz, CH_3, minor), 1.84 (d, *J* = 8 Hz, 3H, CH_3 major), 1.46 (s, 9H, Boc minor), 1.26 (s, 9H, Boc major); ^{13}C NMR (100 MHz, $CDCl_3$) δ 175.8 (major), 175.1 (minor), 143.4 (major), 142,4 (minor), 134.4, 130.3 (major), 130.2 (minor), 128.9 (minor), 128.8 (major), 128.6, 128.3, 127.8, 127.4, 127.2, 126.3 (major), 126.2 (minor), 78.5 (minor), 78.4 (major), 53.0, 45.8, 30.3 (major), 30.2 (minor), 29.8, 28.4 (major), 28.2 (minor), 20.0 (minor), 19.7 (major); HRMS *m/z* value calculated for $C_{24}H_{30}N_2O_3$ is 394.2256, found 394.2250.

4.8 References:

1. (a) Gellman, S. H. *Acc. Chem. Res*. **1998**, *31*, 173. (b) Hill, D. J.; Mio, M. J.; Prince, R. B.; Hughes, T. S.; Moore, J. S. *Chem. Rev*. **2001**, *101*, 3893. (c) Goodman, C. M.; Choi, S.; Shandler, S.; DeGrado, W. F. *Nat. Chem. Biol*. **2007**, *3*, 252. (d) Seebach, D.; Gardiner, *J. Acc. Chem. Res*. **2008**, *41*, 1366. (e) Martinek, T. A.; Fülöp, F. *Chem. Soc. Rev*. **2012**, *41*, 687. (f) Cheng, R. P.; Gellman, S. H.; DeGrado, W. F. *Chem. Rev*. **2001**, *101*, 3219. (g) Seebach, D.; Hook, D. F.; Glattli, A. *Biopolymers* **2006**, *84*, 23.
2. (a) Appella, D. H.; Christianson, L. A.; Karle, I. L.; Powell, D. R.; Gellman, S. H. *J. Am. Chem. Soc*. **1996**, *118*, 13071. (b) Appella, D. H.; Christianson, L. A.; Klein, D. A.; Powell, D. R.; Huang, X. L.; Barchi, J. J.; Gellman, S. H. *Nature* **1997**, *387*, 381.(c) Martinek, T. A.; Mándity, I. M.; Fülöp, L.; Tóth, G. K.; Vass, E.; Hollósi, M.; Forró, E.; Fülöp, F. *J. Am. Chem. Soc*. **2006**, *128*, 13539. (d) Mándity, I. M.; Fülöp, L.; Vass, E.; Tóth, G. K.; Martinek, T. A.; Fülöp, F. *Org. Lett*. **2010**, *12*, 5584. (e) Hayen, A.; Schmitt, M. A.; Ngassa, F.; Thomasson, K. A.; Gellman, S. H. *Angew. Chem., Int. Ed*. **2004**, *43*, 505. (f) Choi, S. H.; Guzei, I. A.; Spencer, L. C.; Gellman, S. H. *J. Am. Chem. Soc*. **2008**, *130*, 6544. (g) Choi, S. H.; Guzei, I. A.; Spencer, L. C.; Gellman, S. H. *J. Am. Chem. Soc*.

2009, *131*, 2917. (h) Choi, S. H.; Guzei, I. A.; Spencer, L. C.; Gellman, S. H. *J. Am. Chem. Soc*. **2010**, *132*, 13879. (i) Seebach, D.; Gademann, K.; Schreiber, J. V.; Matthews, J. L.; Hintermann, T.; Jaun, B.; Oberer, L.; Hommel, U.; Widmer, H. *Helv.Chim. Acta* **1997**, *80*, 2033. (j) Rueping, M.; Schreiber, J. V.; Lelais, G.; Jaun, B.; Seebach, D. *Helv. Chim. Acta* **2002**, *85*, 2577.

3. (a) Hanessian, S.; Luo, X. H.; Schaum, R.; Michnick, S. *J. Am. Chem. Soc*. **1998**, *120*, 8569. (b) Hanessian, S.; Luo, X. H.; Schaum, R. *Tetrahedron Lett*. **1999**, *40*, 4925. (c) Seebach, D.; Brenner, M.; Rueping, M.; Schweizer, B.; Jaun, B. *Chem. Commun*. **2001**, 207. (d) Woll, M. G.; Lai, J. R.; Guzei, I. A.; Taylor, S. J. C.; Smith, M. E. B.; Gellman, S. H. *J. Am. Chem. Soc*. **2001**, *123*, 11077. (e) Khurram, M.; Qureshi, N.; Smith, M. D. *Chem. Commun*. **2006**, 5006. (f) Jones, C. R.; Qureshi, M. K. N.; Truscott, F. R.; Hsu, S. T. D.; Morrison, A. J.; Smith, M. D. *Angew. Chem., Int. Ed*. **2008**, *47*, 7099. (g) Vasudev, P. G.; Ananda, K.; Chatterjee, S.; Aravinda, S.; Shamala, N.; Balaram, P. *J. Am. Chem. Soc*. **2007**, *129*, 4039. (h) Chatterjee, S.; Vasudev, P. G.; Raghothama, S.; Ramakrishnan, C.; Shamala, N.; Balaram, P. *J. Am. Chem. Soc*. **2009**, *131*, 5956. (i) Vasudev, P. G.; Chatterjee, S.; Shamala, N.; Balaram, P. *Acc. Chem. Res*. **2009**, *42*, 1628. (j) Horne, W. S.; Gellman, S. H. *Acc. Chem. Res*. **2008**, *41*, 1399.
4. (a) Driggers, E. M.; Hale, S. P.; Lee, J.; Terrett, N. K. *Nature Rev. Drug Disc*. **2008**, *7*, 608. (b) White, C. J.; Yudin, A. K. *Nature Chem*. **2011**, *3*, 509.
5. (a) Azzarito, V.; Long, K.; Murphy, N. S.; Wilson, A. J. *Nat. Chem*. **2013**, *5*, 161. (b) Jayatunga, M. K. P.; Thompson, S.; Hamilton, A. D. *Bioorg. Med. Chem. Lett*. **2013**, *24*, 717. (c) Kulikov, O. V.; Thompson, S.; Xu, H.; Incarvito, C. D.; Scott, R. T. W.; Saraogi, I.; Nevola, L.; Hamilton, A. D. *Eur. J. Org. Chem*. **2013**, 3433.(d) Thompson, A. D.; Hamilton, S. *Org. Biomol. Chem*. **2012**, *10*, 5780. (e) Tosovsk, P.; Arora, P. S. *Org. Lett*. **2010**, *12*, 1588. (f) Marimganti, S.; Cheemala, M. N.; Ahn, J.-M. *Org. Lett*. **2009**, *11*, 4418. (g) German, E. A.; Ross, J. E.; Knipe, P. C.; Don, M. F.; Thompson, S.; Hamilton, A. D. *Angew. Chem. Int. Ed*. **2015**, *54*, 2649.
6. (a) Saragovi, H. U.; Fitzpatrick, D.; Raktabutr, A.; Nakanishi, H.; Kahn, M.; Greene, M. I. *Science* **1991**, *253*, 792. (b) Vassilev, L. T.; Vu, B. T.; Graves, B.; Carvajal, D.; Podlaski, F.; Filipovic, Z.; Kong, N.; Kammlott, U.; Lukacs, C.; Klein, C.; Fotouhi, N.; Liu, D. A. *Science* **2004**, *303*, 844. (c) Arkin, M. R.; Wells, J. A. *Nature. Rev*. **2004**, *3*,

301. (d) Milroy, L. G.; Grossmann, T. N.; Hennig, S.; Brunsveld, L.; Ottmann, C. Chem. Rev. *Chem. Rev*. **2014**, *114*, 4695.

7. (a) Bandyopadhyay, A.; Mali, S. M.; Lunawat, P.; Raja, K. M. P.; Gopi, H. N. *Org. Lett.* **2011**, *13*, 4482. (c) Mali, S. M.; Bandyopadhyay, A.; Jadhav, S. V.; Ganesh Kumar, M.; Gopi, H. N. *Org. Biomol. Chem*. **2011**, *9*, 6566. (d) Ganesh Kumar, M.; Benke, S. N.; Raja, K. M. P.; Gopi, H. N. *Chem. Comm*. **2015**, *15*, 13397. (e) Bandyopadhyay, A.; Gopi, H. N. *Org. Lett*. **2012**, *14*, 2770.
8. (a) Li, S. C.; Goto, N. K.; Williams, K. A.; Deber, C. M. *Proc. Natl. Acad. Sci. USA.* **1996**, *93*, 6676. (b) Sansom, M. S. P.; Weinstein, H. *Trends Pharmacol. Sci*. **2000**, *21*, 445.
9. (a) Lohr, F.; Jenniches, I.; Frizler, M.; Meehan, M. J.; Sylvester, M.; Schmitz, A.; Gütschow, M.; Dorrestein, P. C.; König, G. M.; Schäberle, T. F. *Chem. Sci*. **2013**, *4*, 4175. (b) Gay, D. C.; Spear, P. J.; Keatinge-Clay, A. T. *ACS Chem. Bio*. **2014**, *9*, 2374.

4.9 Appendix I: Characterization Data for Synthesized Compounds and Peptides

Designation	Description	Page
Boc-Pro-dγPhe-OEt (**P1**)	^{1}H NMR	209
Boc-Pro-dγPhe-Pro-dγPhe-OEt (**P2**)	^{1}H NMR	209
Boc-Pro-dγPhe-Pro-dγPhe-Pro-dγPhe-OEt (**P2**)	MALDI-TOF/TOF	210
Compounds **1(a-g)** &	^{1}H & ^{13}C NMR	210-222
Compounds **2(a-g)**		

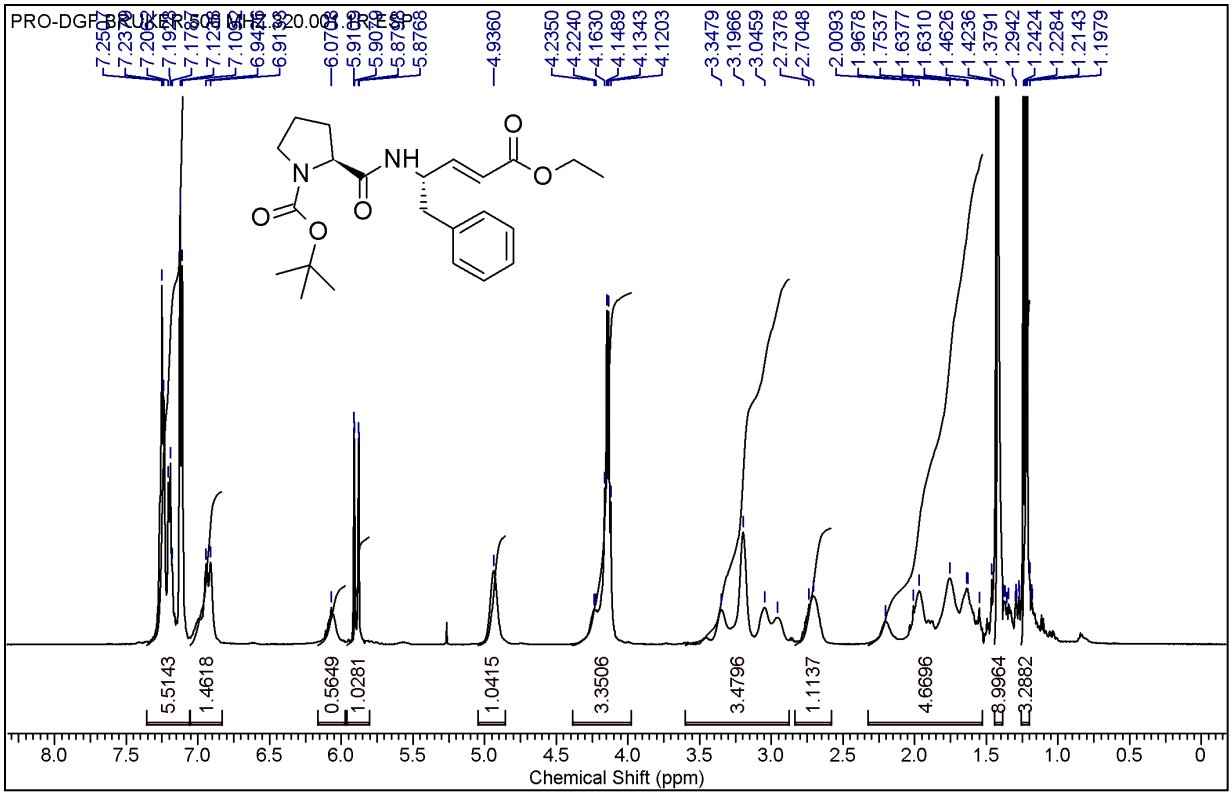
PRO-DGF BRUKER 500 MHz 21.920.03 DPTES
7.2507
7.2307
7.2106
7.1997
7.1763
7.1208
7.1004
6.9445
6.9193
6.0703
5.9129
5.9079
5.8769
5.8768
4.9360
4.2350
4.2240
4.1630
4.1489
4.1343
4.1203
3.3479
3.1966
3.0459
2.7378
2.7048
2.0093
1.9678
1.7537
1.6377
1.6310
1.4626
1.4236
1.3791
1.2942
1.2424
1.2284
1.2143
1.1979
NH
O
N
O
O
O
O
5.5143
1.4618
0.5649
1.0281
1.0415
3.3506
3.4796
1.1137
4.6696
8.9964
3.2882
8.0
7.5
7.0
6.5
6.0
5.5
5.0
4.5
4.0
3.5
3.0
2.5
2.0
1.5
1.0
0.5
0
Chemical Shift (ppm)

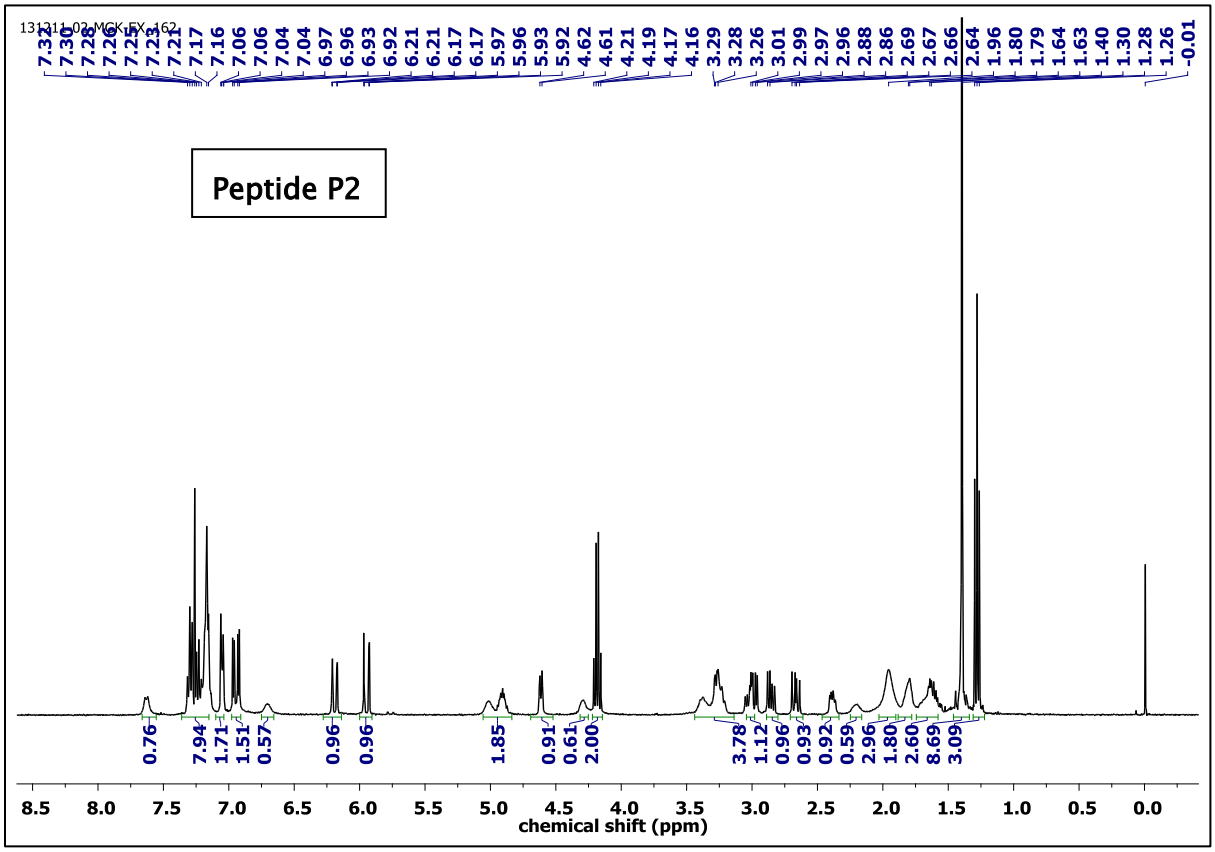
131211_02_MGK_EX_162
7.31
7.30
7.26
7.25
7.23
7.21
7.17
7.16
7.06
7.06
7.04
7.04
6.97
6.96
6.93
6.92
6.21
6.21
6.17
6.17
5.97
5.96
5.93
5.92
4.62
4.61
4.21
4.19
4.17
4.16
3.29
3.28
3.26
3.01
2.99
2.97
2.96
2.88
2.86
2.69
2.67
2.66
2.64
1.96
1.80
1.79
1.64
1.63
1.40
1.30
1.28
1.26
-0.01
Peptide P2
0.76
7.94
1.71
1.51
0.57
0.96
0.96
1.85
0.91
0.61
2.00
3.78
1.12
0.96
0.93
0.92
0.59
2.96
1.80
2.60
8.69
3.09
8.5
8.0
7.5
7.0
6.5
6.0
5.5
5.0
4.5
4.0
3.5
3.0
2.5
2.0
1.5
1.0
0.5
0.0
chemical shift (ppm)

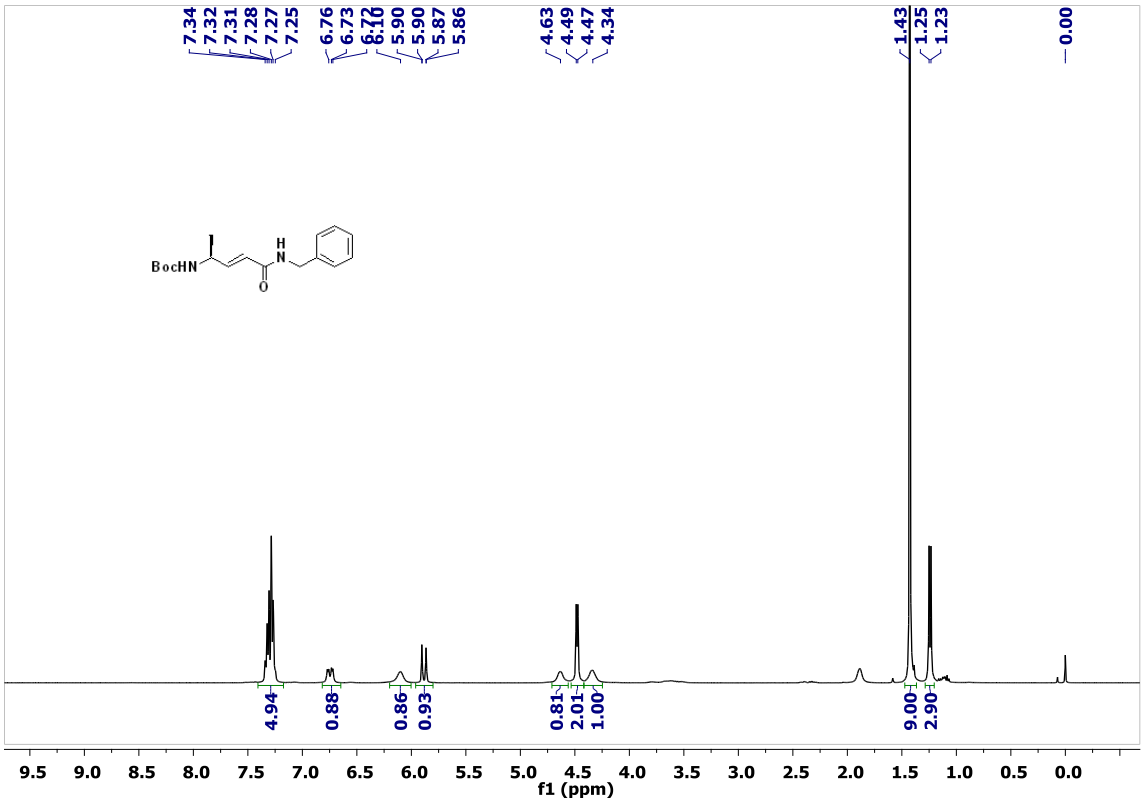
7.34
7.32
7.31
7.28
7.27
7.25
6.76
6.73
6.70
6.10
5.90
5.90
5.87
5.86
4.63
4.49
4.47
4.34
1.43
1.25
1.23
0.00
BocHN
H
N
O
4.94
0.88
0.86
0.93
0.81
2.01
1.00
9.00
2.90
9.5 9.0 8.5 8.0 7.5 7.0 6.5 6.0 5.5 5.0 4.5 4.0 3.5 3.0 2.5 2.0 1.5 1.0 0.5 0.0
f1 (ppm)

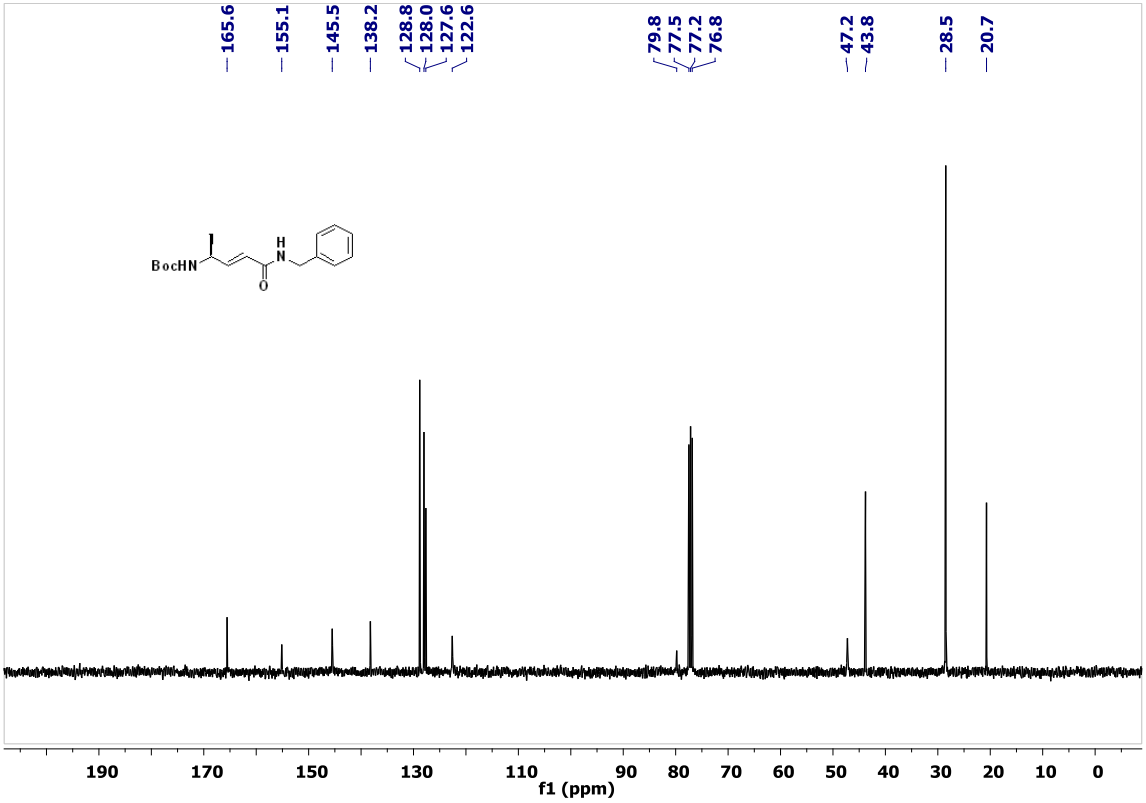
165.6
155.1
145.5
138.2
128.8
128.0
127.6
122.6
79.8
77.5
77.2
76.8
47.2
43.8
28.5
20.7
BocHN
H
N
O
190 170 150 130 110 90 80 70 60 50 40 30 20 10 0
f1 (ppm)

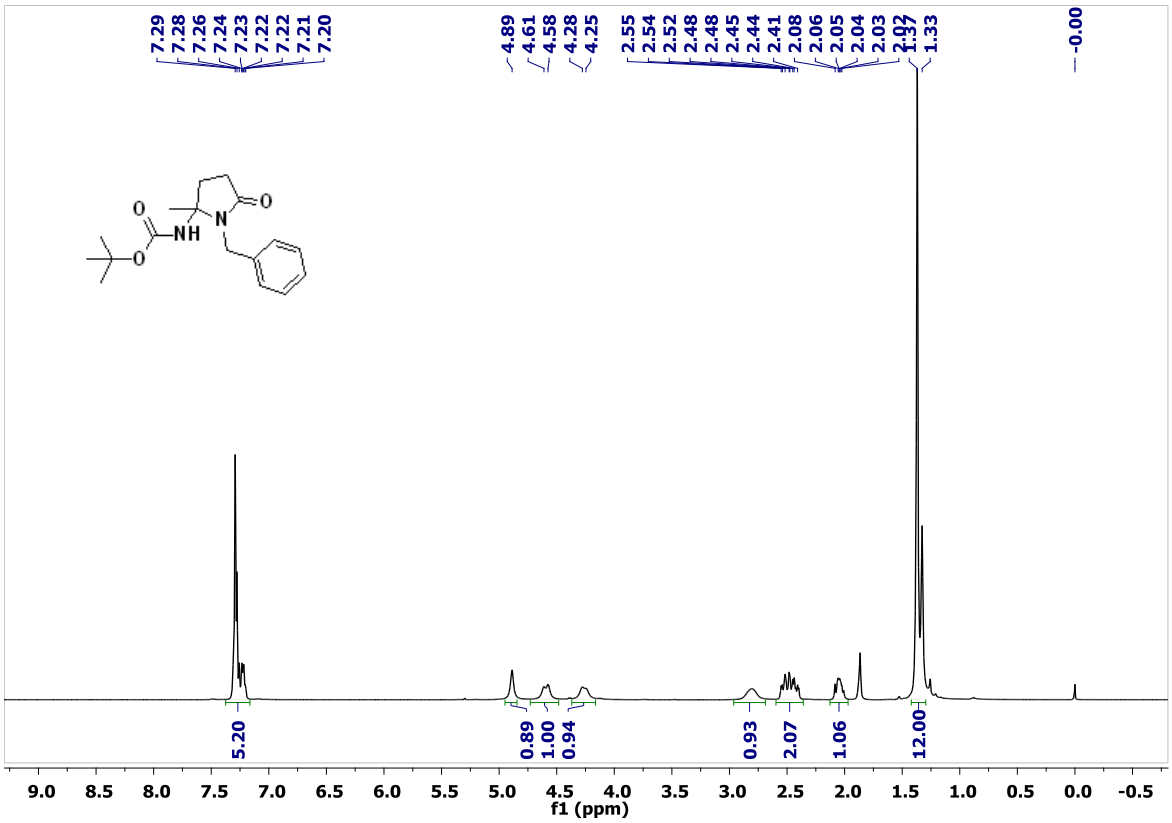
7.29
7.28
7.26
7.24
7.23
7.22
7.22
7.21
7.20
4.89
4.61
4.58
4.28
4.25
2.55
2.54
2.52
2.48
2.48
2.45
2.44
2.41
2.08
2.06
2.05
2.04
2.03
2.02
1.37
1.33
-0.00
5.20
0.89
1.00
0.94
0.93
2.07
1.06
12.00
9.0 8.5 8.0 7.5 7.0 6.5 6.0 5.5 5.0 4.5 4.0 3.5 3.0 2.5 2.0 1.5 1.0 0.5 0.0 -0.5
f1 (ppm)

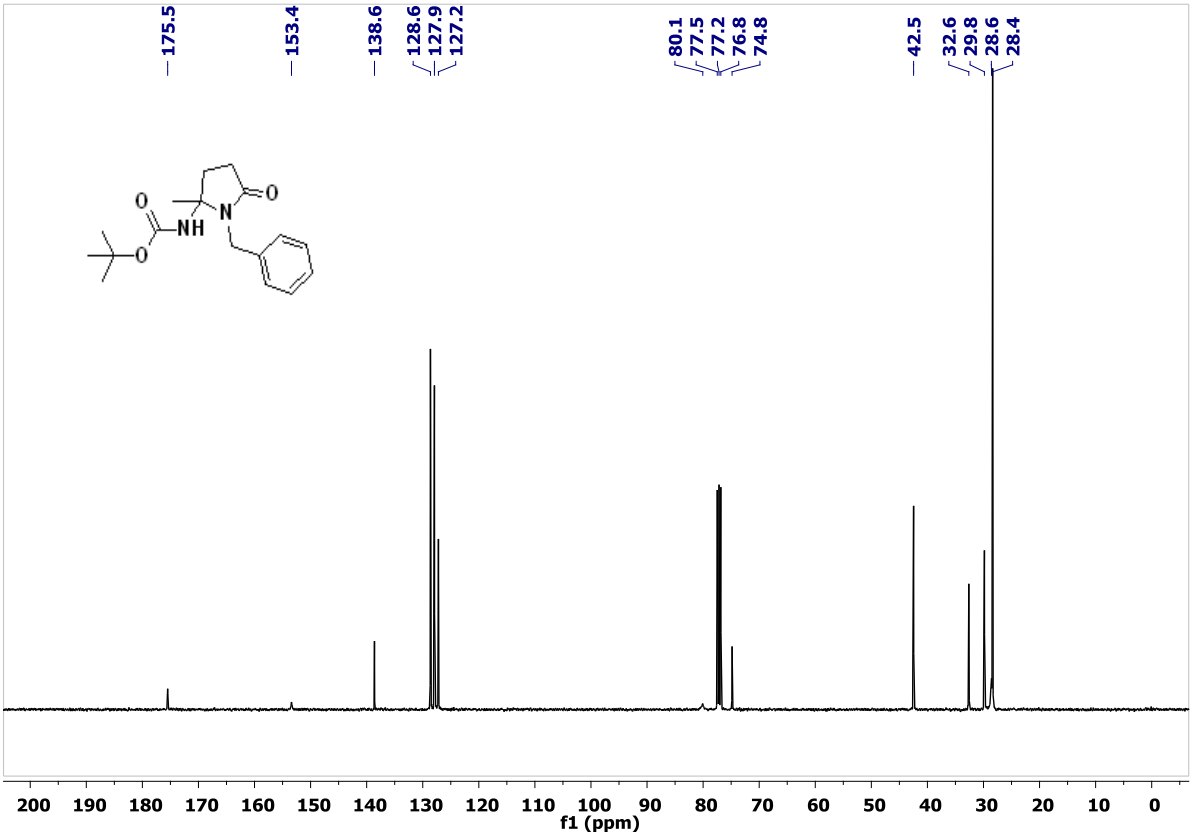
175.5
153.4
138.6
128.6
127.9
127.2
80.1
77.5
77.2
76.8
74.8
42.5
32.6
29.8
28.6
28.4
200 190 180 170 160 150 140 130 120 110 100 90 80 70 60 50 40 30 20 10 0
f1 (ppm)

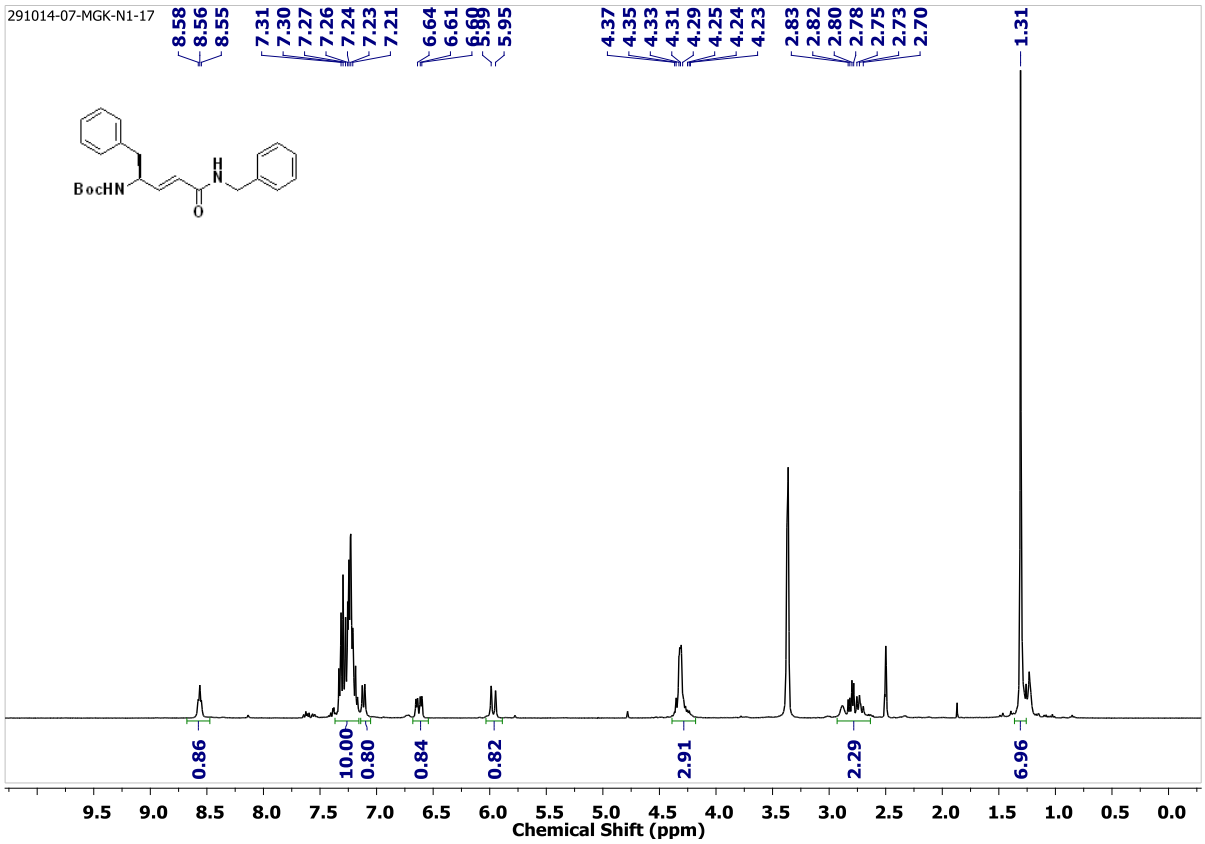
291014-07-MGK-N1-17
8.58
8.56
8.55
7.31
7.30
7.27
7.26
7.24
7.23
7.21
6.64
6.61
6.60
5.99
5.95
4.37
4.35
4.33
4.31
4.29
4.25
4.24
4.23
2.83
2.82
2.80
2.78
2.75
2.73
2.70
1.31
BocHN
H
N
O
0.86
10.00
0.80
0.84
0.82
2.91
2.29
6.96
9.5 9.0 8.5 8.0 7.5 7.0 6.5 6.0 5.5 5.0 4.5 4.0 3.5 3.0 2.5 2.0 1.5 1.0 0.5 0.0
Chemical Shift (ppm)

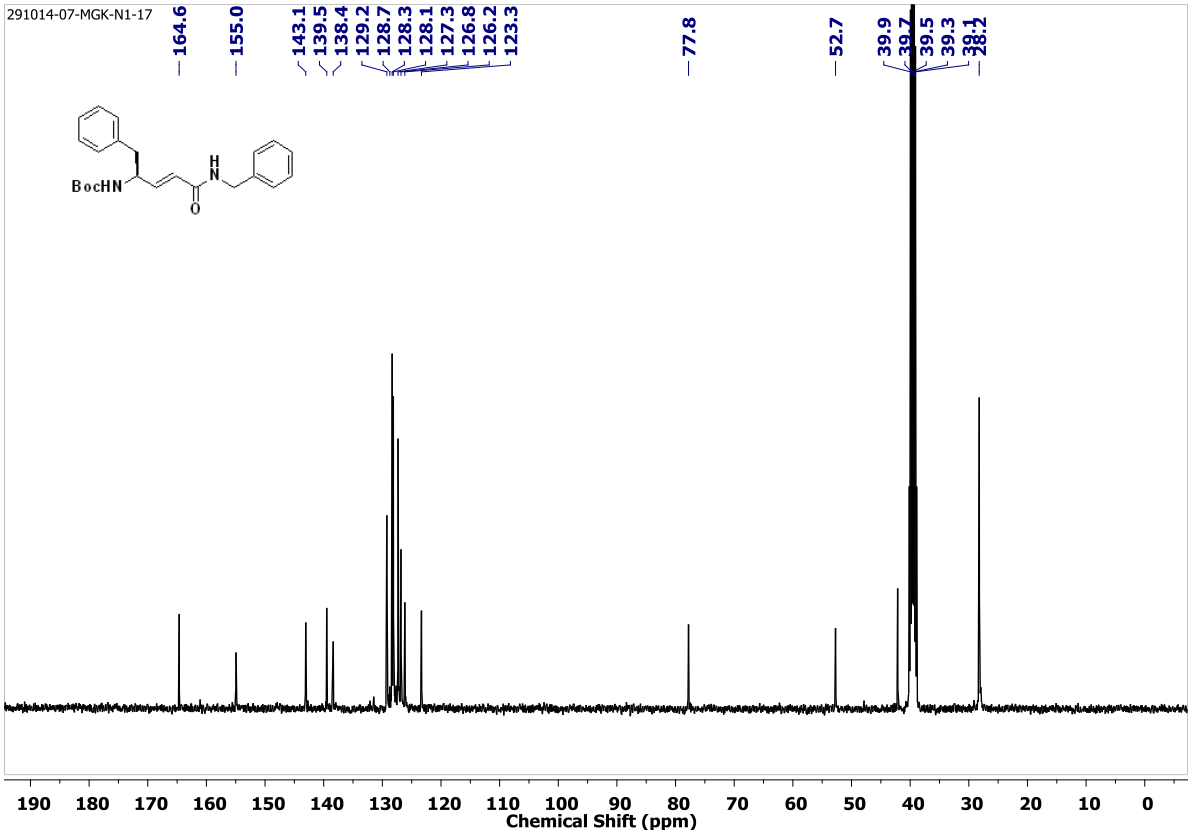
291014-07-MGK-N1-17
164.6
155.0
143.1
139.5
138.4
129.2
128.7
128.3
128.1
127.3
126.8
126.2
123.3
77.8
52.7
39.9
39.7
39.5
39.3
39.1
28.2
BocHN
H
N
O
190 180 170 160 150 140 130 120 110 100 90 80 70 60 50 40 30 20 10 0
Chemical Shift (ppm)

160913-19-MGK-LNB

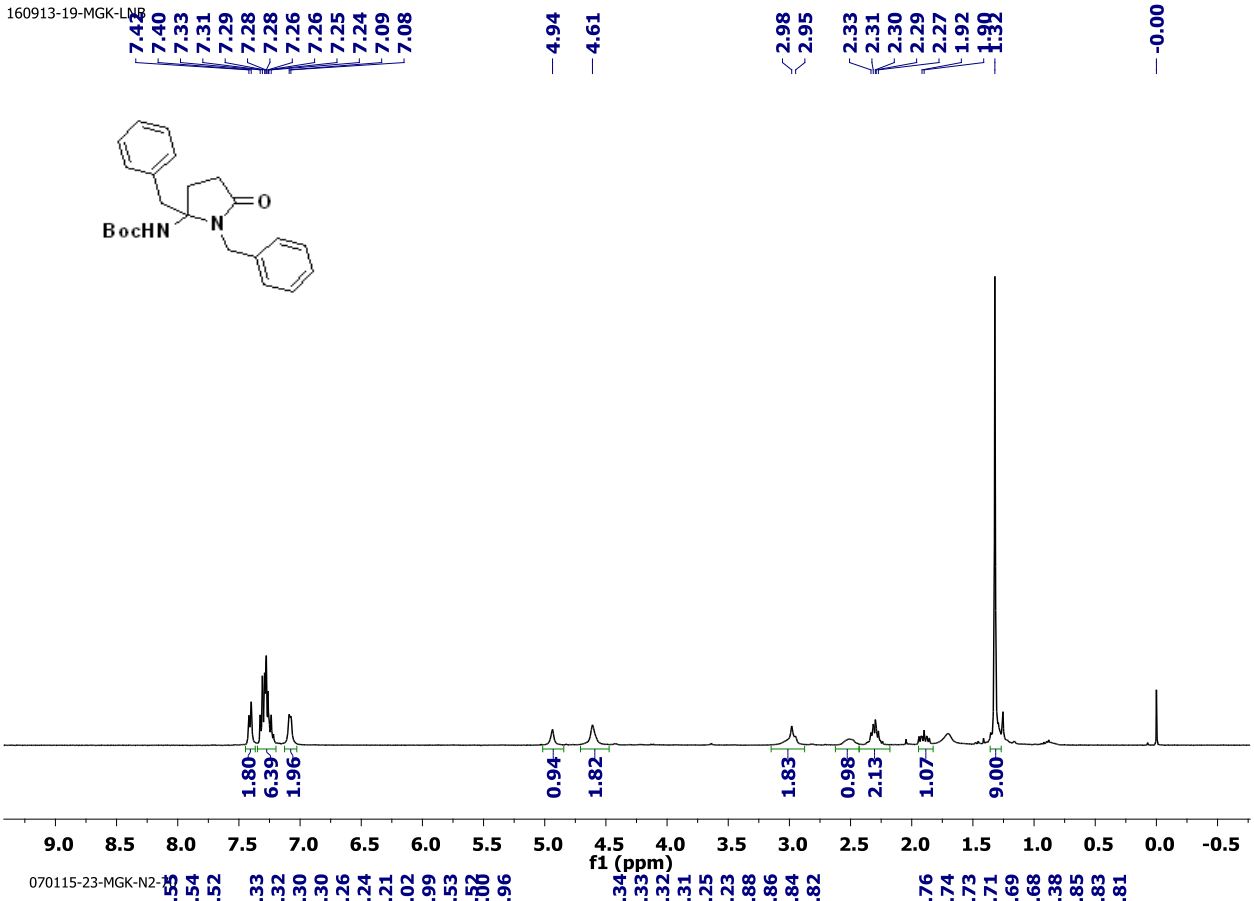

070115-23-MGK-N2-1

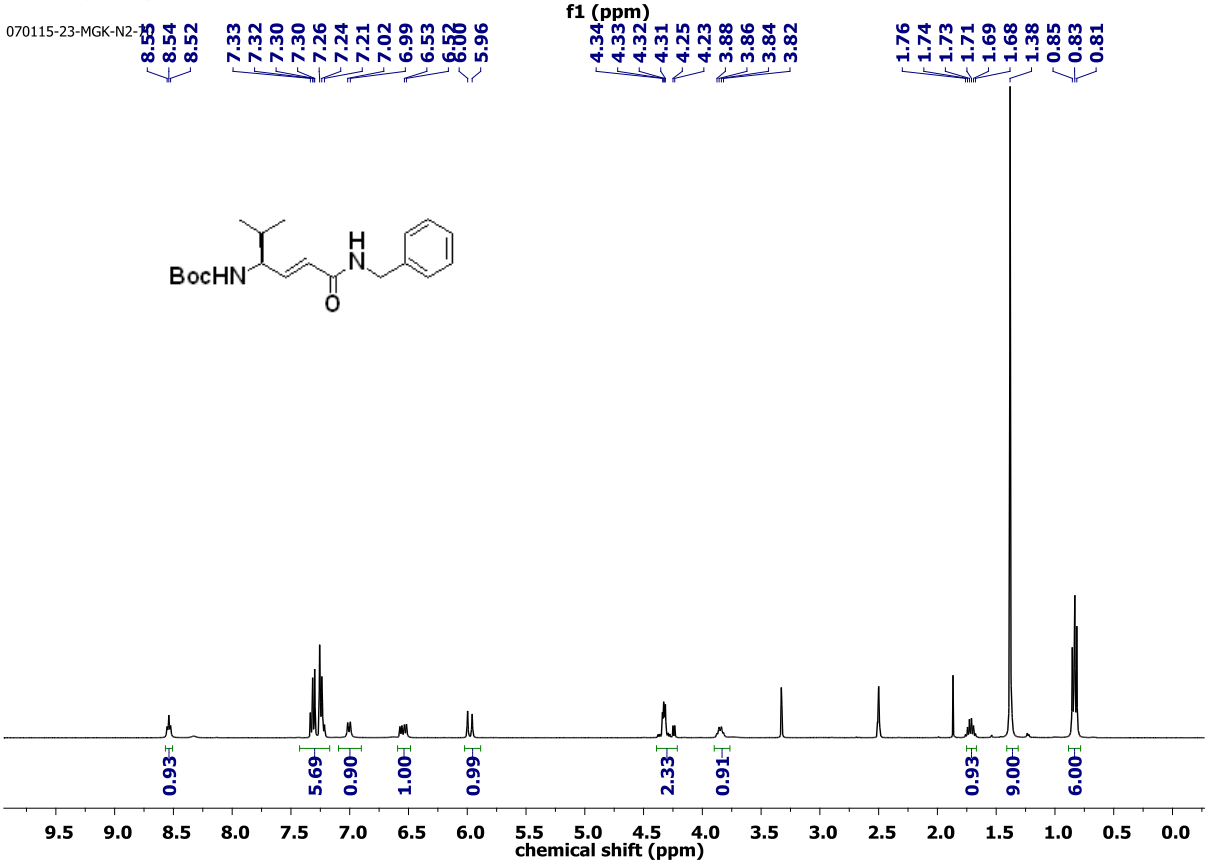

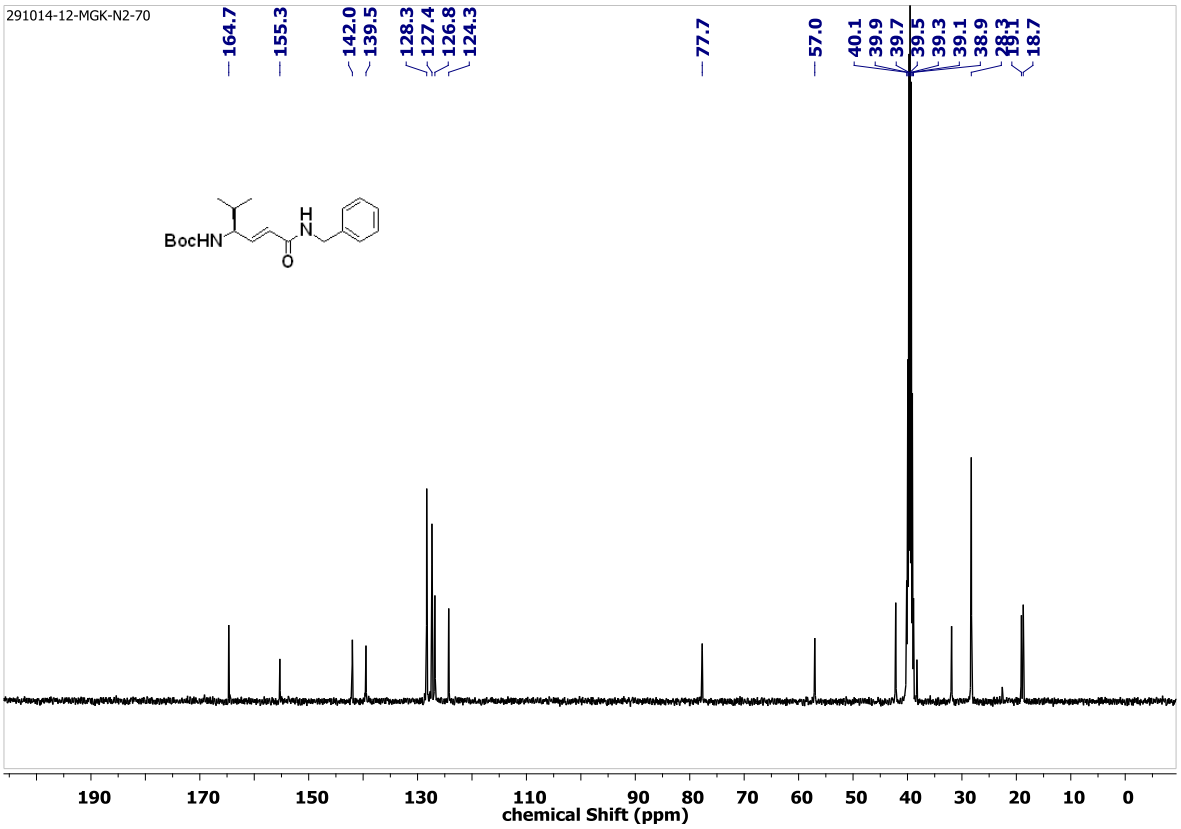
291014-12-MGK-N2-70
164.7
155.3
142.0
139.5
128.3
127.4
126.8
124.3
77.7
57.0
40.1
39.9
39.7
39.5
39.3
39.1
38.9
28.3
19.1
18.7
BocHN
H
N
O
190
170
150
130
110
90
80
70
60
50
40
30
20
10
0
chemical Shift (ppm)

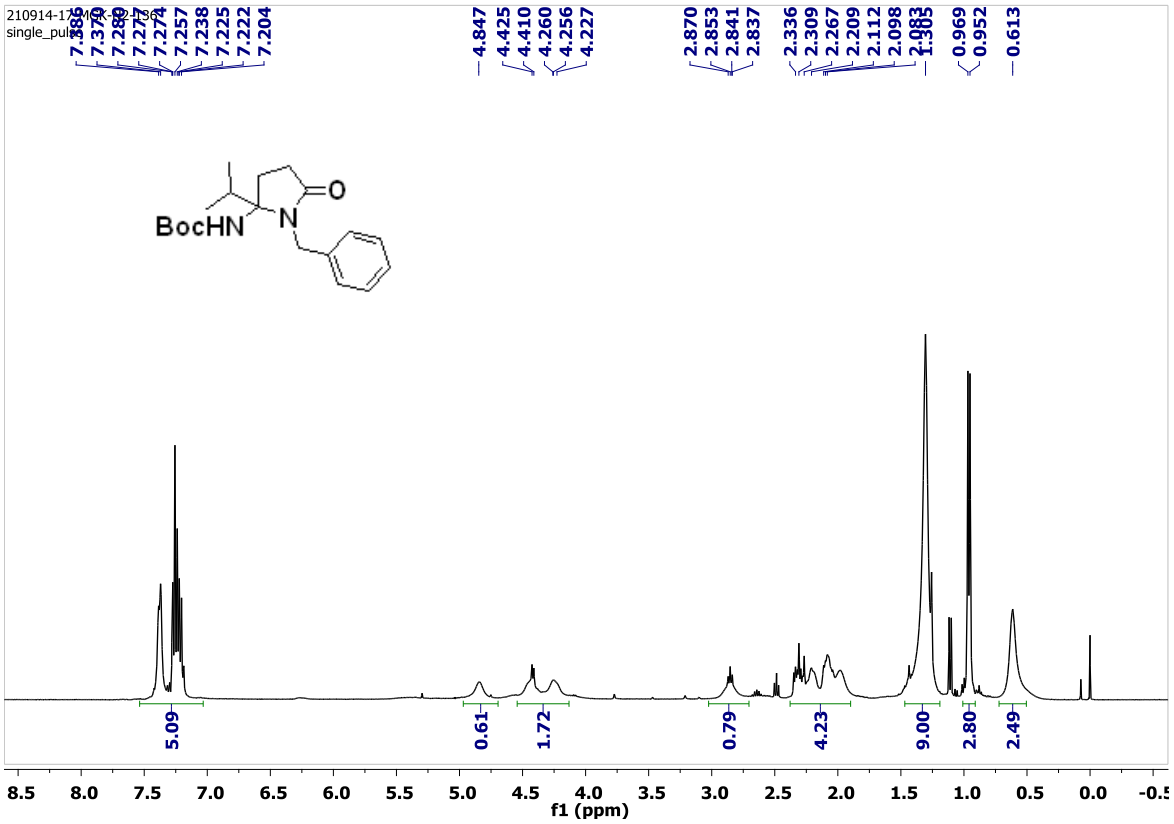
210914-11-MGK-N2-132
single_pulse
7.389
7.370
7.280
7.277
7.274
7.257
7.238
7.225
7.222
7.204
4.847
4.425
4.410
4.260
4.256
4.227
2.870
2.853
2.841
2.837
2.336
2.309
2.267
2.209
2.112
2.098
2.083
1.105
0.969
0.952
0.613
BocHN
N
O
5.09
0.61
1.72
0.79
4.23
9.00
2.80
2.49
8.5
8.0
7.5
7.0
6.5
6.0
5.5
5.0
4.5
4.0
3.5
3.0
2.5
2.0
1.5
1.0
0.5
0.0
-0.5
f1 (ppm)

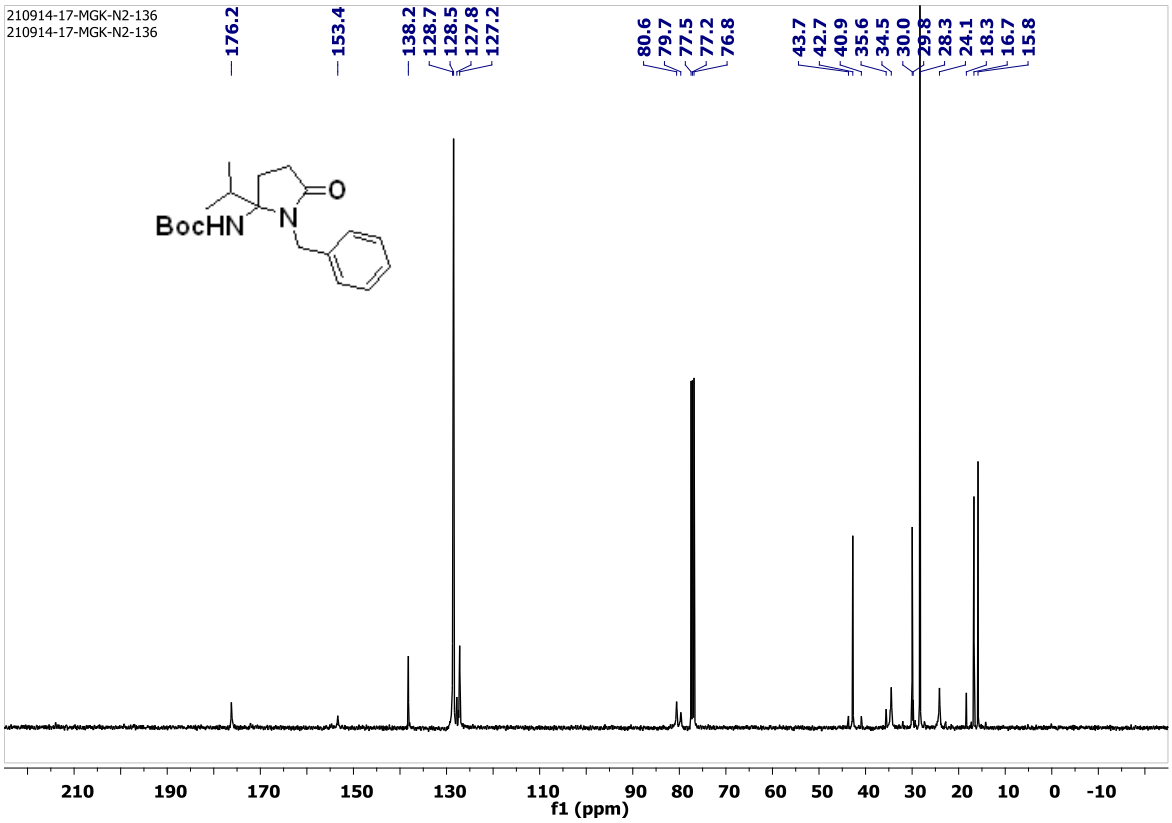
210914-17-MGK-N2-136
210914-17-MGK-N2-136
176.2
153.4
138.2
128.7
128.5
127.8
127.2
80.6
79.7
77.5
77.2
76.8
43.7
42.7
40.9
35.6
34.5
30.0
29.8
28.3
24.1
18.3
16.7
15.8
BocHN
O
N
f1 (ppm)

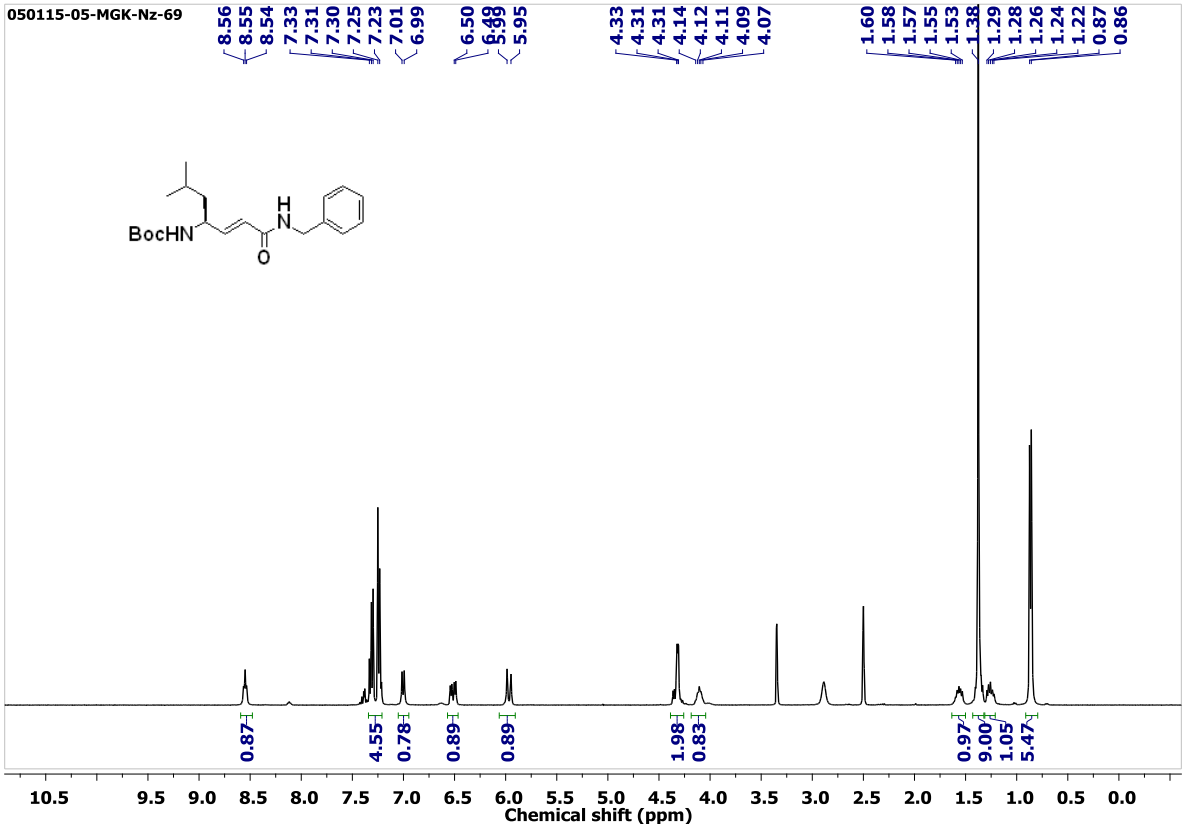
050115-05-MGK-Nz-69
8.56
8.55
8.54
7.33
7.31
7.30
7.25
7.23
7.01
6.99
6.50
6.49
6.49
5.95
4.33
4.31
4.31
4.14
4.12
4.11
4.09
4.07
1.60
1.58
1.57
1.55
1.53
1.38
1.29
1.28
1.26
1.24
1.22
0.87
0.86
BocHN
H
N
O
0.87
4.55
0.78
0.89
0.89
1.98
0.83
0.97
9.00
1.05
5.47
Chemical shift (ppm)

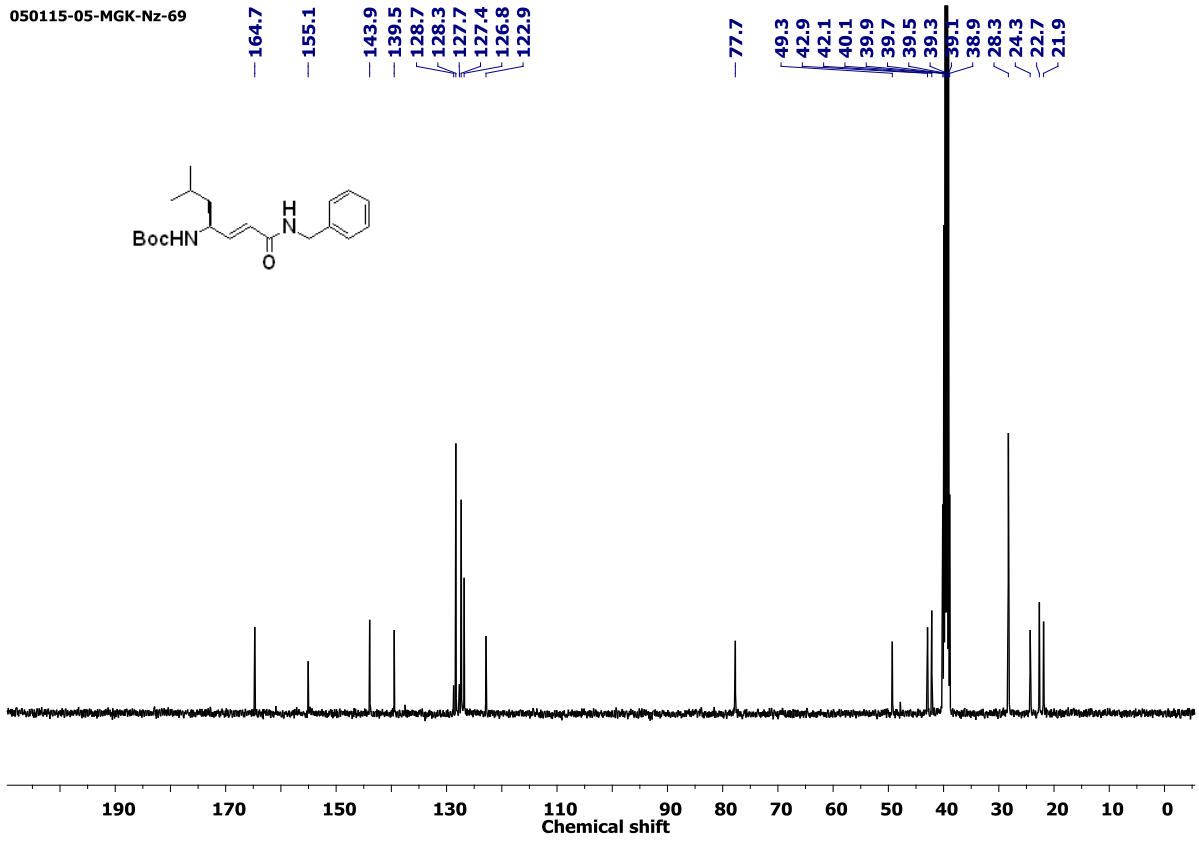
050115-05-MGK-Nz-69
164.7
155.1
143.9
139.5
128.7
128.3
127.7
127.4
126.8
122.9
77.7
49.3
42.9
42.1
40.1
39.9
39.7
39.5
39.3
39.1
38.9
28.3
24.3
22.7
21.9
BocHN
H
N
O
190
170
150
130
110
90
80
70
60
50
40
30
20
10
0
Chemical shift

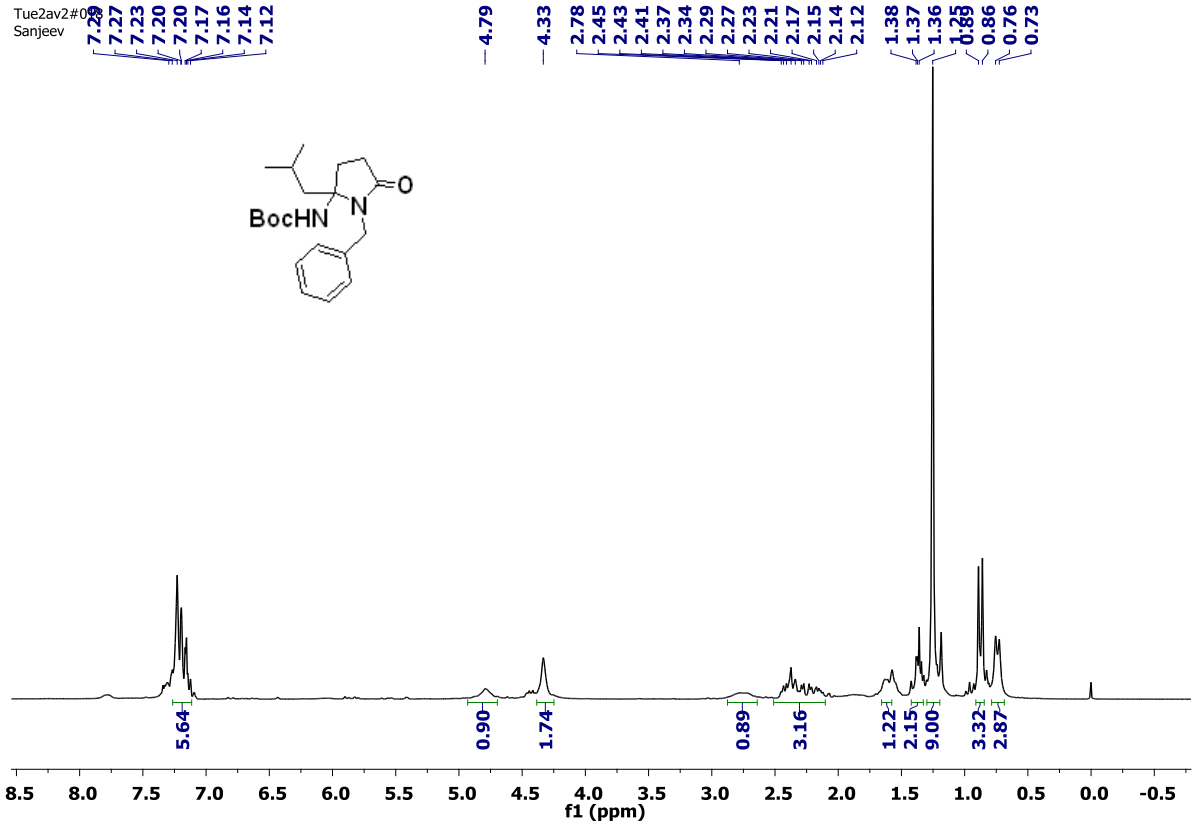
Tue2av2#098
Sanjeev
7.29
7.27
7.23
7.20
7.20
7.17
7.16
7.14
7.12
4.79
4.33
2.78
2.45
2.43
2.41
2.37
2.34
2.29
2.27
2.23
2.21
2.17
2.15
2.14
2.12
1.38
1.37
1.36
1.25
0.89
0.86
0.76
0.73
BocHN
N
O
5.64
0.90
1.74
0.89
3.16
1.22
2.15
9.00
3.32
2.87
8.5
8.0
7.5
7.0
6.5
6.0
5.5
5.0
4.5
4.0
3.5
3.0
2.5
2.0
1.5
1.0
0.5
0.0
-0.5
f1 (ppm)

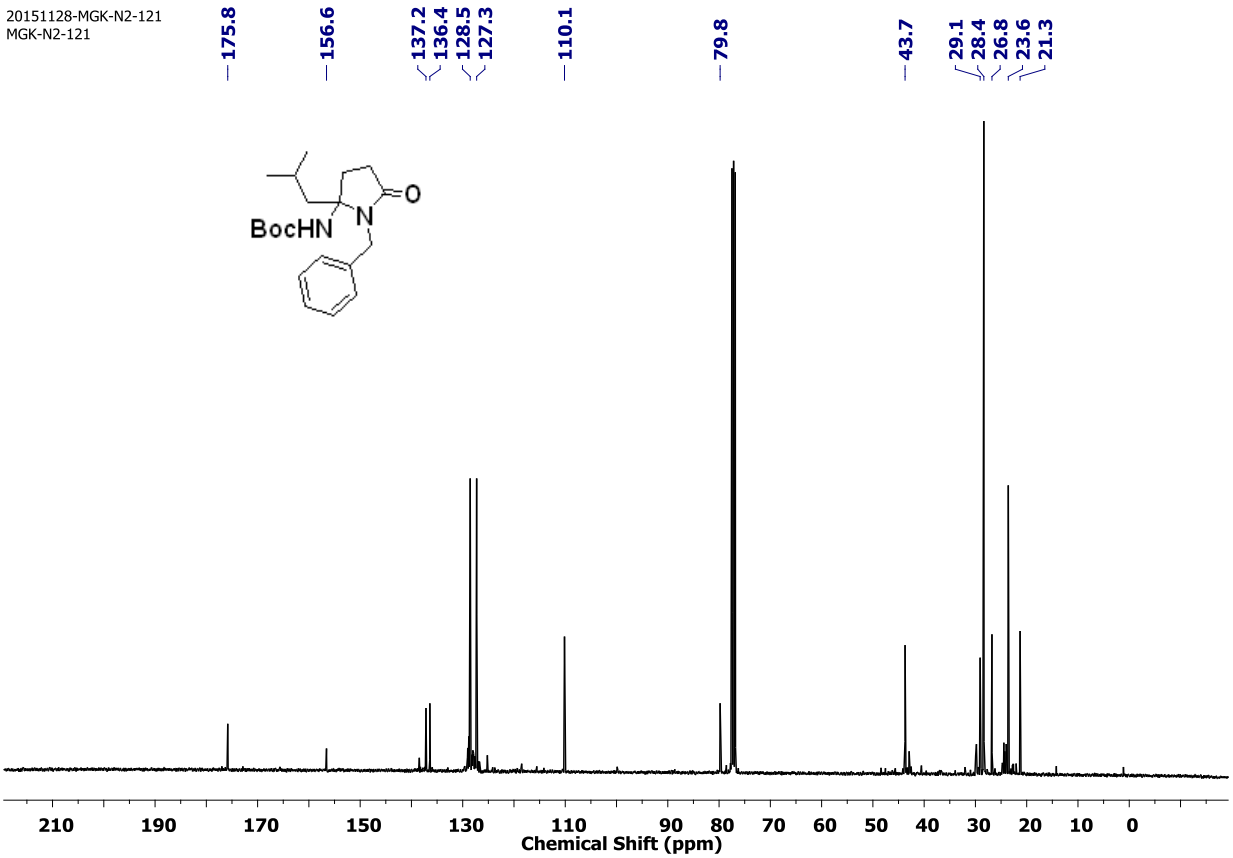
20151128-MGK-N2-121
MGK-N2-121
175.8
156.6
137.2
136.4
128.5
127.3
110.1
79.8
43.7
29.1
28.4
26.8
23.6
21.3
BocHN
N
O
210 190 170 150 130 110 90 80 70 60 50 40 30 20 10 0
Chemical Shift (ppm)

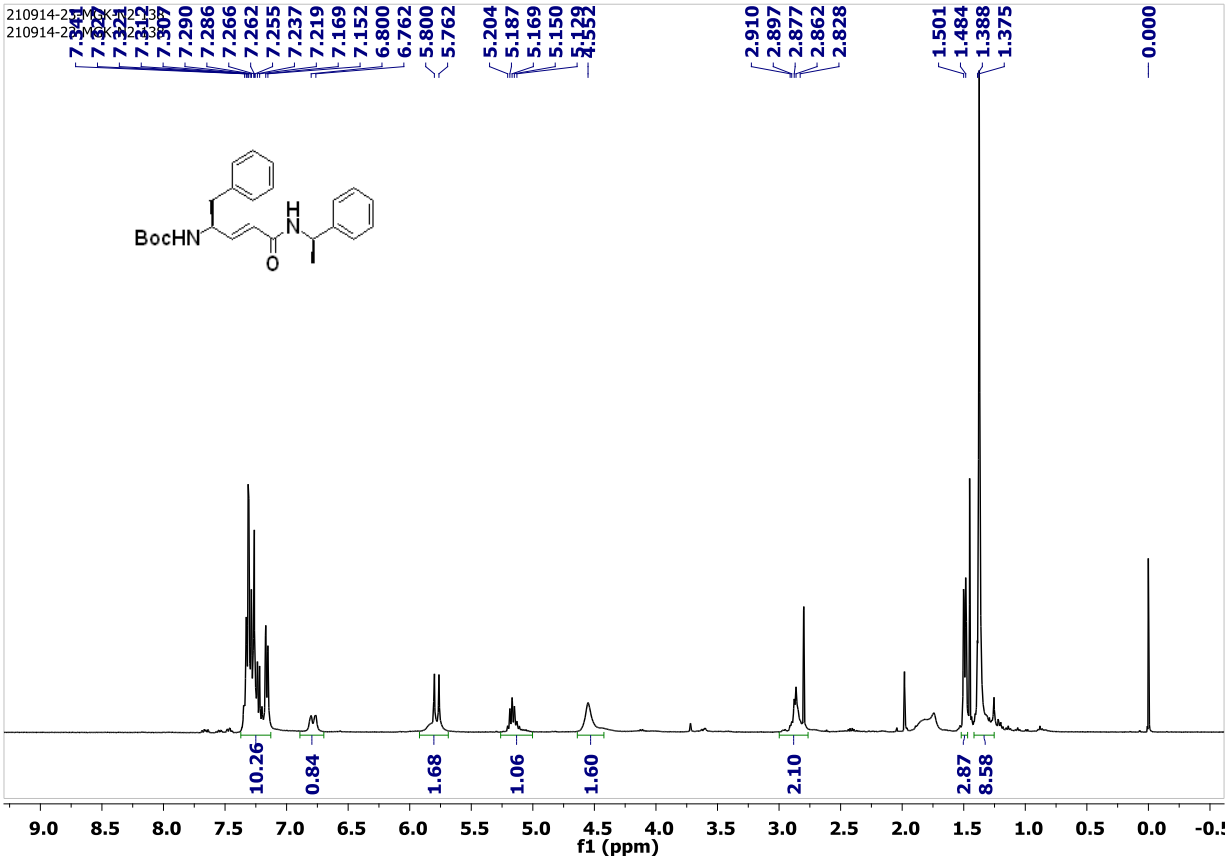
210914-2MGK-N2-133
210914-2MGK-N2-133
7.341
7.327
7.321
7.312
7.307
7.290
7.286
7.266
7.262
7.255
7.237
7.219
7.169
7.152
6.800
6.762
5.800
5.762
5.204
5.187
5.169
5.150
5.129
4.552
2.910
2.897
2.877
2.862
2.828
1.501
1.484
1.388
1.375
0.000
BocHN
H
N
O
10.26
0.84
1.68
1.06
1.60
2.10
2.87
8.58
9.0 8.5 8.0 7.5 7.0 6.5 6.0 5.5 5.0 4.5 4.0 3.5 3.0 2.5 2.0 1.5 1.0 0.5 0.0
f1 (ppm)

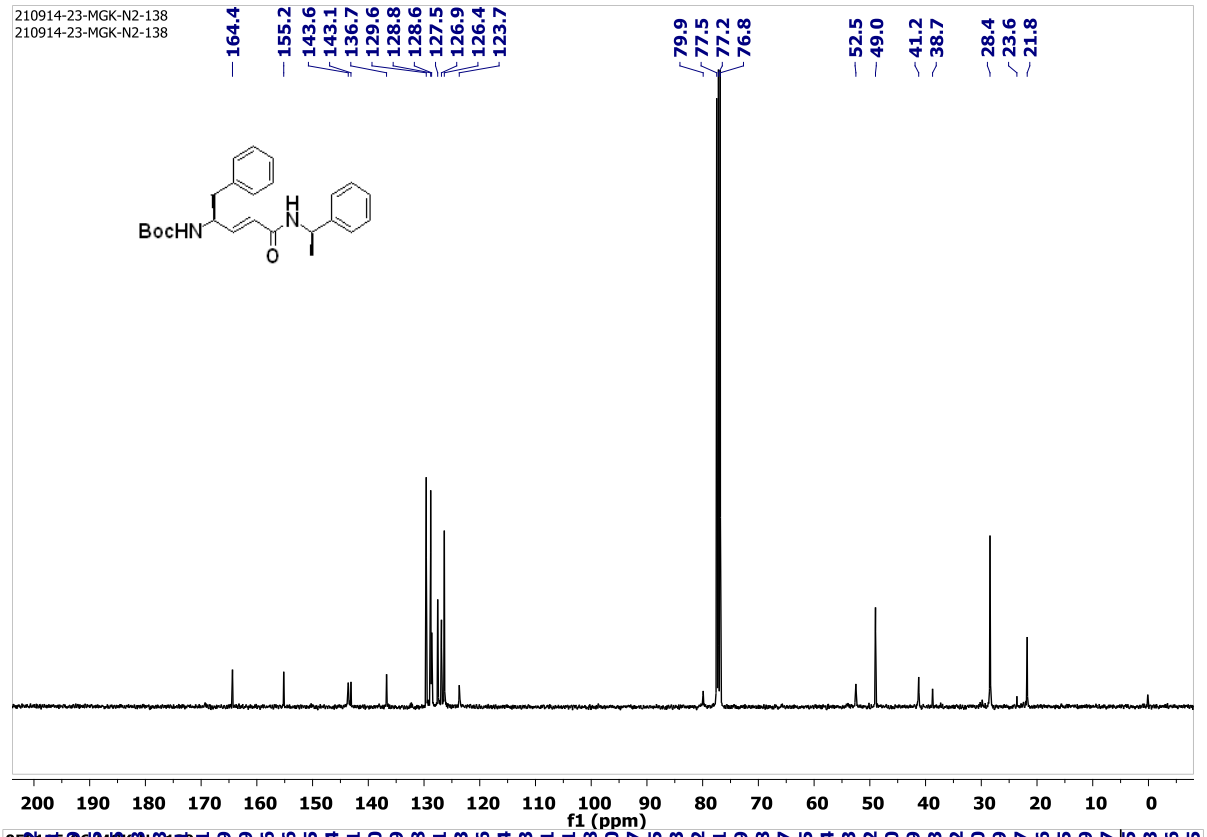
210914-23-MGK-N2-138
210914-23-MGK-N2-138
164.4
155.2
143.6
143.1
136.7
129.6
128.8
128.6
127.5
126.9
126.4
123.7
79.9
77.5
77.2
76.8
52.5
49.0
41.2
38.7
28.4
23.6
21.8
BocHN
H
N
O
200 190 180 170 160 150 140 130 120 110 100 90 80 70 60 50 40 30 20 10 0
f1 (ppm)

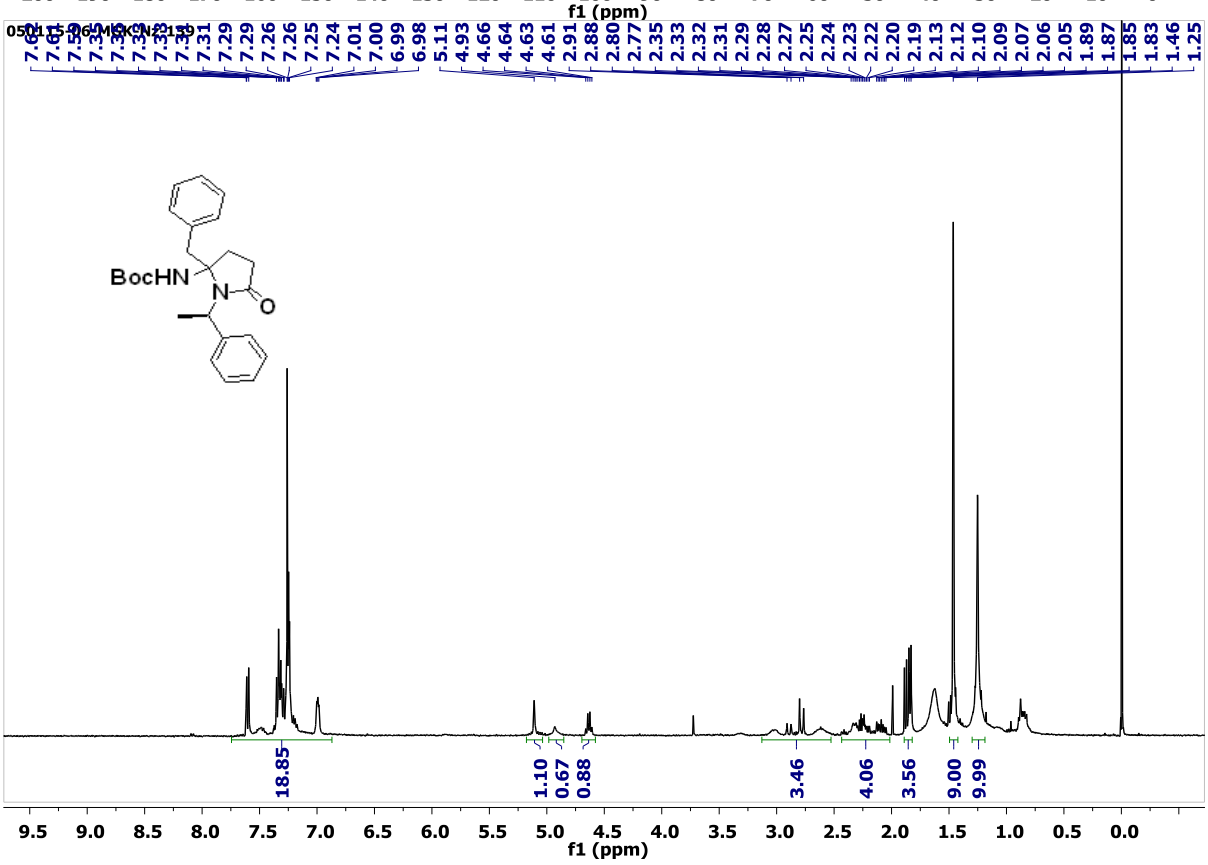
7.61 7.59 7.57 7.35 7.33 7.31 7.29 7.29 7.26 7.26 7.25 7.24 7.01 7.00 6.99 6.98
5.11 4.93 4.66 4.64 4.63 4.61 2.91 2.88 2.80 2.77 2.35 2.33 2.32 2.31 2.29 2.28 2.27 2.25 2.24 2.23 2.22 2.20 2.19 2.13 2.12 2.10 2.09 2.07 2.06 2.05 1.89 1.87 1.85 1.83 1.46 1.25
BocHN
N
O
18.85
1.10
0.67
0.88
3.46
4.06
3.56
9.00
9.99
9.5 9.0 8.5 8.0 7.5 7.0 6.5 6.0 5.5 5.0 4.5 4.0 3.5 3.0 2.5 2.0 1.5 1.0 0.5 0.0
f1 (ppm)

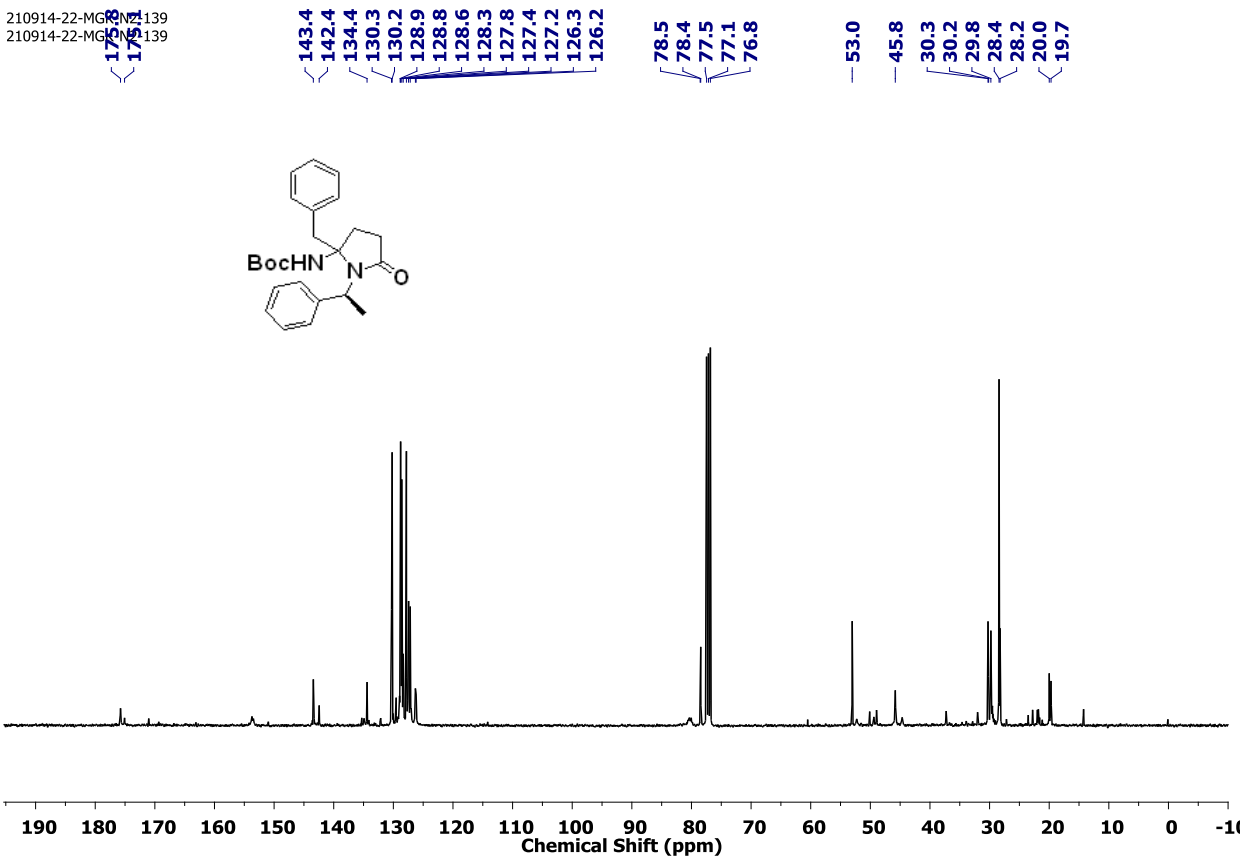
210914-22-MGK-Nz-139
210914-22-MGK-Nz-139
143.4
142.4
134.4
130.3
130.2
128.9
128.8
128.6
128.3
127.8
127.4
127.2
126.3
126.2
78.5
78.4
77.5
77.1
76.8
53.0
45.8
30.3
30.2
29.8
28.4
28.2
20.0
19.7
BocHN
N
O
190 180 170 160 150 140 130 120 110 100 90 80 70 60 50 40 30 20 10 0
Chemical Shift (ppm)

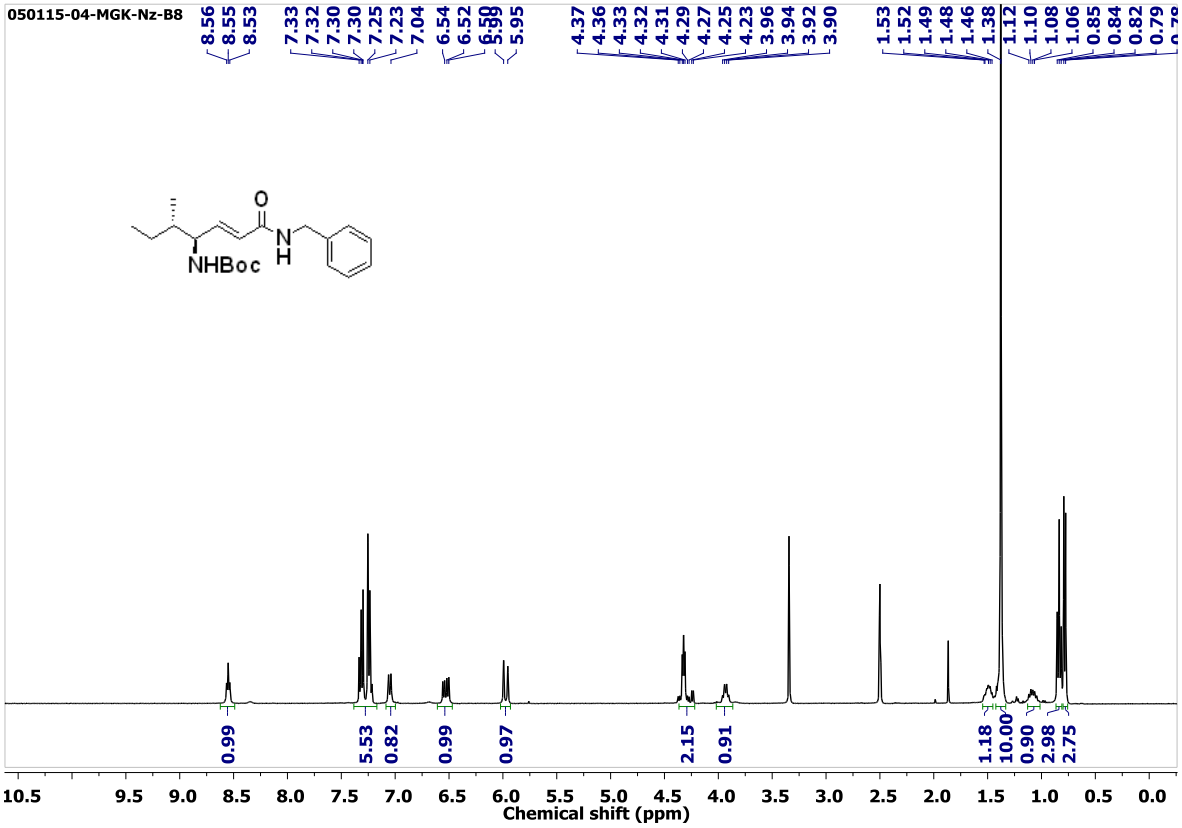
050115-04-MGK-Nz-B8
8.56
8.55
8.53
7.33
7.32
7.30
7.30
7.25
7.23
7.04
6.54
6.52
5.95
4.37
4.36
4.33
4.32
4.31
4.29
4.27
4.25
4.23
3.96
3.94
3.92
3.90
1.53
1.52
1.49
1.48
1.46
1.38
1.12
1.10
1.08
1.06
0.85
0.84
0.82
0.79
O
N
H
NHBoc
0.99
5.53
0.82
0.99
0.97
2.15
0.91
1.18
10.00
0.90
2.98
2.75
10.5 9.5 9.0 8.5 8.0 7.5 7.0 6.5 6.0 5.5 5.0 4.5 4.0 3.5 3.0 2.5 2.0 1.5 1.0 0.5 0.0
Chemical shift (ppm)

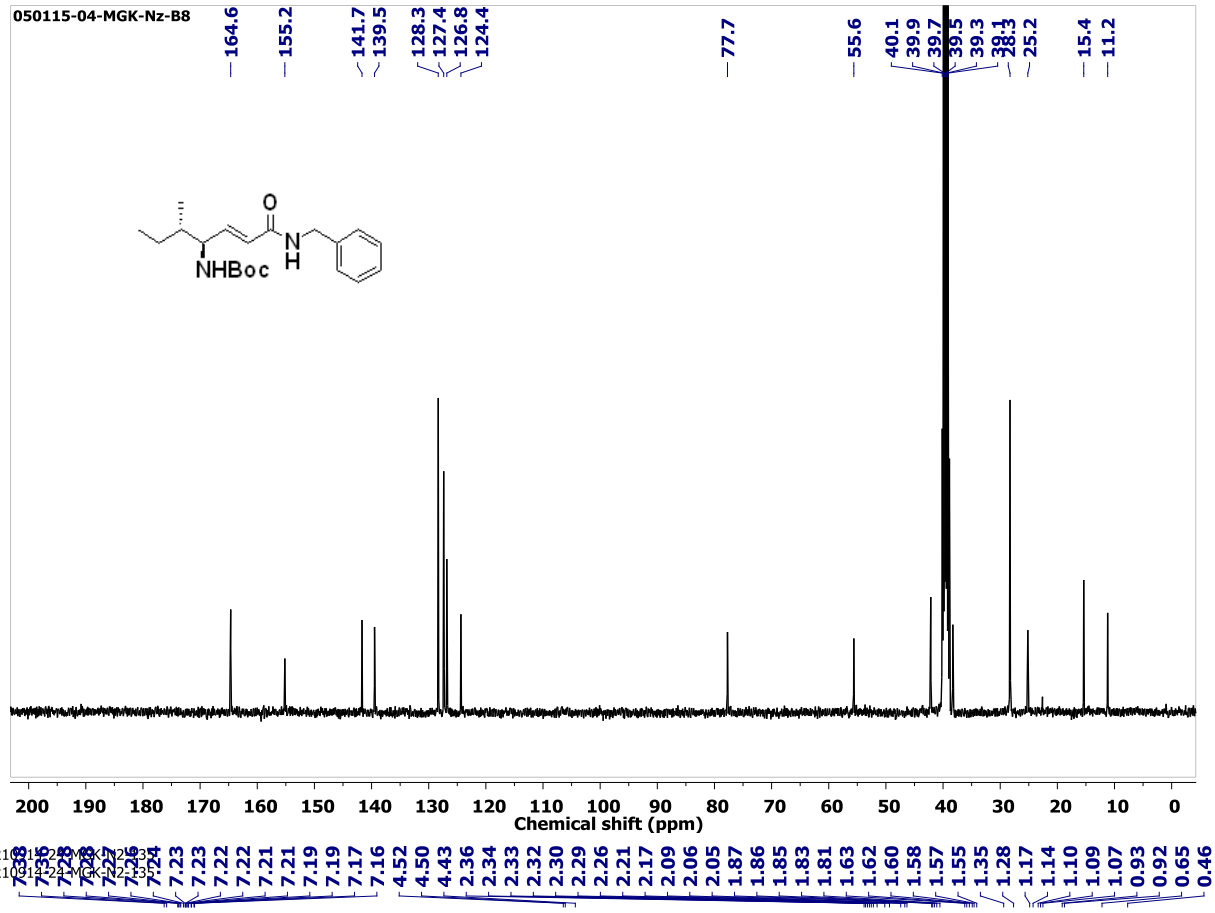
050115-04-MGK-Nz-B8
164.6
155.2
141.7
139.5
128.3
127.4
126.8
124.4
77.7
55.6
40.1
39.9
39.7
39.5
39.3
39.1
28.3
25.2
15.4
11.2
NHBoc
Chemical shift (ppm)

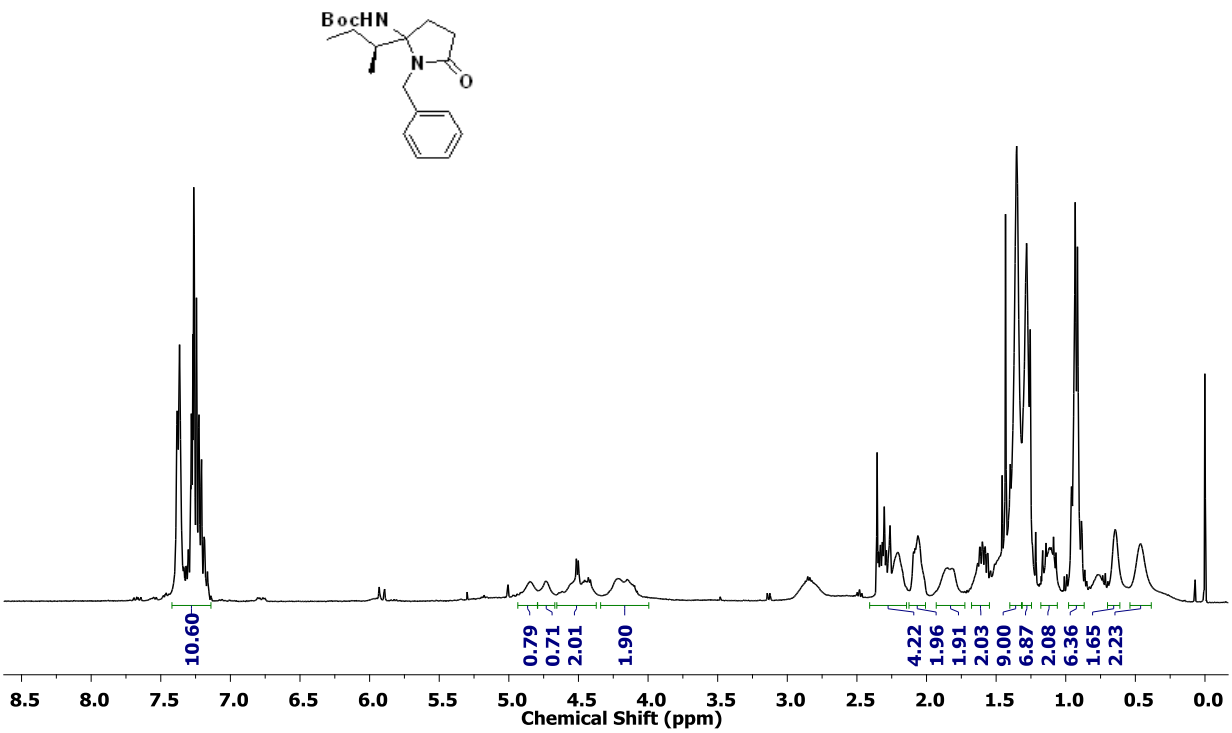
BocHN
10.60
0.79
0.71
2.01
1.90
4.22
1.96
1.91
2.03
9.00
6.87
2.08
6.36
1.65
2.23
Chemical Shift (ppm)

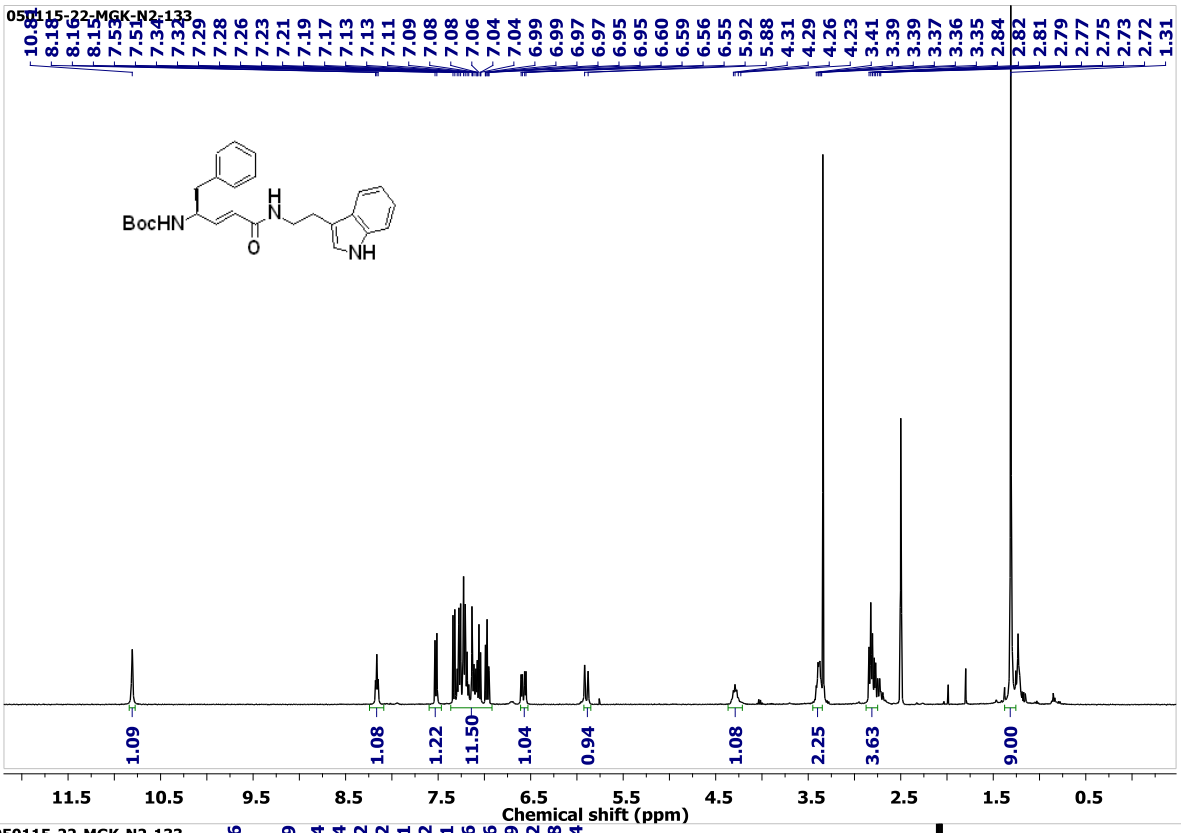
050115-22-MGK-N2-133
10.81 8.18 8.16 8.15 7.53 7.51 7.34 7.32 7.29 7.28 7.26 7.23 7.21 7.19 7.17 7.13 7.13 7.11 7.09 7.08 7.08 7.06 7.04 7.04 6.99 6.99 6.97 6.97 6.95 6.95 6.60 6.59 6.56 6.55 5.92 5.88 4.31 4.29 4.26 4.23 3.41 3.39 3.39 3.37 3.36 3.35 2.84 2.82 2.81 2.79 2.77 2.75 2.73 2.72 1.31
BocHN
H
N
O
NH
1.09 1.08 1.22 11.50 1.04 0.94 1.08 2.25 3.63 9.00
11.5 10.5 9.5 8.5 7.5 6.5 5.5 4.5 3.5 2.5 1.5 0.5
Chemical shift (ppm)

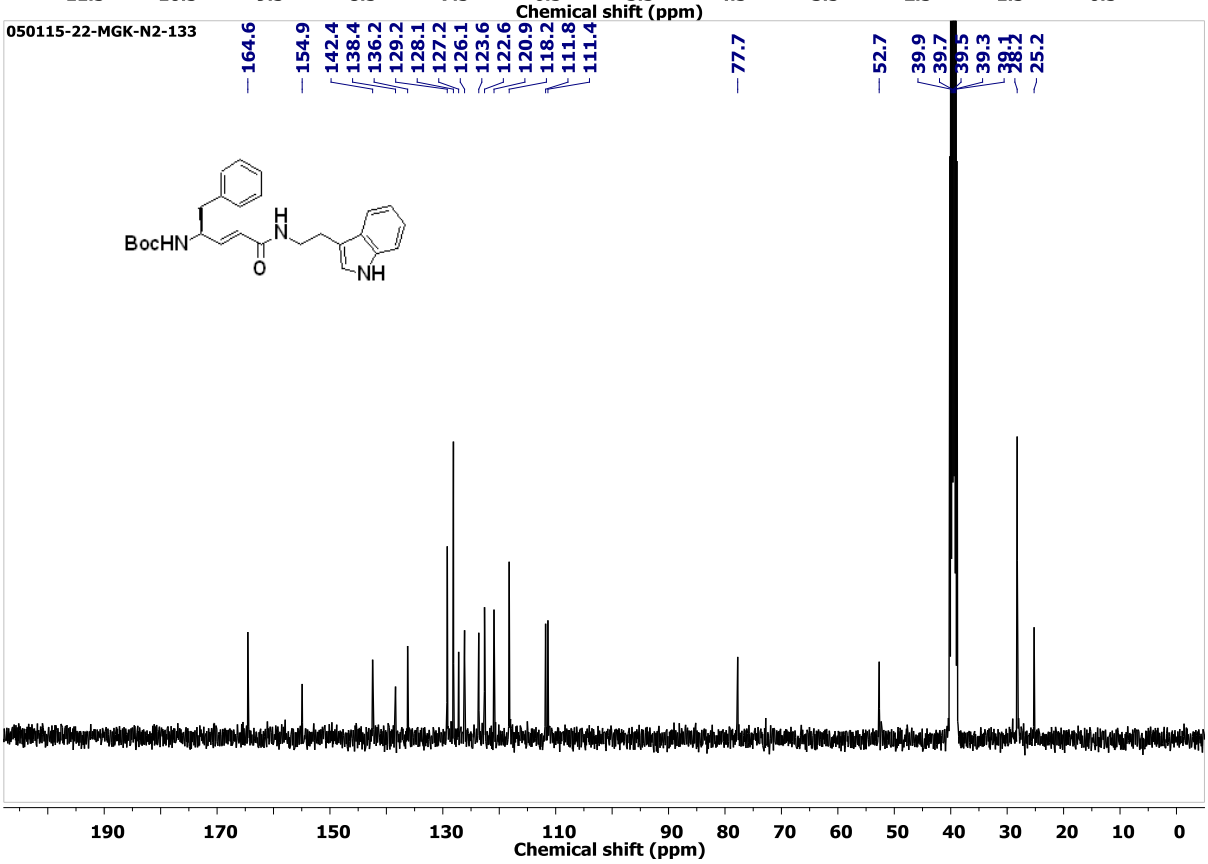
050115-22-MGK-N2-133
164.6 154.9 142.4 138.4 136.2 129.2 128.1 127.2 126.1 123.6 122.6 120.9 118.2 111.8 111.4 77.7 52.7 39.9 39.7 39.5 39.3 39.1 28.1 25.2
BocHN
H
N
O
NH
190 170 150 130 110 90 80 70 60 50 40 30 20 10 0
Chemical shift (ppm)

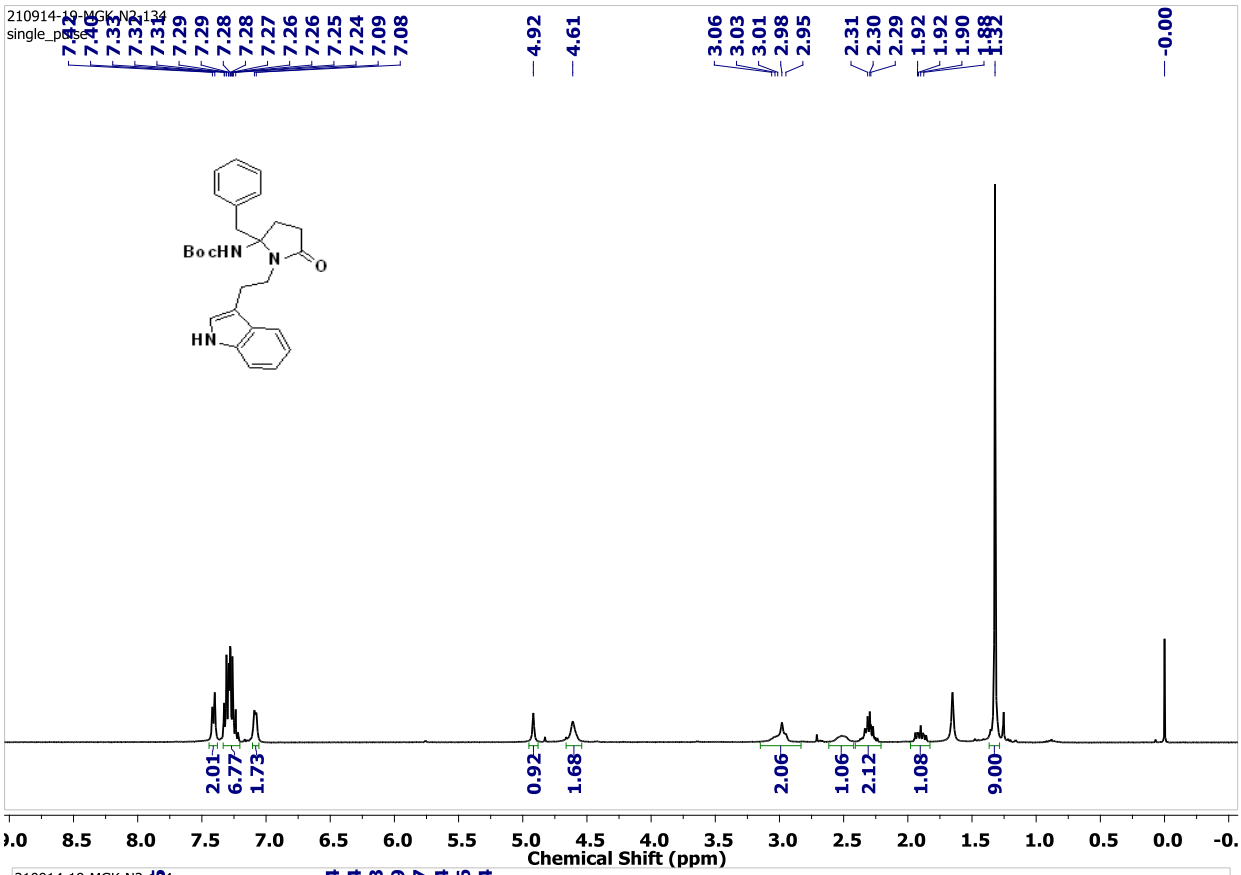
210914-19-MGK-N2-134
single_pulse
7.46 7.45 7.33 7.32 7.31 7.29 7.29 7.28 7.28 7.27 7.26 7.26 7.25 7.24 7.09 7.08
4.92
4.61
3.06 3.03 3.01 2.98 2.95
2.31 2.30 2.29
1.92 1.92 1.90 1.88 1.32
-0.00
BocHN
N
O
HN
2.01
6.77
1.73
0.92
1.68
2.06
1.06
2.12
1.08
9.00
8.5 8.0 7.5 7.0 6.5 6.0 5.5 5.0 4.5 4.0 3.5 3.0 2.5 2.0 1.5 1.0 0.5 0.0
Chemical Shift (ppm)

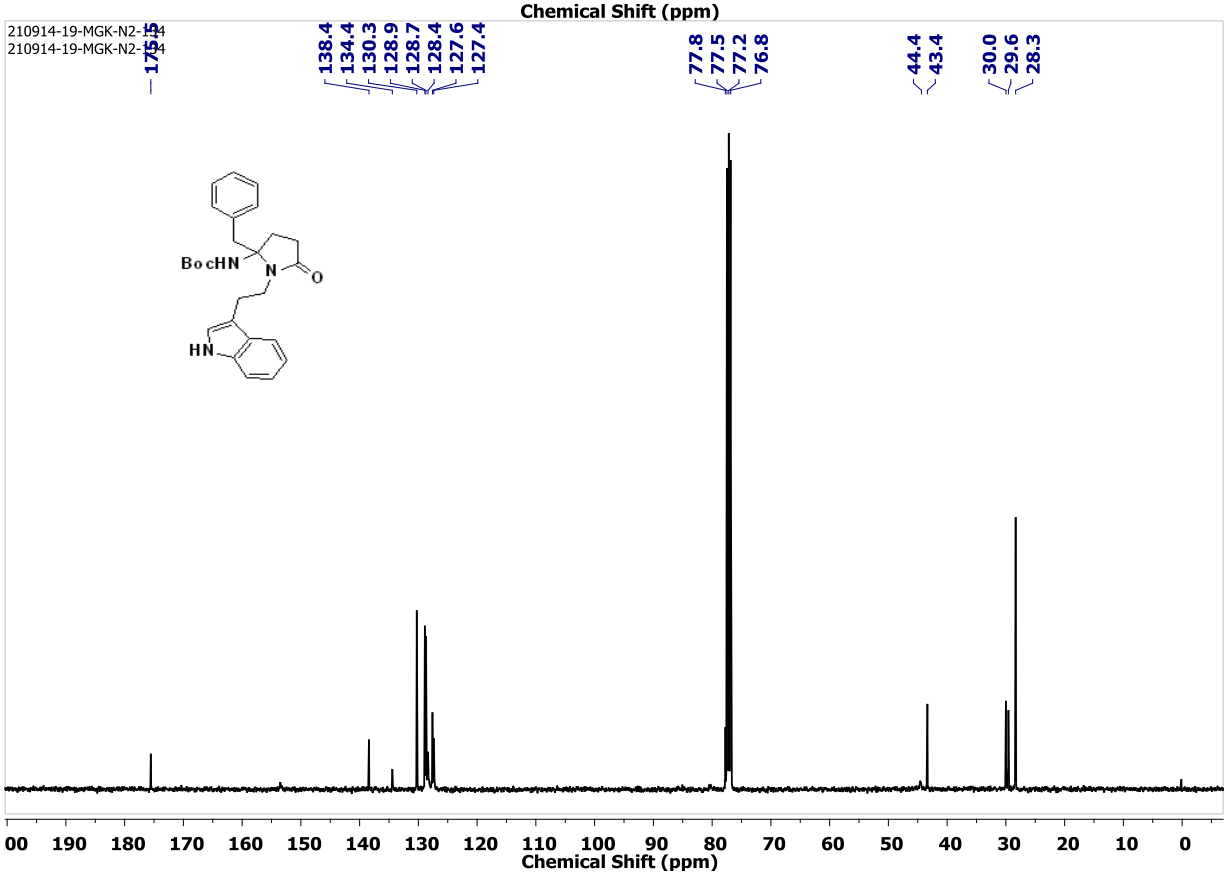
210914-19-MGK-N2-134
210914-19-MGK-N2-134
175.5
138.4
134.4
130.3
128.9
128.7
128.4
127.6
127.4
77.8
77.5
77.2
76.8
44.4
43.4
30.0
29.6
28.3
BocHN
N
O
HN
190 180 170 160 150 140 130 120 110 100 90 80 70 60 50 40 30 20 10 0
Chemical Shift (ppm)